CHEMICAL REVIEWS

pubs.acs.org/CR

Review

Earth-Abundant 3d Transition Metal-Catalyzed Enantioselective C−H Functionalization

Pu-Fan Qian, Jia-Heng Hu,[§] Yan-Xuan Wu,[§] Yuan Xu,[§] Keary M. Engle,[*] and Bing-Feng Shi[*]

Cite This: https://doi.org/10.1021/acs.chemrev.6c00255

Read Online

ACCESS | Metrics & More | Article Recommendations

ABSTRACT: Transition metal-catalyzed enantioselective C−H functionalization has emerged as a next-generation synthetic paradigm, offering numerous opportunities for the *de novo* construction and late-stage modification of complex molecular architectures. In parallel with well-established precious metal catalysts, increasing research efforts have shifted toward the use of earth-abundant 3d transition metals, driven by their distinctive intrinsic properties and reactivity profiles. This review summarizes the rapid progress in 3d metal-catalyzed enantioselective C−H functionalization up to March 2025, encompassing both inner-sphere and outer-sphere mechanisms. Emphasis is placed on the underlying challenges and core strategic solutions that have enabled these developments. To provide a comprehensive perspective, the advancements are categorized based on distinct metal/ligand catalytic systems and subcategorized according to the type of C−H functionalization reactions. Key aspects such as ligand design, reaction development, mechanistic insights, synthetic applications, and current limitations are discussed in detail where appropriate.

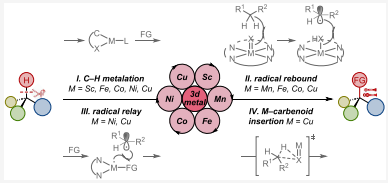

CONTENTS

Received: March 16, 2026
Revised: June 11, 2026
Accepted: June 19, 2026

1. INTRODUCTION

Chiral compounds have myriad applications in biochemistry,[1] pharmaceutical industry,[2] asymmetric catalysis,[3] molecular recognition,[4] material science,[5] deeply embedded in our daily life.[6] Considering the distinct physical, chemical, and biological properties of enantiomers in a chiral milieu,[7] diverse efficient asymmetric approaches to enantiopure molecules have been pursued in the past decades,[3,8] though the majority of these strategies hinge on the availability of pre-existing functional groups or chiral auxiliaries, which require additional installation steps with undesired byproducts generated as stoichiometric waste.[9] Therefore, alternative sustainable synthetic approaches are in highly demanded.[10] C−H bonds are the most common "functional groups" in organic compounds, underscoring the unique promise of transition-metal-catalyzed C−H activation[11] for dramatically simplifying the synthesis of bioactive and functional molecules through innovative disconnection strategies.[12] Nevertheless, within a given molecule, the similar bond strengths and steric environments of inequivalent C−H bonds combined with their ubiquitous presence pose a challenge in devising strategies for their precise functionalization, particularly when viewed through the lenses of enantioselectivity control. To date, most enantioselective C−H functionalization methods have relied on noble 4d and 5d transition metals, especially palladium, rhodium, iridium and ruthenium.[3g,13]

In light of their lower cost, reduced toxicity,[14] and unique reactivity profile,[15,16] earth-abundant 3d transition metals have gradually attracted attention as catalysts for enantioselective C−H functionalization, leading to a burgeoning body of literature that includes numerous novel bioinspired complexes and rationally designed chiral ligands guided by the properties of metal and the associated mechanistic considerations (Table 1).

Table 1. A Summary of Diverse Chiral Ligands Developed for 3d Transition Metal-Catalyzed Enantioselective C−H Functionalization: Structure and Property

metal	chiral ligand	mechanism	section
Sc	Cp^X	(I) C−H metalation	2.1
	anilido-oxazoline		2.2
Mn	Salen	(II) HAA/radical rebound	3.1
	porphyrin		3.2
	aminopyridine		3.3
Fe	porphyrin	(II) HAA/radical rebound	4.1
	Salan		4.2
	pyridine-based ligands		4.3
	NHC	(I) C−H metalation	4.4
Co	phosphine	(I) C−H metalation	5.1
	NHC		5.2
	Cp^X		5.3
	Cp*/CCA		5.4
	CPA		5.5
	Salox		5.6
	porphyrin	(II) HAA/radical rebound	5.7
Ni	SPO	(I) C−H metalation	6.1
	NHC		6.2
	BINOL		6.3
	Salox		6.4
	BOX and analogues	(III) HAA/radical relay	6.5
Cu	NHC	(I) C−H metalation	7.1
	BINOL		7.2
	BOX	(IV) metal−carbenoid insertion	7.3.4
	BOX and analogues	(III) HAA/radical relay	7.3
	CPA		7.4
	phosphine		7.5

Intriguingly, despite the substantial differences in coordination behaviors (ligand type, denticity, *etc.*) as well as the compatible metals and functionalizations, the majority of these ligands possess C2 symmetry, which appears to be a powerful design feature to enhance enantiocontrol in asymmetric catalysis.[3b−g,i,j] Through these efforts, enhanced catalytic performance,

https://doi.org/10.1021/acs.chemrev.6c00255
Chem. Rev. XXXX, XXX, XXX−XXX

Scheme 1. A Brief Overview of 3d Transition Metal-Catalyzed Enantioselective C−H Functionalization: Mechanism and Reactivity

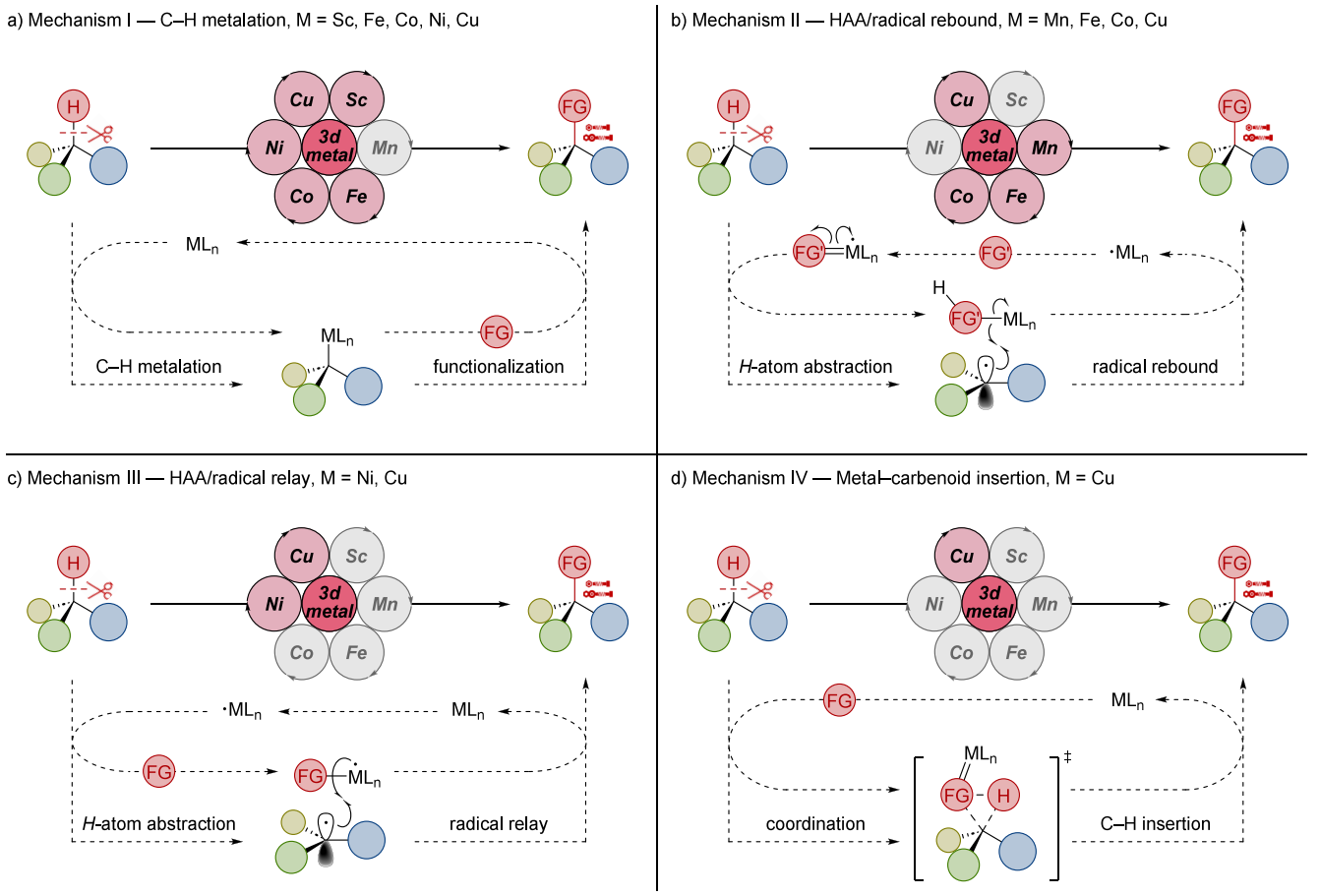

particularly improved kinetic reactivity and enantioselectivity, has been realized, allowing the direct conversion of abundant hydrocarbons into valuable chiral compounds through a variety of mechanistic paradigms.[17] The reactivity of these earth-abundant catalysts is in many cases distinct from noble metal catalysis, offering exciting opportunities for sustainable chemistry. Generally, from a mechanistic perspective, these stereospecific C−H transformations could be categorized into four strategies (Scheme 1).[17a,18] The first one is directed C−H metalation enabled by scandium, iron, cobalt, nickel, and copper, which involves an inner-sphere C−H cleavage for generation of the organometallic metallacycle intermediate, classified as "C−H activation" in the strictest sense of the term (Scheme 1a).[17a,18c,19] In a second approach, the C−H bond is cleaved through hydrogen atom abstraction (HAA) via outer-sphere mechanism without direct association of the cleaved C−H bond to metal center, and then stereoselectively functionalized through radical rebound which is inspired by biocatalytic C−H oxidation (Scheme 1b).[17d,e,20] The third approach begins through a similar HAA pathway then proceeds via a radical relay mechanism (Scheme 1c).[17b,c,21] Lastly, asymmetric metal−carbenoid insertion constitutes another pathway for outer-sphere C−H functionalization with copper catalysis (Scheme 1d).[11d,22]

Despite the rapid advancements in earth-abundant 3d metal-catalyzed C−H functionalization over the past two decades, a comprehensive review summarizing innovations in catalyst and ligand design, reaction development, mechanistic investigations, and synthetic applications, particularly the significant breakthroughs achieved in the past five years, has not yet been compiled. Therefore, in this review, we aim to provide a holistic overview of this cutting-edge area, outlining advancements of 3d-metal-catalyzed enantioselective functionalization of non-activated C−H bonds via both inner-sphere and outer-sphere mechanisms without any deliberate omissions through March 2025.[23] For clarity, this review has been organized into different metal catalysis, including scandium, manganese, iron, cobalt, nickel, and copper. Each section includes in-depth discussion, organized according to the classes of chiral ligand systems and types of functionalizations. Furthermore, challenges, strategies, ligand design principles, and insights into the mechanism of the catalytic transformations is emphasized to explain the origins of reactivity and enantioselectivity. Applications of these methodologies in the synthesis of complex molecules, such as natural products and biologically active compounds, are also illustrated where appropriate. Accordingly, in light of the vast amount of work in this field, a comprehensive and updated overview focusing specifically on 3d metal-catalyzed enantioselective C−H functionalizations is presented. We hope this review will inspire further innovations in 3d-metal-catalyzed enantioselective C−H functionalization and facilitate potential applications, which will appeal to the broad communities of synthetic organic chemistry, asymmetric catalysis, organometallic chemistry, medicinal chemistry, and materials science.

https://doi.org/10.1021/acs.chemrev.6c00255
Chem. Rev. XXXX, XXX, XXX−XXX

2. SCANDIUM CATALYSIS

As the first 3d transition metal, scandium, a rare-earth metal, is a powerful Lewis acid catalyst,[14b] with diverse applications in asymmetric nucleophilic addition, cycloaddition, redox reactions, and olefin polymerization, among others.[24] In contrast to the late transition metals, scandium is extremely electropositive and stable in its common +3 oxidation state; the resulting Sc^{3+} center features an empty 3d shell, leading to highly polarized Sc−C bonds and a distinct reactivity. The electronic structure precludes certain C−H activation mechanisms that require metal-to-C−H σ back-donation process (e.g., oxidative addition). Therefore, scandium-catalyzed C−H activation typically proceeds via a concerted four-center four-electron σ-bond metathesis mechanism,[25] with the enantioselectivity modulated by a chiral cyclopentadienyl (Cp^X) ligand in most cases.[26] Furthermore, the lack of valence shell electrons also restricts outer-sphere reactivity for Sc(III) species.

2.1. Cp^XSc(III) Catalysis

2.1.1. Asymmetric C−H Alkylation. As part of their longstanding interest in half-sandwich rare-earth metal catalysis,[27] in 2014, the Hou group demonstrated the first scandium-catalyzed enantioselective C−H activation (Scheme 2a).[28] By switching from the planar pentamethylcyclopentadienyl (Cp*) ligand[29] to a chiral Cp^X ligand designed by Cramer,[3g] enantioselective C−H alkylation at the 6-position of pyridine **1** was achieved with terminal alkenes or norbornene **2**. They found the necessarity of 2-substitution for high reactivity, which would presumably weaken the coordination of N(sp^2) lone pair electrons to the metal center. An array of alkylated products **3** was obtained in good yields with excellent enantioselectivities. Analogous to their previous mechanistic investigations,[30] the catalytically active species, a chiral η^2-pyridyl Sc(III) cation **Int1**, is formed via deprotonation of 2-picoline **1a** through σ-bond metathesis from precatalyst **Sc1** after treatment with catalytic amount of $[Ph_3C][B(C_6F_5)_4]$. Stereoselective coordination of olefin **2** is steered by steric repulsion between the chiral Cp^X scaffold and the aliphatic chain R^3 of alkene **2**,[31] followed by migratory insertion into the Sc−C bond to yield the scandacycle **Int3**. Eventually, the branched-alkylated chiral pyridine derivative (*R*)-**3** is released with σ-bond metathesis of another substrate molecule **1** for C−H activation, regenerating the η^2-pyridyl Sc(III) cationic catalyst **Int1** simultaneously. This catalytic system was then found to be suitable for manufacture of silicon-stereogenic silanes via intermolecular enantioselective Si−H alkylation with terminal aliphatic olefins.[32] Intriguingly, when the catalyst was replaced with 4d rare-earth metal yttrium and coordinated by the same chiral BINOL-derived TIPS-substituted Cp^X ligand, asymmetric methyl C(sp^3)−H alkylation of similar *ortho*-substituted pyridines with cyclopropenes would occur instead, plausibly due to its larger atomic radius compared with scandium.[33] For intramolecular enantioselective C−H alkylation, catalyzed by TBDPS-substituted half-sandwich catalyst **Sc2**, Hou and coworkers presented an efficient construction of five- or six-membered bicyclic imidazoles **5** featuring an all-carbon quaternary stereocenter from corresponding starting materials **4** with internal 1,1-disubstituted distal alkenyl group in 2020 (Scheme 2b).[34] Styrene, diene, enyne, and 1-monosubstituted alkene were capable in this transformation as well, affording *exo*-selective cyclized products **5** in high enantioselectivities (68−94% *ee*).

Scheme 2. Cp^XSc(III)-Catalyzed Enantioselective C−H Alkylation of Pyridines

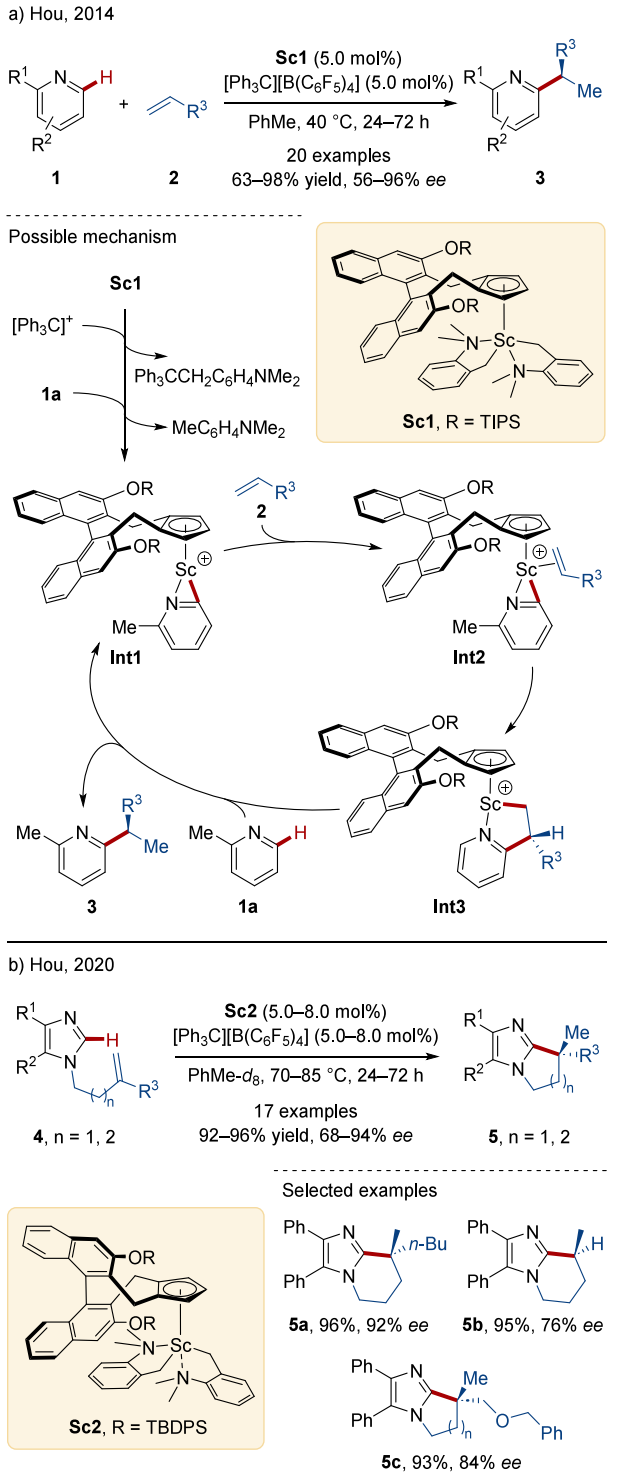

In 2023, Hou, Cong, and colleagues expanded the scope of directing groups (DGs) in Cp^XSc-catalyzed asymmetric C−H activation to aldimines **6**, producing a variety of 1-aminoindanes, including *trans*-**7**, *cis*-**7**, *trans*-**8**, *cis*-**8**, *trans*-**9**, and *cis*-**9**, with further stereoselective intramolecular nucleophilic addition of the Sc−C bond to the imine moiety after enantioselective olefin migratory insertion, providing the corresponding products in high regio-, enantio-, and diastereoselectivity (Scheme 3).[35] Remarkably, the *trans*- versus *cis*-selectivity in the reaction

https://doi.org/10.1021/acs.chemrev.6c00255
Chem. Rev. XXXX, XXX, XXX−XXX

Scheme 3. Cp^XSc(III)-Catalyzed Enantioselective C−H Activation/[3 + 2] Annulation of Aldimines

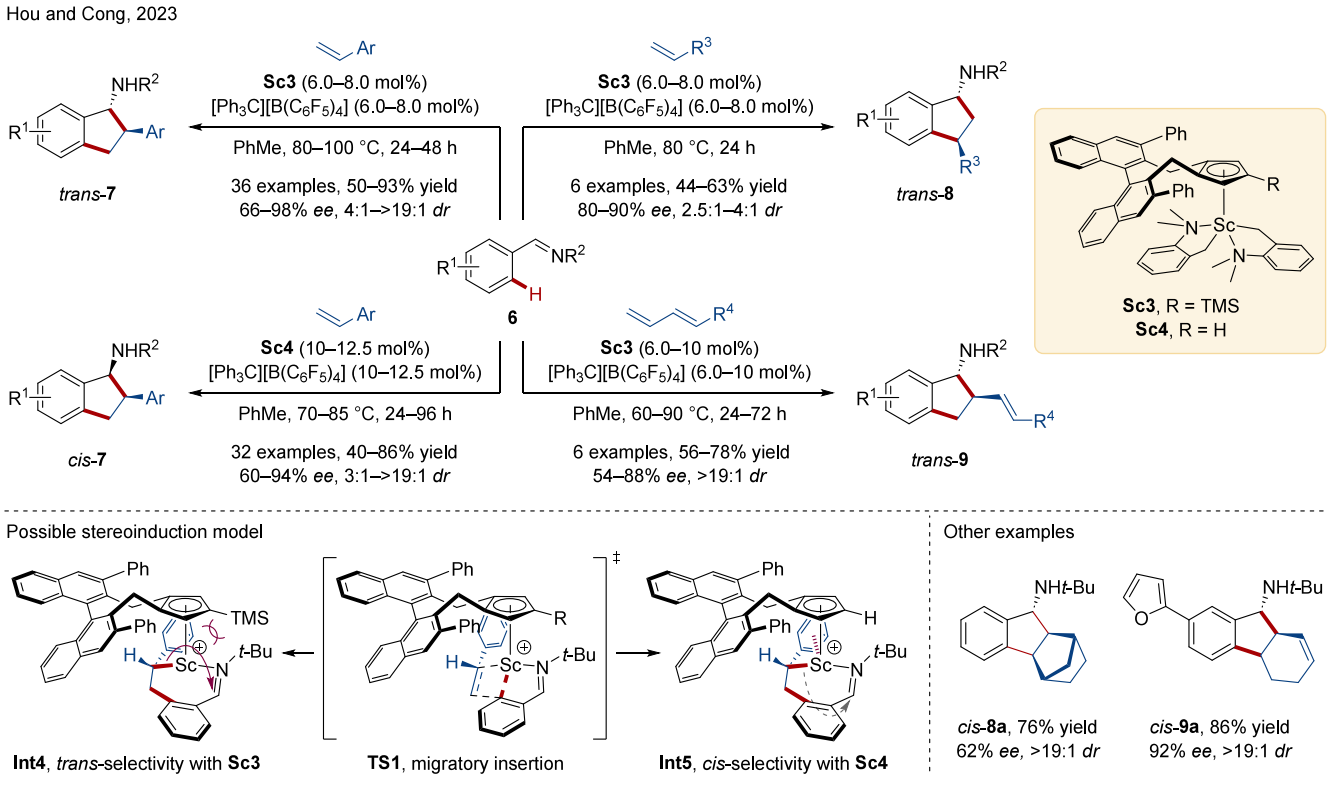

Scheme 4. Cp^XSc(III)-Catalyzed Enantioselective C−H Olefination/Nucleophilic Addition of Quinolines

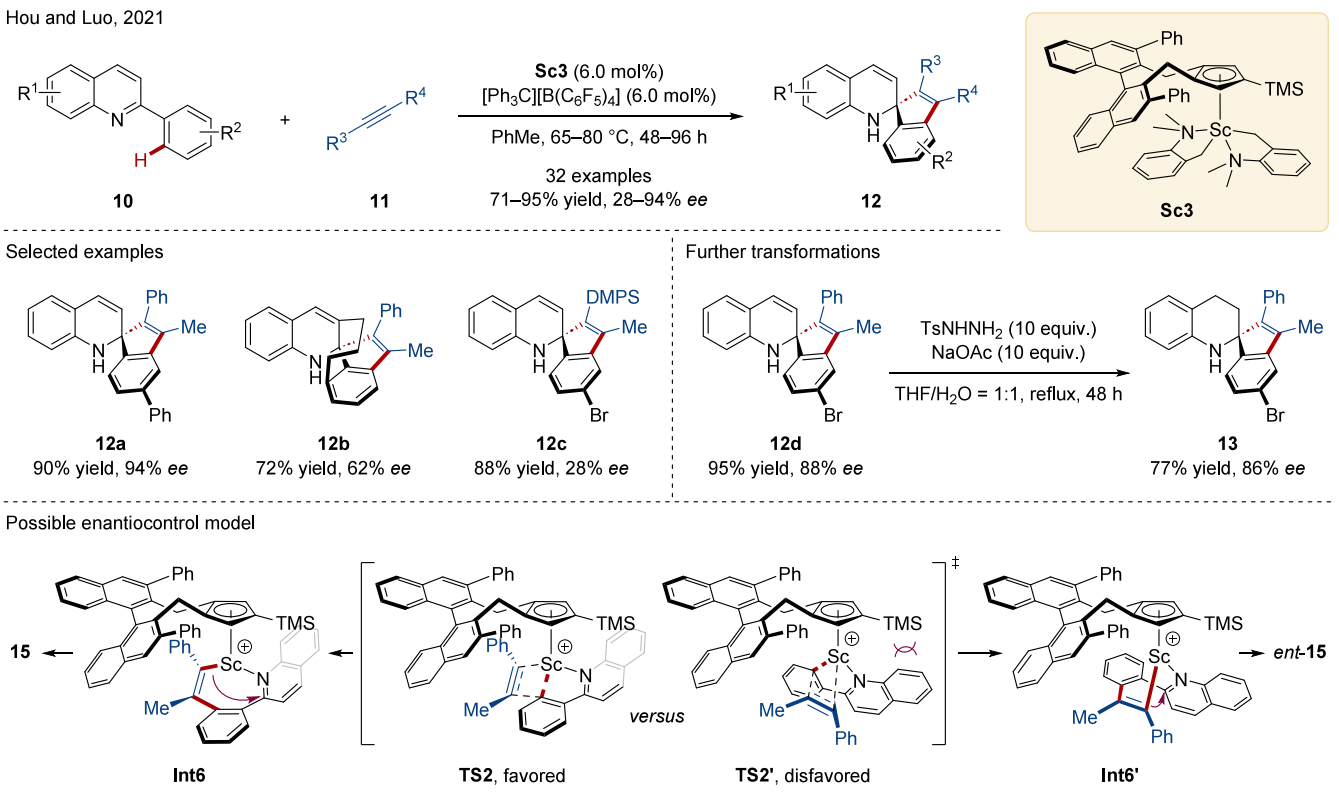

between aldimines and aromatic olefins is tunable through whether a trimethylsilyl (TMS) group is present or not on the chiral Cp^X ligand. In light of the higher steric congestion in TMS-substituted Cp^XSc catalyst **Sc3**, the potential interaction between the phenyl group of the inserted styrene and the scandium center is hampered in intermediate **Int4**, providing *trans*-**7** through Sc−C nucleophilic addition to the imine group from the *Si* face. On the other hand, when using smaller chiral

https://doi.org/10.1021/acs.chemrev.6c00255
Chem. Rev. XXXX, XXX, XXX−XXX

Cp^X-ligated **Sc4** as the catalyst, the arene−metal π-coordination is viable in the absence of bulky TMS group, leading to the (1*S*,2*S*)-7 with *cis*-configuration. Moreover, 1,3-dienes are also compatible in this transformation. With aliphatic α-alkenes, the corresponding 1,3-aminoindanes were formed through 1,2-migratory insertion, albeit with inferior enantioselectivities.[36] For norbornene and cyclohexadiene, the *cis*-polycyclic products were obtained in excellent diastereoselectivities of >19:1 *dr*, mainly due to the rigid architecture of cyclic alkenes. Notably, an analogous transformation was described via stereoselective C(sp^3)−H activation/[3 + 2] annulation directed by an imine with a racemic half-sandwich scandium catalyst.[37]

2.1.2. Enantioselective Nucleophilic Addition. In 2021, Hou, Luo, and co-workers disclosed an enantioselective approach to *spiro*-dihydroquinolines (*spiro*-DHQs) **12** containing an all-carbon quaternary stereocenter via C−H activation/dearomative annulation cascade with a chiral Cp^XSc catalyst (Scheme 4).[38] As with the above examples, the half-sandwich chiral scandium catalyst **Sc3** bearing a TMS-substituted 3,3′-phenyl binaphthyl-based Cp^X ligand was effective in enabling access to diverse enantioenriched *spiro*-DHQs **12** (up to 95% yield and 94% *ee*) from 1-aryl propynes **11**. The products could be hydrogenated with tosyl hydrazide to furnish tetrahydroquinolines (THQs), such as **13**, without significant erosion of *ee*. Strikingly, the polycyclic compound **12b** was synthesized in 87% yield and 82% *ee* from cycloheptaquinoline. Various conjugated enynes, including 1-dimethylphenylsilyl (DMPS) propyne and diphenylacetylene, were tolerated in this system, yielding corresponding products **12** with varying levels of enantioselectivity (28−82% *ee*). Supported by DFT analysis, the migratory insertion of alkyne **11** after regioselective coordination with chiral scandacycle was proposed to be the enantiodetermining step for this asymmetric *spiro*-annulation. Steric repulsion between TMS group on Cp^X ligand and quinoline ring of **10** destabilizes the disfavored transition state **TS2'**. Resembling the chiral Cp^XSc-catalyzed C−H alkylation/nucleophilic addition with alkenes discussed above (Scheme 3),[35] the desired *spiro*-DHQs are formed via σ-bond metathesis between C−H bond of an incoming substrate and the Sc−N bond of the product-bound intermediate formed upon intramolecular dearomative nucleophilic 1,2-addition from intermediate **Int6**. Intriguingly, when the 2-phenylquinoline moiety and alkynyl group were tethered within the same molecule, a new class of rigid stepladder polymers, poly(*spiro*-dihydroquinoline)s, could be gained smoothly with a simplified TMS-substituted Cp*Sc catalyst.[39]

2.1.3. Enantioselective C−H Alkenylation. Beyond establishment of *C*-central chirality through scandium-catalyzed enantioselective C−H activation, in 2021 Hou, Luo, and colleagues reported a modular asymmetric route toward planar chiral products with Cp^XSc catalyst **Sc3** (Scheme 5).[40] A wide range of planar chiral ferrocenes (PCFs) **15** were synthesized in high yields and with excellent enantioselectivities (26 examples, 64−94% yield, 92−98% *ee*). Furthermore, a functionalized ruthenocene **15c** was prepared in 91% yield and 78% *ee*. Analogous to their previous work on regiodivergent C−H alkylation of quinolines to access racemic products,[41] significant H/D exchange was detected at both the C8-position of the quinoline and the *ortho*-positions of the cyclopentadienyl (Cp) ring on the ferrocene in deuterium-labeling experiments, with similar H/D scrambling detected in the absence or presence of the alkyne coupling partner. These results indicated that reversible C−H activation takes place at both the quinolyl and

Scheme 5. Cp^XSc(III)-Catalyzed Enantioselective C−H Alkenylation of Ferrocenes

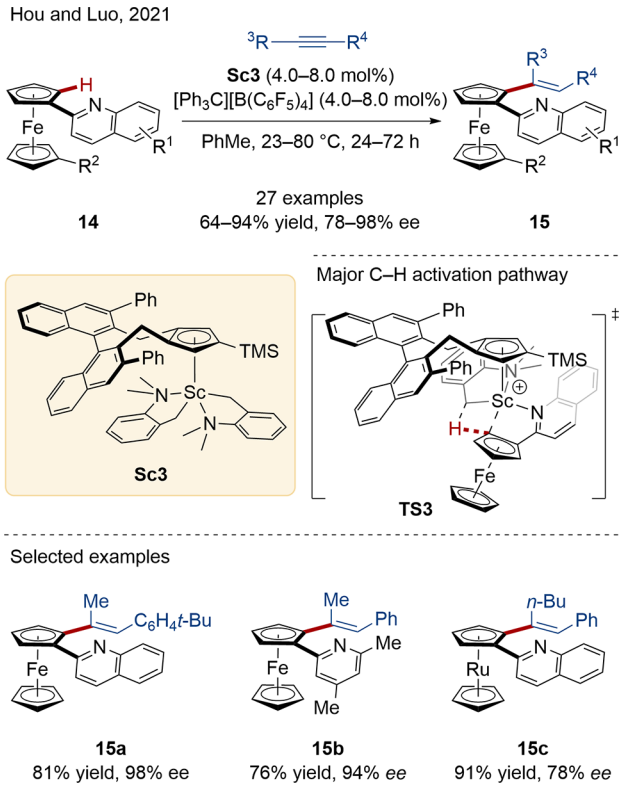

Cp rings, with subsequent enantio- and regiodetermining migratory insertion of the alkyne occurring on the Cp ring. Revealed by DFT calculations, unlike the transformations summarized in section 2.1.1 and 2.1.2, planar chirality is established during the C−H activation step with **TS3** determined as the favored transition state. Unlike the C−H activation/dearomatization of 2-phenylquinolines **10** with alkynes **11** (Scheme 4),[38] further nucleophilic addition does not take place in this reaction.

2.2. Sc(III)/Anilido-Oxazoline Catalysis

Beyond chiral Cp^XSc catalysts, very recently, Xu, Luo, and collaborators discovered that the precoordinated chiral anilido-oxazoline scandium complexes **Sc5** and **Sc6** are powerful catalysts in Sc(III)-catalyzed enantioselective C−H activation, when used in combination with cocatalytic $[PhNHMe_2][B(C_6F_5)_4]$ (Scheme 6).[42] Directed by an aromatic tertiary amine, the reaction proceeded with Markovnikov-selectivity, converting anilines **16** to C−H alkylated compounds **18** in excellent yields (54−98%) and enantioselectivities (86−98% *ee*) under mild conditions. When the *para*-position of the aniline substrate **16** was substituted with aryl group, the scandium complex **Sc6** with a bulkier cyclohexyl (Cy) group offered higher enantioselectivity. Verified by topographic steric maps and density functional theory (DFT) calculations, as shown in **TS4**, stereocontrol is induced by the steric repulsion between the main chain of olefin **17** and the arene of aniline **16** with tight spatial restriction offered by the chiral anilido-oxazoline structure.

3. MANGANESE CATALYSIS

Owing to its rich deposits in the Earth's crust as well as its multiple oxidation states ranging from −3 to +7,[43] manganese

https://doi.org/10.1021/acs.chemrev.6c00255
Chem. Rev. XXXX, XXX, XXX−XXX

Scheme 6. Sc(III)/Anilido-Oxazoline Complex-Catalyzed Enantioselective C−H Alkylation

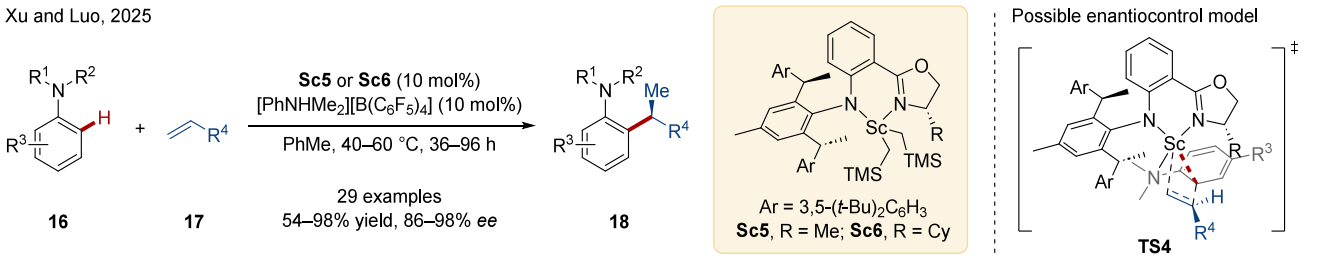

Scheme 7. Mn(III)/Salen-Catalyzed Enantioselective Methylene C−H Hydroxylation

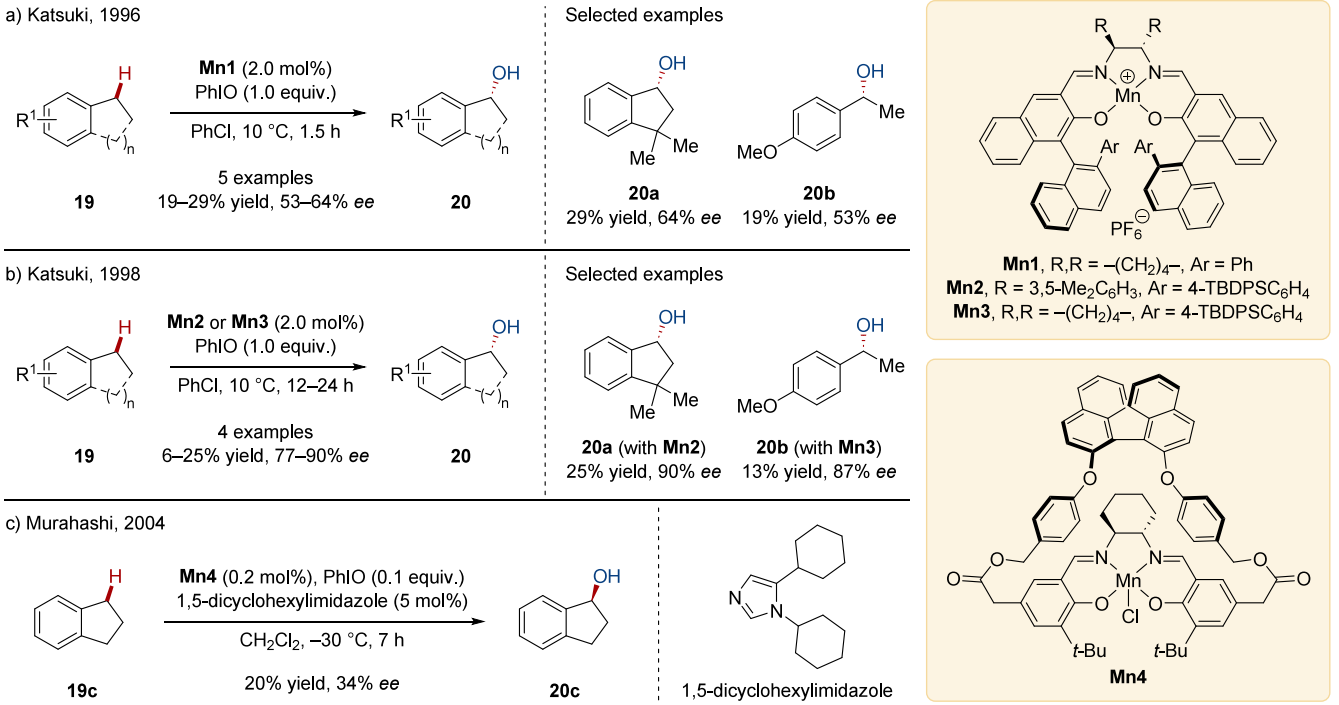

has emerged as a cost-effective and environmentally benign metal with versatile catalytic reactivity in organic synthesis,[14b,44] such as asymmetric epoxidation.[8b,44b,45] Moreover, manganese is also regarded as a vital trace element for living organisms with broad biological relevance,[46] participating in several metabolic processes as an essential cofactor for binding of molecular oxygen, such as in superoxide dismutase (Mn-SOD) and arginase.[14] Stimulated by its role in biochemistry, chemists have developed a series of asymmetric C−H hydroxylation, oxygenation, amination, amidation, and halogenation reactions catalyzed by high-valent manganese species, which generally proceed via a radical rebound pathway.[17e,44b,47] In contrast, though C−H activation via inner-sphere mechanisms has been well-developed with low-valent manganese catalysis in recent years,[48] to date, enantioselective variants remain elusive, presumably due to the lack of effective chiral ligands.

3.1. Mn(III)/Salen Catalysis

3.1.1. Enantioselective C−H Hydroxylation. Spurred on by Jacobsen's discovery of a diastereoselective C−H hydroxylation via kinetic resolution of 1,2-dihydronaphthalene oxides generated by asymmetric epoxidation with Mn(III)/Salen catalysis in 1994,[49] Katsuki and co-workers designed a chiral cyclohexanediamine-derived binaphthyl ligand for enantioselective benzylic C−H hydroxylation.[50] Chelated by a tailored *N*,*N*′-bis(salicylaldiminato)ethylenediamine (Salen) ligand, the corresponding chiral manganese(III) complex ($S_\sigma R_a$)-**Mn1** was revealed to be a competent catalyst with iodosylbenzene PhIO as an oxidant, affording secondary alcohols **20** in low yields (19−29%) with moderate enantioselectivities (53−64% *ee*) from both cyclic and linear substrates **19** (Scheme 7a). Shortly afterward, they modified the Mn(III)/Salen catalyst to **Mn2** and **Mn3** possessing a deeper chiral pocket, improving the enantioselectivity of the process (Scheme 7b).[51] In 2004, the Murahashi group developed a strapping biaryl framework-base chiral Mn(III)/Salen complex **Mn4**, which turned out to be an unsatisfactory catalyst for enantioselective methylene C−H hydroxylation of indane **19c** (Scheme 7c).[52]

Among the foundational investigations depicted in Scheme 7, ketones arising from overoxidation were commonly detected as major side-products, underscoring the challenge of facile overoxidation under the reaction conditions for methylene C−H hydroxylation, which would then ablate the newly generated stereocenter and undermine the yield of the chiral product.[53] Asymmetric C−H oxidation of a *meso* or prochiral compound is an alternative strategy that grants access to enantioenriched products containing multiple contiguous stereocenters. In such substrates the more rigid and conformationally constrained nature of the substrates can lead to particularly high enantiomeric excess. In 1998, the Katsuki group unveiled an

https://doi.org/10.1021/acs.chemrev.6c00255
Chem. Rev. XXXX, XXX, XXX−XXX

Scheme 8. Mn(III)/Salen-Catalyzed Desymmetrization of *Meso*-Tetrahydrofuran and Pyrrolidine Derivatives

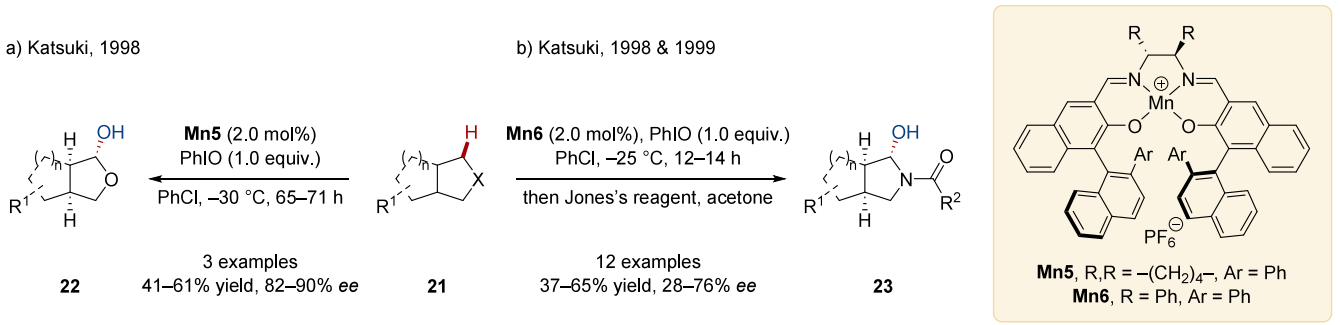

Scheme 9. Mn(III)/Salen-Catalyzed Enantioselective Tertiary C–H Hydroxylation

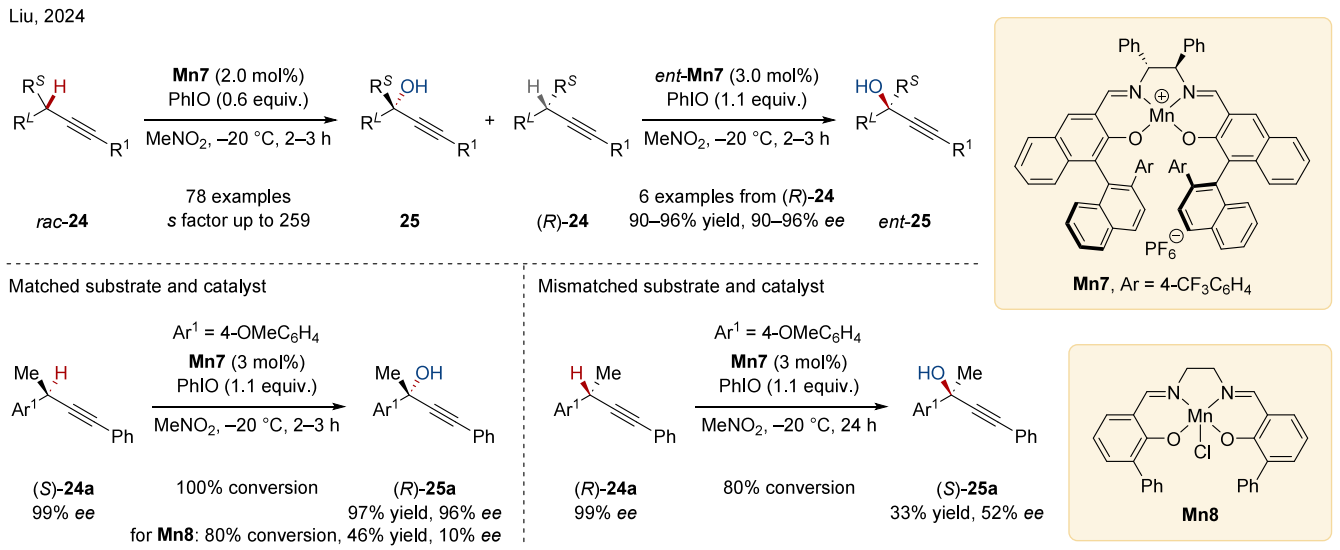

elegant desymmetrization of *meso*-tetrahydrofurans **21** through enantioselective α-C–H hydroxylation (Scheme 8a).[54] Catalyzed by Mn(III)/Salen species (R_c,R_a)-**Mn5**, three consecutive *C*-stereocenters were established simultaneously, providing target chiral *exo*-lactols **22** in moderate yields (41–61%) and high enantioselectivities (82–90% *ee*). Additionally, in this case only trace quantities of the overoxidized lactones were observed. The slow rate of overoxidation is due to the fact that the remaining *endo*-C–H bond at the hydroxylated carbon atom is sterically hindered. Subsequently, Katsuki also reported asymmetric α-C–H hydroxylation for production of chiral pyrrolidine derivatives **23** with moderate *ee* values (28–76% *ee*) catalyzed by **Mn6** (Scheme 8b).[55]

In an approach distinct from their previous ionic redox deracemization,[56] in 2024, Liu and colleagues described an ingenious kinetic resolution of acyclic alkynes *rac*-**24** via enantioselective tertiary propargylic C–H hydroxylation (Scheme 9).[57] A broad scope (78 examples) of chiral tertiary alcohols **25** and enantioenriched starting materials **24** were acquired with *s* factors ranging from 58 to 259 catalyzed by Mn(III)/Salen complex **Mn7**. Asymmetric C–H oxidation of the recovered optically active substrates (*R*)-**24** was also carried out with *ent*-**Mn7** for the generation of *ent*-**25**. In mechanistic experiments, the **Mn7**-catalyzed C–H oxidation was found to be highly efficient for configurationally matched enantiopure (*S*)-**24a**, while the mismatched substrate (*R*)-**24a** was hydroxylated to the opposite enantiomer (*S*)-**25a** along with a significant decline of reactivity, chemoselectivity, and stereoselectivity. Subjecting enantioenriched (*S*)-**24a** (99% *ee*) to racemic manganese catalyst **Mn8** led to (*R*)-**25a** 10% *ee*. Collectively, these results indicated that the tertiary C–H bond of matched alkyne enantiomers is preferentially cleaved through an enantiodifferentiating HAA assisted by the pocket-like chiral manganese species **Mn7**, and the oxygen recombination is a stereoretentive process.

3.1.2. Enantioselective C–H Oxygenation. Based on the tendency of these catalytic systems to give overoxidation, asymmetric 2-fold C–H oxygenation of a *meso* or prochiral compound is more straightforward than monoselective C–H hydroxylation in some respects. In 1998, Murahashi and coworkers reported the enantioselective benzylic 2-fold C–H oxygenation.[58] In the presence of excess oxidant, PhIO, chiral ketone **27** was formed in modest enantioselectivity (22% *ee*) with 50 mol% 4-phenylpyridine-*N*-oxide (4-PPN) via desymmetrization of 2-methyl-1,3-diphenylpropane **26** catalyzed by Mn(III)/Salen complex **Mn9** (Scheme 10a). An improved *ee* value of 70% was measured for cyclic β-siloxyketone **29** due to the rigid indane structure with **Mn10**. In 2005, the same group employed this Mn(III)/Salen catalytic system in desymmetrizing α-C–H oxidation of *cis*-1,3- or 1,4-disilylethers **30**, giving chiral γ- or δ-siloxyketones **31** in modest to excellent enantioselectivities (16–93% *ee*) with **Mn10** (Scheme 10b).[59]

3.1.3. Enantioselective C–H Oxidative Kinetic Resolution. Mn(III)/Salen-catalyzed oxidative kinetic resolution offers an appealing avenue to synthesize chiral secondary alcohols.[60] Beyond the direct two-electron oxidation of alcohols,

https://doi.org/10.1021/acs.chemrev.6c00255
Chem. Rev. XXXX, XXX, XXX–XXX

Scheme 10. Mn(III)/Salen-Catalyzed Enantioselective Benzylic C−H Oxygenation

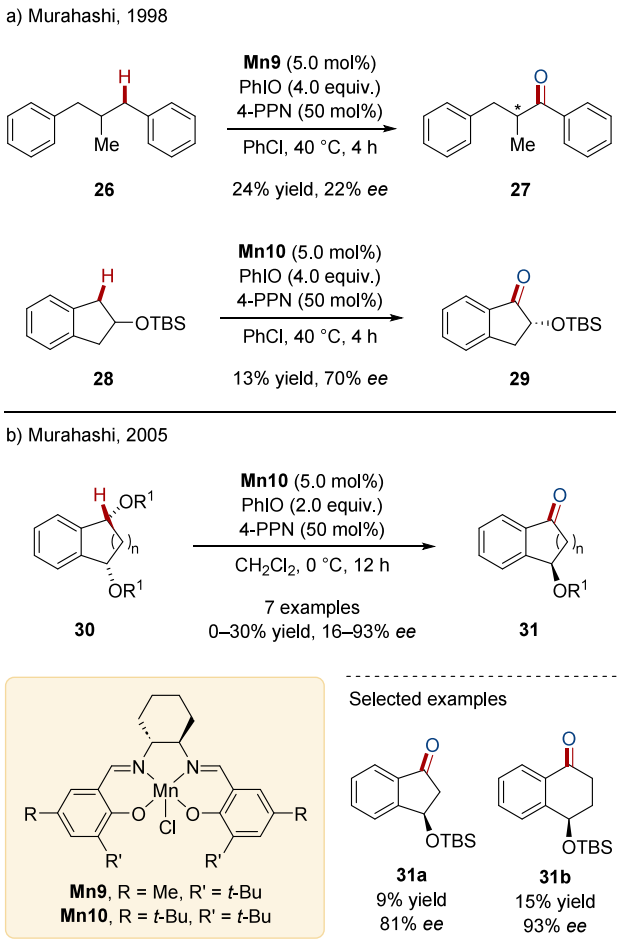

in 2020, Liu, Zhang, and collaborators accomplished an expeditious synthesis of chiral cyclic esters **32** containing multiple stereocenters with ketones **33** as the byproducts (Scheme 11a).[61] Catalyzed by Mn(III)/Salen **Mn11**, a site- and enantiodifferentiating C−H hydroxylation takes place as an additional key step on the stereochemically matched starting material *ent*-**32** to generate the corresponding chiral or achiral ketone **33**, while leaving intact the enantioenriched 5- to 10-membered oxacycle **32** bearing distinctive substituent patterns. The reaction proceeded with moderate to excellent enantiodiscrimination (51−98% *ee*), offering a convenient approach to access tetrahydrofuran or tetrahydropyran-based bioactive molecules such as (−)-centrolobine. DFT calculations indicated that unlike the previously reported C−H oxidative KR, this transformation likely proceeds through a radical rebound mechanism, with the two enantiomers in the racemic substrate distinguished by catalyst **Mn11** through stabilizing $\pi-\pi$ interactions between the 4-methoxyphenyl (PMP) group in the substrate *rac*-**32** and the binaphthyl groups of the Salen ligand. This site- and enantioselective C−H oxidative kinetic resolution was also applicable for the asymmetric construction of α-substituted 1,3-dihydroisobenzofurans, 1,2-dihydrobenzofurans, and 6*H*-benzo[*c*]chromenes with *s* factor up to 211 (Scheme 11b).[62] Interestingly, the oxidative kinetic resolution strategy could be adapted to Ti(IV)/Salen catalysis, and the same group then achieved the formation of enantioenriched hydroxylamines via asymmetric N−H oxidation.[63]

By leveraging benzylic C−H oxidation at the α-position of azido group, in 2020, the Liu group reported an efficient kinetic resolution of organic azides *rac*-**36** and *rac*-**38** catalyzed by **Mn13** or **Mn14** with *s* factor up to 95 (Scheme 12).[64] For tetrahydroquinoline (THQ) substrates *rac*-**36**, oxidation of stereomatched (*R*)-**36** triggers loss of nitrogen and dimerization of the resulting iminyl radical **Int8** to the corresponding azo-compound **37** as the oxidized byproduct. With indolines (*R*)-**38** on the other hand, the stereomatched substrate is oxidized to 2-cyanophenylamide **39** through Mn(V)−oxo-mediated HAA,

Scheme 11. Mn(III)/Salen-Catalyzed Enantioselective C−H Oxidative Kinetic Resolution of Oxacycles

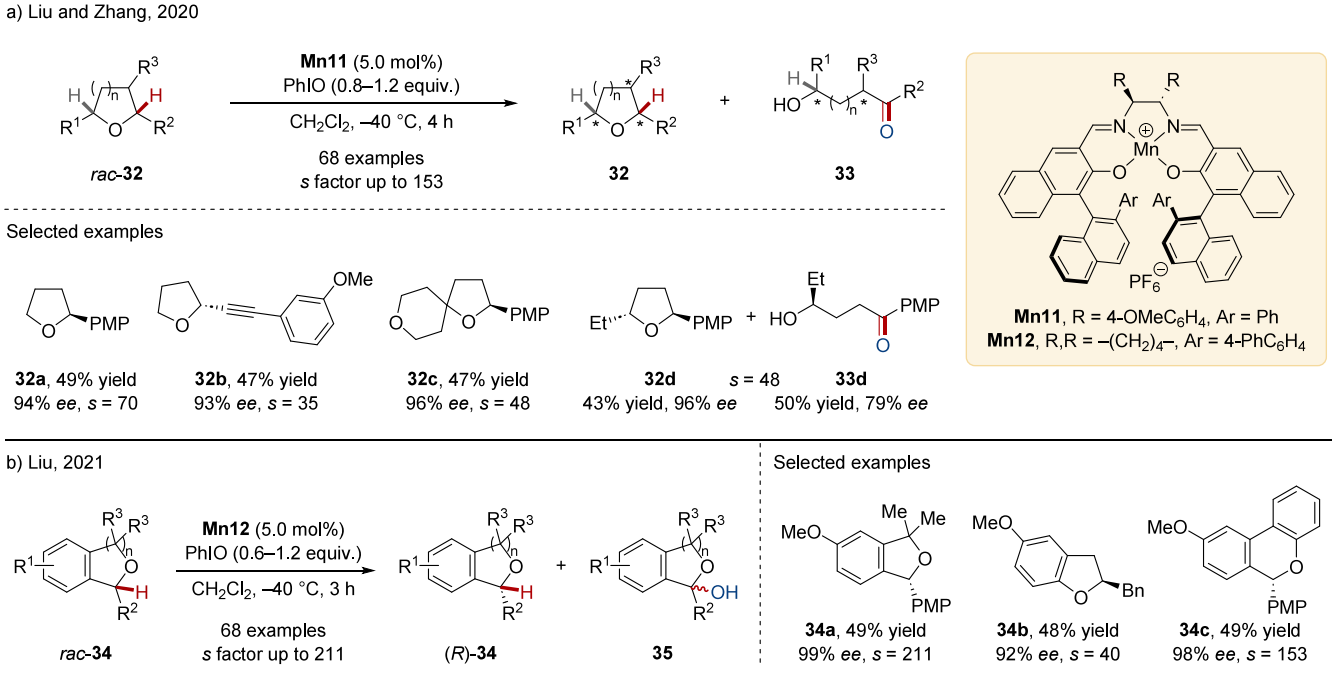

https://doi.org/10.1021/acs.chemrev.6c00255
Chem. Rev. XXXX, XXX, XXX−XXX

Scheme 12. Mn(III)/Salen-Catalyzed Enantioselective C−H Oxidative Kinetic Resolution of Organic Azides

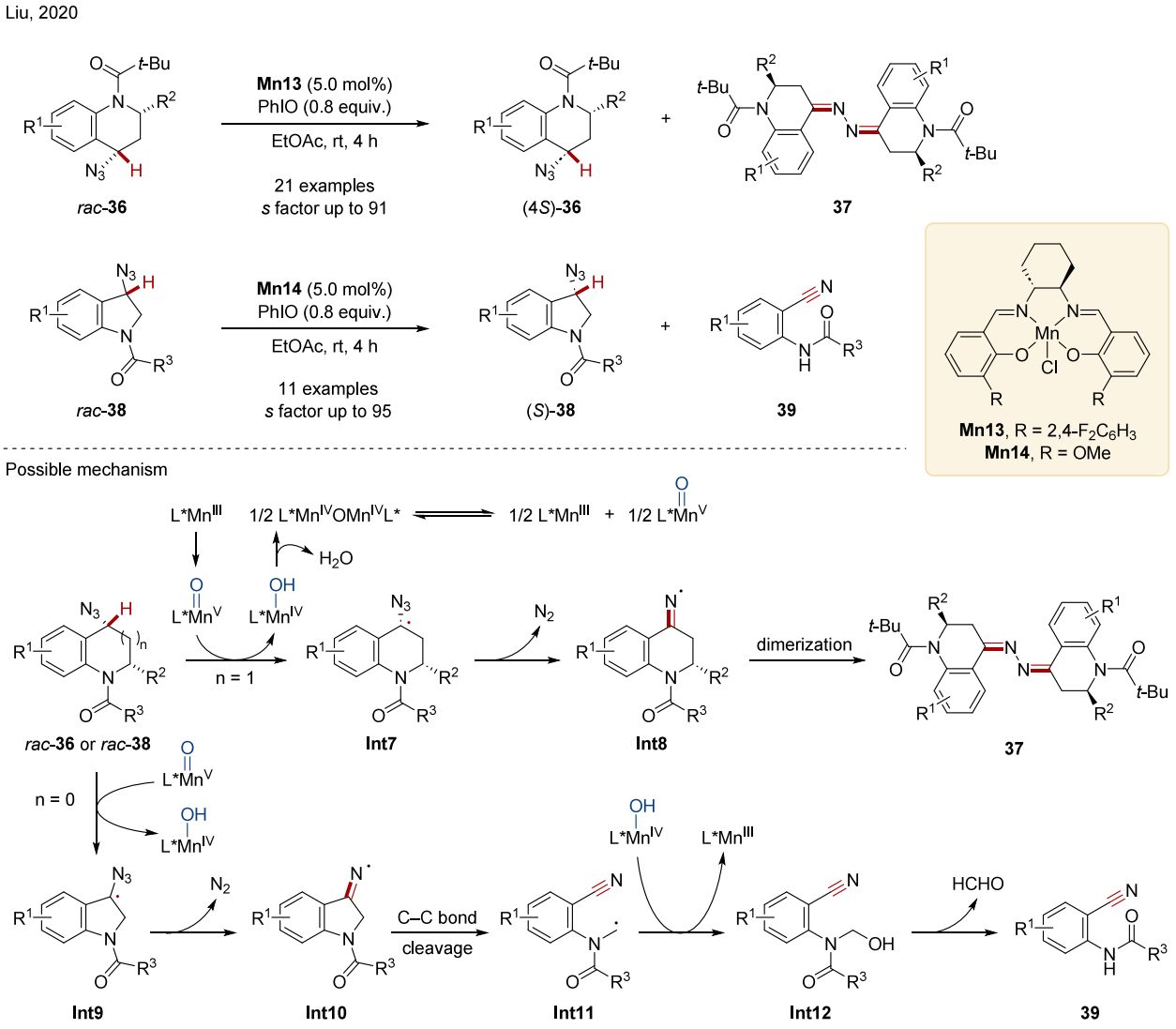

azide collapse, C−C bond cleavage, oxygen atom rebound, and hemiaminal decomposition. The excellent levels of enantiocontrol are attributed to the hydrogen-bond interactions, as revealed by DFT calculations.

3.1.4. Enantioselective C−H Azidation. In reactive chiral $(X)_2Mn(IV)$/Salen complexes, considerable distortion is observed when coordinated with certain axial ligands, such as N_3^- and $CF_3CH_2O^-$, tuning the chiral environment and amplifying stereoinduction in some cases.[65] In 2015, the Groves group employed the manganese Salen species for C−H azidation in the presence of aqueous sodium azide solution, and **Mn10** was found to be an efficient catalyst for asymmetric functionalization of celestolide **40**, preparing C−H azidated product **41** in 60% yield and 70% *ee* (Scheme 13a).[66] In order to improve the enantioselectivity, Liu and colleagues developed a novel binaphthyl-derived Mn(III)/Salen complex **Mn15** with bulky adamantyl substituents at both the 6- and 6′-positions of the binaphthyl motifs, allowing synthesis of various enantioenriched *N*-acyl azidoindolines **43** via tertiary or secondary benzylic C−H azidation (Scheme 13b).[67] Radical clock experiments and Hammett analysis revealed that C−H functionalization proceeds through a radical rebound pathway. In a control experiment oxidative kinetic resolution of racemic secondary azide was tested under standard conditions, a low conversion and poor stereoselectivity (s = 7.2) was obtained, implying that the excellent enantioselectivities of most examples originate from asymmetric C−H azidation. The origins of enantioinduction were probed by DFT calculations, which revealed an important stabilizing $\pi-\pi$ interaction between the phenyl group located on the axially chiral binaphthyl moiety and indoline framework in the favored transition state for the *R*-configured product.

3.2. Mn(III)/Porphyrin Catalysis

Metalloporphyrin catalysts have been extensively utilized in oxidation reactions as artificial analogues of CYP450.[68] Building on the pioneering work of Groves,[69] in 2012, the Simonneaux group illustrated enantioselective C−H hydroxylation with H_2O_2 as an oxidant (Scheme 14).[70] After introducing four sulfonate groups into the Halterman porphyrin[71] by means of their previously developed methods,[72] the chiral norbornane-appended manganese porphyrin **Mn16** was turned to be water-soluble, allowing benzylic C−H hydroxylation of compound **44** in phosphate buffered saline (PBS) solution in high yields (50−90%) and moderate enantioselectivities (32−57% *ee*), with the high-valent Mn(V)−oxo porphyrin proposed as a key intermediate in this transformation.[69,73] For 4-ethyltoluene,

https://doi.org/10.1021/acs.chemrev.6c00255
Chem. Rev. XXXX, XXX, XXX−XXX

Scheme 13. Mn(III)/Salen-Catalyzed Enantioselective C−H Azidation

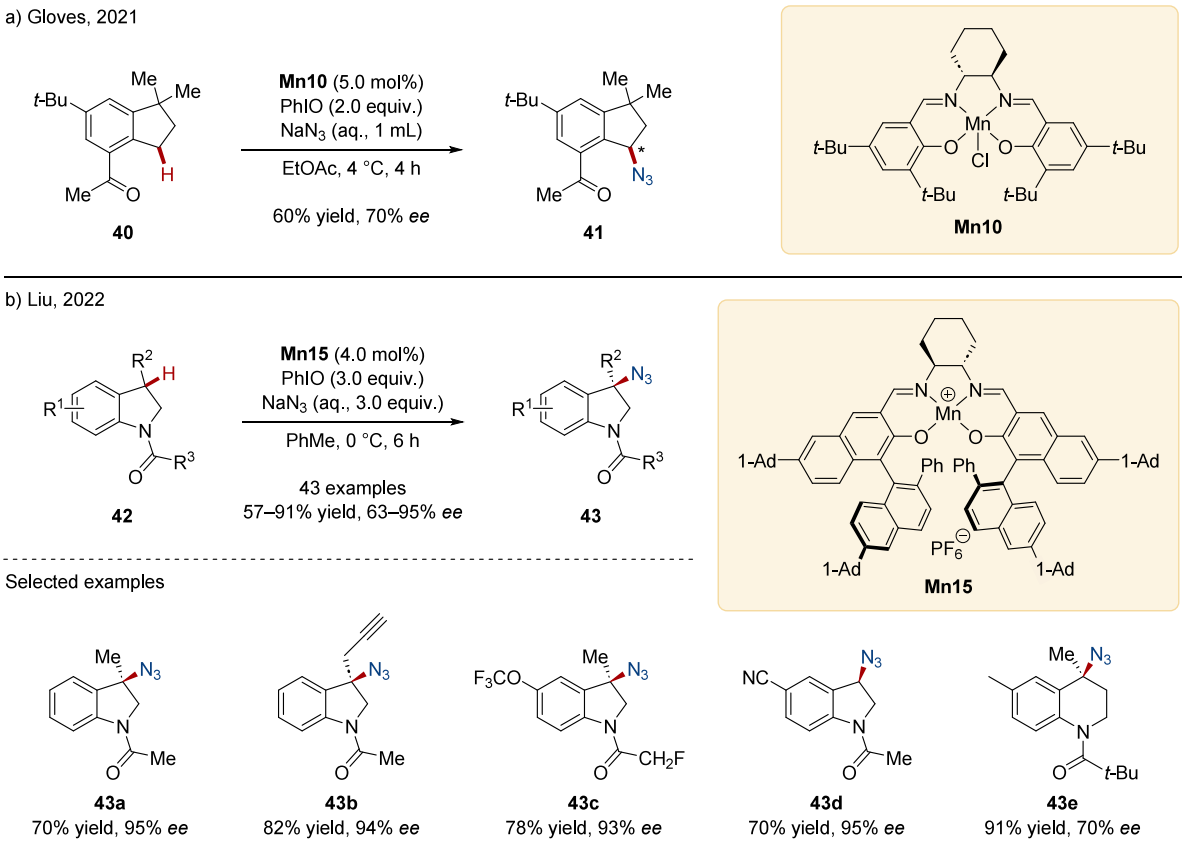

only secondary C−H oxidized product **45a** was observed, illustrating the higher reactivity of the secondary C−H bonds than the primary benzylic C−H bonds.

Building on their previous accomplishments in ruthenium-catalyzed enantioselective C=C epoxidation and C−H oxygenation modulated by molecular self-assembly between catalyst and substrates through hydrogen-bond interactions,[74] in 2018 Bach et al. demonstrated the asymmetric synthesis of 3,4-dihydroquinolones (DHQs) **47** with a manganese porphyrin complex **Mn17** featuring a similar remote recognition site (Scheme 15a).[75] Inspired by Crabtree's ground breaking contributions,[76] a distal lactam moiety was appended to the porphyrin backbone, allowing the 3,4-DHQ substrate **46** to dock through two N−H···O hydrogen bonds, positioning the target C−H bonds adjacent to the reactive Mn(V)−oxo species, as shown in **Int13**. In this way, one specific endocyclic pro-*S* C−H bond is hydroxylated in a highly stereoselective manner. In 2020, the same group then realized the site- and enantioselective benzylic C−H oxidation of alkyl-substituted quinolones **48** catalyzed by **Mn17** with the oxidant PhIO as the limiting reagent, furnishing the exocyclic methylene hydroxylated compounds **49** in moderate yields (21−62%) and outstanding enantioselectivity (80−98% *ee*). A unique mode of site-selectivity was exhibited in this asymmetric C−H hydroxylation, with functionalization taking place adjacent to the amide group even in substrates containing multiple potential reactive sites, such as in chiral quinolones **49c−f**. This patterns stands in contrast to the results with manganese(III) 5,10,15,20-tetrakis-(pentafluorophenyl)porphyrin (TPFPP) chloride, which lacks the molecular recognition site, as catalyst, as illustrated in **Int14** (Scheme 15b).[77] Moreover, the elegantly designed chiral porphyrin ligand was found to be effective in iron-catalyzed remote enantiodifferentiating epoxidation as well.[78]

3.3. Mn(II)/Aminopyridine Catalysis

3.3.1. Enantioselective C−H Hydroxylation. Encouraged by White's pioneering work on selective C−H oxidation in iron catalysis,[79] the tetradentate N4 ligand was identified as a multifunctional platform for biomimetic C−H functionalization, with the chirality at the metal atom (Λ and Δ) determined by the aminopyridine ligand. In 2017, Bryliakov and colleagues disclosed the asymmetric hydroxylation of benzylic C−H bonds with a precoordinated manganese aminopyridine catalyst **Mn18**, Boc-L-proline as an auxiliary ligand, and H_2O_2 as an eco-friendly oxidant (Scheme 16a).[80] Though the yields and enantioselectivities of the corresponding products were low, it is still worth mentioning that this transformation could be carried out under an extremely low loading of **Mn18** (0.05 mol%) with high turnover number (TON) up to 340, revealing **Mn18** to be a highly reactive catalyst for benzylic C−H oxidation. Improved results were then obtained by Costas, Bietti, and collaborators in 2,2,2-trifluoroethanol (TFE) at −35 °C[81] and by the Bryliakov group in 2,2-difluoroethanol (DFE) at −30 °C.[82] In these cases solvent suppresses further oxidation of the product by reversing the polarity through hydrogen-bonding interactions. Meanwhile, HFIP was another advantageous fluorinated alcohol solvent for this benzylic C−H oxidation.[83] In 2021, Gebbink and co-workers also developed an alternative chiral Mn(II)/aminopyridine catalyst **Mn19** for asymmetric benzylic C−H hydroxylation, affording secondary alcohols in moderate yield and enantioselectivity (Scheme 16b).[84]

For cyclic prochiral reactants, Sun and colleagues developed an enantioselective methylene C(sp^3)−H hydroxylation of 3-

https://doi.org/10.1021/acs.chemrev.6c00255
Chem. Rev. XXXX, XXX, XXX−XXX

Scheme 14. Mn(III)/Porphyrin-Catalyzed Enantioselective Benzylic C−H Hydroxylation

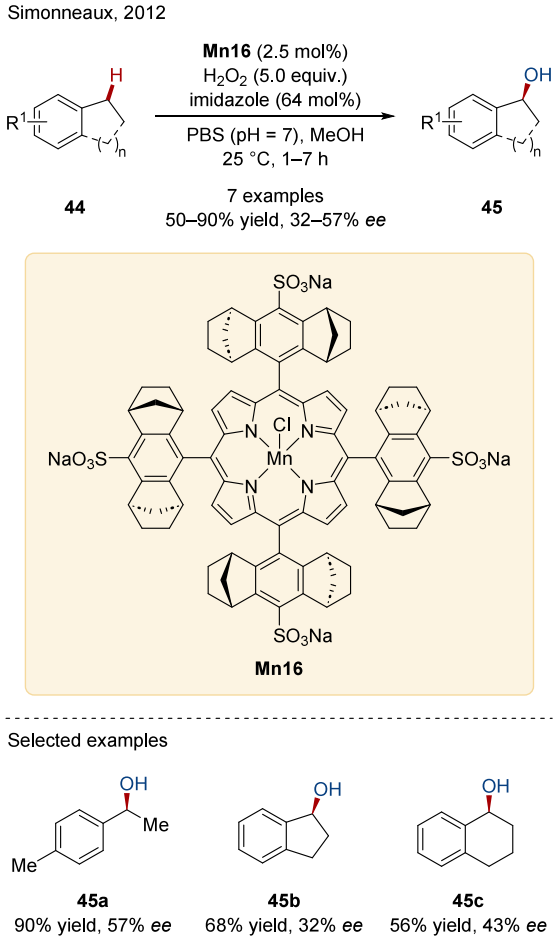

benzoylindans **52** with H_2O_2 assisted by 2,2-dimethylbutanoic acid (DMBA), constructing secondary alcohols **53** featuring two continuous stereocenters in a *cis*-configuration with moderate yields and good stereoselectivity (Scheme 17a).[85] Surprisingly, once the carbonyl group in substrate **52** was replaced with $-CH_2-$ or $-CH(OH)-$, the reactivity of these analogues significantly decreased, suggesting a probable intermolecular hydrogen-bonding interaction among the solvent TFE, the 3-benzoylindane substrate **52**, and a carboxylate ligand on the Mn(V)−oxo species, which may account for the good enantio- and diastereoselectivity. In 2023, an enantioselective tertiary C−H hydroxylation of trisubstituted cyclohexanes **54** was also reported by Costas, Bietti, Osuna et al. (Scheme 17b).[86] Catalyzed by the bulky TIPS-substituted complex **Mn21**, a broad range of products were generated in the presence of phthaloyl-L-*tert*-leucine, among which the (3*R*,5*R*)-3-hydroxy-3,5-dimethylcyclohexan-1-one could further be converted to diverse macrolides after Baeyer−Villiger oxidation and $LiAlH_4$ reduction.

3.3.2. Enantioselective C−H Oxygenation. In 2017, Costas, Bietti, and co-workers unveiled a site- and enantioselective methylene C−H oxidation of *N*-cyclohexylamides **56** catalyzed by manganese complex **Mn22** bearing a *trans*-(1*R*,2*R*)-diaminocyclohexane-derived linear tetraazadentate ligand with excess cyclopropyl carboxylic acid as additive (Scheme 18a).[87] The transformation formed diverse 3-substituted cyclohexanones **57** with moderate to excellent regio- and enantioselectivities (55−96% *ee*). Subsequently, the same authors recognized that, due to the torsional effects, the *cis*-1,4-, *trans*-1,3-, and *cis*-1,2-substituted diamino-cyclohexanes **58** could be site-selectively oxidized whereas the opposite diastereoisomers are unreactive under the same conditions. By leveraging this effect, the *cis*/*trans* mixture of 4-substituted 1-aminocyclohexanes could be converted to 4-alkylcyclohexanone **59** with H_2O_2 as oxidant and *rac*-**Mn23** as catalyst (Scheme 18b).[88] When the recovered *trans*-1,4-substrates were retreated with enantioenriched manganese catalyst **Mn23**, acetic acid, and hydrogen peroxide, several C3- or C2-oxygenated compounds were obtained with variable enantioselectivities (4−90% *ee*). Very recently, Costas, Bietti, Sigman, Call et al. performed predictive statistical modeling, which provided rationalized nonobvious enantioselective trends across these C(sp^3)−H oxidation, despite some of the mechanistic uncertainty.[89]

In 2018, Sun, Nam, and collaborators demonstrated a **Mn20**-catalyzed enantioselective benzylic C−H oxygenation of spirocyclic tetralones and indanones **61** for the construction of all-carbon quaternary stereocenters via a radical rebound mechanism. HAA of the methylene C−H bond of **61** was identified as the turnover-limiting step (Scheme 19a).[90] Assisted by DMBA, multifarious *spiro*-*β*,*β*′-diketones **62** bearing both electron-donating and -withdrawing substituents were obtained with good to excellent stereoselectivity (67−98% *ee*). In the following year, the same group also realized the asymmetric C−H oxygenation of nitrogen-containing spirocyclic molecules **63**, yielding several *spiro*-oxindoles **64** in a similar manner (Scheme 19b).[91] Unexpectedly, when the 2,3-dihydro-quinolin-4(1*H*)-one-based compound was examined under the standard conditions, a considerable amount of corresponding hydroxylated product was isolated in 26% yield. With slight modification of conditions, a few *spiro*-dihydroquinolinones **65** featuring two consecutive *C*-stereocenters was then synthesized with good to excellent enantio- and diastereoselectivities (up to 99% *ee* and >19:1 *dr*).

3.3.3. Enantioselective C−H Acyloxylation. In previous studies on enantioselective C−H hydroxylation and oxygenation catalyzed by bioinspired nonheme manganese(II) complexes with linear tetraazadentate aminopyridine ligands, an external carboxylic acid was usually used as a vital additive to facilitate the cleavage of H_2O_2 during the oxidation process en route to generation of the reactive electrophilic Mn(V)−oxo intermediate.[92] In 2020, Costas, Bietti, and co-workers envisioned that the Mn-bound carboxylate could serve as a directing group (DG) to fix the substrate orientation and rigidify the transition state and based on this hypothesis developed highly enantioselective intramolecular *γ*-C−H lactonization of adamantaneacetic acids **66** with **Mn24** as catalyst in TFE, a strong hydrogen-bond donor (HBD) solvent (Scheme 20a).[93] Intriguingly, for substrates bearing 3′-alkyl or -aryl substituents, which are non-hydrogen bond acceptor (non-HBA) groups, proximal lactones **67** were obtained as the major positionl isomers catalyzed by **Mn24**, while the distal C−H lactonized products **68** or **69** were mainly generated with **Mn24** or **Mn25** when the 3′-position of the adamantyl group was substituted by HBA groups, such as ether, ester, amide, halogen and so on. In 2023, the same group demonstrated another enantioselective lactonization of primary and secondary *γ*-C−H bonds with up to >99% *ee* (Scheme 20b).[94] Remarkably, these bioinspired Mn(II)-catalyzed stereoselective intramolecular *γ*-C−H acyloxylation could be employed as a powerful tool in the synthesis of artificial *α*-amino acids and natural products.[95]

https://doi.org/10.1021/acs.chemrev.6c00255
Chem. Rev. XXXX, XXX, XXX−XXX

Scheme 15. Mn(III)/Porphyrin-Catalyzed Enantioselective C−H Hydroxylation Assisted by H-Bond Interactions

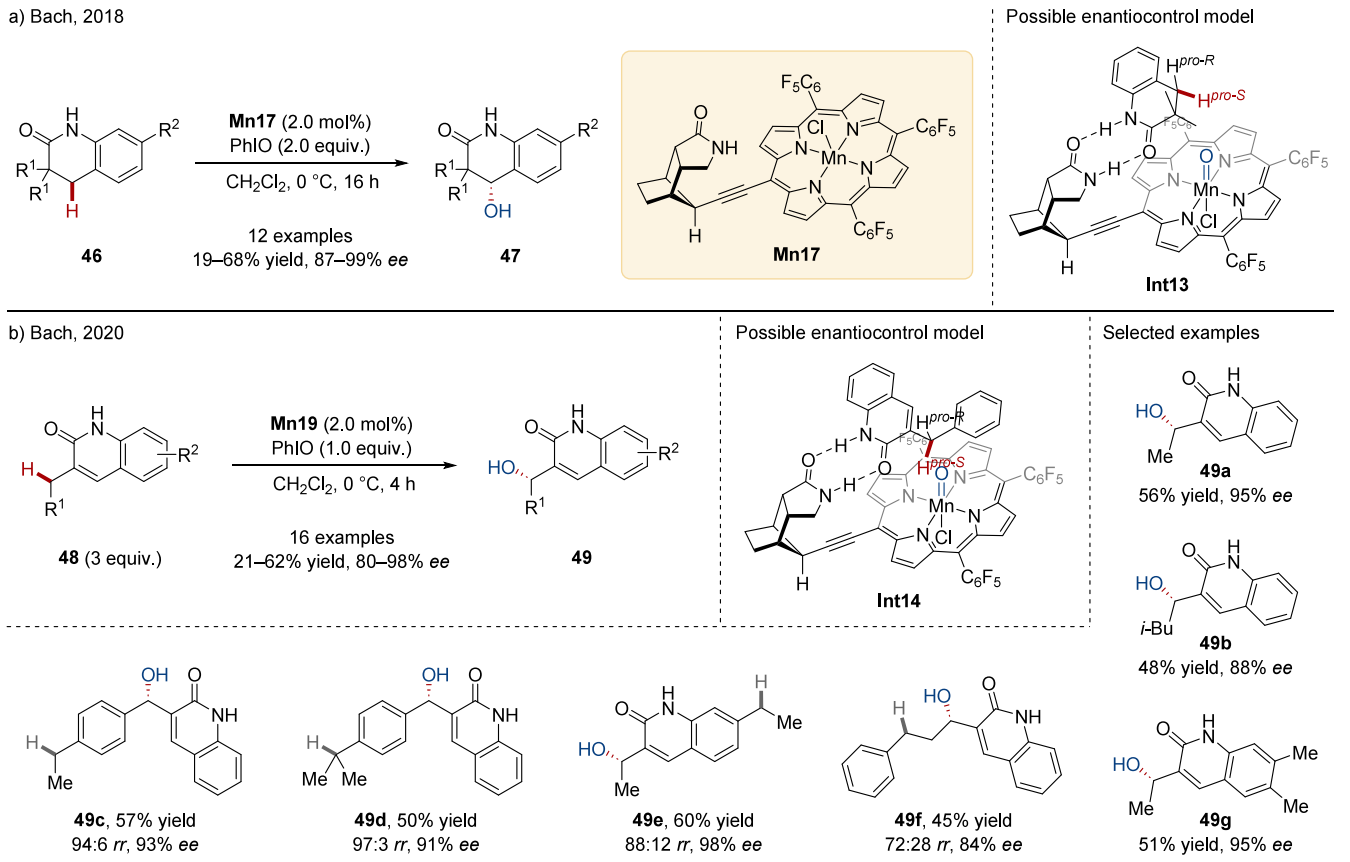

4. IRON CATALYSIS

Iron is the fourth most abundant element in the earth's crust, constituting approximately 5% of its mass, which far exceeds that of any other transition metal.[43] Owing to the widespread presence of iron as a reactive center of essential proteins involved in vital biological processes *in vivo*, such as heme-containing cytochrome P450, several iron-based enzymatic redox systems have evolved the ability to cleave inert C−H bonds under selective pressure, although most chiral hydroxylated products are formed with low enantiomeric excess.[47a,96] Benefiting from its low cost, low toxicity,[97] and diverse reactivity,[14b,16b,98] Fe-catalyzed C−H functionalization has attracted increasing attention in organic synthesis,[15a,b,d,99] particularly via the radical rebound pathway.[20,100] Consequently, a series of bioinspired enantioselective C−H hydroxylation, amination, amidation, and dehydrogenation reactions have been accomplished with chiral porphyrin, Salen, and pyridine-based ligands or stereogenic-at-iron catalysts by Groves, Simonneaux, Chattopadhyay, Meggers, Che, Liu, et al.[47c,e,f,101] Recently, with a nucleophilic low-valent iron species formed under reducing reaction conditions,[16b,98c,99a] several examples of Fe(II)-catalyzed inner-sphere enantioselective C−H functionalization enabled by chiral *N*-heterocyclic carbene (NHC) ligands have also been achieved.

4.1. Fe(III)/Porphyrin Catalysis

4.1.1. Enantioselective C−H Hydroxylation. Spurred on by their earlier mechanistic investigations,[102] from 1989 to 1990 the Groves group described an enantioselective benzylic C−H hydroxylation with iodosobenzene as the oxidant (Scheme 21a).[103] In order to emulate the catalytic active site of cytochrome P450, heme, the authors developed a vaulted binaphthyl porphyrin-chelated chiral iron catalyst **Fe1** for this stereoselective transformation, constructing a few secondary alcohols **73** in modest to good enantiomeric excess (40−78% *ee*) through a radical rebound mechanism. Moreover, this novel iron−porphyrin catalyst **Fe1** was also suitable for enantioselective epoxidation of substituted styrenes.[103b] Notably, the identical concept of chiral porphyrin ligand design was then found to be productive in Ru/porphyrin-catalyzed benzylic tertiary C−H hydroxylation by Gross and co-workers as well.[104] In 2012, employing their previously developed sulfonate-containing Halterman porphyrin as a precoordinated ligand in chiral iron catalyst **Fe2**,[70−72] Simonneaux and colleagues realized another enantioselective C−H hydroxylation of alkyl aromatics **72** with iodosobenzene diacetate in the presence of imidazole under argon (Scheme 21b).[105]

4.1.2. Enantioselective C−H Amination. In 2020, the Chattopadhyay group achieved the iron(III)/porphyrin-catalyzed intramolecular denitrogenative aliphatic C−H amination of 1,2,3,4-tetrazoles **74**. When the chiral porphyrin iron complex **Fe3** was utilized, the corresponding product **75** could be acquired with moderate enantioselectivity (95%, 46% *ee*) as a single example (Scheme 22a).[106] Building on this early work, in 2023, Che, Liu, Dang, and collaborators illustrated a highly enantioselective intramolecular C−H amination of azides **76** under the irradiation of 410 nm visible light (Scheme 22b).[107] When (*S*,*R*)-cmcporFeCl **Fe4** was used, annulated compounds **77** were obtained in up to 99% yield and 90% *ee*. The stereoselectivity could be reversed with another chiral iron(III)/porphyrin catalyst **Fe5**. Arylsulfonyl azides were also tolerated in this transformation (34 examples, 0−99% yield, 24−93% *ee*). As

https://doi.org/10.1021/acs.chemrev.6c00255
Chem. Rev. XXXX, XXX, XXX−XXX

Scheme 16. Mn(II)/Aminopyridine-Catalyzed Enantioselective Benzylic C−H Hydroxylation

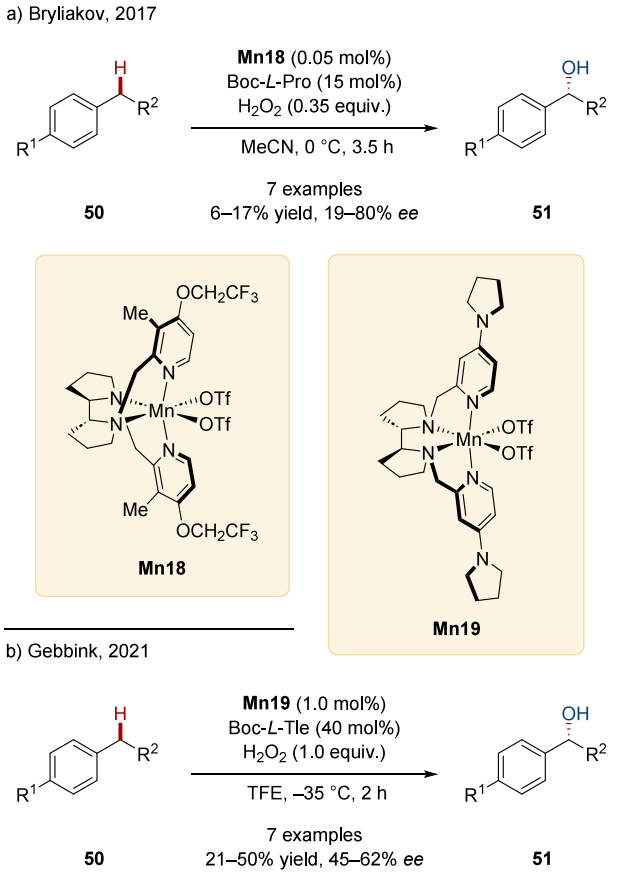

Scheme 17. Mn(II)/Aminopyridine-Catalyzed C−H Oxidative Desymmetrization

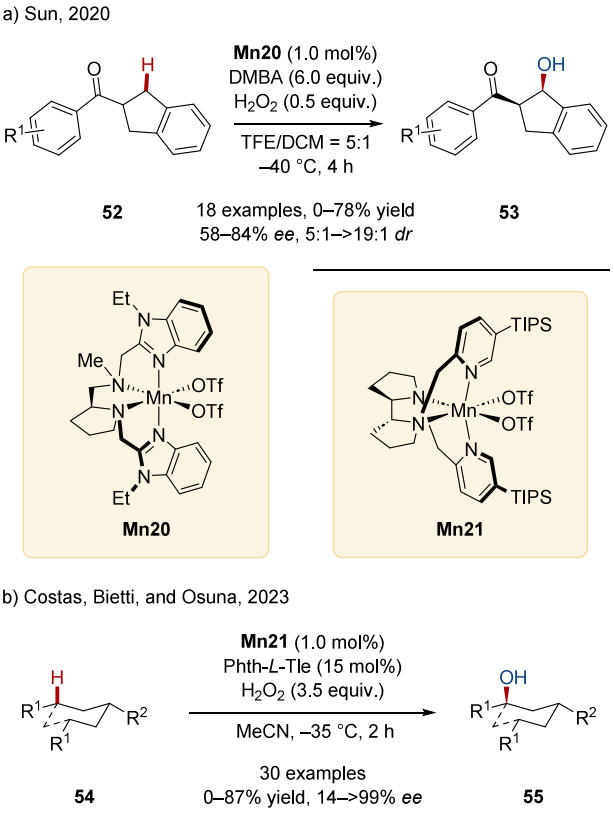

revealed by DFT calculations, an iron−nitrene intermediate in the quartet state is generated under photochemical conditions, which cleaves the target C−H bond through an HAT process. The final cyclized products **77** are then formed through asymmetric radical rebound amination.

4.2. Fe(III)/Salan Catalysis

In 2019, Liu and co-workers discovered an enantioselective synthesis of 5,6-dihydrophenanthridines and 1,2-dihydroquinolines **79** (Scheme 23).[108] With chelation of a strongly electron-donating chiral *N*,*N*′-bis(2-hydroxybenzyl)ethylenediamine (Salan) ligand, the imine-hydrogenated form of the corresponding Salen ligand[109], the dimeric iron(III) complexes **Fe6** and **Fe7** were identified as efficient catalysts for aerobic C−H dehydrogenative KR of amines *rac*-**78** in the assistance of 4-methoxy-1-naphthol, providing diverse chiral cyclic secondary amines **79** with *s* factor up to 91. In contrast, no enantiocontrol was observed when the monomeric Fe(III)/Salan species was tested as a catalyst. Control experiments were consistent with a Fe(III)/Fe(IV) redox cycle,[110] as opposed to a Fe(III)/Fe(II) cycle.[111] The activated binuclear iron(III) catalyst **Fe8** was initially formed *in situ* with the replacement of μ_2−OH by a 1-naphthoxy ligand, followed by oxidation with molecular oxygen. A single-electron transfer (SET) process then takes place between the obtained iron radical cation **Int15** and the configurationally matched reactants (*S*)-**78**, generating iron(III)-bound amine radical cation **Int16**. Hydrogen atom and proton abstraction with superoxide radical eventually gives dehydrogenated products **79**, allowing for recovery of the unreacted *R*-configured enantioenriched amide **78**.

4.3. Fe(II)/Pyridine-Based Complex Catalysis

Stimulated by the progresses on nonheme Fe-based enzyme mimics catalyzing C−H oxidation[79,99e,112] and building on their previous achievements in asymmetric chiral-at-metal iridium[113] and ruthenium catalysis,[114] in 2022 the Meggers group demonstrated a convenient approach to chiral α-amino acids **81** from presynthesized Troc-azanyl esters **80** via stereocontrolled 1,3-nitrogen migration with good regio- and enantioselectivity (Scheme 24a).[115] Subsequently, the same group unveiled a similar stereoselective radical rebound amidation of secondary and tertiary C−H bonds with *N*-Boc-protected azanyl ester substrates **80** prepared *in situ* (Scheme 24b).[116] Both desymmetrization and dynamic kinetic resolution (DKR) were feasible with this protocol, producing versatile linear and α-branched α-amino acids **82** in modest to excellent yields and enantioselectivities (41−98% yield, 12−92% *ee*). Meanwhile, when the TIPS-substituted tetraazadentate ligated Fe(II) species **Fe10** was employed as a catalyst, various chiral 2-imidazolidinones **84**, a class of prevalent bioactive structural motifs, were obtained from prochiral or racemic *N*-aroyloxyureas **83** via 1,5-HAT in an enantioselective or enantioconvergent manner (Scheme 24c).[117] This transformation was also realized in 2024 by the Cen group in low to moderate enantioselectivities with amino acid-derived chiral phenanthroline ligand **L1** (Scheme 24d).[118] Very recently, Schomaker, Liu, and colleagues disclosed an asymmetric benzylic C−H sulfamidation of sulfamate esters **87** via 1,5-nitrene transfer with PyBOX ligands **L2** or **L3** (Scheme 24e).[119] Experimental and computational mechanistic studies revealed that both the 1,6-HAT (**TS5**) and radical rebound amidation (**TS6**) processes are stereoselective, with the latter one acting as the enantiodetermining step.

https://doi.org/10.1021/acs.chemrev.6c00255
Chem. Rev. XXXX, XXX, XXX−XXX

Scheme 18. Mn(II)/Aminopyridine-Catalyzed Enantioselective C−H Oxygenation of Cyclohexane

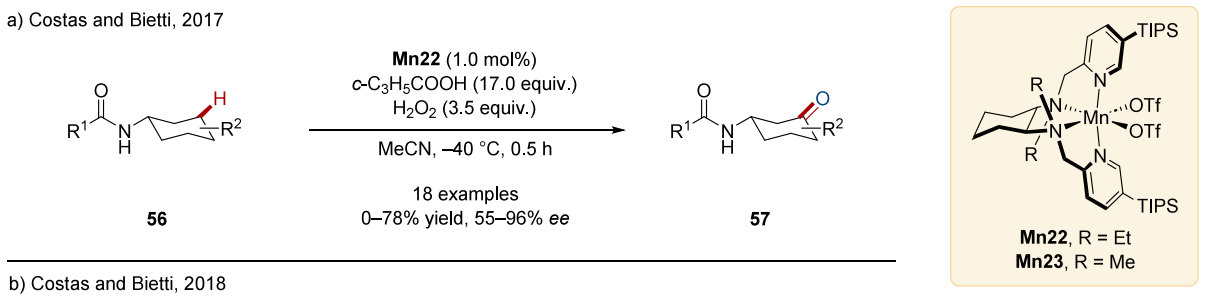

Scheme 19. Mn(II)/Aminopyridine-Catalyzed Enantioselective C−H Oxygenation for the Construction of All-Carbon Quaternary Stereocenters

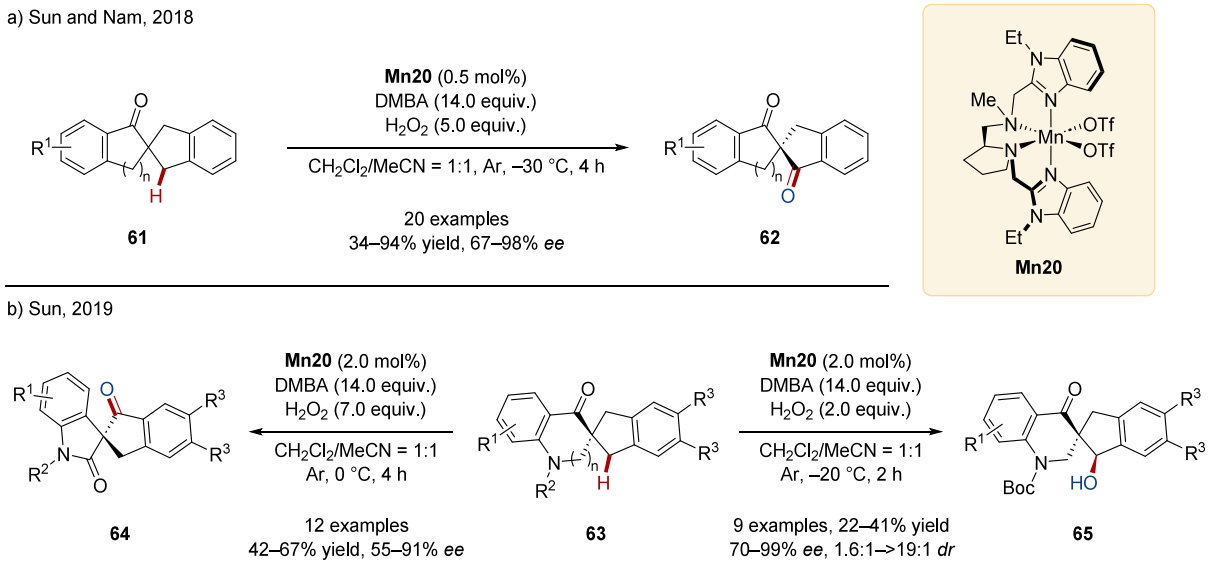

Beyond intramolecular functionalization, in 2023, the more challenging regio- and enantioselective intermolecular C−H amidation was successfully achieved after minor adjustments to original reaction conditions by Meggers and co-workers (Scheme 25).[120] α-Aryl amino acids were obtained in generally higher yields than α-alkyl amino acids (**91a** versus **91b**), and α,α-disubstituted carboxylic acids **89** were also compatible in this transformation. Mechanistic experiments suggested an irreversible stereoablative process, likely C−C bond rotation of long-lived diradical intermediate formed from HAT within the coordination sphere of the metal, prior to enantiodetermining C−N bond formation.

4.4. Fe(II)/NHC Catalysis

In contrast to outer-sphere radical rebound C−H functionalization, iron-catalyzed asymmetric C−H activation proceeding through an inner-sphere mechanism has developed at a much slower pace, due in part to the lack of effective chiral ligands.[15a−c] In their 2016 study on low-valent Fe-catalyzed C−H allylation assisted by a triazole-based bidentate auxiliary, the Ackermann group detected a low but reproducible *ee* value of 7% with chiral bisphosphine ligand (*S,S*)-DIPAMP.[121] Soon after, a slightly improved enantiomeric excess of 46% *ee* was obtained in the arylation of *N*-(quinolin-8-yl) ferrocenoyl carboxylic amide with (*R,R*)-bis(diphenylphosphino)butane by Butenschön et al., with the C−H cleavage identified as the enantiodetermining step.[122]

Building on these fundamental reports, in 2017, Ackermann and collaborators disclosed a highly enantioselective imine-directed C−H alkylation of (aza)indoles **92** with terminal olefins (vinyl ferrocene or arylethylenes) **93** (Scheme 26a).[123] Based on the rich history of chiral NHC ligands in asymmetric catalysis,[124] the authors designed a novel *meta*-1-Ad-decorated chiral NHC ligand **L4** for this asymmetric transformation informed by Yoshikai's nonstereoselective transformation.[125] A broad array of aldehyde products **94** (obtained following hydrolytic workup) were prepared featuring both electron-donating and -withdrawing groups. With azaindole substrates the non-hydrolyzed imine products could be isolated directly. Meanwhile, when the standard olefin, vinylferrocene, was exchanged

https://doi.org/10.1021/acs.chemrev.6c00255
Chem. Rev. XXXX, XXX, XXX−XXX

Scheme 20. Mn(II)/Aminopyridine-Catalyzed Enantioselective C−H Lactonization

a) Costas and Bietti, 2020

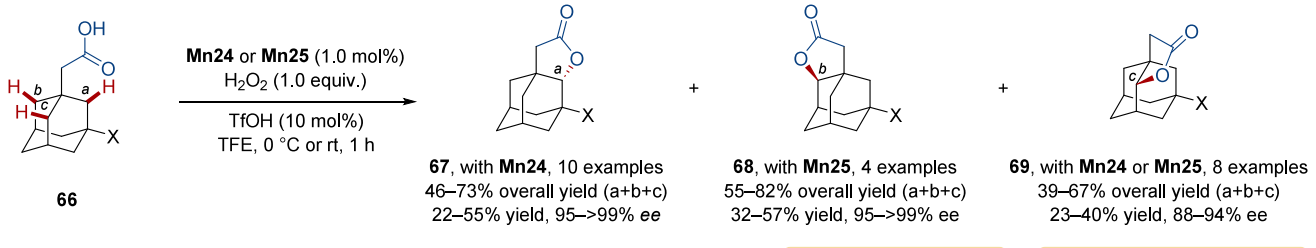

b) Costas, Bietti, and Call, 2023

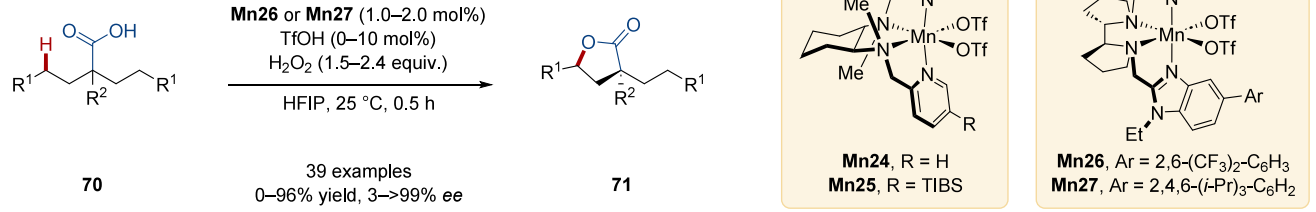

Scheme 21. Fe(III)/Porphyrin-Catalyzed Enantioselective C−H Hydroxylation

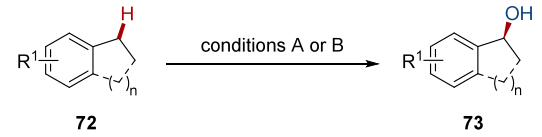

a) Groves, 1989 & 1990 conditions A: **Fe1** (0.1 mol%) PhIO (0.1 equiv.) CH_2Cl_2, 0 °C, 1 h

7 examples
19–47% yield
40–78% *ee*

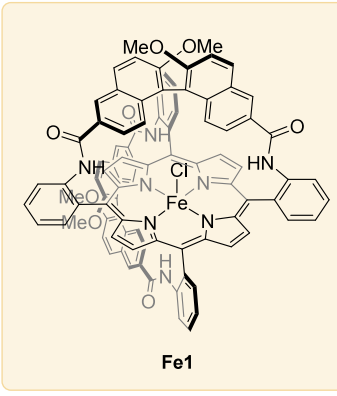

b) Simonneaux, 2012 conditions B: **Fe2** (0.1 mol%) imidazole (1.0 mol%) $PhI(OAc)_2$ (0.1 equiv.) CH_3OH/H_2O = 5:1 Ar, rt, 1 h

8 examples
20–82% yield
7–78% *ee*

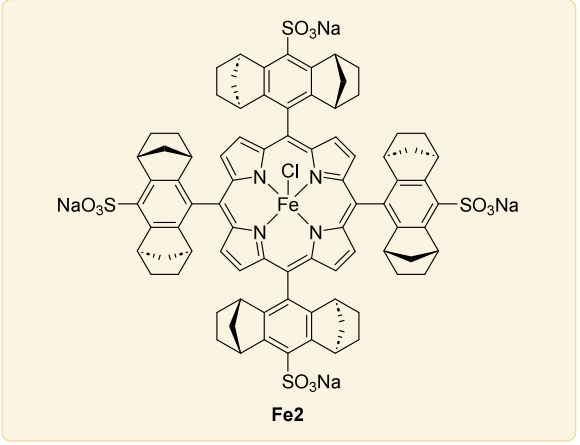

with arylethylenes **93**, the yields of product **94** increased significantly, albeit with attenuated enantioselectivities. Through mechanistic investigations,[126] a plausible catalytic cycle was proposed, involving an irreversible coordination-induced stereoselective migratory insertion (**Int18** to **Int19**) and a ligand-to-ligand hydrogen transfer (LLHT)-type C−H activation (**TS7**).[127]

In 2024, Ackermann, Wencel-Delord, Neidig, and co-workers demonstrated the establishment of both C−N axially and *C*-centrally chiral molecules **97** via Fe/NHC-catalyzed enantio- and diastereoselective C−H alkylation (Scheme 26b).[128] Similar to their previous work, the C−H activation was hypothesized to proceed via an LLHT process (**TS8**) rather than classic C−H bond oxidative addition. LLHT establishes the *C*-stereogenic center, whereas the C−N axis is set during ultimate atroposelective C−C reductive elimination step.

5. COBALT CATALYSIS

Cobalt is an essential trace element in living organisms, primarily found in vitamin B12 (cobalamin) and various enzymes,[129] and it also plays an important role in organic synthesis, promoting a range of useful transformations, including hydroformylation, cycloaddition, cross-coupling, and Pauson−Khand reaction, among others.[14b,130] Since the initial exploration in $Co_2(CO)_8$-catalyzed C−H activation by Murahashi in the 1950s,[131] numerous Co-mediated C−H functionalizations have been realized over the past 70 years.[15d,132] Through the development of innovative chiral ligands, the past decade has witnessed explosive growth in cobalt-catalyzed enantioselective C−H activation, encompassing low-valent Co(I)/phosphine and Co(I)/NHC catalysis, high-valent pseudotetrahedral Cp^XCo(III) and Cp*Co(III)/CCA catalysis, high-valent octahedral Co(II)/CPA and Co(II)/Salox catalysis, and Co(II)/porphyrin metalloradical catalysis (MRC). Among the 3d metal catalysts, cobalt stands out for having the greatest number of catalytic asymmetric C−H functionalization examples and the most diverse underlying mechanisms.[13e,i,k,17d,133]

https://doi.org/10.1021/acs.chemrev.6c00255
Chem. Rev. XXXX, XXX, XXX−XXX

Scheme 22. Fe(III)/Porphyrin-Catalyzed Enantioselective C−H Amination

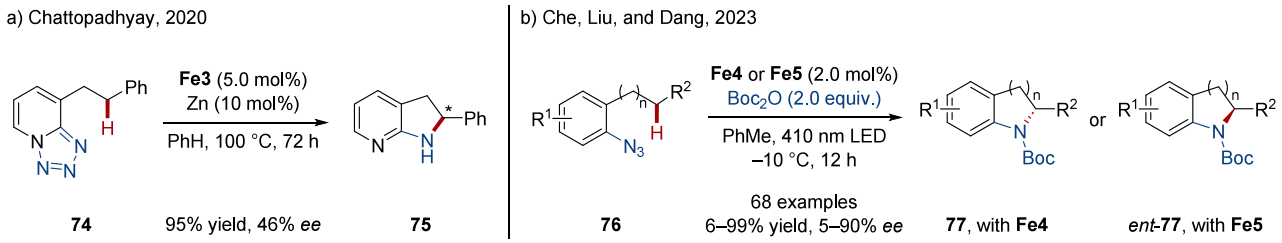

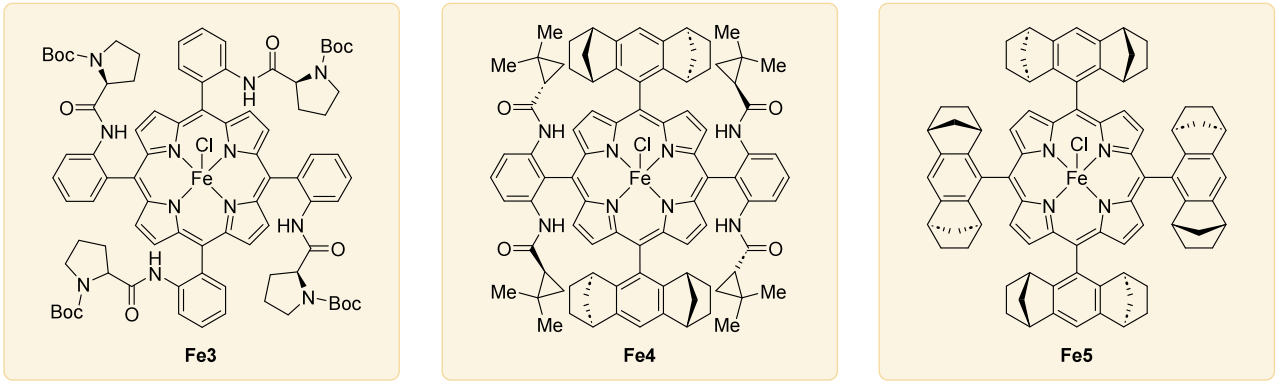

Scheme 23. Fe(III)/Salan-Catalyzed Enantioselective C−H Dehydrogenative Kinetic Resolution

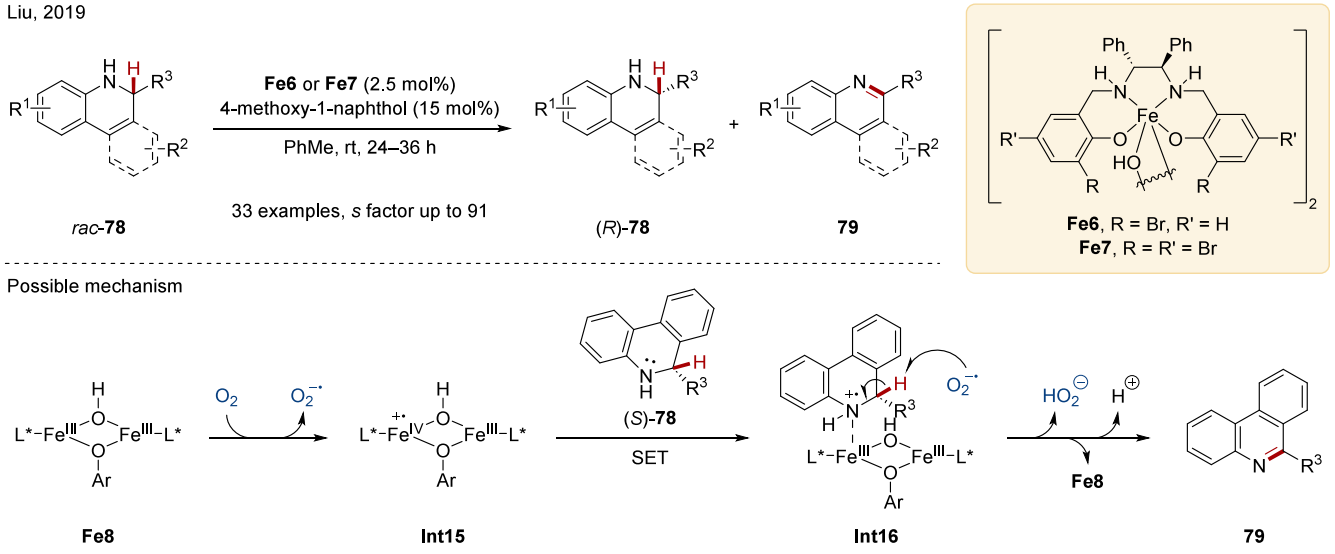

5.1. Co(I)/Phosphine Catalysis

5.1.1. Asymmetric Formyl C−H Annulation. Inspired by progress in Rh-catalyzed enantioselective hydroacylation[134] and their own lab's previous work in cobalt catalysis,[132a,135] in 2014 the Yoshikai group demonstrated a cobalt-catalyzed enantioselective formyl C−H oxidative activation/intramolecular annulation with chiral bisphosphine ligands (*R*,*R*)-BDPP **L6** or (*R*,*R*)-Ph-BPE **L7** (Scheme 27a).[136] With the low-valent Co(I) species generated *in situ* from simple cobalt chloride or bromide salts and a heterogeneous metallic reductant, a small collection of indanones **99** and a broad range of phthalides **100** were formed in good to excellent enantioselectivities (82−98% *ee*), with the narrower scope in the former case attributed to the sensitivity of the reaction to substituents on the arene. Overall, the transformation represents convenient means of accessing to enantioenriched carbonyl compounds. Deuterium-labeling experiments showed complete intramolecular H atom transfer without any H/D crossover during the hydroacylation process, excluding a Tishchenko-type mechanism involving a freely diffusing cobalt−hydride species.[137]

With minor modifications of reaction conditions, in 2017 the same group then disclosed the enantio- and diastereoselective construction of indanones **102** containing two proximal C-stereocenters from *E*/*Z* mixtures of 2-alkenylbenzaldehyde substrates **101** (Scheme 27b).[138] Based on the mechanistic experiments and previous reports,[139] the authors speculated that only the reductive elimination process c from **Int21** as well as c′ are irreversible, with the good to excellent diastereoselectivity attributed to epimerization of *cis*-**102** to *trans*-**102** at the α-position of carbonyl group. In the same year, Dong and collaborators also achieved an efficient enantioselective synthesis of chiral cyclobutanones **104** with both α-quaternary and -tertiary carbon stereocenters via desymmetrization of **103** with an *ent*-**L6**-precoordinated cobalt catalyst (Scheme 27c).[140]

https://doi.org/10.1021/acs.chemrev.6c00255
Chem. Rev. XXXX, XXX, XXX−XXX

Scheme 24. Enantioselective Intramolecular C−H Amidation Catalyzed by Fe(II)/Pyridine-Based Complexes

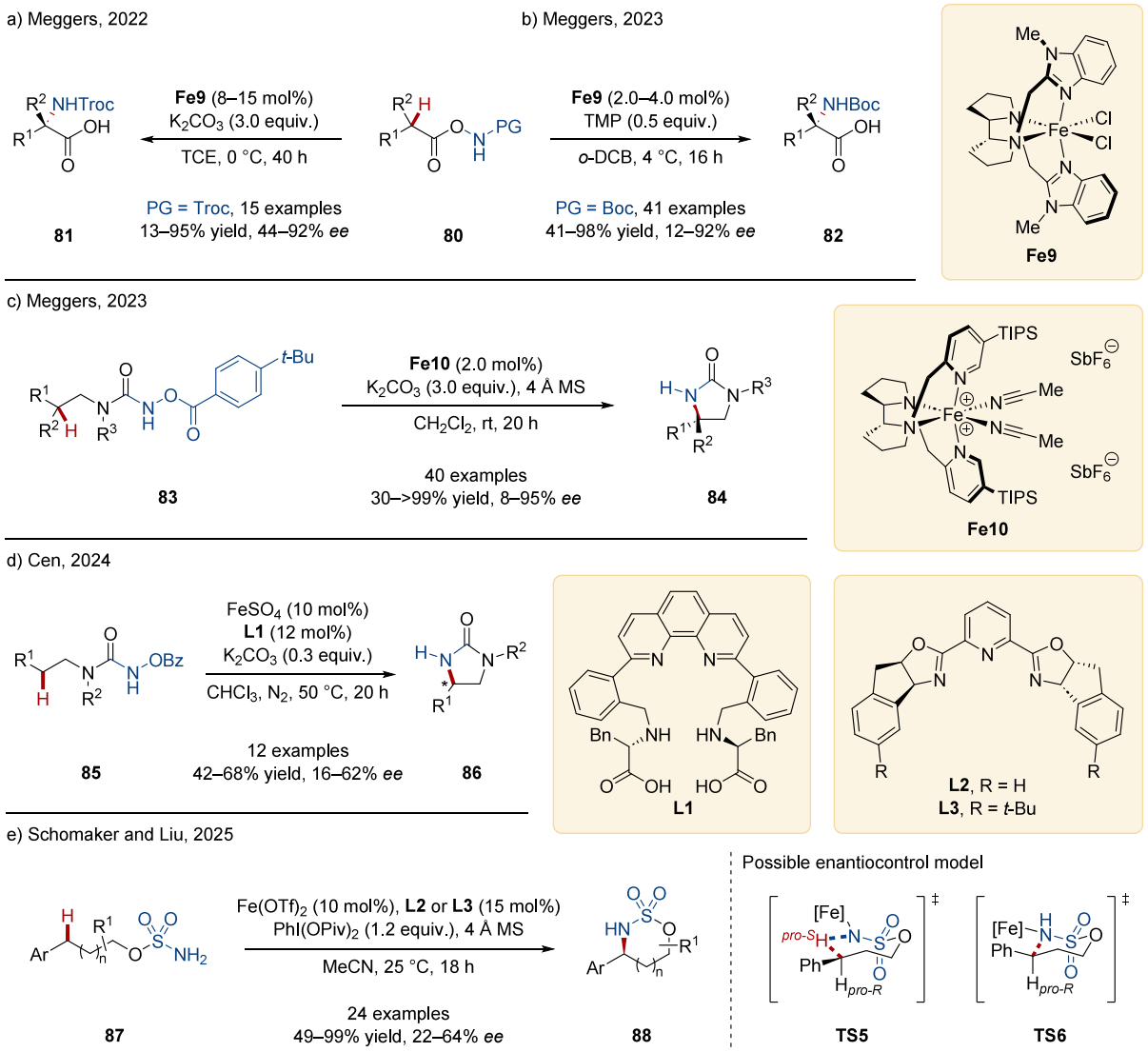

Scheme 25. Fe(II)/Aminopyridine-Catalyzed Enantioselective Intermolecular C−H Amidation

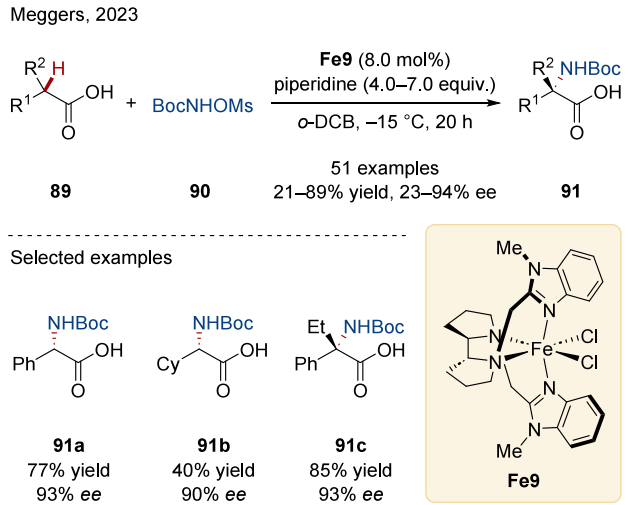

In 2020, the Lautens group accomplished the cobalt-catalyzed enantioselective intermolecular hydroacylation of 1,6-enynes **107** with (*S*,*S*)-BDPP ligand *ent*-**L6**, affording diverse ketones **108** via a formyl C−H activation/cyclization cascade with up to 98% *ee* (Scheme 28).[141] The deuterium-labeling and kinetic isotope effect (KIE) experiments indicated that the H atom of the formyl group was transferred entirely to the newly formed methyl group in **108**, ruling out an LLHT mechanism.[127,142] Meanwhile, C−H bond cleavage is not the rate-determining step, which was consistent with Cheng's report.[143] In analogy to previous results,[140,143,144] the authors proposed a catalytic cycle with multiple plausible pathways from reactive chiral cationic cobalt(I) complex **Int23**, as mechanistic investigations could not completely disambiguate whether the reaction is initiated through C−H oxidative addition or oxidative cyclization.

5.1.2. Asymmetric Indole C−H Alkylation. In 2015, the Yoshikai group disclosed an enantioselective C−H alkylation at the C2-positon of *N*-Boc-protected indoles **109** with styrenes catalyzed by Co(acac)$_3$ and chiral phosphoramidite **L8** (Scheme 29).[145] Branched products **110** were selectively obtained in moderate to good yields and enantioselectivities with the imine directing group hydrolyzed *in situ* upon workup. As revealed by further mechanistic investigations, C−H oxidative addition and migratory insertion are reversible in the putative catalytic cycle,

https://doi.org/10.1021/acs.chemrev.6c00255
Chem. Rev. XXXX, XXX, XXX−XXX

Scheme 26. Fe(II)/NHC−Catalyzed Enantio- and Diastereoselective C−H Alkylation

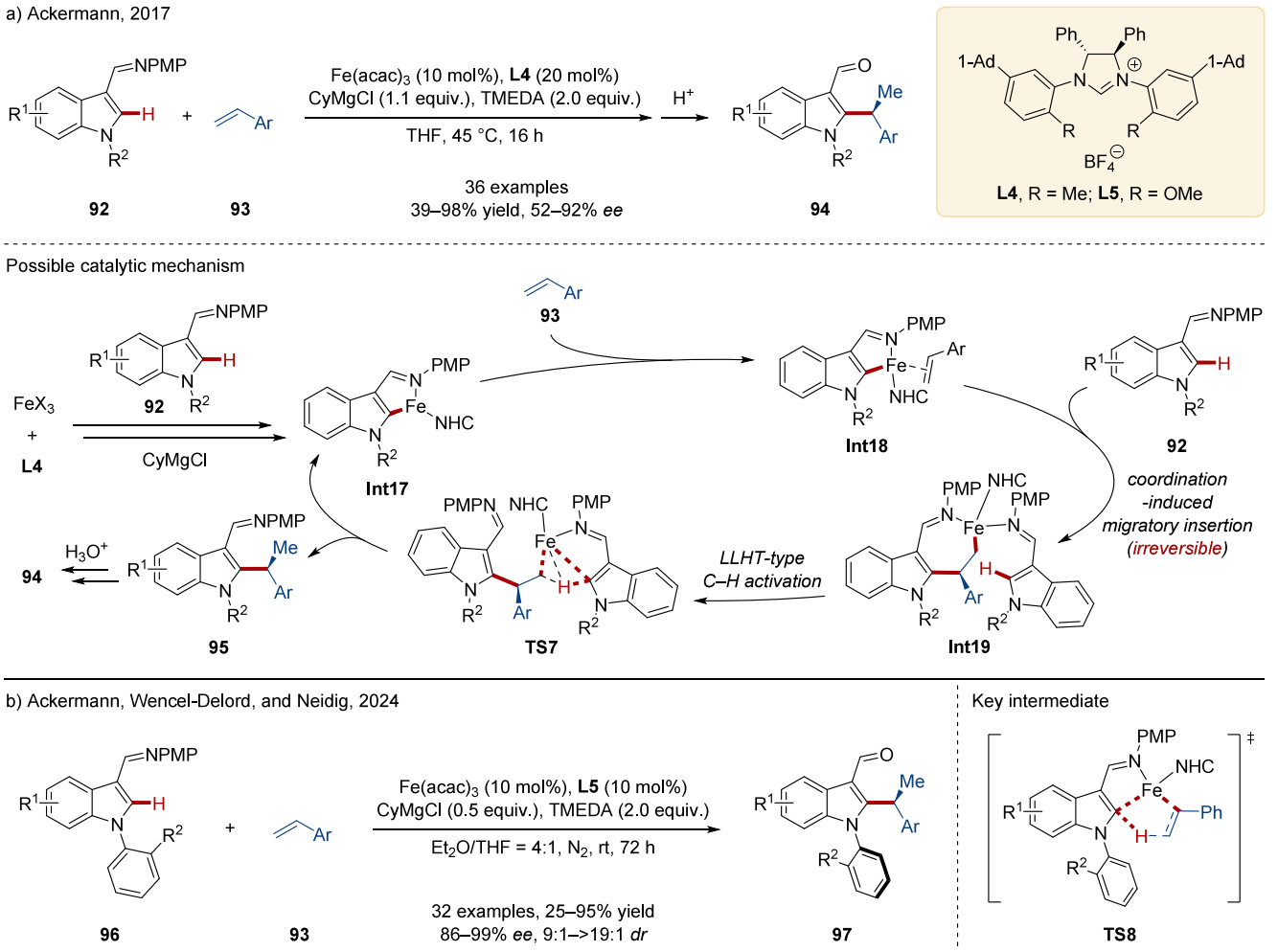

with the regio- and enantioselectivity determined in both the migratory insertion and reductive elimination steps.

In 2020, Lautens and co-workers combined Co-catalyzed pyridyl-directed C−H activation with hydroarylative cyclization of 1,6-enynes **107**, establishing an enantioselective C2-functionalization of various indoles **111** in excellent regio- and stereoselectivity with the bisphosphine (*R*,*R*)-QuinoxP* **L9** as ligand (Scheme 30).[146] The deuterium labeling and crossover experiments also exclude an LLHT mechanism, which is frequently invoked in cobalt-catalyzed C−H activation, for the C−H bond cleavage process.[127,142] The chelating effect between the enyne substrates and cobalt catalyst seems to be important, as no desired products **112** were observed when either the alkynyl or alkenyl group was removed from the enyne. Similar to findings from another study performed by the same group (Scheme 28),[141] the authors concluded that either oxidative cyclization or C−H oxidative addition pathways could potentially rationalize the available mechanistic data.

5.1.3. Enantioselective Allylic C−H Functionalization. Unlike enantioselective allylic C−H functionalization with noble metal catalysts, such as Pd or Rh,[147] allyl functionalization with earth-abundant metal catalysts remains underdeveloped. In 2017, Sato and colleagues reported promising proof-of-concept data, demonstrating 25% yield and 81% *ee* in the coupling between 1-allyl-3-methoxybenzene and acetone with Co(acac)$_2$/(*R*)-difluorphos/AlMe$_3$ catalysis in DMF at 60 °C.[148] Encouraged by this finding, in 2021, the Meng group then achieved the asymmetric allylic C−H activation/nucleophilic addition to aldehydes and α-ketoesters with improved enantio- and diastereoselectivities (up to 96% *ee* and >19:1 *dr*), furnishing a broad range (86 examples) of chiral homoallylic alcohols **114** or **115** with Co(acac)$_2$/(*S*,*S*)-Et-BPE as the catalytic system (Scheme 31).[149] Meng's method offered high stereo-, site-, and chemoselectivity, as the authors noted that other phosphine ligands led to isomerized or methylated olefin side product rather than aldehyde addition, underscoring the importance of the (*S*,*S*)-Et-BPE ligand. Intriguingly, this methodology simplified the total synthesis of (−)-dihydrodehydrodiconiferyalcohol **116** and (−)-lithospermic acid.

Recently, Yamamoto, Yasui, and collaborators disclosed a photopromoted enantioselective cyclization of unsaturated substrates **117** and **119** featuring a 1,6-diyne moiety via chemoselective C−H desymmetrization or chemodivergent parallel kinetic resolution (PKR). C−H cleavage via σ-complex assisted metathesis (σ-CAM) acts as the enantiodetermining step (Scheme 32).[150] Regarding other aspects of the mechanism, DFT calculations indicated that the trivalent-cobaltacycle, generated through oxidative cyclization of the 1,6-diyne,[151] has four possible conformations, and a hydrogen-bonding interaction was recognized to be crucial for excellent enantiocontrol. In the more stable intermediate **Int44**, which

https://doi.org/10.1021/acs.chemrev.6c00255
Chem. Rev. XXXX, XXX, XXX−XXX

Scheme 27. Co(I)/Phosphine-Catalyzed Asymmetric Intramolecular Formyl C−H Annulation

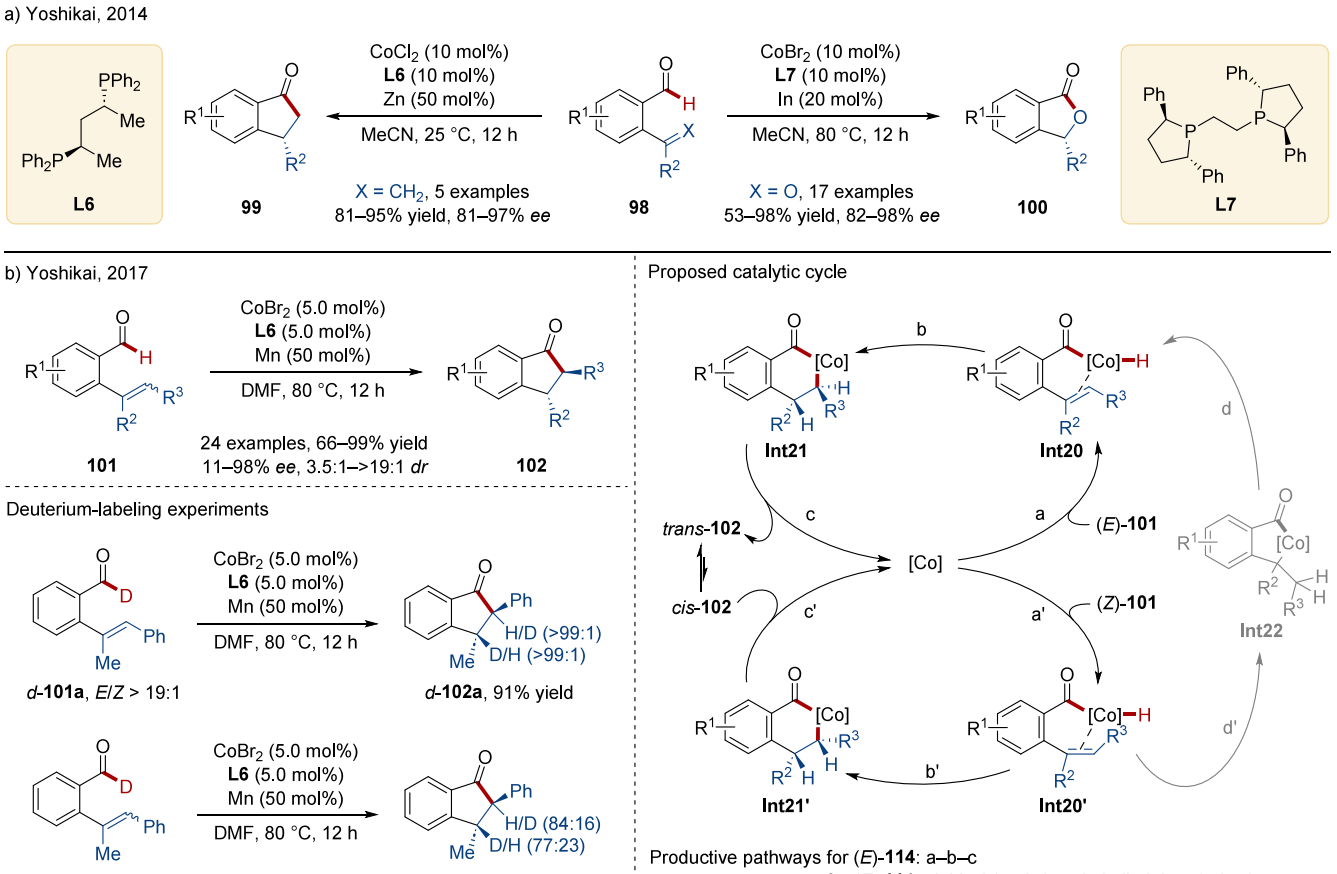

ultimately leads to the major product (*E*)-**118**, steric repulsion between the ligand and substrate is minimized.

5.2. Co(I)/NHC Catalysis

Having demonstrated success in enantioselective Fe/NHC catalyzed C−H activation,[121,123] in 2022 Wencel-Delord, Ackermann, and colleagues demonstrated a cobalt-catalyzed atroposelective C−H arylation of indoles **122** (Scheme 33a).[152] By utilizing a *meta*-1-adamantyl-substituted NHC ligand **L12**, numerous C−C axially chiral indole-3-aldehydes were synthesized in moderate to excellent yields and enantioselectivities (up to 99% yield and 96% *ee*). On the other hand, no desired arylated product **124b** was detected when the 1-chloronaphthalene coupling partner **123** contained a 2-methoxy group. As shown in **TS9**, C−H cleavage occurs via an LLHT mechanism instead of a classic C−H oxidative addition pathway.[153] In the key transition state **TS10** for the rate-limiting and enantiodetermining C−Cl oxidative addition step, DFT calculations suggested that stabilizing C−H···π interactions along with attractive dispersion forces were vital for the outstanding level of enantiocontrol.

Remarkably, this Co/NHC catalytic system was also suitable for the construction of chiral *N*-aryl indole-3-carbaldehydes **126** containing *vicinal* C−C and C−N stereogenic axes via simultaneous atroposelective C−H desymmetrization and kinetic resolution (Scheme 33b).[154]

5.3. Cp^XCo(III) Catalysis

5.3.1. Enantioselective C−H Alkylation. Since Kanai and Matsunaga's seminal investigation in 2013,[155] Cp*Co(III)-catalyzed C−H functionalization has emerged as a powerful synthetic tool, complementing more well-established rhodium- and iridium-catalyzed processes.[132c,e,i,156] One intuitive strategy for realizing the corresponding enantioselective transformations is to leverage chiral Cp^XCo(III) complexes as catalysts.[13e] Prompted by the advent of chiral Cp^X ligands in noble metal catalysis,[3g] in 2019 the Cramer group synthesized and screened a set of Cp^XCo(III) species, funding that a *tert*-butyl-substituted Cp^XCo(CO)I_2 **Co1** complex efficiently catalyzed construction of enantioenriched dihydroisoquinolones **129** facilitated by a redox-active *N*-chloroamide moiety as the DG (Scheme 34a).[157]

https://doi.org/10.1021/acs.chemrev.6c00255
Chem. Rev. XXXX, XXX, XXX−XXX

Scheme 28. Co(I)/Phosphine-Catalyzed Asymmetric Intermolecular Formyl C−H Annulation

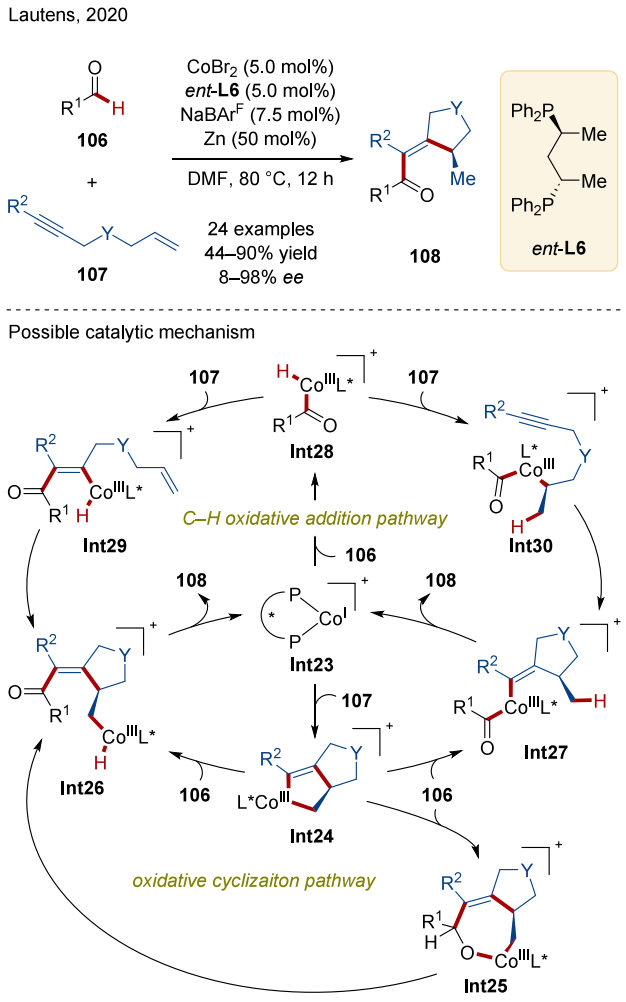

Scheme 29. Co(I)/Phosphine-Catalyzed Asymmetric Indole C−H Alkylation

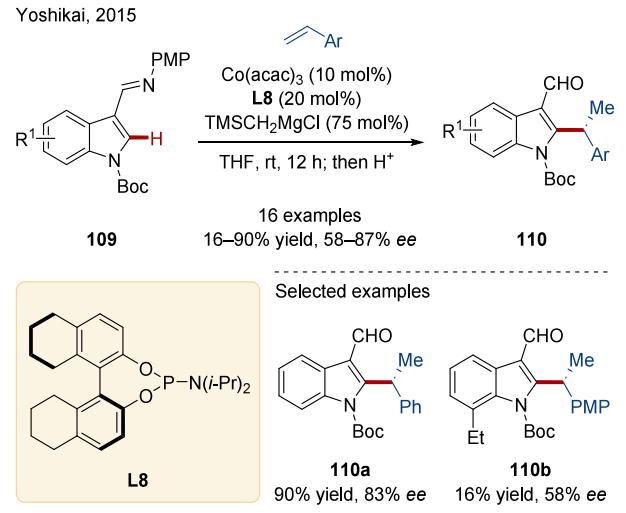

To rationalize the superior catalytic performance of **Co1**, the authors compared the X-ray crystallography and IR spectroscopy data of **Co1** to that of the analogous chiral cobalt(III) complex lacking the *t*-Bu group, as well as achiral complexes

Scheme 30. Co(I)/Phosphine-Catalyzed Asymmetric Cyclization with 1,6-Enynes

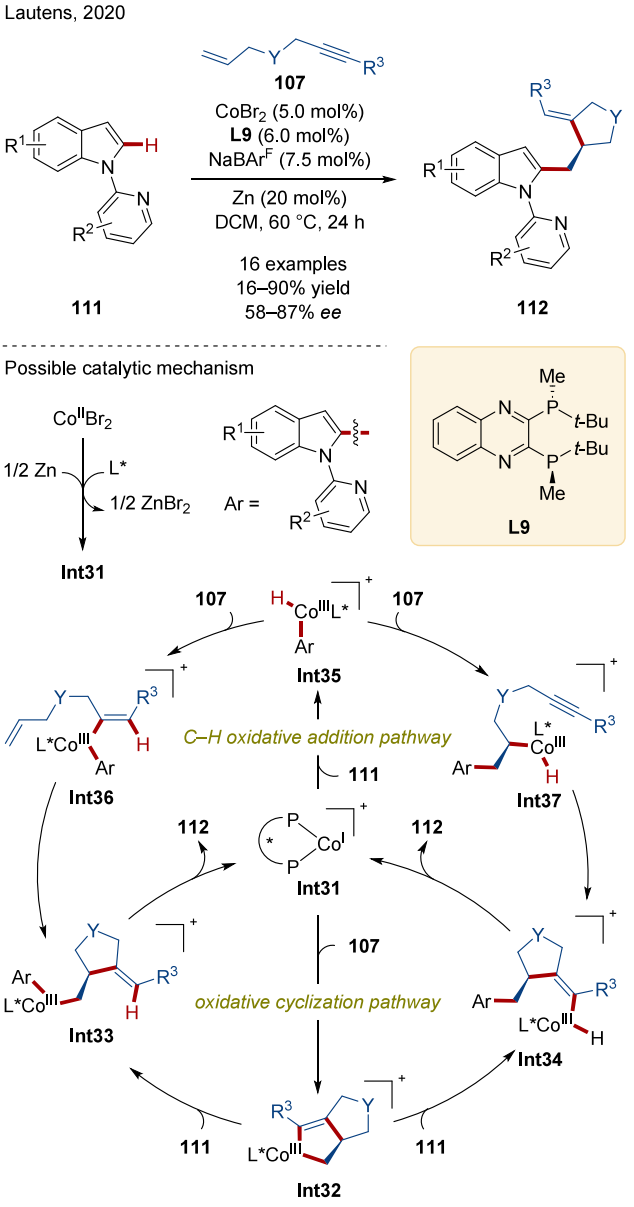

CpCo(CO)I_2[158] and Cp*Co(CO)I_2.[159] Interestingly, the bulky *t*-Bu group in **Co1** exhibits a significant remote effect in increasing the dihedral angle of the binaphthyl backbone of the Cp^X ligand, slightly opening up the chiral pocket, thereby improving both the reactivity and enantioselectivity dramatically. Two years later, the same group also demonstrated an enantioselective intermolecular carboamination of acrylates and bicyclic olefins with *N*-phenoxyamides **130** catalyzed by Cp^XCo(III) complexes (Scheme 34b),[160] which exemplified the reactivity and mechanistic differences between Cp*Co(III) catalysis[161] and its Cp*Rh(III) counterparts.[162]

Beyond carboamination, You and co-workers uncovered a Cp^XCo(III)-catalyzed stereoselective ring-opening C−H alkylation of *N*-pyrimidin-2-yl indoles **133** with 7-oxabenzonorbornadienes **134** in 2023 (Scheme 34c).[163] Notably, when switching from the Cp^XCo(III) catalyst **Co1** to Cp*Co(CO)I_2 under optimal conditions, the diastereoselectivity was reversed such that *trans*-products were favored rather than *cis*-products

https://doi.org/10.1021/acs.chemrev.6c00255
Chem. Rev. XXXX, XXX, XXX−XXX

Scheme 31. Co(I)/Phosphine-Catalyzed Asymmetric Allylic C−H Activation/Nucleophilic Addition

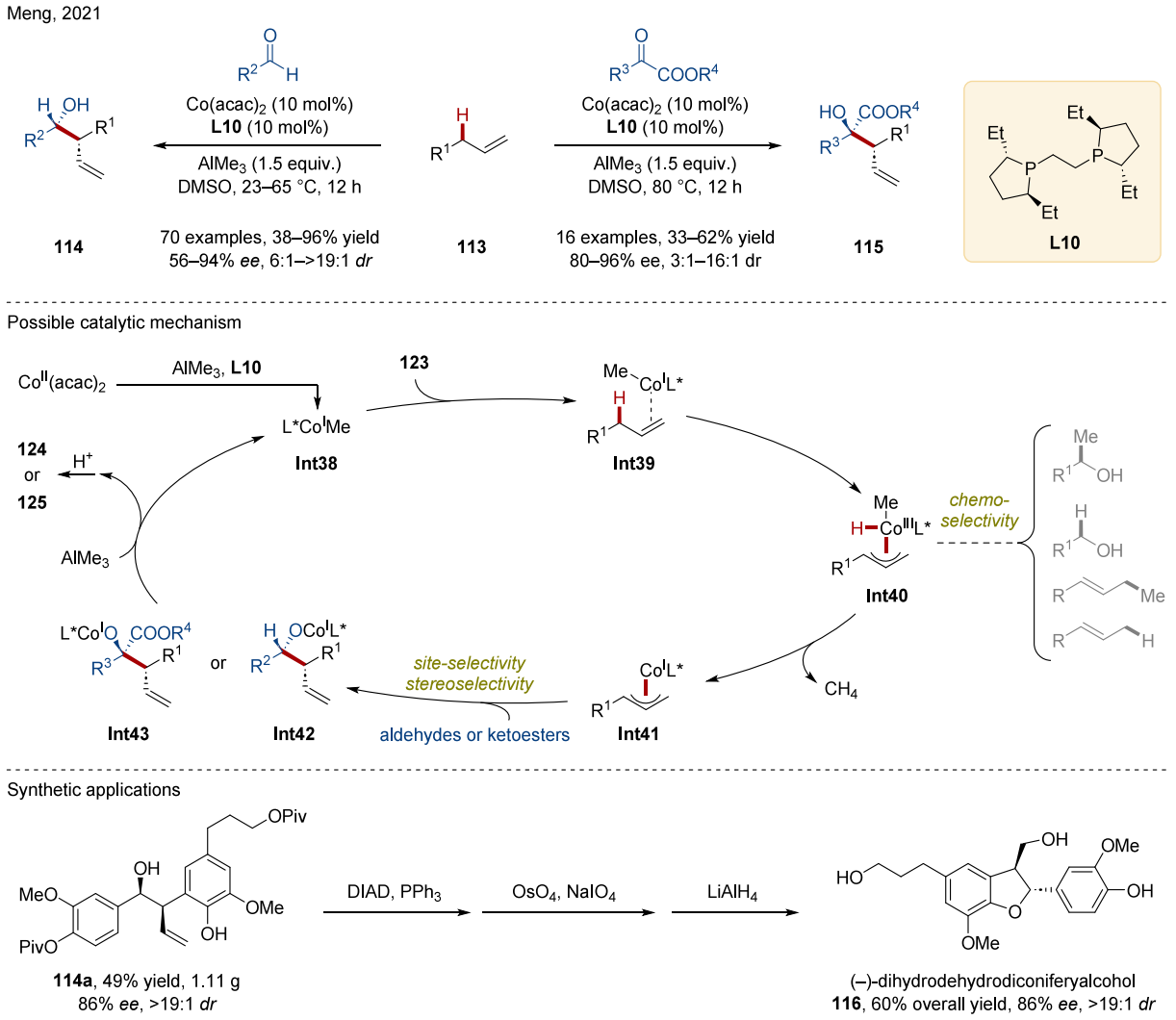

135. DFT calculations indicated that *β*-oxygen elimination is the rate- and stereodetermining step and thus that all preceding steps in the catalytic cycle are reversible. With the achiral Cp*Co(III) catalyst, an additional acetate ligand coordinates during the *trans*-*β*-oxygen elimination step, lowering the energetic barrier by 3.2 kcal·mol^{-1} compared with the alternative *cis*-*β*-oxygen elimination process. On the contrary, an acetate ligand cannot be accommodated around the bulkier Co center of **Co1**, substantially raising the transition state energy for *trans*-*β*-oxygen elimination via **Int47′**, while the transition state for *cis*-*β*-elimination from **Int47** is stabilized by weak coordination between cobalt and the bridging ether [B(Co−O) = 2.02 Å]. Therefore, *cis*-*β*-oxygen elimination from **Int47**, generated from alkene *exo*-migratory insertion from **Int46**, is favored with the chiral Cp^{X}Co(III) **Co1** catalyst, yielding the *cis*-(1*S*,2*R*)-**135** as the major product. Moreover, 7-azabenzonorbornadienes **136** were also compatible in this transformation catalyzed by **Co3**, in which the *cis*- and *trans*-selectivities could be flipped by simply changing the reaction solvent from TFE to toluene as well as the acetate additive.

Recently, the Cramer group employed cyclopropenes as a one-carbon synthon, disclosing an enantioselective [4 + 1] annulation of *N*-chlorobenzamides **138** with exceptional *E*/*Z*-selectivity catalyzed by **Co4** (Scheme 35).[164] Numerous biologically relevant chiral isoindolinones were prepared through C−H activation, cyclopropene coordination, migratory insertion, C−C bond cleavage for cyclopropane ring opening, oxidative addition, nitrene insertion, and protonation. Surprisingly, when switching from **Co4** to its chiral Cp^X-chelated Rh(III) homologue the more common [4 + 2] cyclization via direct N−Cl oxidative addition and C−N reductive elimination was observed. DFT calculations indicated that the change in product selectivity originates from more facile cyclopropane ring opening after migratory insertion with cobalt (**Int50** → **Int51**) compared to rhodium.

Multicomponent transformations offer the opportunity to rapidly generate molecular and stereochemical complexity in a single step. However, these transformations also introduce added challenges in terms of reactivity and selectivity control. Stimulated by Ellman's three-component C−H functionalization with [Cp*Co(C$_6$H$_6$)][B(C$_6$F$_5$)$_4$]$_2$,[165] in 2021 Cramer and colleagues reported the enantio- and diastereoselective version of this coupling among substrates **140**, vinyl ketones, and aldehydes (Scheme 36).[166] Regarding the reaction mechanism, after pyrazole-directed C−H activation, a selective Michael addition occurs, and the vinyl ketone is proposed to be oriented such that the R^2 group points in the open space within the substrate binding pocket created by the chiral ligand. This leads

https://doi.org/10.1021/acs.chemrev.6c00255
Chem. Rev. XXXX, XXX, XXX−XXX

Scheme 32. Co(I)/Phosphine-Catalyzed Cycloaddition/Asymmetric Allylic C−H Activation

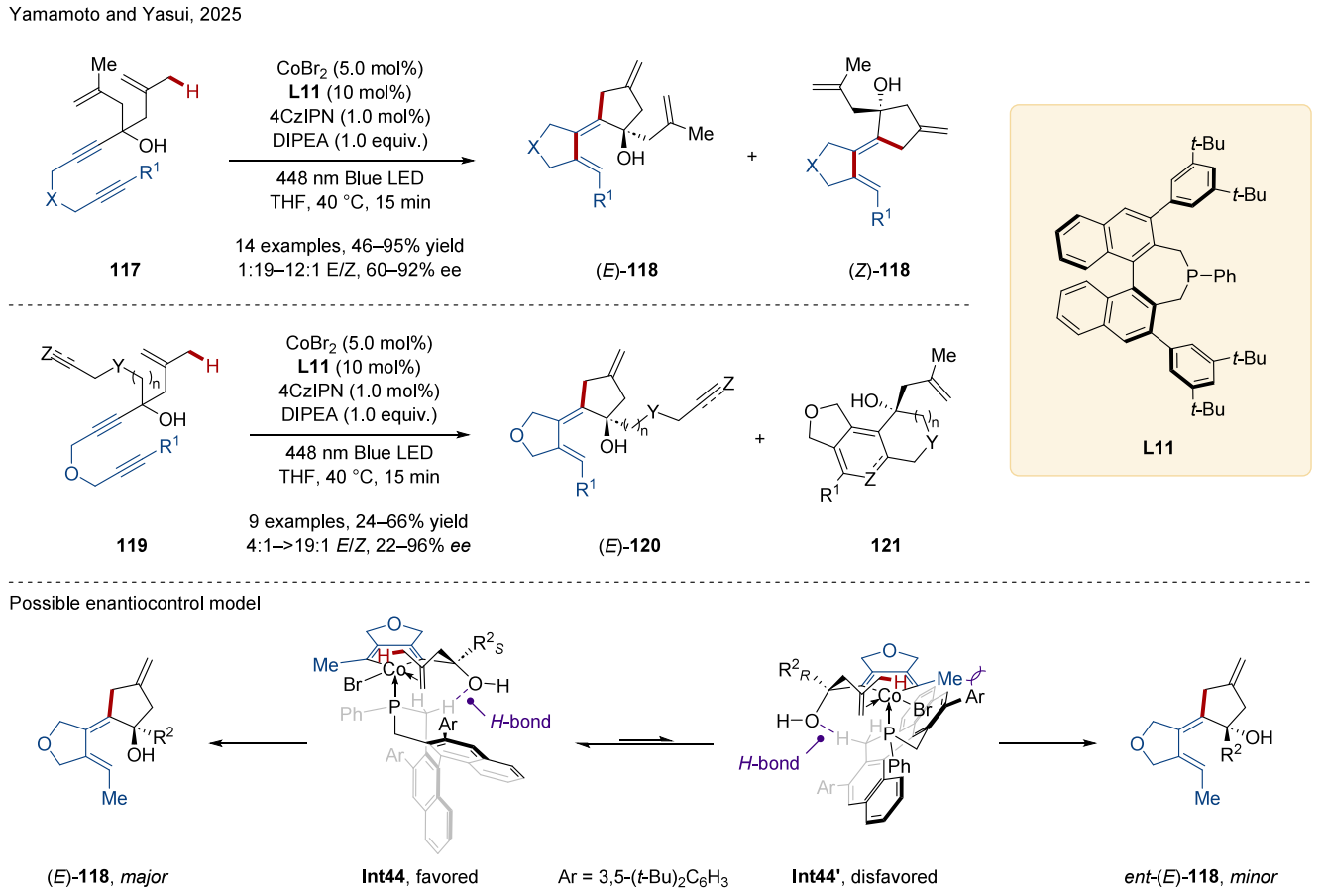

to preferential formation of corresponding cobalt enolate **Int54**, which possesses less steric crashing. Similarly, in the subsequent nucleophilic addition to the aldehyde coupling partner, the R^3 substituent is preferentially positioned at the opposite end of the Cp^X sidewall (as illustrated in the dotted-line box in Scheme 36), leading to the major (2*R*,3*S*)-configuration of the products **141**.

5.3.2. Enantioselective C−H Allylation. In 2024, You and colleagues unveiled an enantioselective C−H allylation for the construction of planar chiral ferrocenes **144** (Scheme 37).[167] Large ^{13}C KIE values were observed for the carbons where the new $C(sp^2)-C(sp^3)$ bond was formed, implicating migratory insertion of allyl carbonate **143** as the turnover-limiting step. With a reversible C−H activation step, further computational studies then established that migratory insertion is also the enantiodetermining step, as the energy of favored transition state **TS12**, which is stabilized through attractive C−H···π interactions, is 2.1 kcal·mol^{-1} lower than the disfavored **TS12′**.

5.4. Cp*Co(III)/CCA Catalysis

5.4.1. Enantioselective C−H Alkylation. Since high-valent cobalt catalyzed C−H cleavage process are generally promoted by carboxylates through a concerted metalation−deprotonation (CMD) mechanism,[132e,168] the utilization of a chiral carboxylic acid (CCA) as the external chiral ligands is an alternative strategy to achieve enantiocontrol.[169] In 2018, the Ackermann group adopted a C_2-symmetric chiral carboxylic acid **L13**, establishing the branched-selective asymmetric C−H alkylation of *N*-pyridyl indoles **145** with terminal olefins (Scheme 38a).[170] As suggested by H/D scrambling and computational studies, irreversible protodemetalation was identified as the enantiodetermining step. Unfortunately, when removing the aromatic ring at the allylic position of the olefin, the enantioselectivity of the corresponding product **146c** decreased dramatically, implying the importance of π-chelating effect in this transformation. Recently, informed by a machine learning (ML) model, Ackermann, Hong, and colleagues realized the simultaneous construction of *C*-central and C−N axial chirality in **147** under similar conditions by changing the amide moiety from benzoyl in **L13** to 3-furanoyl in **L14** (Scheme 38b).[171]

In 2020, Matsunaga, Yoshino, and co-workers expanded the scope of olefins to *N*-protected maleimides **149**, disclosing an asymmetric hydroarylation with *N*-5-methylpyrimidin-2-yl indoles **148** via an analogous reversible migratory insertion (from **Int56** to **Int57** and **Int57′**) and irreversible stereoselective protodemetalation (from **Int57** to products **150**) mechanism (Scheme 38c).[172] Instead of the C_2-symmetric CCAs **L13** and **L14**, the authors designed the C_1-symmetric (*S*)-2′-phenyl-[1,1′-binaphthalene]-2-carboxylic acid **L15** as the sole chiral proton source for this transformation. Later, several chiral CCAs based on an axially chiral styrene backbone were also employed in this transformation.[173] Among those surveyed, CCA **L16** synthesized by Zhang, Zhong, and collaborators in 2022, afforded compound **150a** with a higher enantiomeric excess of 82% (Scheme 38d).[174]

Leveraging multiple noncovalent interactions (NCI)[175] between a redesigned pyridyl directing group and CCA ligand, in 2021 our group demonstrated a branched-selective asymmetric C−H alkylation of *N*-pyridyl indoles **151** with unactivated terminal aliphatic olefins (Scheme 39),[176] further

https://doi.org/10.1021/acs.chemrev.6c00255
Chem. Rev. XXXX, XXX, XXX−XXX

Scheme 33. Co(I)/NHC-Catalyzed Asymmetric Allylic C−H Activation/Nucleophilic Addition

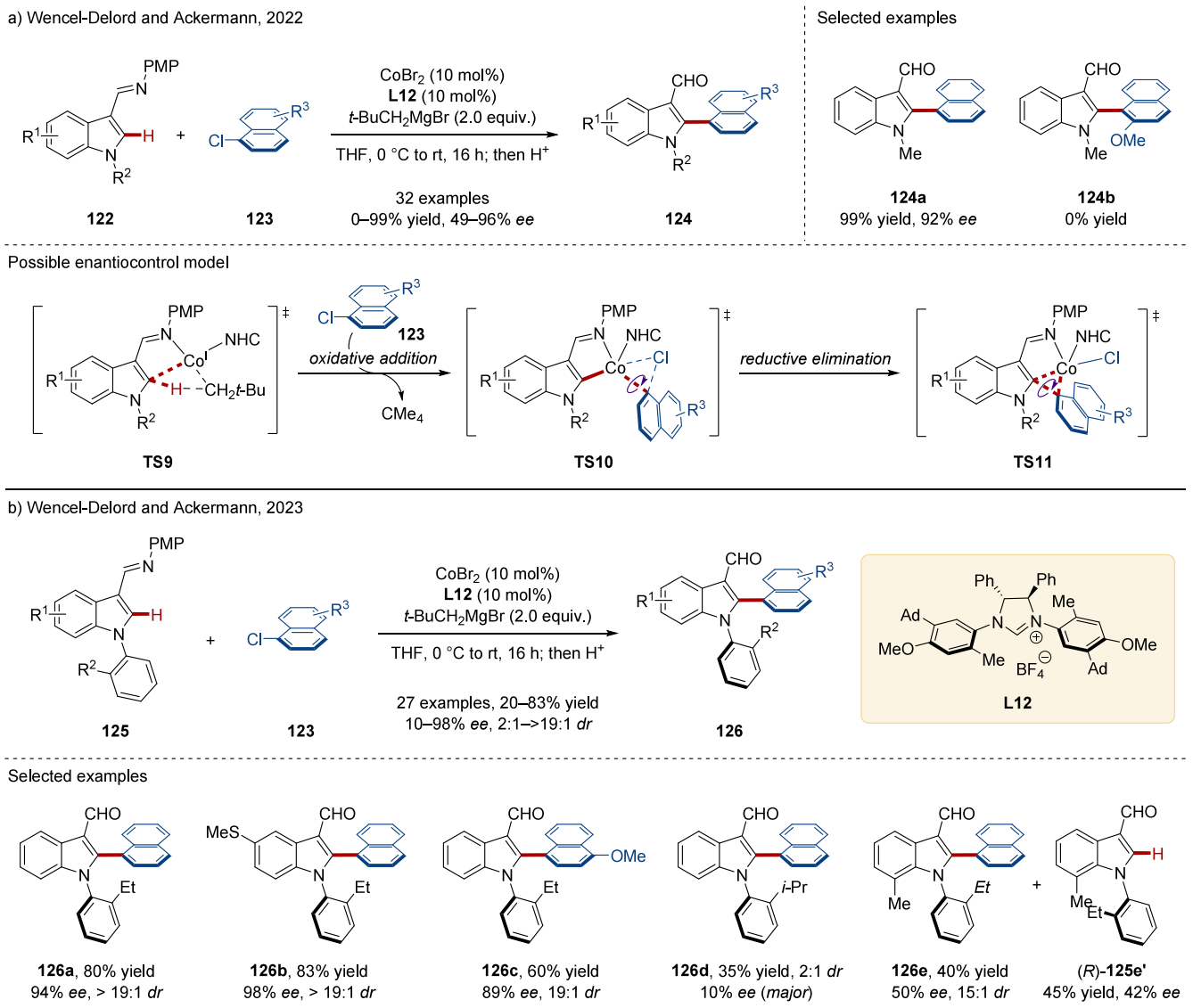

enhancing the enantiocontrol compared with Ackermann's work (Scheme 38a).[170] To enable this investigation, a library of noncanonical bulky amino acids (AAs) were synthesized on gram scale in one step from commercially available *N*-Phth-Tle-OH by means of previously developed palladium(II)-catalyzed C(sp^3)−H arylation methodology.[177] This effort led to identification of the optimal bisaryl-substituted CCA ligand **L17**. As revealed by DFT calculations, during the irreversible alkene migratory insertion step, a strong $\pi-\pi$ stacking interaction between the electron-deficient 3,5-$(CF_3)_2C_6H_3$ fragment in the substrate **151** and the electron-rich 4-methoxy-3-methylbenzyl group on **L17**, along with a C−H···π interaction between the aliphatic olefin and the other 4-methoxy-3-methylbenzyl group, stabilizes transition state **TS13**, leading to extraordinary stereochemical induction through precise molecular recognition among the substrate, alkene, Cp*Co(III), and the tailored ligand.

5.4.2. Enantioselective C−H Amidation. In 2019, Matsunaga, Yoshino, and co-workers established a convenient synthetic approach to various chiral β-amino thiocarbonyl amides **155** bearing a quaternary *C*-stereocenter via Cp*Co(III)/CCA-catalyzed enantioselective C(sp^3)−H amidation with dioxazolones **154** (Scheme 40a).[178] Drawing on Dixon and Seayad's nonstereoselective transformations,[179] a Tle-derived centrally chiral ligand **L18** and a ferrocene-based planar chiral carboxylic acid **L19** were used to achieve good enantiocontrol for α-alkyl and α-aryl thioamides **153** respectively. Meanwhile, our group simultaneously uncovered an asymmetric C(sp^2)−H amidation of ferrocenyl thioamides **153** with a novel *N*-monoprotected amino acid (MPAA) **L20** as the chiral ligand via enantiodetermining CMD process (Scheme 40b).[180]

In 2022, our group[181] and the group of Matsunaga and Yoshino[182] independently reported an enantioselective amidation of sulfoximines **159**, with each group a different optimal CCA (Scheme 45), establishing the stereogenic sulfur center via cobalt-catalyzed C−H activation.[183] In the report from Matsunaga and Yoshino, the major pathway is hypothesized to proceed via **TS14**, which benefits from stabilizing C−H···π interactions between the sulfoximine **159** and the *pseudo*-C_2-symmetric H_8-binaphthyl ligand **L21**. With this method, diverse benzothiadiazine-1-oxides bearing both electron-donating and -withdrawing groups were synthesized in moderate to good yields and enantioselectivities (Scheme 41a, 43−96% yield, 82−96% *ee*).[182] In the report from our group, the major pathway

https://doi.org/10.1021/acs.chemrev.6c00255
Chem. Rev. XXXX, XXX, XXX−XXX

Scheme 34. Cp^XCo(III)-Catalyzed Asymmetric Olefin Hydroarylation

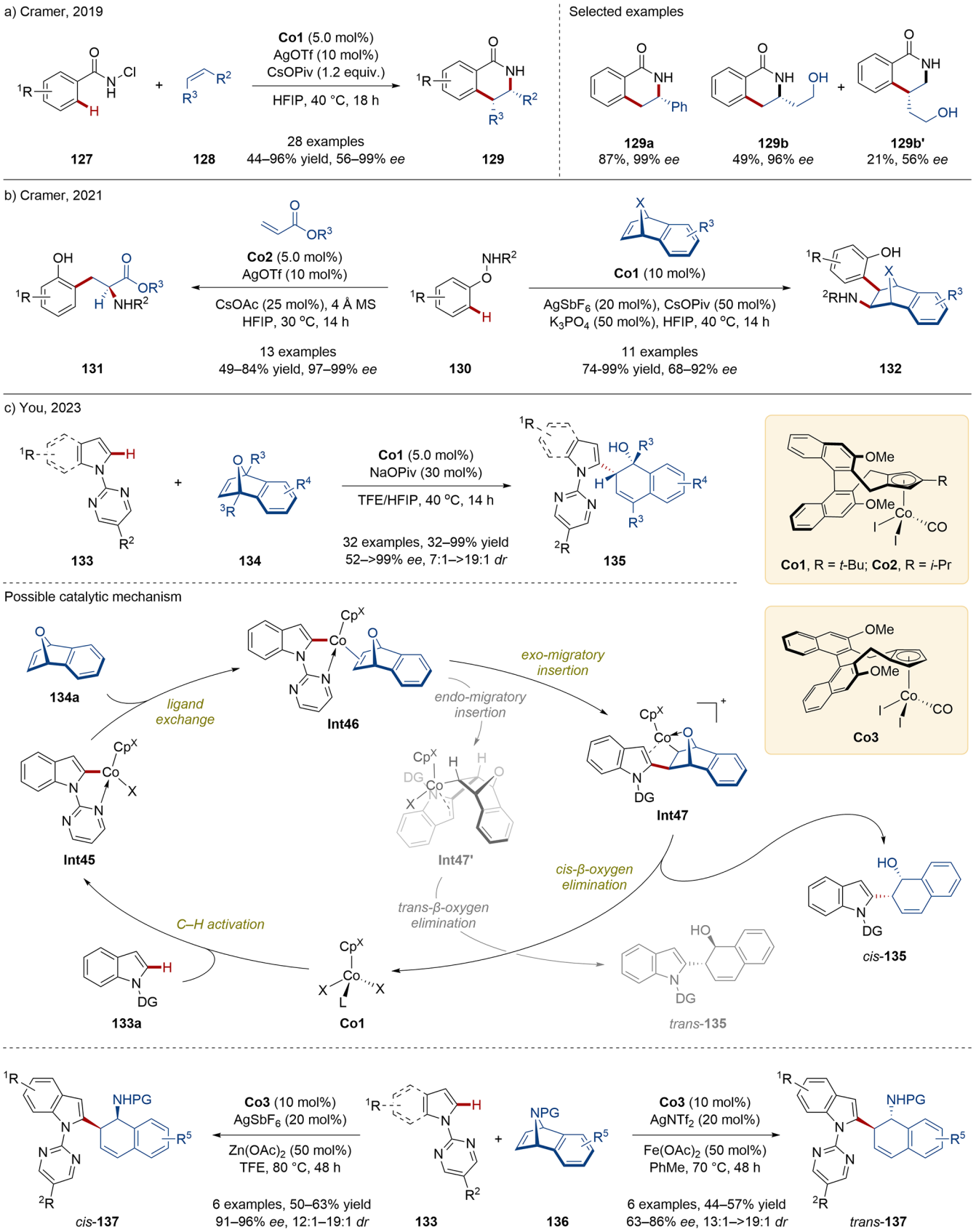

(**TS15**) is stabilized by a hydrogen-bonding interaction between N−H of the sulfoximine **159** and the *N*,*N*-diisopropyl carboxylamide group on CCA **L22** (or **L23**), which is the origin of the excellent levels of enantiocontrol.[184] This transformation afforded either cyclic and acyclic products (**161** and **162**, respectively) in up to 97% *ee* depending on the

https://doi.org/10.1021/acs.chemrev.6c00255
Chem. Rev. XXXX, XXX, XXX−XXX

Scheme 35. $Cp^XCo(III)$-Catalyzed Asymmetric C−H Activation/[4 + 1] Annulation

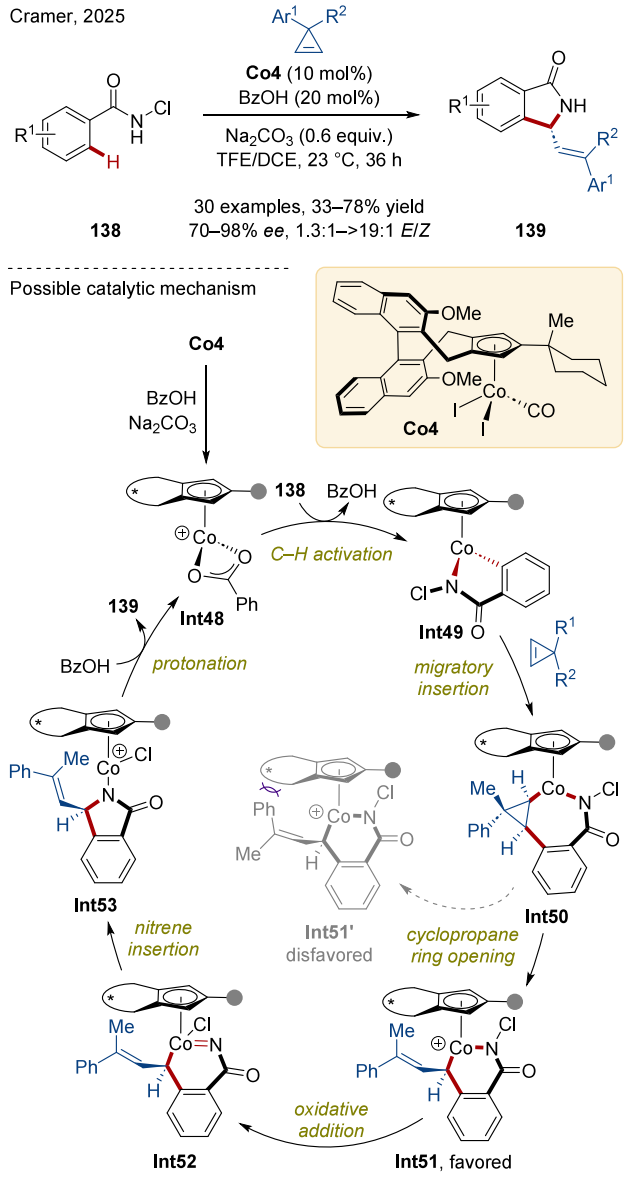

Scheme 36. $Cp^XCo(III)$-Catalyzed Asymmetric C−H Three-Component Functionalization

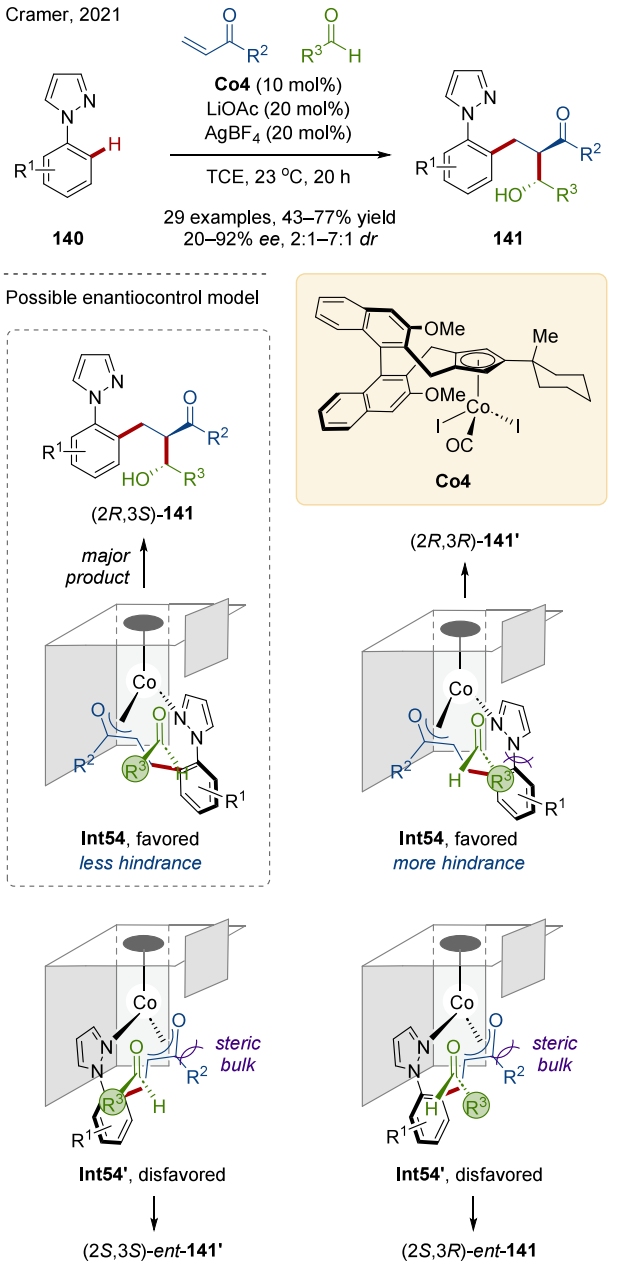

substituents on the dioxazolones **160** and the reaction conditions. The products could be reduced to access an intriguing class of *N*,*S*-chiral sulfoxide ligands (Scheme 41b).[181]

5.4.3. Enantioselective C−H Olefination. In 2024, Dixon, Hamlin, and co-workers disclosed a regio- and enantioselective C(sp^3)−H olefination of prochiral α-dimethyl β-aryl thioamides **163** assisted by *N*-Phth-Tle-OH **L18** (Scheme 42).[185] Using but-2-ynoate esters **164** as the alkenylation reagents, a series of desymmetrized compounds **165** containing a quaternary *C*-stereocenter were obtained in moderate yields and enantiomeric excess. β-Alkyl thioamides **163** were also suitable in this transformation, furnishing the corresponding products with lower enantioselectivities.

5.5. Co(II)/CPA Sequential Catalysis

Beyond progress on C−H activation with pseudotetrahedral $Cp^XCo(III)$ or Cp*Co(III)/CCA catalytic systems, in 2021, our group demonstrated a sequential achiral C−H alkenylation/asymmetric [4 + 1] spirocyclization of *N*-(quinolin-8-yl)-benzamides **166** using a simple Co(II) salt that could be oxidized to the active Co(III) catalyst *in situ* (Scheme 43a).[186] Instead of developing a novel chiral ligand for high-valent cobalt catalysis, we adopted the 2,2′,3,3′-tetrahydro-1,1′-spirobiindene-based 6,6′-bulky aryl-substituted chiral phosphoric acid (CPA) **L24**, a member of the commonly employed (*S*)-STRIP ligand class in metal−organocatalysis,[187] to achieve enantiocontrol during subsequent aza-1,4-Michael addition spirocyclization. As shown in **Int59**, (*S*)-STRIP **L24** is proposed to coordinate with the Co complex **Int58**, which accompanies self-assembly with the C−H olefinated intermediate utilizing hydrogen-bonding interaction between the phosphate and amide groups. In 2023, Ackermann and co-workers extended this Co(II)/CPA sequential catalysis to the asymmetric construction of these *spiro*-γ-lactams **168** using CPA **L25** under electrooxidative conditions, operating via the same mechanism pathway (Scheme 43b).[188]

https://doi.org/10.1021/acs.chemrev.6c00255
Chem. Rev. XXXX, XXX, XXX−XXX

Scheme 37. Cp^XCo(III)-Catalyzed Enantioselective C−H Allylation

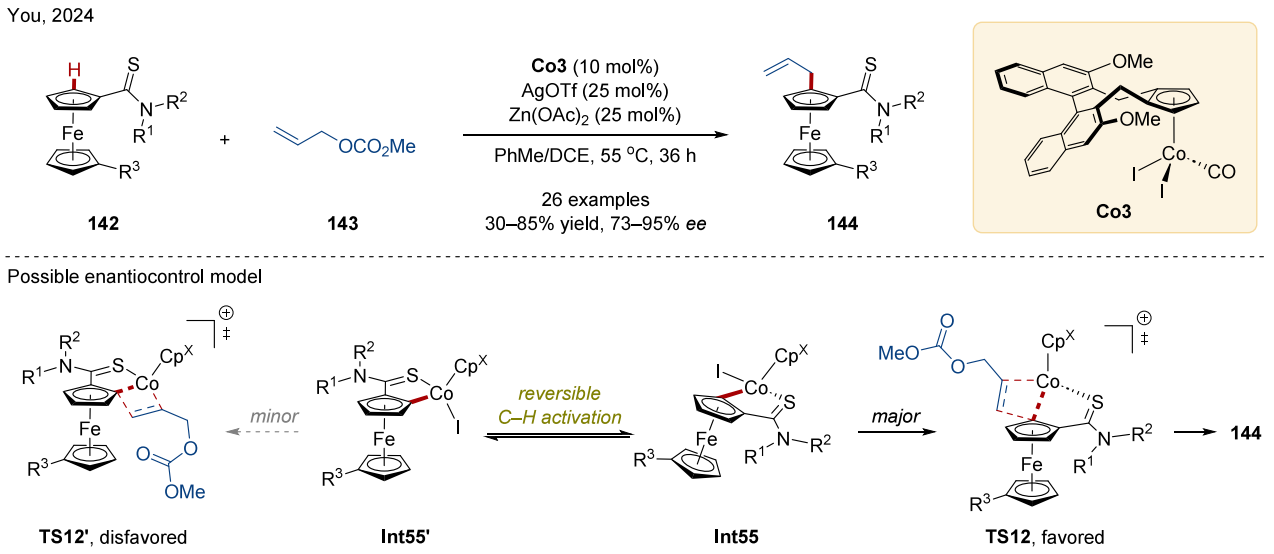

5.6. Co(II)/Salox Catalysis

5.6.1. Enantioselective C−H [4 + 2] Annulation with Alkynes and Allenes. *5.6.1.1. Construction of Central Chirality.* As a seminal study in 2014, Daugulis and co-workers reported the first Cp free cobalt-catalyzed C−H alkenylation/annulation using a commercially available cobalt(II) salt as catalyst, enabled by strongly coordinating bidentate DGs such as 8-aminoquinoline and picolinamide.[189] Mechanistic studies revealed that the *N*-(quinolin-8-yl) benzamide substrate acts as a monoanionic bidentate ligand (MBL) to facilitate oxidation of the precatalyst, Co(II) salt, to the active Co(III) catalyst, which features higher reactivity since it is more suitable for C−H cleavage via a two-electron metalation step than open-shell Co(II) complexes. Drawing on this insight, we envisioned that a rational-designed chiral MBL could mimic the coordination pattern and catalytic function of *N*-(quinolin-8-yl) amide, thereby achieving the first enantioselective C−H activation catalyzed by an octahedral cobalt complex.[133d] To this end, we eventually found salicyloxazoline (Salox) ligands as capable candidates for this concept. First introduced by Bolm and co-workers,[190] Salox ligands represent a novel class of air-stable and conformational-rigid chiral ligands that are readily accessible via $ZnCl_2$-catalyzed condensation of salicylonitriles and enantiopure β-amino alcohols.[191]

In a proof-of-concept study reported by our group in 2022, diverse *P*-stereogenic chiral phosphinamides **172** were constructed with 98% to >99% *ee* via enantioselective C−H annulation of aryl phosphinamides **169** with alkynes **170** or allenes **171** assisted by Salox ligand **L26** (Scheme 44).[190] For unsymmetrical phosphamides *rac*-**169**, kinetic resolution was also viable, and an excellent *s*-factor of 206 could be reached. In further mechanistic control experiments, NaOPiv was found to be critical for C−H metalation, indicating a CMD mechanism in this catalytic system. Several key intermediates were investigated by synthesis of their stabilized analogues which allow for isolation and analysis by single-crystal X-ray diffraction, clarifying the operative stereoinduction model that gives rise to extraordinary enantioselectivities observed. In the proposed catalytic cycle, precise assembly of substrate **169** and Salox **L26** with cobalt(III) center (**Int61**) is attributed to the $\pi-\pi$ stacking interactions between phenyl ring of oxazoline in **L26** and the quinoline ring in **169**, as well as the $\pi-\pi$ stacking between the phenolic moiety in **L26** and one of the aryl groups in **169**. Enantiodetermining C−H activation then forms the pincer-type cobaltacycle *mer*-(S_c,S_p)-**Int62** in the presence of NaOPiv. Following this study, the Ackermann group and the Ling group also achieved the asymmetric synthesis of various *P*-stereogenic chiral phosphinamides **172**−**174** via electrocatalysis, whereby holes replace the chemical oxidant, $Mn(OAc)_2{\cdot}4H_2O$, used in the prior system.[188,192]

In 2024, Sundararaju and co-workers reversed the regioselectivities of the Co(II)/Salox-catalyzed asymmetric C−H/N−H [4 + 2] annulation using 1-bromoalkynes as the coupling partners with a Bn-substituted Salox **L28** (Scheme 45).[193] In the proposed mechanism, initial formation of cyclized intermediate **177** establishes the regioselectivity, with the alkyl or aryl group positioned adjacent to the *P*-stereogenic center due to the presence of the bulky bromine atom. A subsequent oxidative addition of the C−Br bond occurred with the freshly liberated Co(I) species, and the final products **176** are then formed with following ligand exchange and C−O reductive elimination.

Subsequently, our group realized that picolinamide (PA) and its derivatives could serve as a class of alternative directing group that could exhibit analogous $\pi-\pi$ stacking interactions with the phenyl ring of oxazoline on the Salox ligand.[194] A wide range of C1-stereogenic chiral 1,2-dihydroisoquinolines (DHIQs) **179** were produced via desymmetrization or kinetic resolution (Scheme 46). The obtained DHIQs **179** have proven to be key intermediate products in the gram-scale asymmetric total synthesis of 1,2,3,4-tetrahydroisoquinoline (THIQ) natural alkaloids, including (−)-norlaudanosine **180**, (−)-xylopinine **181**, (+)-laudanosine **182**, (+)-sebiferine **183**, (+)-cryptostyline II **184**, and (+)-solifenacin, as well as other bioactive molecules such as FR115427, and (+)-NPS R-568.

5.6.1.2. Construction of Axial Chirality. In parallel to our lab's discovery of the Co(II)/Salox catalytic system described in the preceding section, Niu and co-workers also discovered Co(II)/Salox catalysts to be effective for atroposelective C−H activation/annulation.[195] Facilitated by Salox **L27**, a set of C−N axially chiral isoquinolinones **186** were constructed via atroposelective C−H/N−H [4 + 2] annulation with alkynes using O_2 as the terminal oxidant (Scheme 47a, Condition A).

https://doi.org/10.1021/acs.chemrev.6c00255
Chem. Rev. XXXX, XXX, XXX−XXX

Scheme 38. Cp*Co(III)/CCA-Catalyzed Enantioselective C−H Alkylation

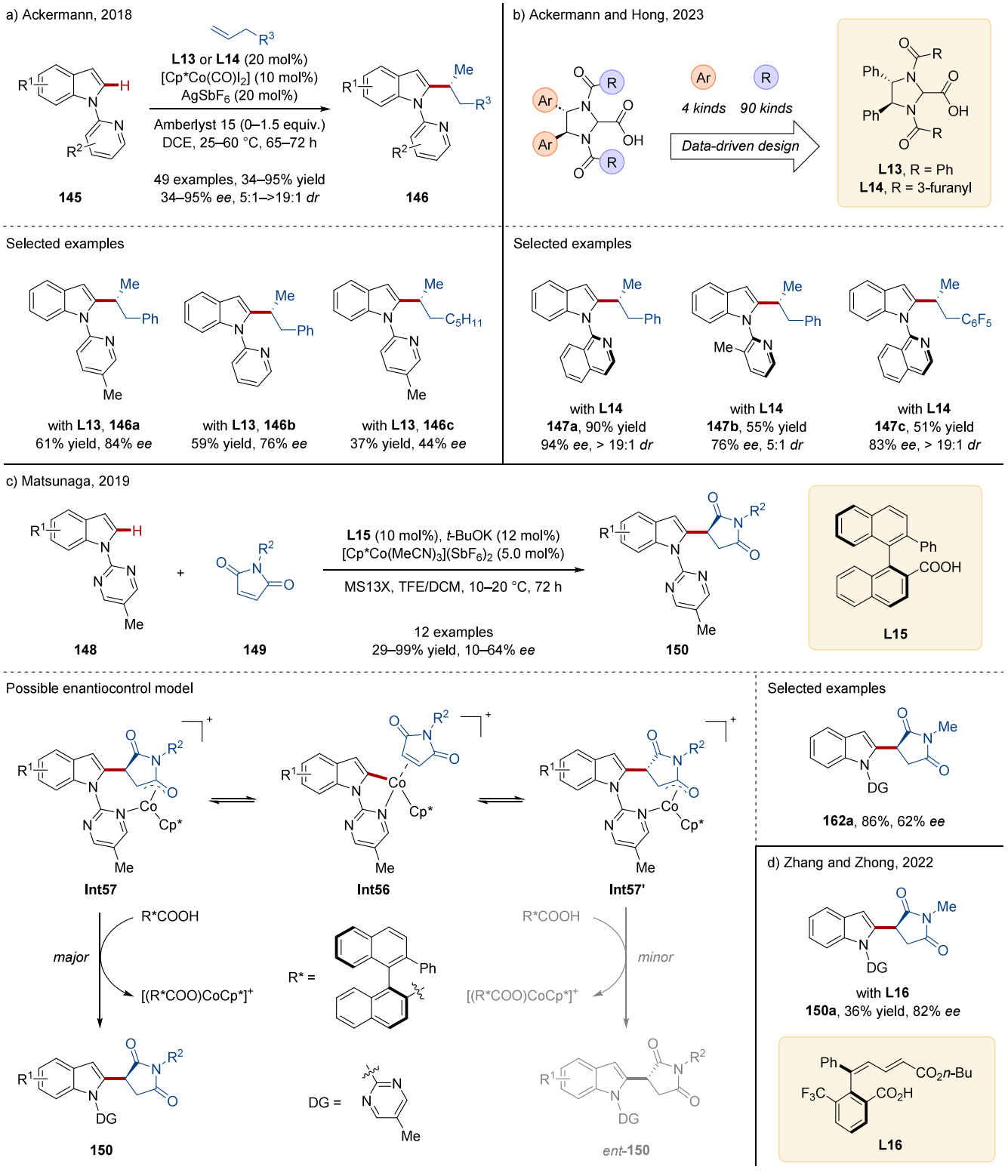

Subsequently, the same group also employed allenes in this cobalt-catalyzed atroposelective isoquinolinone synthesis with the solvent exchanged from 1,4-dioxane to $PhCF_3$, yielding the C═C double bond-isomerized products **187** in up to >99% *ee* (Scheme 47a, Condition B).[196] Several electro- and photochemical variants have been reported, and the reaction could be scaled up with continuous flow technique (Scheme 47b).[188,197,198] In 2003, Niu, Yang, and colleagues then demonstrated the asymmetric synthesis of chiral sultams **193** and **194** bearing a C−N axis via Co/**L30**-catalyzed C−H activation of aryl sulfonamides **192** with alkynes and allenes as the coupling partners, respectively (Scheme 47c).[199] The pyridine-*N*-oxide auxiliary was also identified as an alternative effective directing group for this cobaltaelectro-catalyzed

https://doi.org/10.1021/acs.chemrev.6c00255
Chem. Rev. XXXX, XXX, XXX−XXX

Scheme 39. Cp*Co(III)/CCA-Catalyzed Enantioselective C−H Alkylation Modulated by NCIs

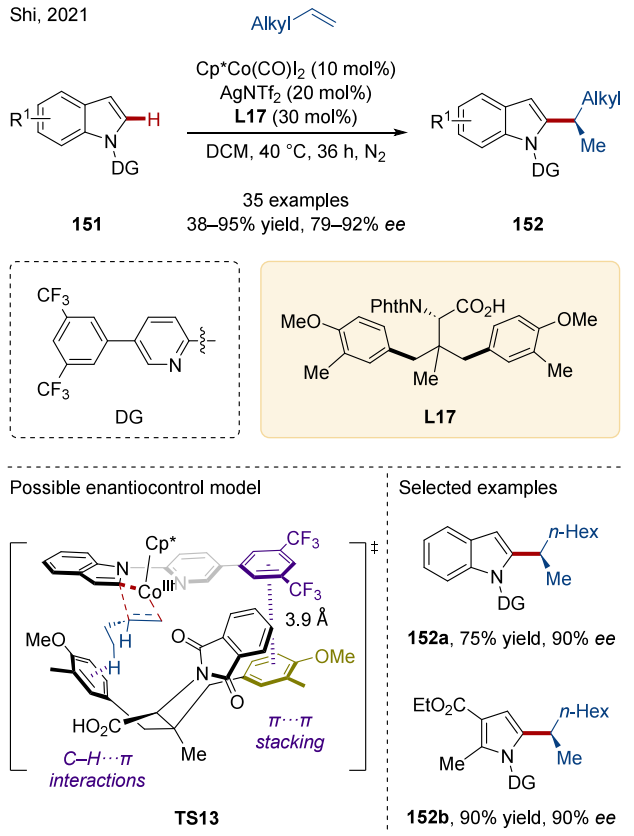

atroposelective C−H activation/annulation, allowing the establishment of a chiral C−N axis through key transition state **TS16** (Scheme 47d).[200]

Compared with C−N axially chiral molecules, those with a N−N axis are comparatively rare. The N−N axis was long believed to be unstable based on its deplanarized structure. Nevertheless, the rotational barrier of the N−N bond can actually be enhanced through repulsion between lone pairs at two proximal nitrogen atoms, allowing for stable chiral N−N axes through appropriate substitution.[201] In 2023, Niu, Yang, and co-workers disclosed a Co(II)/Salox-catalyzed C−H annulation with alkynes utilizing 1*H*-pyrrolo[2,3-*b*]pyridine-1-yl amide as a directing group, affording isoquinolinones **199** containing a fixed N−N axis with excellent atroposelectivities (Scheme 48).[202] The gram-scale synthesis of **199a** with ethynyldiphenylphosphine oxide was conducted smoothly (1.08g, 60% yield, 99% *ee*). Upon reduction of **199a**, the obtained N−N axially chiral phosphine **201** turned out to be an efficient ligand in enantioselective Tsuji−Trost allylic alkylation. When O_2 was replaced with direct current electricity for reoxidation, the corresponding compounds were generated in slightly inferior yields and enantioselectivities,[203] and the alkyne coupling partner could also be replaced by allenes.[204]

For more challenging diaxially chiral atropisomers,[205] we initially achieved a facile access to *vicinal* C−C and C−N chiral axes via intramolecular C−H activation/[4 + 2] annulation with Co(II)/Salox catalysis in 2022 (Scheme 49a).[206] These two chiral axes in **205** were proposed to be constructed separately in the alkyne migratory insertion and C−N reductive elimination steps. Therefore, the tight coordination of Salox **L26** around the cobalt center is essential for high levels of stereoinduction by offering a long-lasting chiral environment that persists throughout the entire catalytic cycle. Very recently, our group also reported the cobalt-catalyzed atroposelective synthesis of pyridoindolones **208** bearing two distinct and remote C−N axes (Scheme 49b).[207] In contrast to the intramolecular C−H/N−H [4 + 2] annulation discussed above in which the two axes were constructed in different steps, the pyridoindolone synthesis establishes the chirality of both C−N axes during the C−H metalation step. An unexpected asymmetric amplification was detected, which may be attributed to the inhibition of reactivity by the minor enantiomer with nonenantiopure Salox **L32**. The minor enantiomer of the Salox ligand presumably gives rise to a heterochiral 2:1 (or even 3:1) ligand:metal complex that is unreactive. Intriguingly, these diaxial atropisomers exhibited exceptional chiroptical properties as potential fluorescent organic materials.

5.6.1.3. Construction of Inherent Chirality. Inherent chirality arises from the bending of a planar structure into three-dimensional space with curvature that breaks the

Scheme 40. Cp*Co(III)/CCA-Catalyzed Enantioselective C−H Amidation of Thioamides

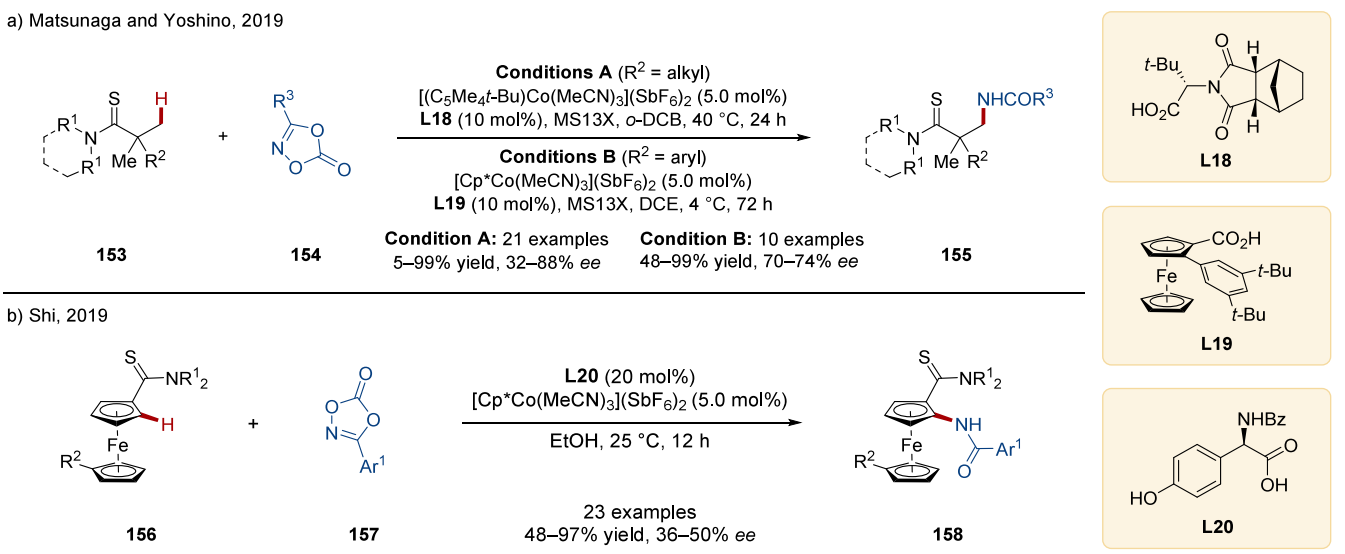

https://doi.org/10.1021/acs.chemrev.6c00255
Chem. Rev. XXXX, XXX, XXX−XXX

Scheme 41. Cp*Co(III)/CCA-Catalyzed Enantioselective C−H Amidation of Sulfoximines

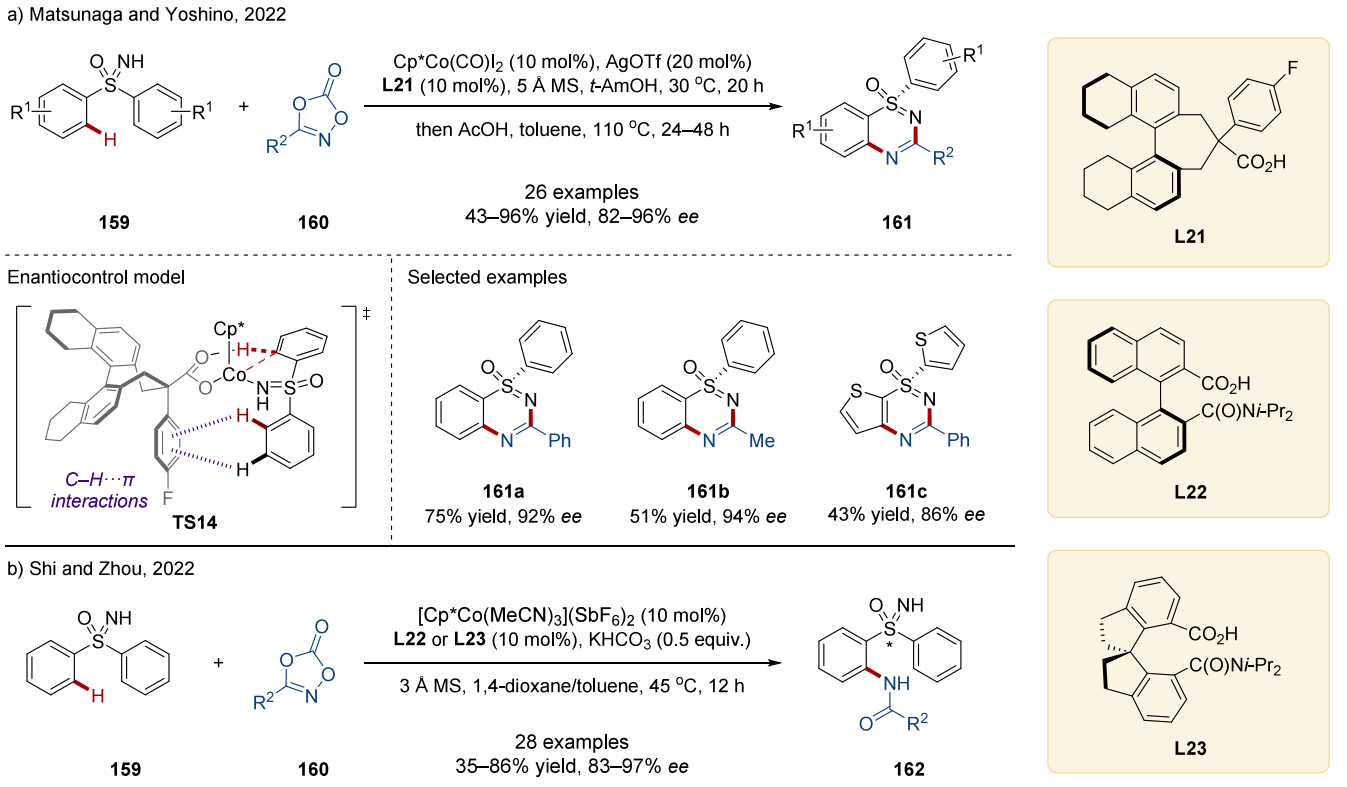

Scheme 42. Cp*Co(III)/CCA-Catalyzed Enantioselective C−H Olefination

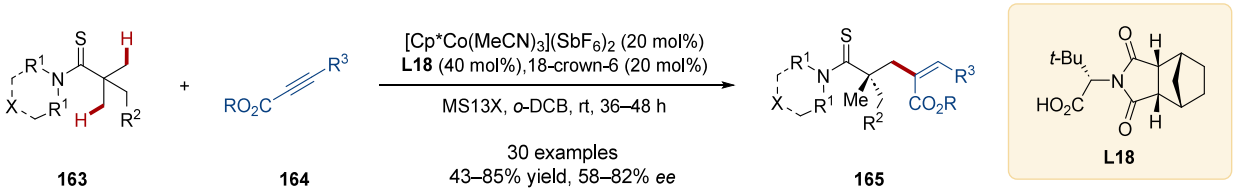

molecular symmetry. Enantioselective synthetic approaches to inherently chiral molecules have been less explored to date compared with those containing other types of chirality, since their unique molecular architectures poses challenges to traditional methods.[208] In 2024, we applied the Co(II)/Salox-catalyzed enantioselective C−H annulation to establish inherent chirality, accomplishing the desymmetrization of calix[n]arenes **211** (Scheme 50a).[209] Meanwhile, a large number of both inherently and axially chiral calix[4]arenes **211** were also accessed in outstanding enantio- and diastereoselectivities with this protocol. Both chemo- (i.e., $Mn(OAc)_3{\cdot}2H_2O$) and electrooxidation systems could be employed. At nearly the same time, Niu, Yang, and colleagues also demonstrated the construction of both inherently and C−N axially chiral calix[4]arenes **213** using 3-substituted pyrid-2-yl *N*-oxide directing groups (Scheme 50b).[210]

5.6.2. Enantioselective C−H [4 + 2] Annulation with Alkenes. As established by previous mechanistic investigations,[190,206] the Salox ligand coordinates to cobalt in a bidentate fasion with high fidelity within the resulting Co(III) metallacycle intermediates [e.g., *mer*-(S_c,S_p)-**Int62**] in Co(II)/Salox catalysis. This coordination mode establishes a well-defined chiral environment following C−H cleavage, thereby providing a versatile platform for realizing C−H functionalization reactions in which the enantiodetermining step occurs after the C−H metalation through judicious tuning of the Salox ligands. In

https://doi.org/10.1021/acs.chemrev.6c00255
Chem. Rev. XXXX, XXX, XXX−XXX

Scheme 43. Co(II)/CPA-Catalyzed Enantioselective Sequential C−H [4 + 1] Spirocyclization

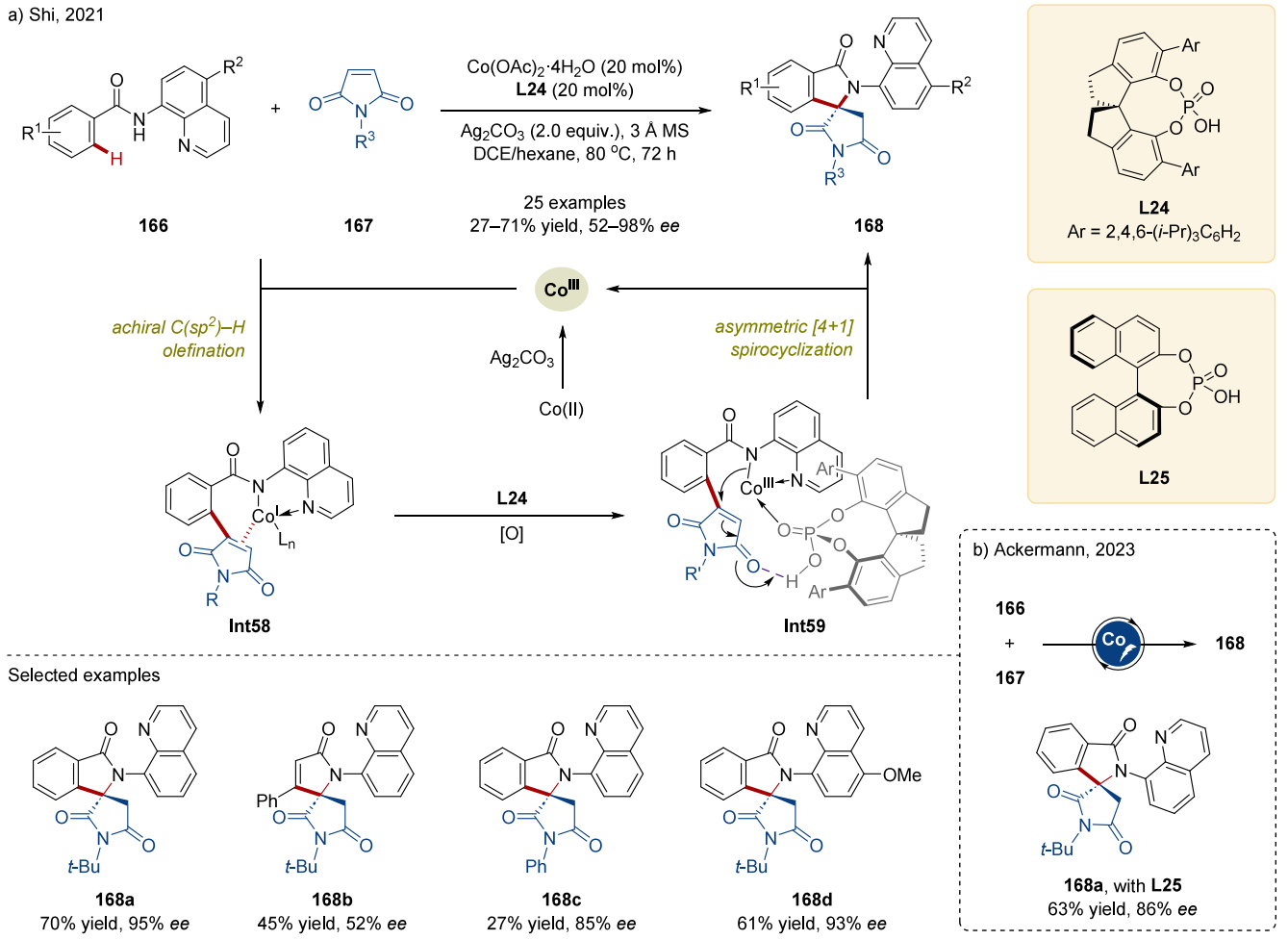

2023, our group achieved the electrooxidative Co(II)/Salox-catalyzed regio- and enantioselective C−H annulation with olefins (Scheme 51a).[211] It should be noted that this reaction was the first 3d metallaelectrocatalyzed asymmetric C−H activation. Through rational design, the chiral Salox ligand *ent*-**L31** was used to enable the stereoselective migratory insertion of alkene. The $\pi-\pi$ interaction between the oxazoline phenyl group of the Salox ligand and the quinoline motif of the benzamide facilitates the precise assembly of a chiral octahedral Co(III) intermediate **Int68**. In addition, the installation of a sterically bulky *tert*-butyl group at the *ortho*-position of phenolic hydroxyl effectively block the front direction of the cobalt complex, thereby directing olefin coordination with high precision such that the larger substituent is oriented toward the open rear side of the chiral pocket. For α-olefins, an appropriate electron-deficient pyridine ligand, 3,4,5-trichloropyridine, was essential for satisfactory regio- and enantiocontrol. A plausible role of the substituted pyridine is as a transient ligand to dynamically occupy the free coordination site in the chiral pocket.

Simultaneously, Niu, Song, Wei, and co-workers realized a similar transformation with chemical oxidants (Scheme 51b).[212] Interestingly, when styrenes are used as coupling partners, the absolute configuration of the products (e.g., **217a−c**) is opposite compared with when cyclic or heteroatom-substituted terminal alkenes are used (e.g., **217d** and **217e**), as confirmed by single-crystal X-ray analysis. Following these studies, in 2024 the Ackermann group reported a closely related cobaltaelectrocatalyzed C−H/N−H [4 + 2] annulation with alkenes to construct analogues with contiguous stereogenic elements comprising both *C*-central and axial chirality using the 7-methyl-8-aminoquinolyl group as the DG (Scheme 51c).[213]

In 2024, our group extended the scope of substrates to bridged bicyclic olefins **222** and aryl hydrazones **224**, accomplishing an unprecedented Co-catalyzed enantioselective domino C−H activation/nucleophilic [3 + 2] annulation (Scheme 52).[214] For benzamides **221**, diverse chiral [2.2.1]-bridged compounds **223** bearing four consecutive tertiary *C*-stereocenters were synthesized through an additional nucleophilic substitution to remove the 8-aminoquinolyl directing group after olefin migratory insertion. In the mechanism, coordination of the coupling partner alkene **222** to the cobaltacycle intermediate is controlled by the *ortho*-butyl Salox **L31**, which plays a vital role in enantioinduction. Recently, the Ackermann group reported the same transformation through an electrocatalysis approach.[215] When aryl hydrazones **224** were used as the substrates, we rationalized upon C−H-metalation the substrate would bind as a κ^3 (X,L,X) tridentate ligand instead of the κ^3 (X,X,L) coordination mode for quinolyl benzamides **221**, which could reverse the binding orientation of the bidentate Salox ligand due to the trans effect (Scheme 52).[214] Therefore, the residue at the α-position of the nitrogen atom on the oxazoline ring was modified judiciously, and the 1-(*tert*-butoxy)ethyl Salox **L35** showed optimal enantiocontrol.

https://doi.org/10.1021/acs.chemrev.6c00255
Chem. Rev. XXXX, XXX, XXX−XXX

Scheme 44. Co(II)/Salox-Catalyzed Enantioselective Construction of *P*-Central Chirality through $\pi-\pi$ Interactions

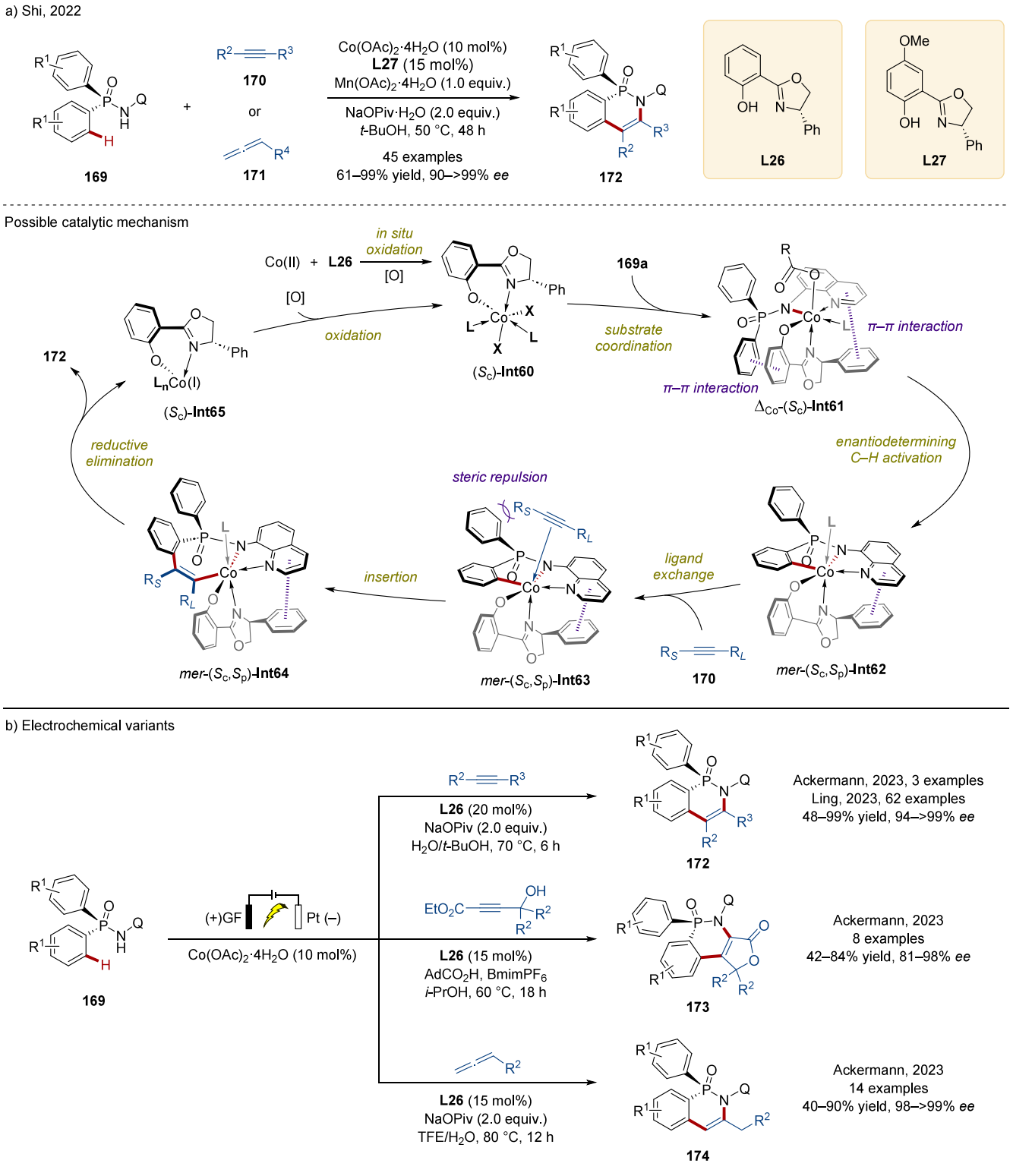

Numerous chiral polycyclic products **225** were formed after nucleophilic addition to the C═N double bond.

This Co(II)/Salox catalytic system was then found to be effective in the asymmetric dearomatization of indoles **228** through cobaltaphotoredox C−H functionalization (Scheme 53a).[216] The photocatalyst 4CzIPN is excited by white LED light to 4CzIPN*, which oxidizes the Co(II) species formed from combining $Co(OAc)_2{\cdot}4H_2O$ and **L31** *in situ*, furnishing the catalytically active trivalent cobalt catalyst to initiate the reaction. Then the ground state 4CzIPN is regenerated by oxidation with molecular oxygen of the $4CzIPN^{\bullet-}$ radical anion. The reduction byproduct, superoxide radical ($O_2^{\bullet-}$) was confirmed by EPR with 5,5-dimethyl-1-pyrroline *N*-oxide (DMPO) as the spin trap. Within the cobalt cycle, Co(III)-mediated C−H activation and indole migratory insertion sets the stage for reductive elimination, delivering the product and

https://doi.org/10.1021/acs.chemrev.6c00255
Chem. Rev. XXXX, XXX, XXX−XXX

Scheme 45. Co(II)/Salox-Catalyzed Enantioselective Construction of *P*-Central Chirality with 1-Bromoalkynes

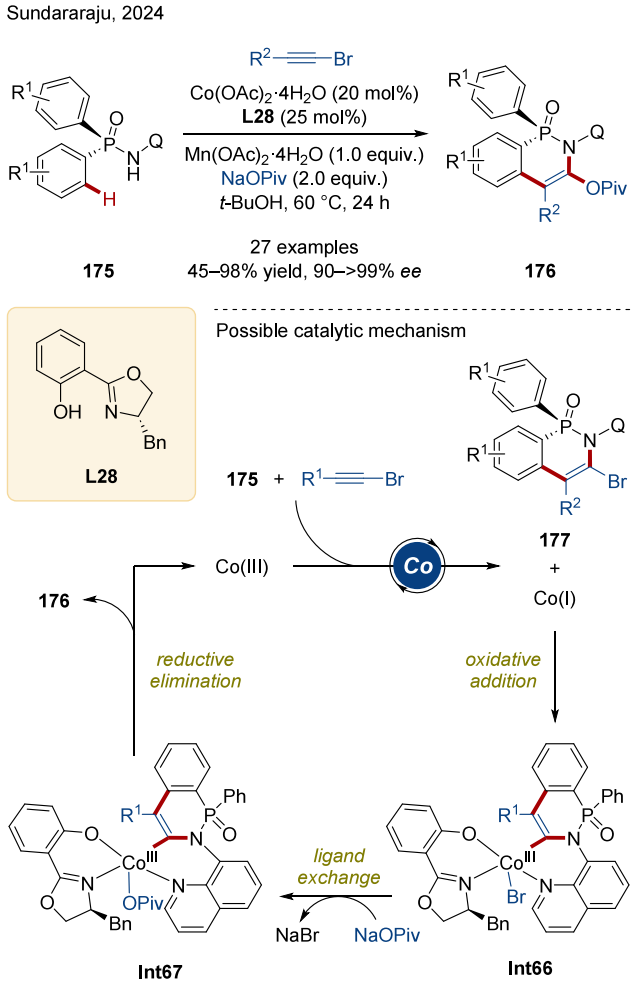

Co(I), which is then reoxidized to Co(III) by excited 4CzIPN* or reactive oxygen species (ROS). At the same time as the report from our group, this photochemical transformation was also demonstrated by the Sundararaju group[217] and the Ackermann group[198] with slightly different Salox ligands **L34** and **L30** as well as different photosensitizers Na_2EosionY and Rhodamine 6G, respectively (Scheme 53b,c).

5.6.3. Enantioselective C−H Alkoxylation, Amination, and Acyloxylation. In 2022, our group then employed the Co(II)/Salox system in the enantioselective dehydrogenative C−H alkoxylation and amination of phosphamides **229** with free alcohols and amides (Scheme 54a).[218] As revealed by mechanistic studies, the reaction is proposed to involve NaOPiv- and Ag_2CO_3-mediated generation of a key anionic alkoxy-bound Co(IV) species **Int72**, which undergoes C−O reductive elimination. This mechanism differs from the Co(III)/Co(I) redox cycle for C−H annulation with alkynes and alkenes discussed above in Section 5.6.1. The Co(II)/Co(III)/Co(IV) catalytic cycle in this case was further supported in our study on Co(II)/Salox-catalyzed electrooxidative C−H alkoxylation (Scheme 54b).[219] During the course of that study, we synthesized, isolated, and characterized an isolated neutral MeOH-ligated cyclometalated cobalt(III) complex. When this Co(III) complex was treated with various reaction components, the C−O reductive elimination product **230** was not observed unless it was oxidized to Co(IV). In 2023, the Ackermann group also followed an electrooxidative approach to couple the same substrates **229** and free alcohols with Salox **L26** (Scheme 54c).[188] Subsequently, the enantioselective dehydrogenative C−H alkoxylation of picolinamides **233** was demonstrated by us in the context of desymmetrization, KR, and PKR (Scheme 55).[220] In addition, our group, the Niu group, and the Ling group then presented the enantioselective C−H acyloxylation with carboxylic acids or carboxylates for the construction of planar chirality,[221] inherent chirality,[222] and *P*-central chirality,[223] respectively (Scheme 56). A representative transition state **TS17** for the enantiodetermining C−H activation step was depicted in Scheme 56a.

5.6.4. Enantioselective C−H [4 + 1] Annulation. In 2023, Niu, Yang, and collaborators applied isonitrile **242** as a C1 synthon, affording diverse heterobiaryl compounds **243** bearing a five−six C−N axis via atroposelective C−H [4 + 1] annulation (Scheme 57a).[224] The obtained iminoisoindolinone products **243** could be transformed to monophosphines through phosphorylation and reduction, which proved to be useful ligands in asymmetric Tsuji−Trost allylic substitution. Subsequently, our group unveiled the asymmetric synthesis of isoindolinones **245** from picolinamides **244** with carbon monoxide as a C1 source. The picolinoyl directing group could be easily removed when treated with Zn and HCl in 1,4-dioxane, giving rise to a valuable intermediate in the total synthesis of bioactive pharmaceutical molecules such as (*S*)-PD172938 **247** and (*S*)-pazinaclone **249** (Scheme 57b).[225]

5.6.5. Enantioselective C−H Arylation. In 2023, we reported a Co(II)/Salox-catalyzed atroposelective direct C−H arylation of biaryls **250** with arylboronic acids via DKR (Scheme 58).[226] In addition to the well-investigated $\pi-\pi$ interaction between picolinoyl DG and phenyl ring of the oxazoline, which mutually organizes the self-assembly of Salox ligand **L32** and picolinamide **250**, we speculated a $\pi-\pi$ interaction between the naphthyl group of **250** and the salicyl group is critical. This interaction stabilizes the favored substrate-chelated intermediate **Int74** before transannular C−H activation, the enantiodetermining step in the catalytic cycle. Then, single-electron oxidation of cobaltacycle **Int75** takes place to form a Co(IV) species, and the final arylated products **251** are generated upon reductive elimination.

5.7. Co(II)/Porphyrin Catalysis

5.7.1. Enantioselective C−H Amidation and Amination. Stimulated by the development of metal−porphyrin catalysis,[227] the Zhang group envisioned that chiral Co(II)/porphyrin complexes would open up new horizons for enantioselective C−H functionalization through metalloradical catalysis (MRC),[17d,228] a special case of radical rebound catalysis.[17b] In 2017, a preliminary study of enantioselective C−H amidation using a chiral porphyrin-chelated cobalt species was conducted by de Bruin and colleagues with a single example, in which the product was obtained in low yield (22%) and enantiomeric excess (46% *ee*).[229] Subsequently, with their experience in MRC-enabled nonstereoselective C−H amidation,[17d,230] Zhang and co-workers reported a robust enantioselective intramolecular C(sp^3)−H amination/1,6-cyclization of sulfamoyl azides **252** that proceeded with high enantioselectivities with a D_2-symmetric chiral Co(II)/amidoporphyrin catalyst **Co5** (Scheme 59a).[231] The cyclic sulfamide products **253** could be transformed to chiral α,γ-diaminobutyric acid esters after desulfonylation. In 2019, the same group achieved intramolecular enantiodivergent 1,5-amination of secondary

https://doi.org/10.1021/acs.chemrev.6c00255
Chem. Rev. XXXX, XXX, XXX−XXX

Scheme 46. Co(II)/Salox-Catalyzed Enantioselective Construction of C−Central Chirality and Its Application in Total Synthesis

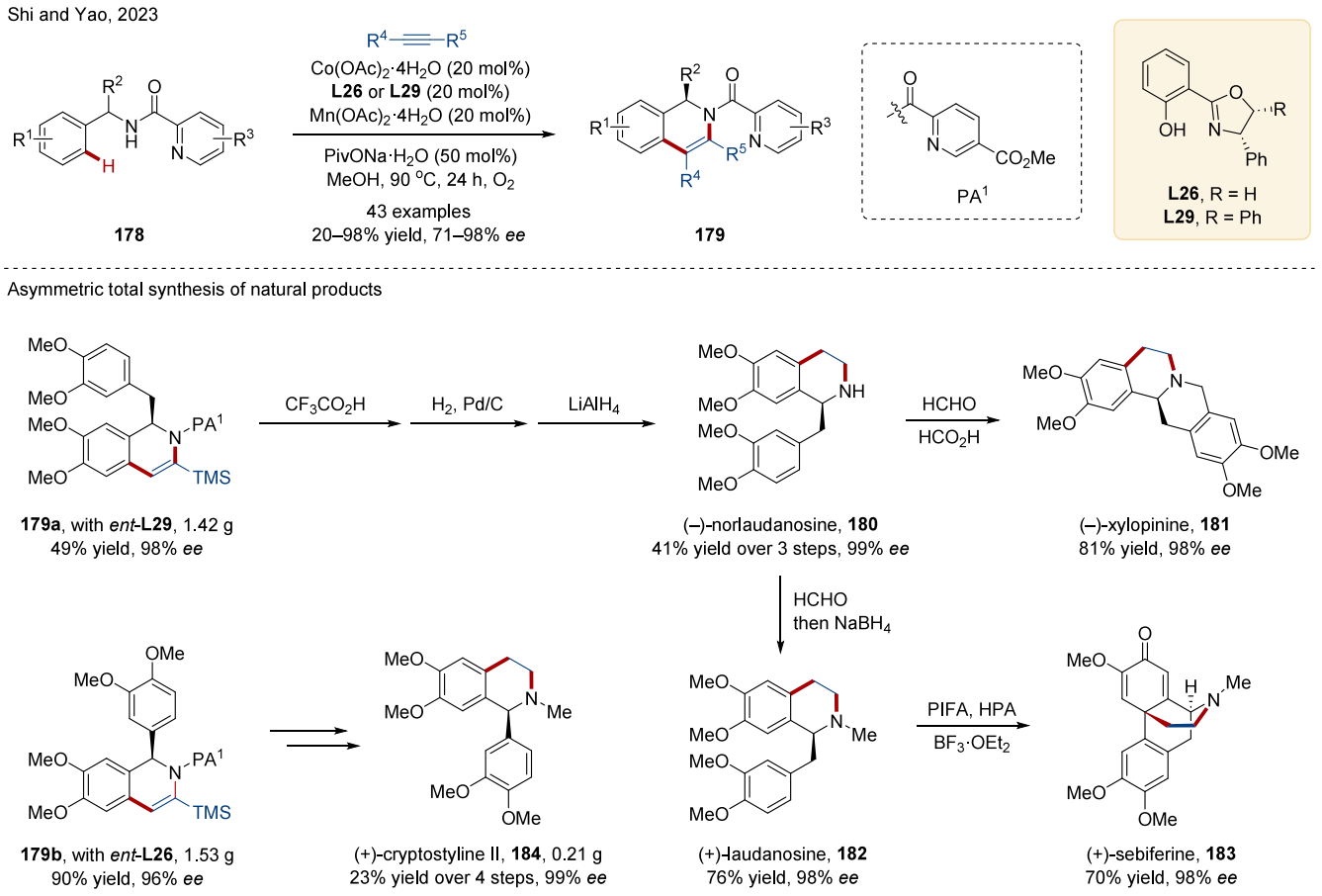

prochiral C(sp^3)−H bonds in sulfamoyl azides **254** (Scheme 59b).[232] Intriguingly, the absolute configuration of the amidated products **255** could be reversed by changing the bridge length and remote nonchiral substituents of the distal-linked D_2-symmetric chiral amidoporphyrin,[233] offering completely different chiral environment for enantiodifferentiative HAA process. The DKR of racemic sulfamoyl azides *rac*-**256** was then demonstrated via intramolecular enantioconvergent amination of tertiary C(sp^3)−H bonds, in which radical substitution was identified as the major enantiodetermining step (Scheme 59c).[234] Meanwhile, the intramolecular regio- and enantioselective metalloradical C−H amination of alkoxysulfonyl azides **258** (Scheme 59d),[235] **260** (Scheme 59e),[236] arylsulfonyl azides **264**, and alkylsulfonyl sulfonamides **266** (Scheme 60)[237] was also realized by the Zhang group. In these transformations, irrespective of whether the process proceeds through 1,5-HAT or 1,6-HAT, the C−H amination/cyclization consistently occurs at the benzylic, allylic, or propargylic position.

In 2020, Zhang and colleagues achieved intermolecular enantioselective benzylic C−H amination of arylactate esters, arylcrotonate esters, and aryltetrolate esters **268** with electron-deficient aryl azides **269** through Co(II)/porphyrin-based MRC (Scheme 61a).[238] The synergy of multiple noncovalent interactions among substrates **268**, azides **269**, and cobalt complex **Co11** is indispensable for this transformation. Subsequently, the same group also disclosed a more challenging intermolecular enantioselective allylic C−H amination of an isomeric mixture of alkenes **271** prepared by Horner−Wadsworth−Emmons reaction (Scheme 61b).[239] The DFT analysis exposed three key noncovalent interactions that give rise to excellent enantioinduction: a two-point hydrogen-bonding interaction between substrate **271** and the cobalt catalyst, a two-point hydrogen-bonding interaction between the azide **269** and the cobalt catalyst, and a $\pi-\pi$ stacking interaction between the substrate **271** and the azide **269**.

5.7.2. Enantioselective C−H Alkylation. Diazo compounds and hydrazones are ideal carbene precursors in metal catalysis. In 2015, Zhang and co-workers uncovered an enantio- and diastereoselective synthesis of sulfolanes **274** featuring two adjacent tertiary *C*-stereogenic centers from α-methoxycarbonyl-α-diazosulfones **273** through desymmetrization of prochiral benzylic, allylic, and allenic C−H bonds (Scheme 62a).[240] Regarding the origins of stereoinduction, two N−H···O hydrogen-bonding interactions between the sulfuryl and carbonyl groups on substrates **273** and amide moiety on the porphyrin ring in the α-Co(III)-alkyl radical intermediate were proposed, explaining the ligand acceleration effects observed in this reaction. Encouraged by the previously described non-stereoselective transformation,[241] the Zhang group later reported another intramolecular enantioselective C(sp^3)−H 1,5-alkylation of arylaldehyde-derireved hydrazones **275** for the construction of indolines **276** (Scheme 62b),[242] as well as an analogous transformation of alkylaldehyde-derived hydrazones **277** (Scheme 62c).[243] Additionally, in 2021 the authors also demonstrated the more difficult metalloradical C−C annulation via enantioselective benzylic 1,4-HAA through use of the bridge-linked catalyst **Co6**. This method offers a convenient approach

https://doi.org/10.1021/acs.chemrev.6c00255
Chem. Rev. XXXX, XXX, XXX−XXX

Scheme 47. Co(II)/Salox-Catalyzed Enantioselective Construction of C−N Axial Chirality

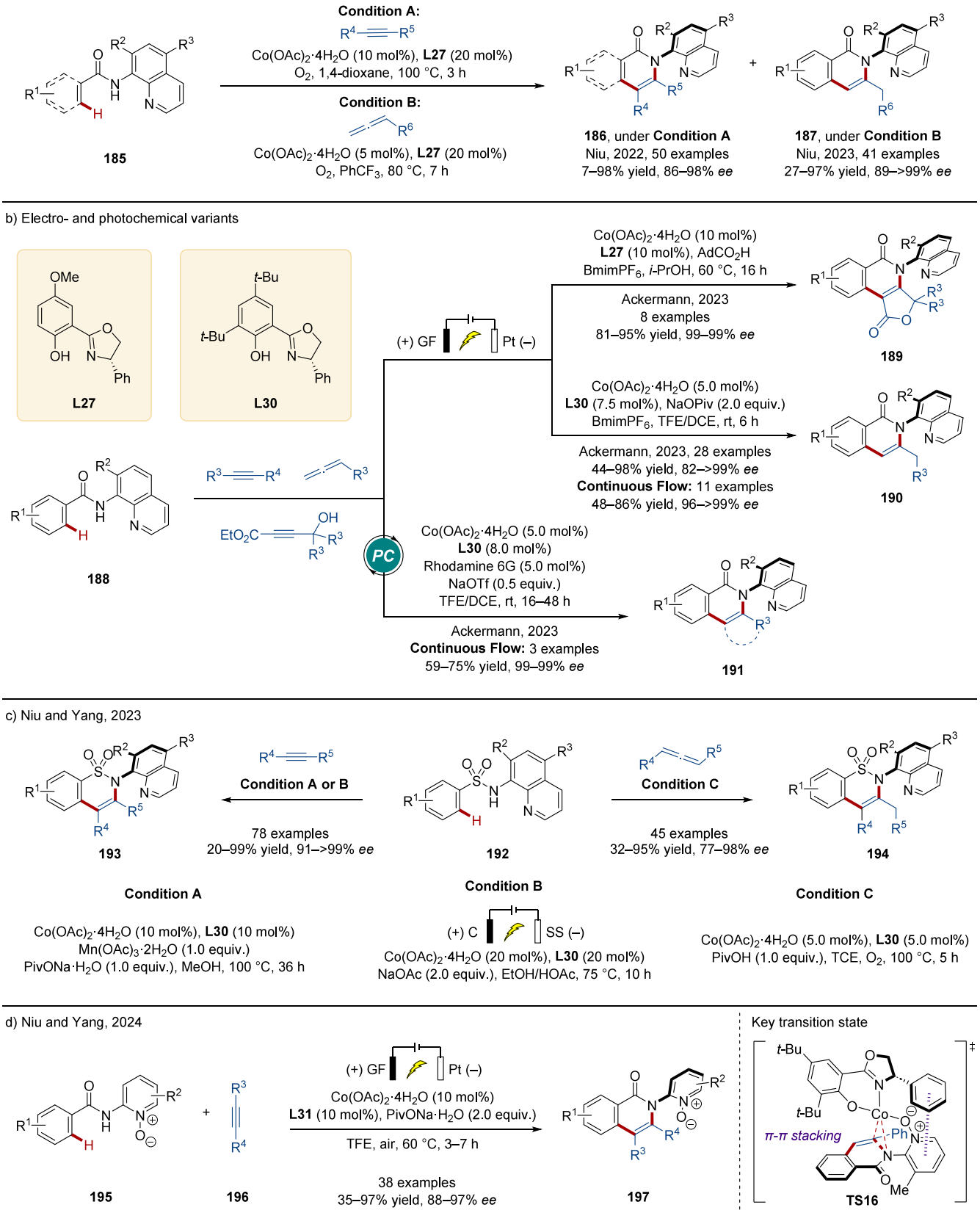

to highly strained α,β-chiral cyclobutanones **280** (Scheme 62d).[244]

https://doi.org/10.1021/acs.chemrev.6c00255
Chem. Rev. XXXX, XXX, XXX−XXX

Scheme 48. Co(II)/Salox-Catalyzed Enantioselective Construction of N−N Axial Chirality

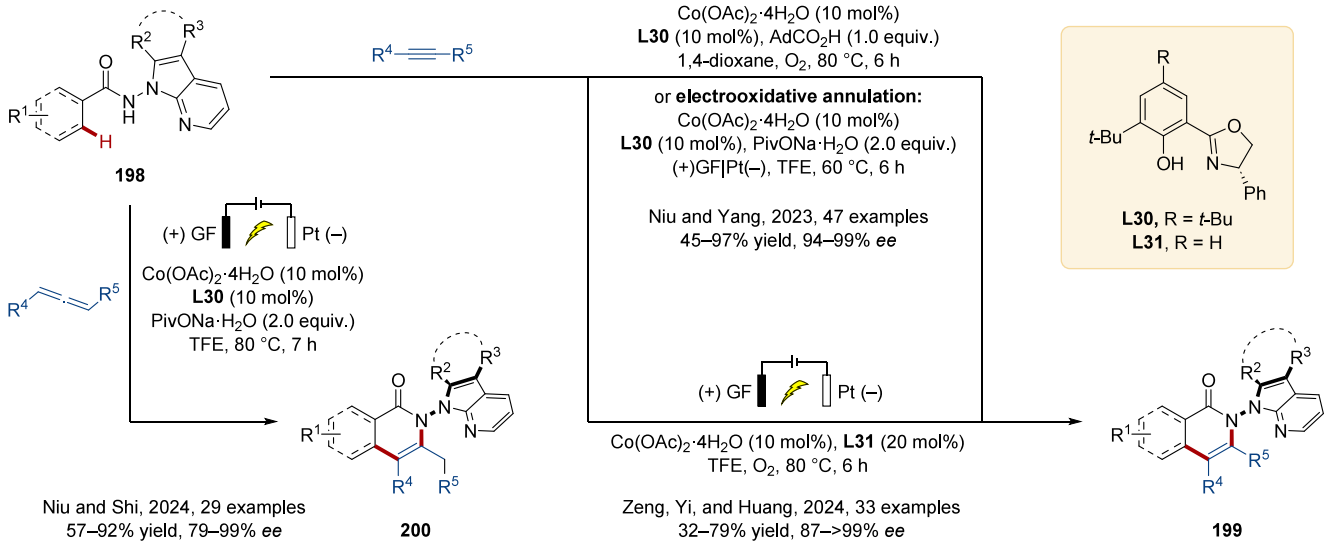

Gram scale and synthetic applications (Niu and Yang, 2023)

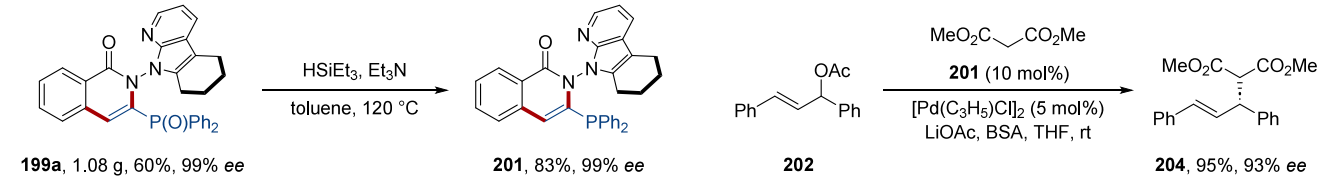

199a, 1.08 g, 60%, 99% *ee* **201**, 83%, 99% *ee* **202** **204**, 95%, 93% *ee*

Scheme 49. Co(II)/Salox-Catalyzed Enantioselective Construction of Diaxial Chirality

a) Shi and Yao, 2022

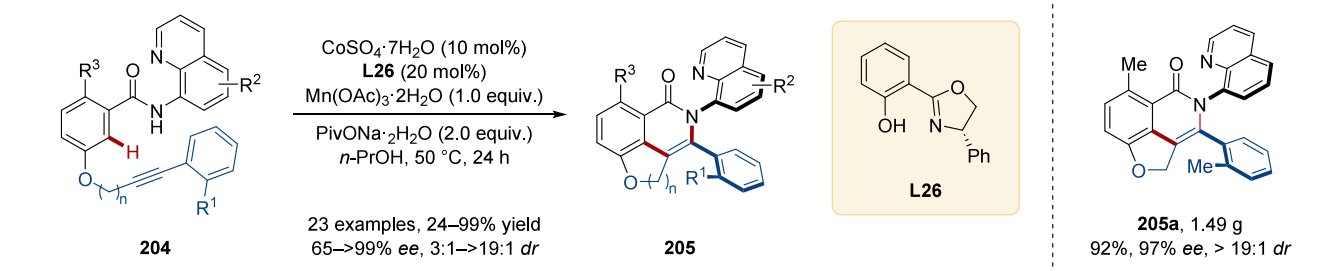

204 205

Gram-scale synthesis

205a, 1.49 g
92%, 97% *ee*, > 19:1 *dr*

b) Shi, 2025

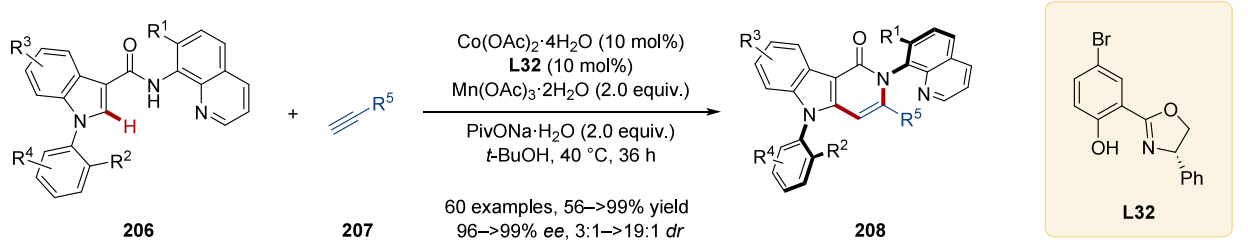

206 207 208

6. NICKEL CATALYSIS

Nickel is a promising and cost-effective alternative to its group 10 counterpart, palladium, due to its significantly higher abundance in the earth's crust.[97] As a catalyst, nickel exhibits a distinct reactivity profile, making it useful in diverse reactions, including difunctionalization of alkenes and alkynes,[245] cross-coupling,[16a,246] and metallaphotoredox radical chemistry.[246d,247] The breadth of catalytic reactivity stems from its ability to smoothly undergo one- and two-electron redox processes, thereby easily toggling among various oxidation states from 0 to +3 and participating in Ni(0)/Ni(II), Ni(I)/Ni(III), and Ni(I)/Ni(II)/Ni(III) catalytic cycles.[245b,246e,247b,248] In 1963, Dubeck isolated a five-membered nickelacycle from azobenzene and nickelocene via C−H metalation.[249] That early contribution set the stage for the eventual development of nickel-catalyzed C−H functionalization reaction. With especially rapid progress in recent years,[15b,250] catalytic enantiose-

https://doi.org/10.1021/acs.chemrev.6c00255
Chem. Rev. XXXX, XXX, XXX−XXX

Scheme 50. Co(II)/Salox-Catalyzed Enantioselective Construction of Inherent Chirality

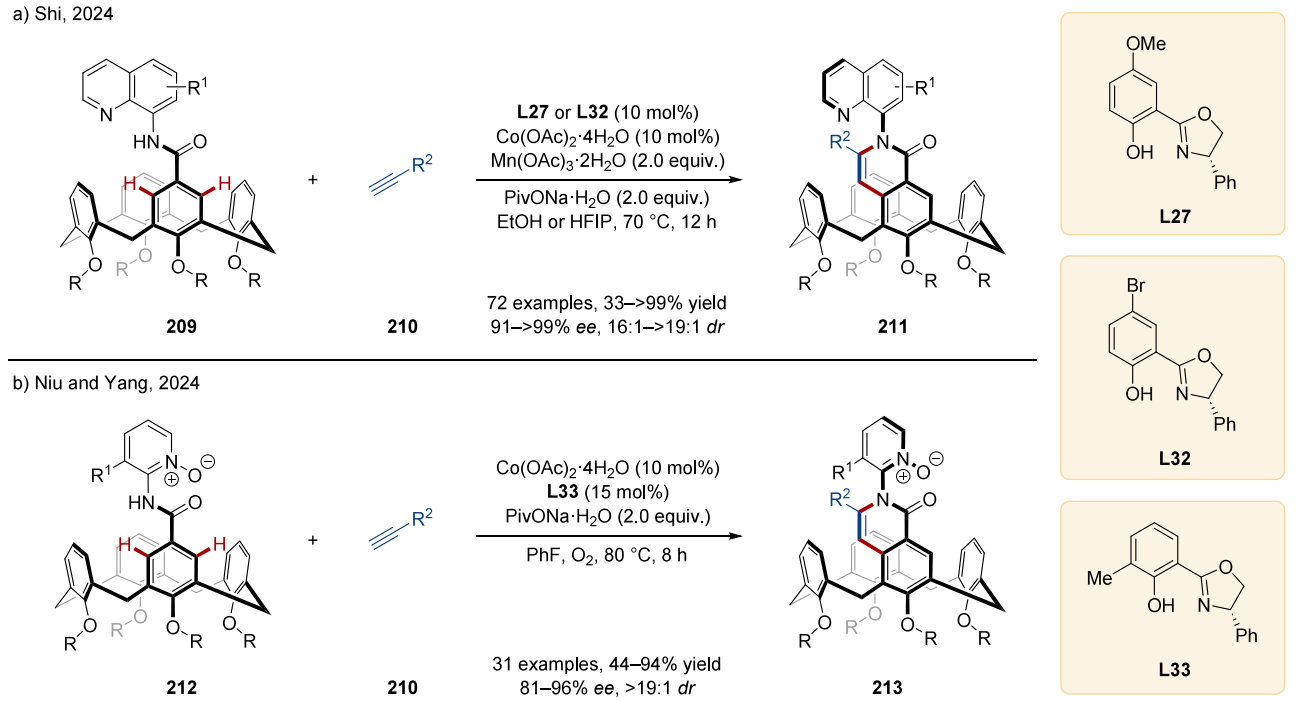

Scheme 51. Co(II)/Salox-Catalyzed Enantioselective C–H Annulation with Olefins

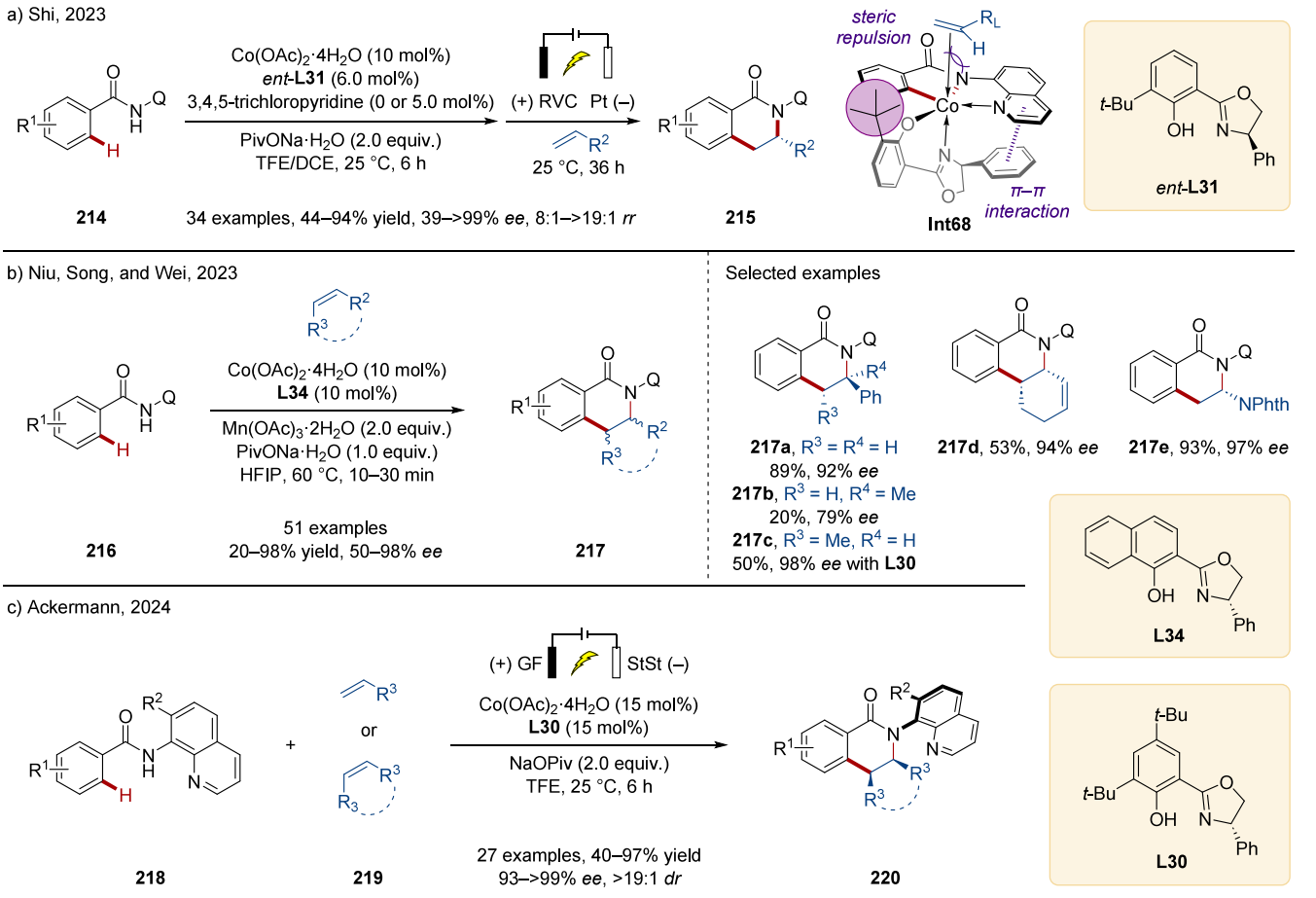

lective Ni-catalyzed C–H functionalization reactions have been enabled by the evolution of a growing collection of effective chiral ligands, including secondary phosphine oxide (SPO), NHC, BINOL, Salox, and BOX ligands and their derivatives, which have found applications in both inner-sphere C–H metalation and outer-sphere radical relay mechanisms.[251]

https://doi.org/10.1021/acs.chemrev.6c00255
Chem. Rev. XXXX, XXX, XXX–XXX

Scheme 52. Co(II)/Salox-Catalyzed Enantioselective C−H Nucleophilic Annulation with Bridged Bicyclic Olefins

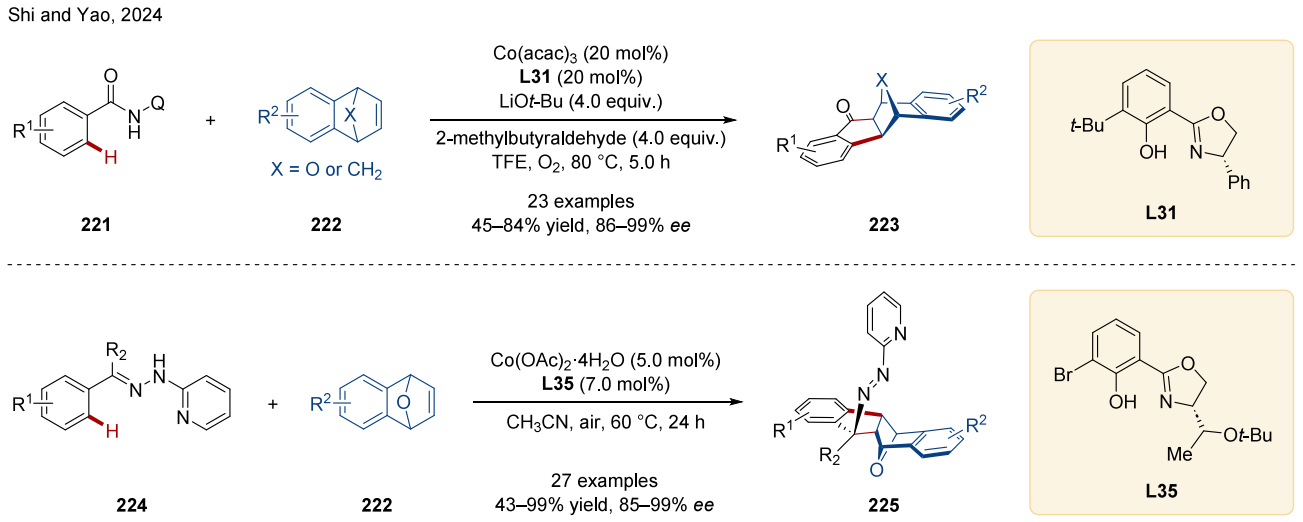

Scheme 53. Co(II)/Salox-Catalyzed Photoredox Enantioselective C−H Annulation

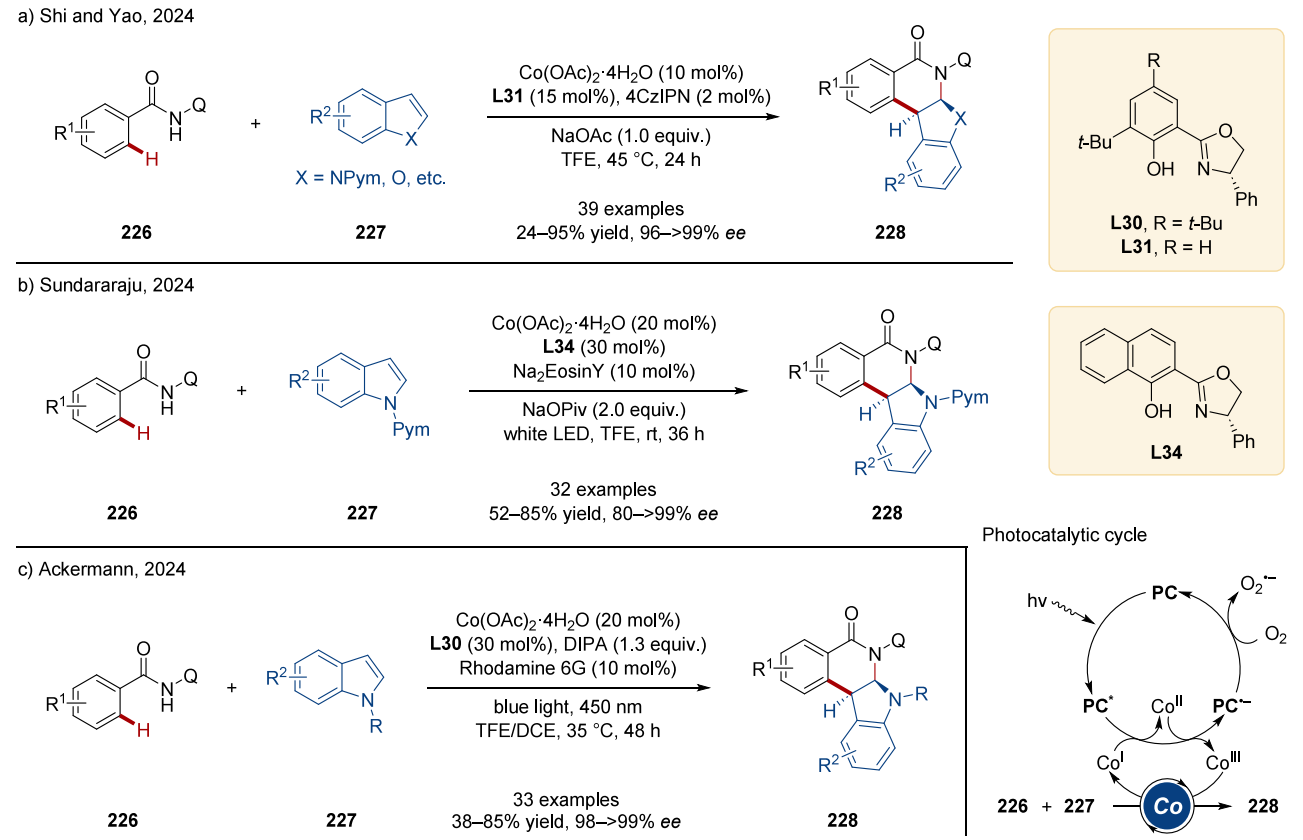

6.1. Ni(0)/SPO Catalysis

6.1.1. Intramolecular Asymmetric C−H Annulation. Building on Nakao and Hiyama's earlier work,[252] the Cramer group applied air- and moisture-stable chiral secondary phosphine oxide (SPO) ligands[253] in Ni(0) catalysis, achieving the first nickel-catalyzed enantioselective C−H activation of alkenyl formamides **281** in 2013 (Scheme 63a).[254] A bimetallic strategy[255] was used in this process, with a catalytic amount of the hard Lewis acid, $AlMe_3$, acting as a bridge between the oxygen-atom of the phosphinous acid tautomer of the SPO ligand **L33** and the carbonyl group of the substrate **281**, accelerating the insertion of nickel(0) into the formamide C−H bond. Diverse α-tertiary *C*-chiral pyrrolidones **282** were synthesized in moderate to excellent yields and enantioselectivities. To probe the reaction mechanism, deuterated formamide **281a** was tested, and complete deuterium transfer was observed. Recently, Ye, Huang, and co-workers reported the asymmetric construction of γ-lactams **284** featuring an α-quaternary *C*-stereogenic center via C−H annulation (Scheme 63b).[256]

Beyond formamide C−H bonds, the Ye group demonstrated an enantioselective C−H *exo*-selective alkylation/cyclization of imidazoles **285** containing an intramolecularly tethered C═C

https://doi.org/10.1021/acs.chemrev.6c00255
Chem. Rev. XXXX, XXX, XXX−XXX

Scheme 54. Co(II)/Salox-Catalyzed Enantioselective C−H Alkoxylation and Amination

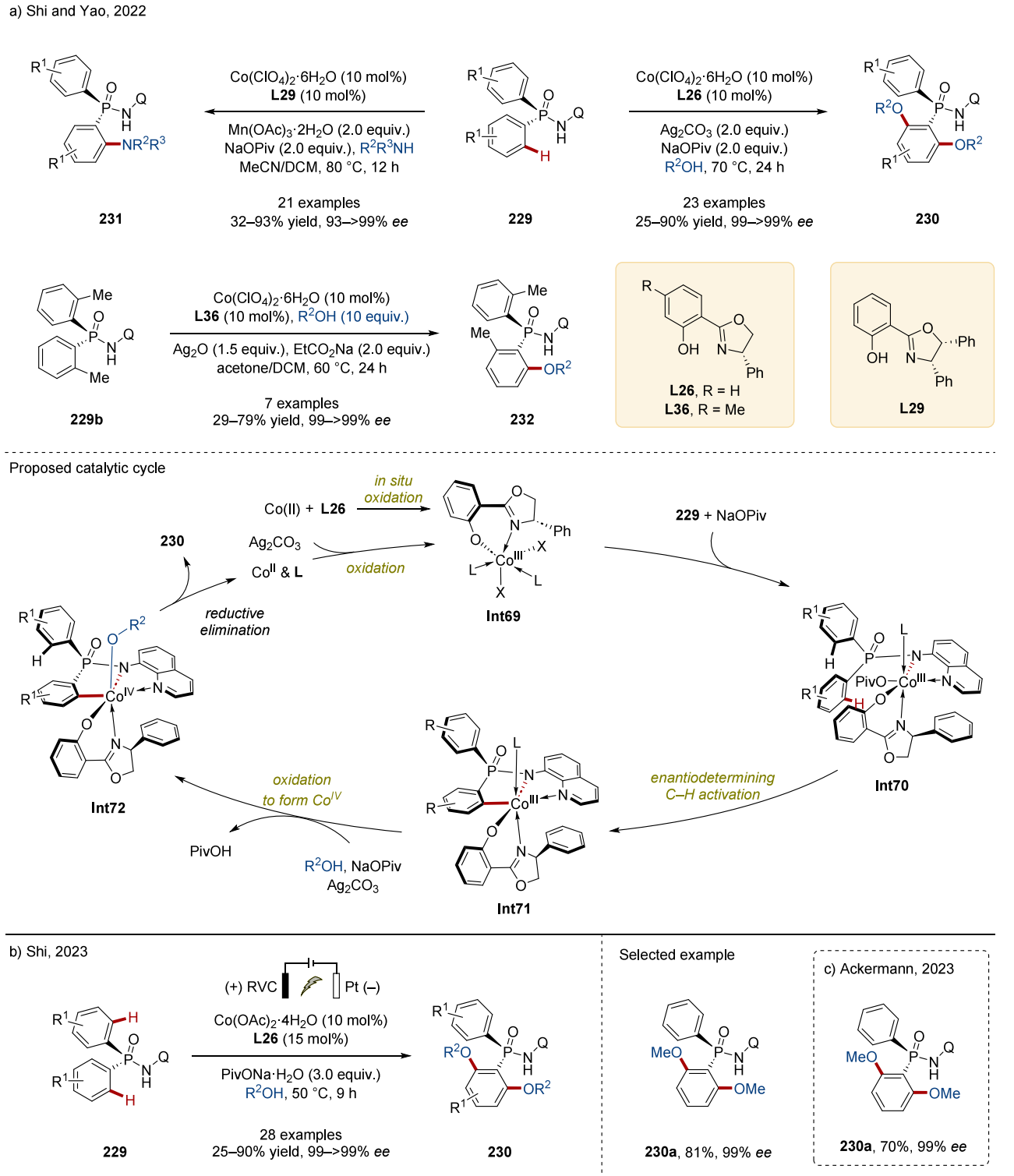

bond via Ni−Al bimetallic catalysis with Taddol-based SPO ligand **L35** (Scheme 64a).[257] Similarly, the reaction begins with generation of an active phosphine oxide-ligated Ni−Al bimetallic complex, and the C−H bond is cleaved through an LLHT or oxidative addition mechanism. This reaction takes place at a lower reaction temperature compared with an analogous rhodium-catalyzed system.[258] In 2023, Qiu and colleagues then realized the Ni−Al-catalyzed C−H *exo*-annulation of 4-oxoquinazolines **287** (Scheme 64b).[259] When trimethylaluminum was removed from this catalytic system and JoSPOphos **L39** was used as ligand,[260] another nickel-catalyzed asymmetric C−H alkylation/cyclization of imidazoles **289** was achieved with reversed *endo*-selectivity (Scheme 64c).[261]

6.1.2. Intermolecular Asymmetric C−H Alkylation. The Ni−Al bimetallic catalysis has also been employed for the intermolecular enantioselective C−H alkylation with 1,3-dienes **292** by Ye, Huang, and colleagues in 2022, in which a C_1-symmetric SPO **L40** was used as the chiral ligand (Scheme

https://doi.org/10.1021/acs.chemrev.6c00255
Chem. Rev. XXXX, XXX, XXX−XXX

Scheme 55. Co(II)/Salox-Catalyzed Enantioselective C−H Alkoxylation of Picolinamides

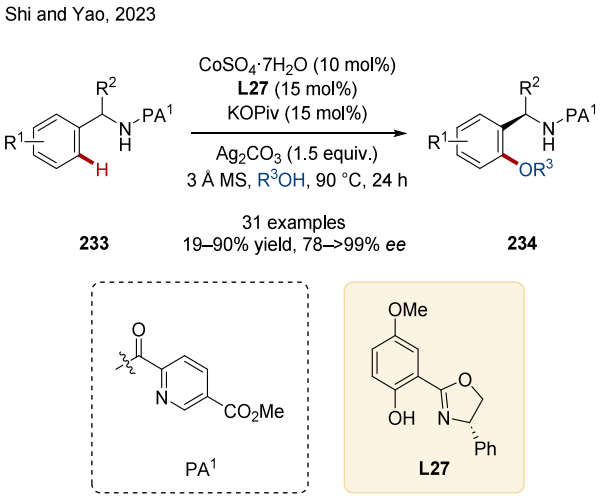

65a).[262] As revealed by DFT calculations, the C2−H activation of pyridines **291** proceeds via a reversible LLHT mechanism, in which the hydrogen atom is transferred to the 1,3-diene **292** after the coordination of pyridine nitrogen to aluminum. This step is followed by rapid isomerization of the allylnickel intermediate from η^1 to η^3 coordination. The subsequent C−C reductive elimination step is the turnover-limiting and enantiodetermining step. A C−H···π interaction between the phenyl group of the 1,3-diene **292** and the *N*-aryl moiety on the SPO ligand **L40** was found to stabilize the favored transition state **TS18**, while steric repulsion between the allylic framework and the Ni−Al bimetallic catalyst was observed in the disfavored diastereomeric transition state. In 2024, Ackermann, Hong, and collaborators disclosed a bimetallic Ni−Al/SPO-catalyzed linear-selective atroposelective C−H alkylation of benzimidazoles **294** to establish a chiral C−N axis (Scheme 65b).[263] 1,3-Dienes were also suitable for this reaction, generating the branch-alkylated products such as **296b** with excellent enantio- and diastereoselectivities.

6.1.3. Enantioselective C−H Olefination. In 2020, the Ye group demonstrated a Ni−Al/SPO-catalyzed twofold enantioselective C−H activation/annulation of ferrocene formamides **297** with alkynes **298** (Scheme 66a).[264] After the formation of a Ni−H species through oxidative addition of the formyl C−H bond, migratory insertion of the alkynes **298** occurs, generating the key intermediate **Int79**. The bicyclic nickel complex **Int80** is obtained through a second C−H activation step, with the ferrocenyl C−H bond cleaved enantioselectively through an S_EAr mechanism,[265] as mediated by the SPO ligand **L42**. Direct C−C reductive elimination byproducts are detected with other SPO ligands. In 2022, building on their previous non-stereoselective transformations,[266] a variety of dihydropyridones **302** were synthesized from formamides **300** and alkynes **301** (Scheme 66b).[267] A formyl C−H activation of Ni−Al complex

Scheme 56. Co(II)/Salox-Catalyzed Enantioselective C−H Acyloxylation

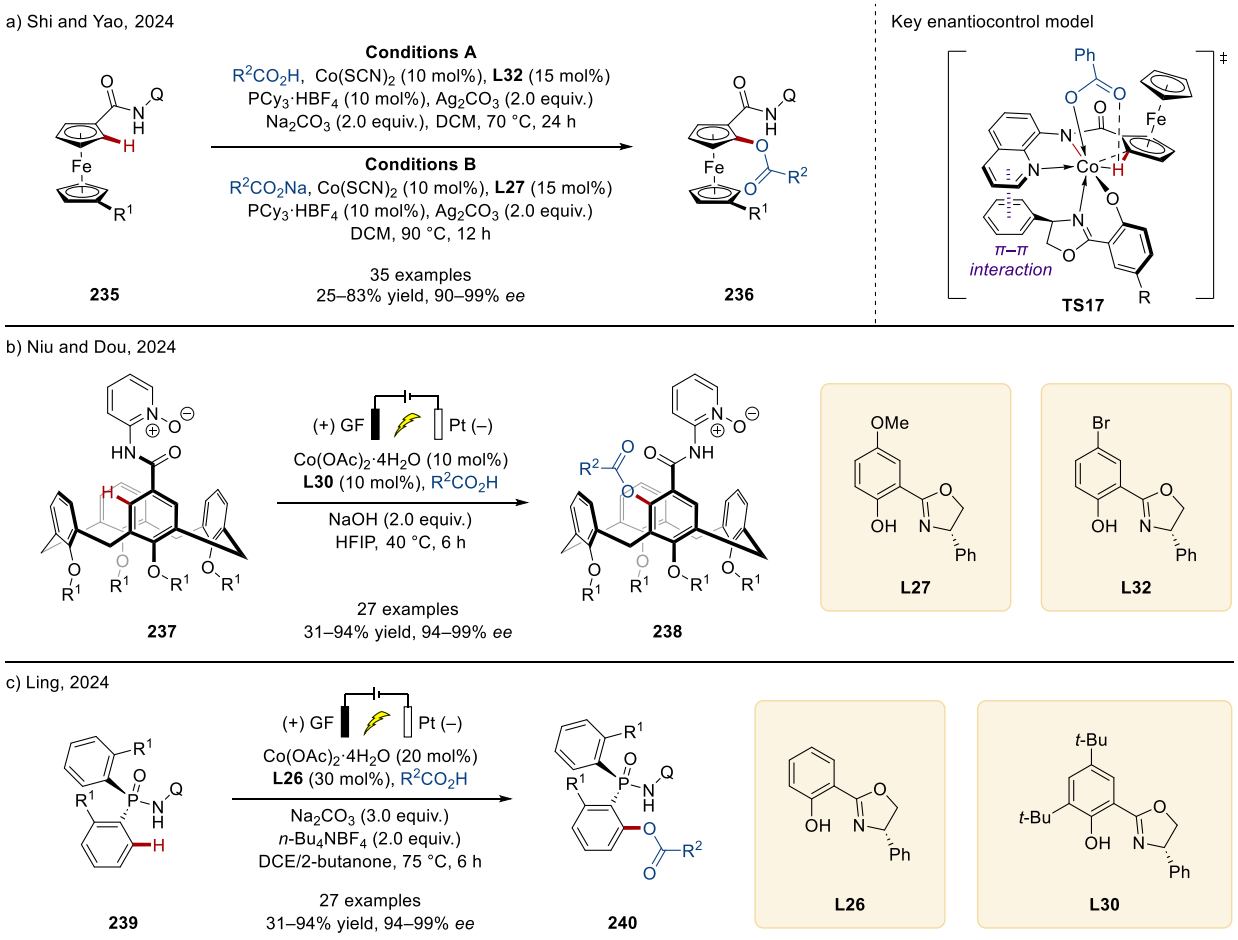

https://doi.org/10.1021/acs.chemrev.6c00255
Chem. Rev. XXXX, XXX, XXX−XXX

Scheme 57. Co(II)/Salox-Catalyzed Enantioselective C−H [4 + 1] Annulation

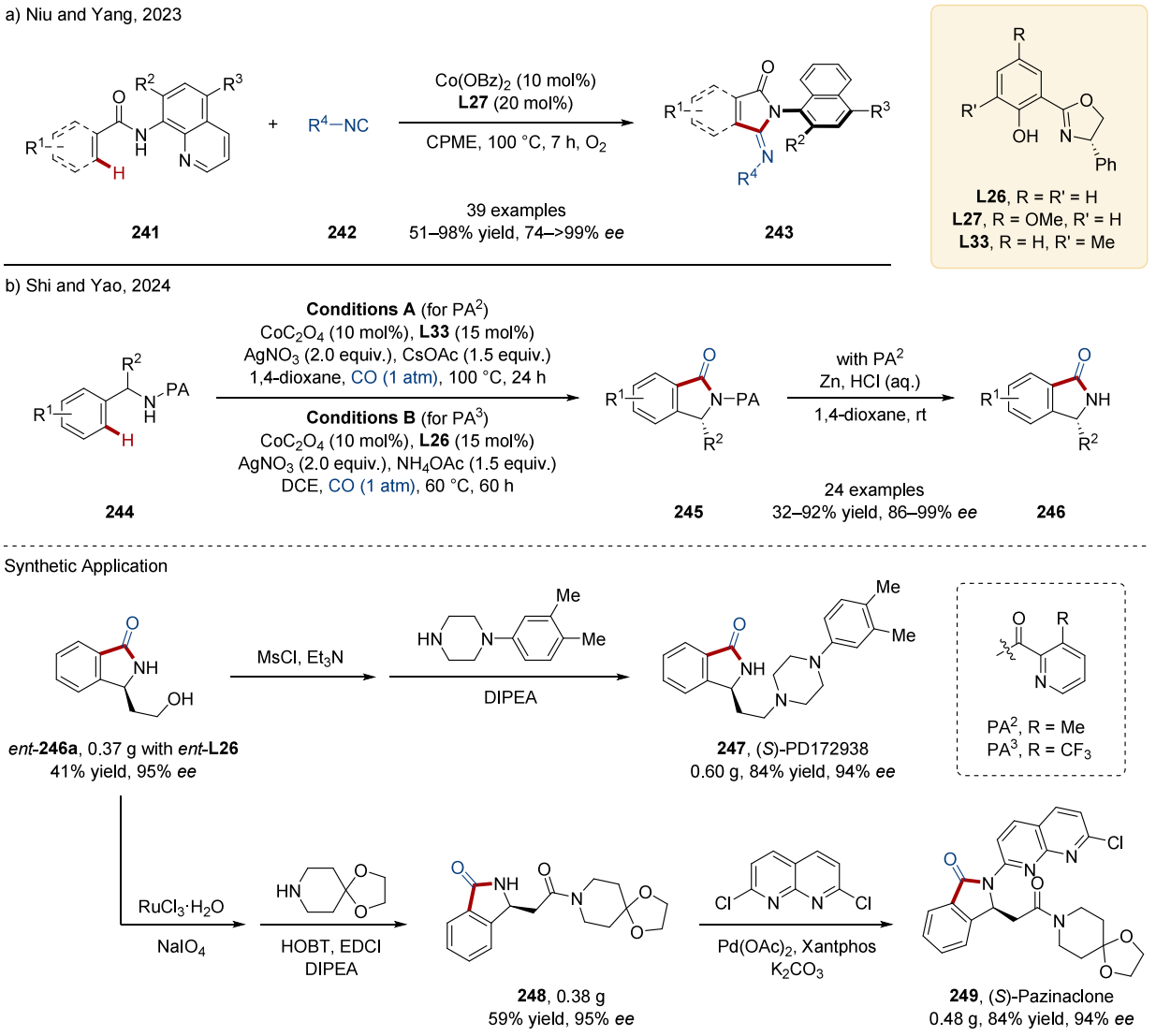

Int81 takes place via an LLHT or oxidative addition mechanism with a H_8−BINOL-derived SPO **L43**, and subsequent turnover-limiting and enantiodetermining methyl or methylene C(sp^3)−H annulation then forms the target products **302**.

6.2. Ni(0)/NHC Catalysis

6.2.1. Intramolecular Asymmetric C−H Annulation. NHC ligands, well established in nickel catalysis, have also proven to be powerful purveyors of stereochemistry in Ni(0)-catalyzed enantioselective C−H functionalization.[124,268] In 2015, the Cramer group observed a preliminary result of 57% *ee* with a C_1-symmetric chiral NHC ligand[269] in their research of ligand-controlled regiodivergent Ni-catalyzed C−H *exo*- or *endo*-annulation of pyridones.[270] By further optimization of reaction conditions, Cramer and co-workers found that, the combination of a bulky NHC ligand **L44** designed by Gawley[271] and a bulky organoaluminum cocatalyst MAD developed by Yamamoto,[272] was highly effective in this Ni(0)/NHC-catalyzed intramolecular C−H alkylation of 2- or 4-pyridones **303**, affording *endo*-annulated products **304** in moderate to excellent yields and enantioselectivities (Scheme 67a).[273] Nevertheless, this methodology proved ineffective for the modulation of *C*-central chirality at the *α*-position of pyridones, such as **304b**, which was obtained in a completely racemic form. A similar transformation has also been achieved with a slightly modified NHC precursor **L45** for improved reactivity and enantiocontrol by Xu, Shi, and colleagues.[274]

In 2019, the Shi group and the Cramer group then independently realized the Ni-catalyzed enantioselective C−H alkylation/cyclization of pyridines **305** (Scheme 67b)[275] and indoles **307** (Scheme 67c)[276] with **L45** and **L46**, respectively. Interestingly, in Shi's report, the C4−H bond was activated selectivity with substrates **305** containing an alkenyl chain tethered at the C3 position. The excellent regioselectivities in this case might be caused by the coordination of nitrogen-atom on the pyridine skeleton to the bulky organoaluminum cocatalyst MAD, as illustrated in **TS19**, which would block the C2−H bond. Beyond heteroarenes, a nickel/NHC-catalyzed enantioselective C−H *endo*-annulation of polyfluoroarenes **309** was disclosed contemporaneously by Shi and collaborators, allowing access to a broad range of enantioenriched fluorotetralins **310** in high yields with outstanding enantioselectivities (Scheme 67d).[277]

6.2.2. Intermolecular Asymmetric C−H Alkylation. In 2016, Cramer and co-workers demonstrated a Ni-catalyzed three-component reductive coupling/C−H alkylation of

https://doi.org/10.1021/acs.chemrev.6c00255
Chem. Rev. XXXX, XXX, XXX−XXX

Scheme 58. Co(II)/Salox-Catalyzed Enantioselective C−H Arylation

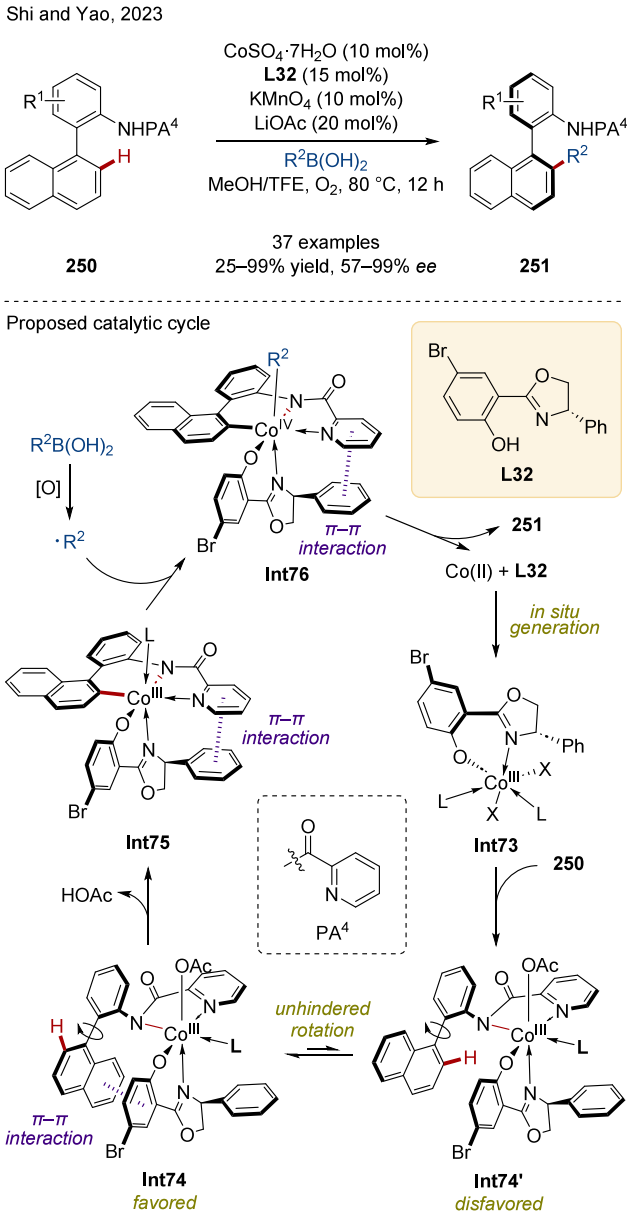

aromatic aldehydes **311** with norbornenes **312** and silanes **313** (Scheme 68).[278] Since an NHC ligand was found to be essential in the previous nonstereoselective version of the reaction,[279] the authors designed a bulky chiral C_2-symmetric NHC **L47**, which takes inspiration from a chiral imidazolidin-2-ylidene that was previously employed enantioselective ruthenium-catalyzed ring-closing metathesis with Grubbs-type catalysts.[280] The catalytic system provided good enantiocontrol with high reactivity, generating polycyclic indanol derivatives **314** containing five continuous tertiary *C*-stereocenters as single diastereoisomers. Intriguingly, one equivalent of the norbornene **312** serves as sacrificial oxidant, undergoing hydrometalation with Ni−H species **Int85** and then accepting a hydrogen atom from the aryl group bond upon C−H activation, while noncyclized side products **316** are formed via direct reductive elimination in some instances.

6.3. Ni(II)/BINOL Catalysis

Though Ni(0)-catalyzed enantioselective C−H functionalizations have steadily grown in prominence, the use of highly toxic, air- and moisture-sensitive, and flammable $Ni(cod)_2$ as well as organoaluminum cocatalysts still limits their practical utility in stereoselective synthesis of functional molecules. In 2024, our group devised a novel approach to high-valent nickel(II)-catalyzed enantioselective C−H functionalization, developing the enantioselective C−H alkynylation of ferrocenes **317** with alkynyl bromides **318** using simple, unadorned BINOL **L48** as a ligand (Scheme 69).[281] Both desymmetrization and KR were possible with this transformation, offering numerous functionalized planar chiral ferrocenes **319** as well as ruthenocene **319c** in high yields and excellent enantioselectivities (90−99% *ee*). When the enantioenriched undeuterated substrate (*R*)-**317a** was alkynylated under standard conditions, the excellent diastereoselectivity (98% *de* with **L48** and >99% *de* with *ent*-**L48**) indicated that the stereocontrol is not affected by existing planar chirality, and the chemical shifts of H_a and H_b on **317a** in ^{1}H NMR were assigned at the same time. We then carefully designed a set of diastereoselective H/D scrambling experiments to further elucidate the origins of enantioselectivity. Interestingly, only the D_a atom at "a" position of (*R*)-d_2-**317a** was exchanged by H atom when **L48** was used as the ligand (right arrow), while only a significant loss of deuterate ratio of H_b in (*R*)-d_a-**317a** was detected with *ent*-**L48** (left arrow). These results are consistent with a scenario in which reversible C−H cleavage is the enantiodetermining step. A pair of pyridine-stabilized nickelacycle enantiomers were also isolated, which could be alkynylated to (*R*)-**319b** or (*S*)-**319b**, respectively in stoichiometric experiments. The structure of this air-stable planar chiral nickelacycle **Ni1** was subsequently elucidated by single-crystal X-ray diffraction with 1,8-diazabicyclo[5.4.0]-7-undecene (DBU) as the neutral axial stabilizing ligand. Based on in-depth mechanistic experiments and previous reports,[282] we proposed a mechanism in which enantioselective C−H activation of the ferrocene substrate **317** proceeds via a CMD process with the binaphtholate ligand as internal base as shown in **TS20** to generate the enantioenriched planar chiral nickelacycle. The following oxidative addition of the alkynyl bromide coupling partner **318** and C−C bond reductive elimination then delivers the final product **319**.

6.4. Ni(II)/Salox Catalysis

Leveraging our prior insights into coordination and enantiocontrol modes of Salox ligands in cobalt catalysis,[133d,190] in 2025 we adopted several chiral Salox ligands containing a bulky substituent at the 6-position of salicyl moiety in nickel(II)-catalyzed C−H alkylation/annulation with oxabicyclic alkenes **321** (Scheme 70).[283] In contrast to the reaction outcomes observed with the Co(II)/Salox catalytic system discussed above (Scheme 52), where domino C−H alkylation/nucleophilic [3 + 2] annulation was observed under similar conditions,[214] here direct C−N reductive elimination was observed, allowing chemodivergent access to enantioenriched [2,2,1]-bridged bicyclic molecules. A DBU-stabilized achiral C−H-metalated Ni(II) species and a Salox-chelated chiral trivalent nickelacycle **Int93** were isolated and characterized by single-crystal X-ray diffraction. Treatment of stoichiometric Ni(III) complex **Int93** with the olefin **321** in the absence of the Ag(I) oxidant furnished the desired product in 52% yield and 96% *ee* (compared to 64% yield and 96% *ee* with $EtCO_2Ag$), excluding the intermediacy of a Ni(IV) species in the subsequent

https://doi.org/10.1021/acs.chemrev.6c00255
Chem. Rev. XXXX, XXX, XXX−XXX

Scheme 59. Co(II)/Porphyrin-Catalyzed Intramolecular Enantioselective C−H Amidation

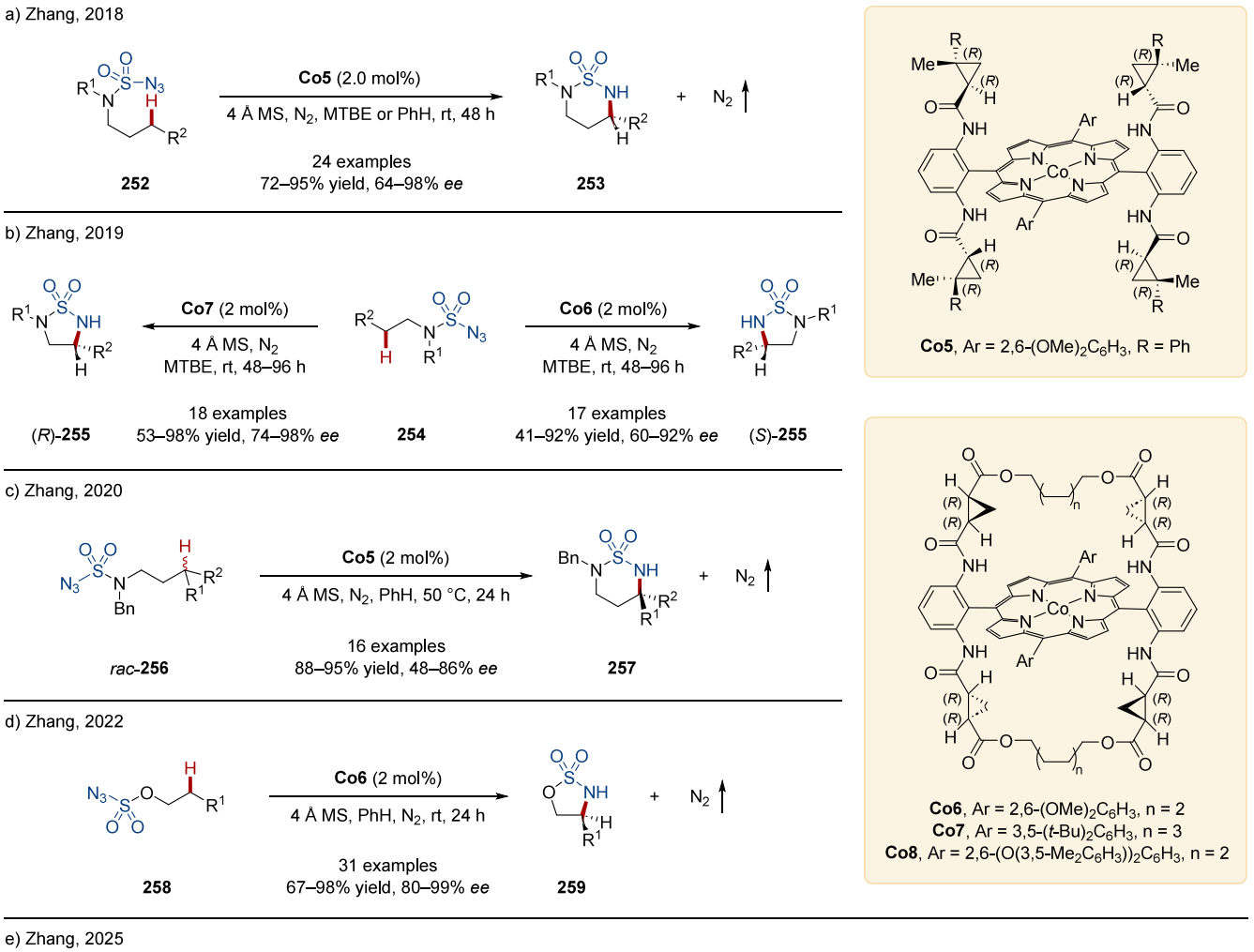

Scheme 60. Co(II)/Porphyrin-Catalyzed Enantioselective C−H Amidation of Arylsulfonyl and Alkylsulfonyl Azides

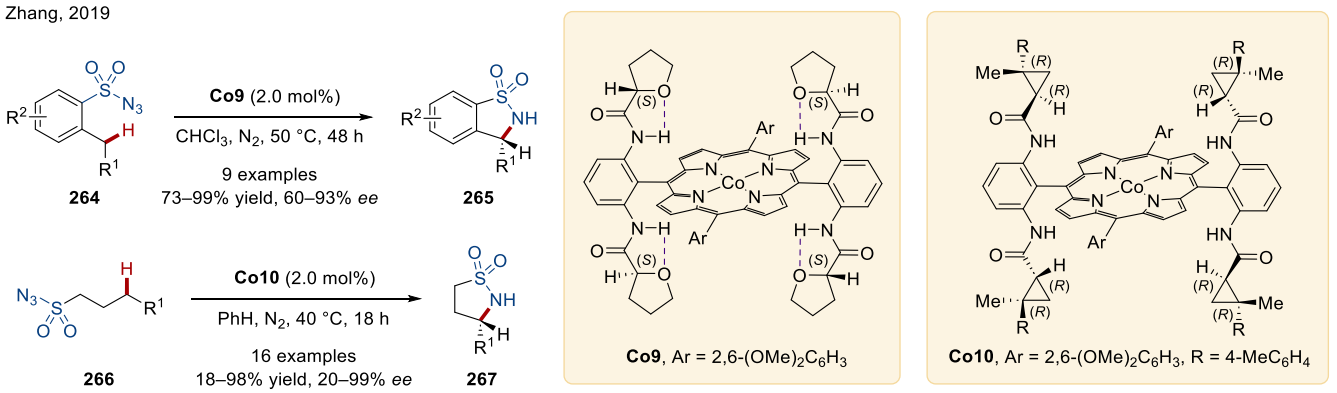

functionalization process. Based on these insights, a plausible mechanism was proposed, which differs markedly from previously reported Co(II)/Salox-catalyzed reaction.[214] In the proposed pathway, benzamide **320a** initially coordinates to the Ni(II) catalyst, enabling Ni(II)-catalyzed C−H cleavage to form the achiral square-planar Ni(II) species **Int92**. This intermediate

https://doi.org/10.1021/acs.chemrev.6c00255
Chem. Rev. XXXX, XXX, XXX−XXX

Scheme 61. Co(II)/Porphyrin-Catalyzed Intermolecular Enantioselective C−H Amination

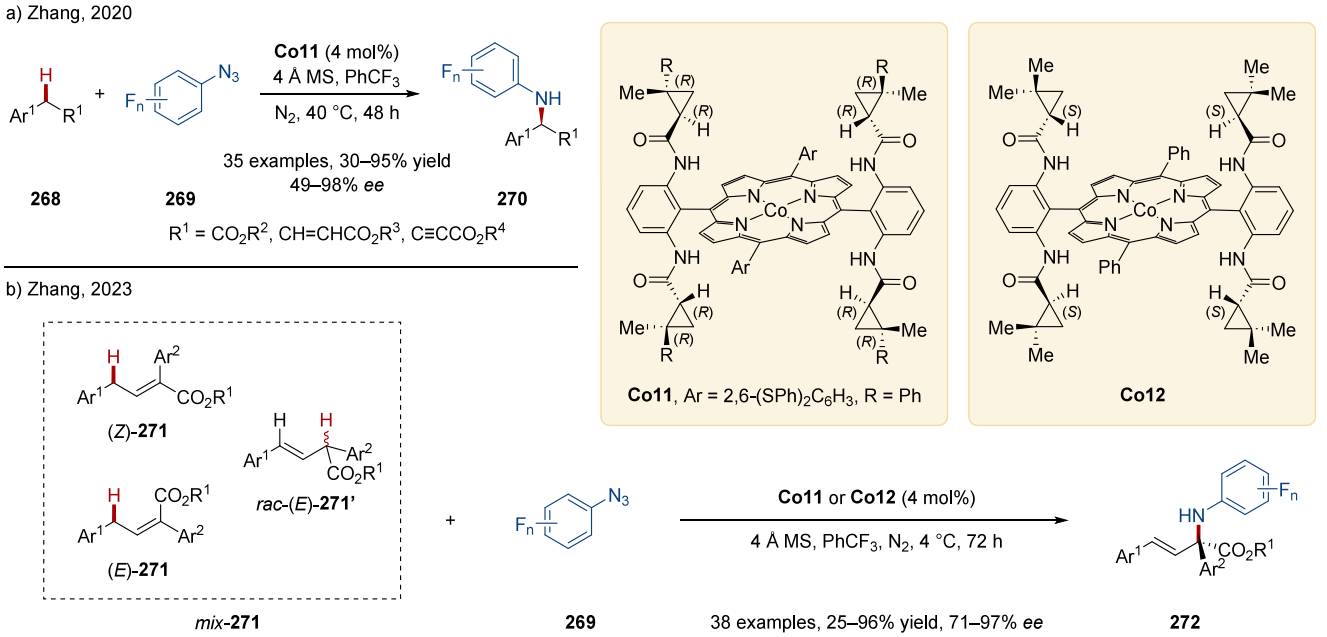

Scheme 62. Co(II)/Porphyrin-Catalyzed Intermolecular Enantioselective C−H Alkylation

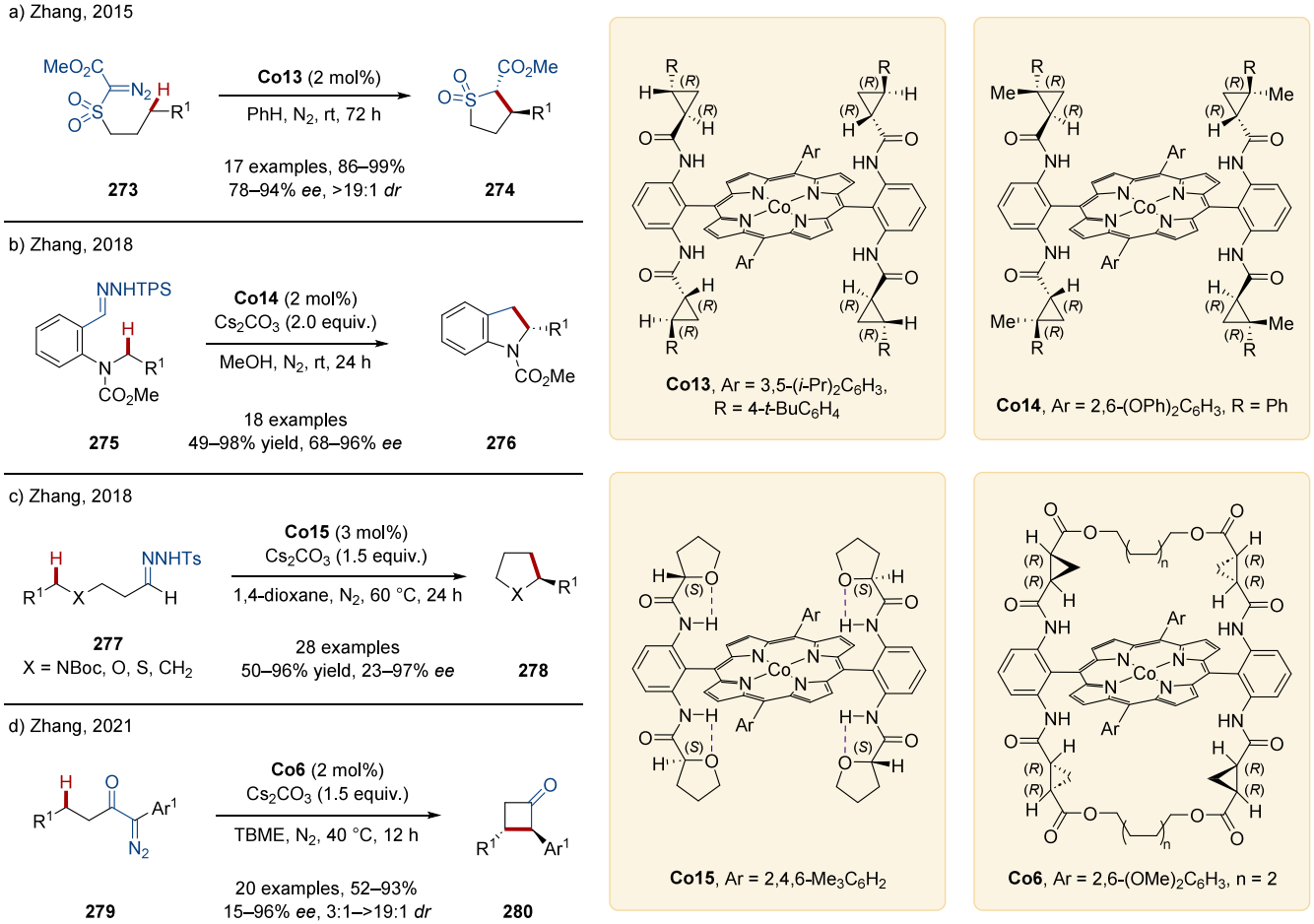

Int92 subsequently undergoes oxidation to afford the chiral Ni(III) species **Int93**, facilitated by the TMS-Salox **L49**. The precise stereoselective coordination of Salox **L49** is likely governed by the $\pi-\pi$ stacking interactions between the 8-quinolyl moiety of substrate **320** and the phenyl group of the oxazoline arm of the Salox ligand **L49**. Meanwhile, as depicted in **Int94** and **Int95**, the steric repulsion provided by the bulky TMS group of Salox **L49** plays a crucial role in directing the

https://doi.org/10.1021/acs.chemrev.6c00255
Chem. Rev. XXXX, XXX, XXX−XXX

Scheme 63. Ni(0)/SPO-Catalyzed Intramolecular Enantioselective Formamide C−H Annulation

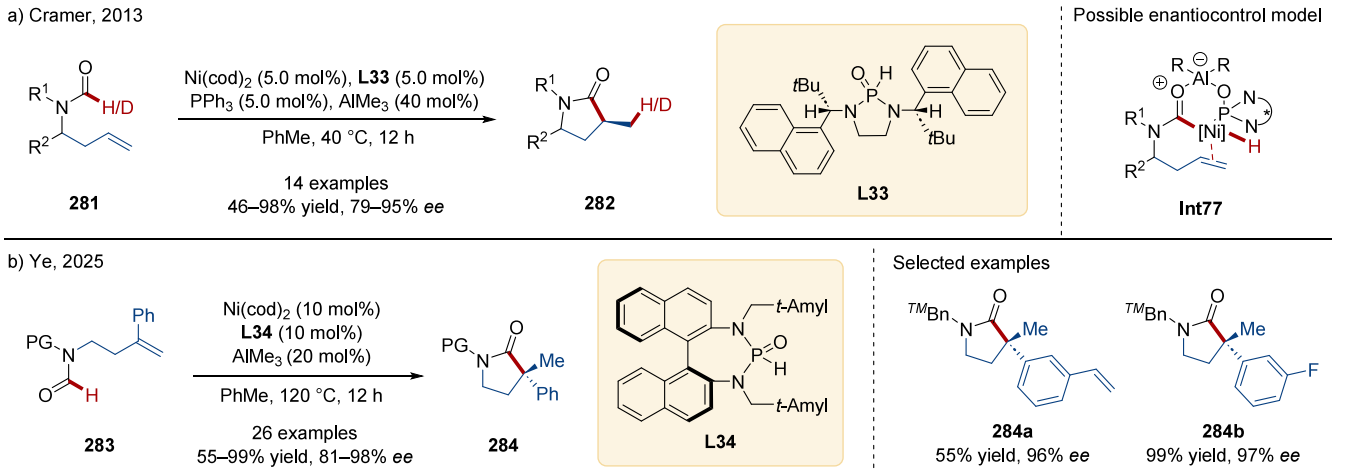

Scheme 64. Ni(0)/SPO-Catalyzed Intramolecular Enantioselective Heteroarene C−H Annulation

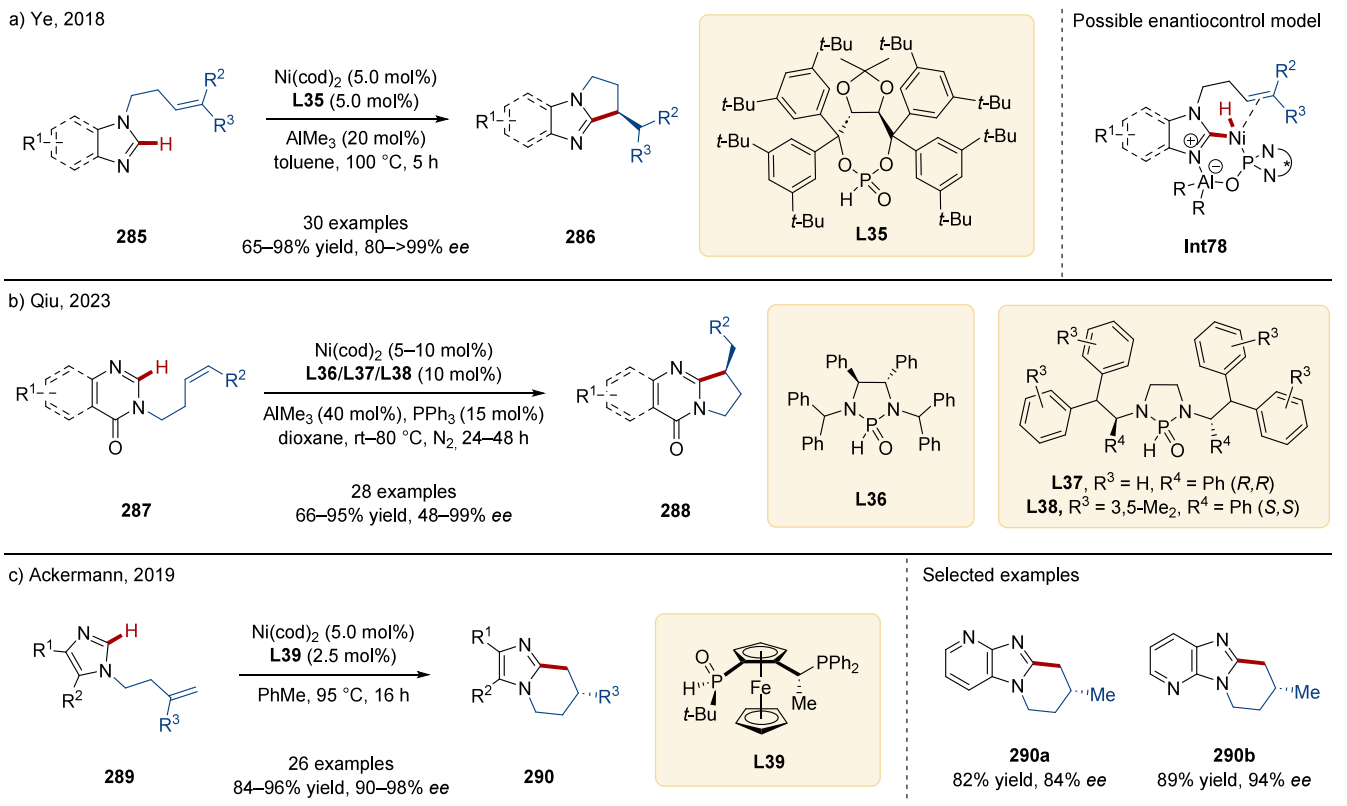

enantioselective coordination of the oxabicyclic alkene **321** to the nickel(III) center and controlling the subsequent migratory insertion step. The stereochemical control ultimately dictates the configuration of all four *C*-stereocenters in the resulting [2,2,1]-bridged bicyclic product **322**. Afterwards, Ackermann and colleagues also accomplished the same transformations, replacing the Ag(I) oxidant with holes through an electro-oxidative platform with ferrocene Cp_2Fe as the redox mediator.[215]

6.5. Ni Catalysis with BOX ligands and Their Analogues

6.5.1. Enantioselective C−H Arylation. Inspired by MacMillan and Doyle's achievements on the combination of photoredox with nickel catalysis for the $C(sp^3)-C(sp^2)$ cross-coupling of *α-N, O,* or phenyl-substituted carboxylic acids with aryl halides,[284] as well as the application of photoredox catalysis in C−H functionalization,[285] the Lu group initially realized a nickel-catalyzed enantioselective benzylic C−H arylation with aryl bromides **324** through photoredox radical relay in 2019 (Scheme 71a).[286] Diverse chiral 1,1-diaryl alkanes **325** were synthesized in moderate to high yields and enantioselectivities with $Ir(dFCF_3ppy)_2(dtbbpy)Cl$ and bis(4-methoxyphenyl)-methanone (DMBP) as cophotocatalysts,[287] together with their newly designed sterically hindered chiral biimidazoline (BiIM) ligand **L50**. Anchored in their mechanistic studies and previous literature,[287,288] a plausible catalytic cycle was proposed. The reaction starts with the oxidative addition of aryl bromide **324** to the *in situ* generated Ni(0) species **Int96**. The resulting aryl Ni(II) bromide complex **Int97** could be

https://doi.org/10.1021/acs.chemrev.6c00255
Chem. Rev. XXXX, XXX, XXX−XXX

Scheme 65. Ni(0)/SPO-Catalyzed Intermolecular Enantioselective C−H Alkylation

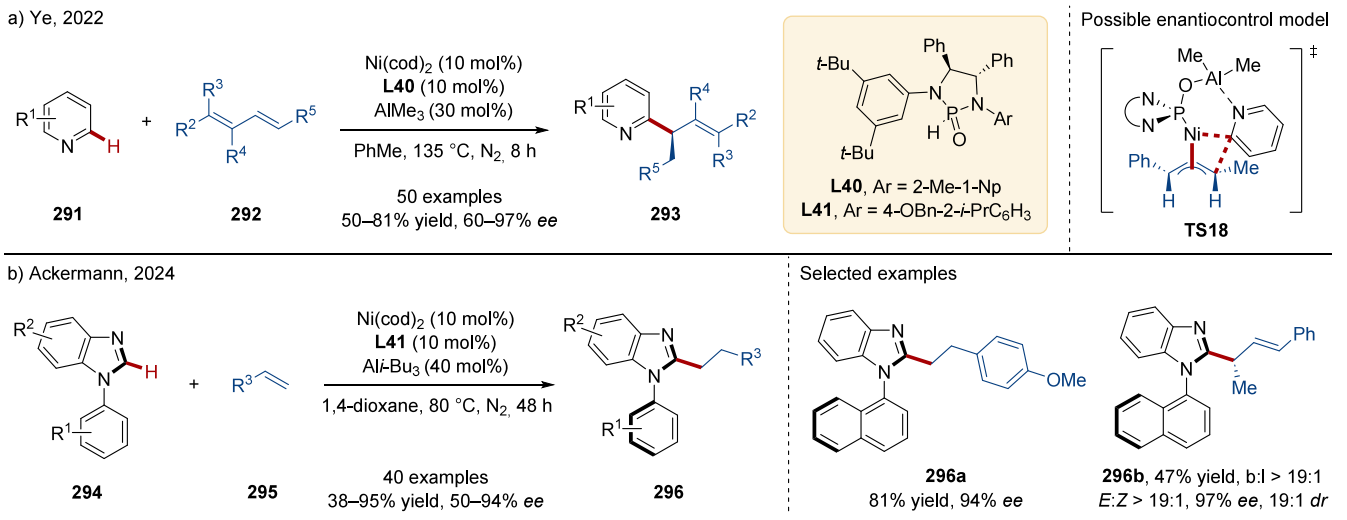

Scheme 66. Ni(0)/SPO-Catalyzed Intermolecular Enantioselective C−H Olefination

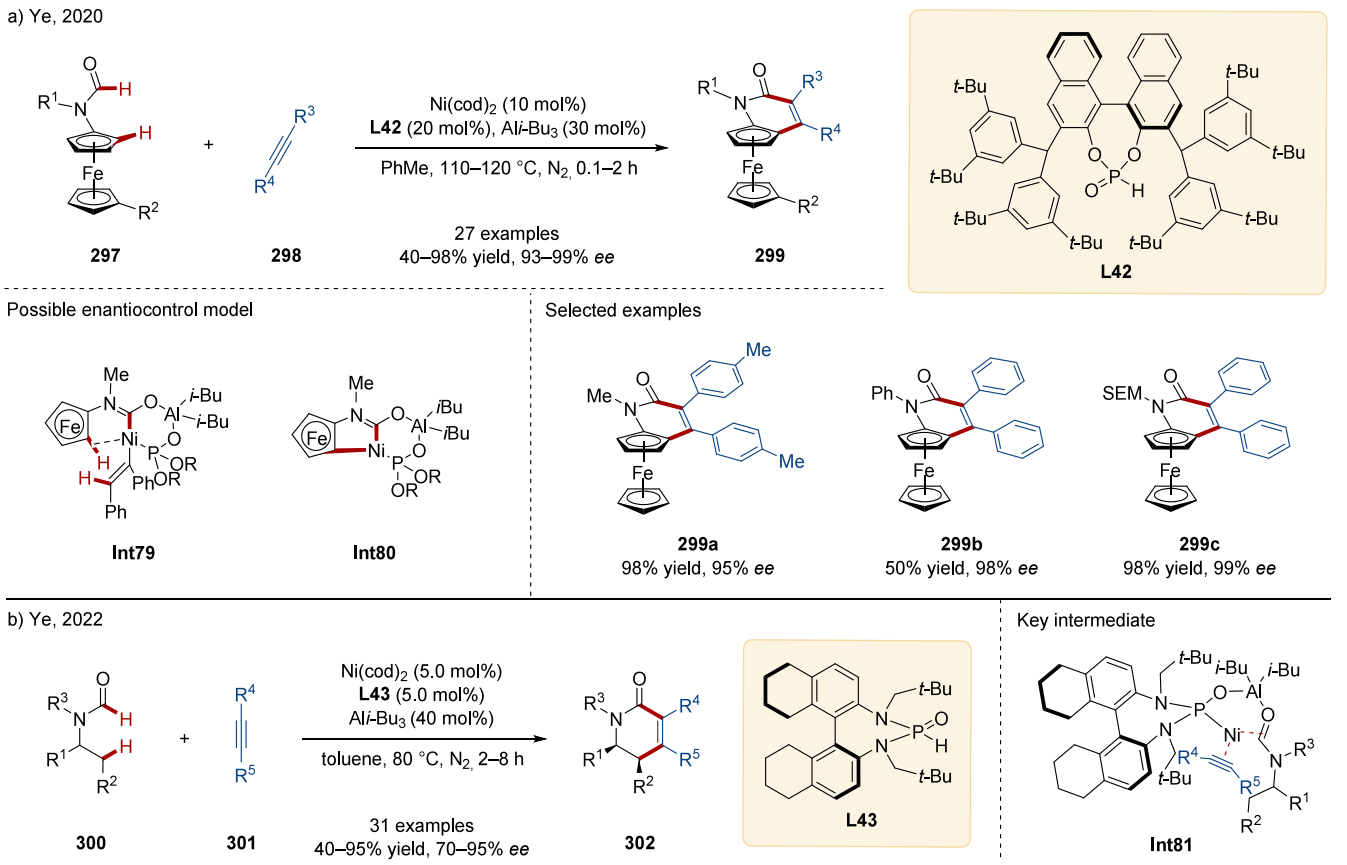

oxidized to the corresponding Ni(III) species by the excited state of [Ir(III)]* through an SET process, releasing a free bromine radical **Int99** that promotes HAT of alkyl benzene **323**. The benzylic radical **Int100** is then intercepted by aryl Ni(II) species **Int98** to form a Ni(III) intermediate **Int101**, which undergoes reductive elimination to afford the target product **325** and a nickel(I) complex, which undergoes single-electron reduction with iridium(II) to regenerate the L*Ni(0) species **Int96** and the ground state Ir(III) photocatalyst. In 2021, Huo and collaborators also demonstrated an asymmetric benzylic C(sp^3)−H arylation of amides **326** with aryl bromides **327** using a chiral bisoxazoline (BOX) ligand **L51**. The β-amide motif on the substrate **326** is proposed to serve as DG to stabilize the alkyl nickel species and impart enantiocontrol (Scheme 71b).[289]

Subsequently, this nickel/photoredox dual C−H/C−X cross-coupling paradigm has enabled the enantioselective α-hetero alkyl C(sp^3)−H arylation of saturated azacycles and linear *N*-alkyl benzamides **329** (Scheme 72a)[290] as well as oxacycles **332** (Scheme 72b)[291] with chiral BiIM **L50** and PHOX **L52** ligands, respectively. The functionalized chiral α-(hetero)aryl oxacycle products **324** could be converted into a series of biologically active molecules and pharmaceuticals, including adenosine

https://doi.org/10.1021/acs.chemrev.6c00255
Chem. Rev. XXXX, XXX, XXX−XXX

Scheme 67. Ni(0)/NHC-Catalyzed Intramolecular Enantioselective C−H Annulation

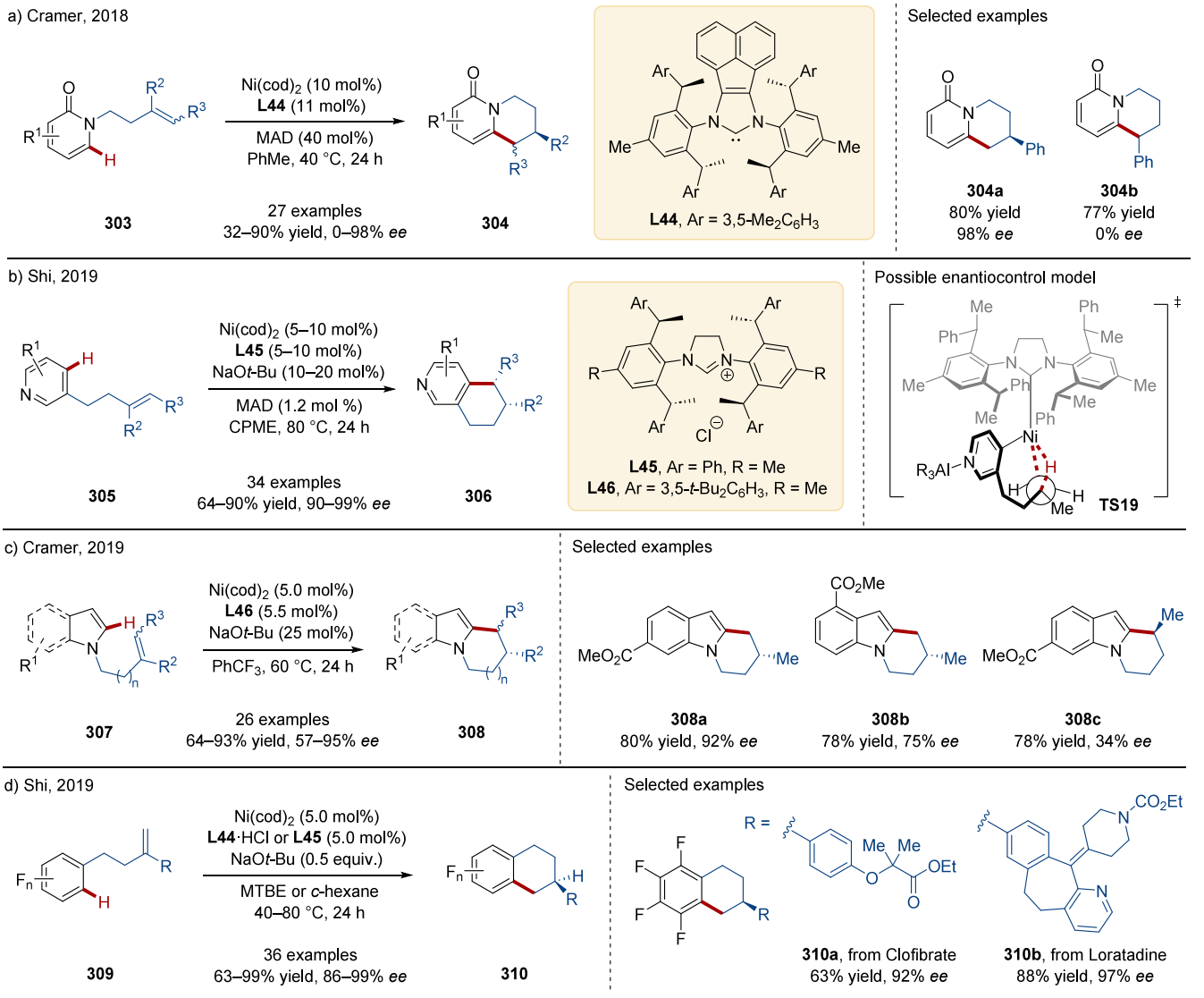

monophosphate-activated protein kinase (AMPK) activator **335**, the natural product analogue **336** of cassumunol F and H, the neural serotonin reuptake inhibitor (*R*)-norfluoxetine **337**, the antidepressants (*S*)-tomoxetine **338**, (*S*)-nisoxetine **339**, and (*S*)-fluoxetine **340**, the acetylcholine esterase and selective serotonin reuptake inhibitor **342**, and a retinol binding protein 4 (RBP4) lowering agent **343**.

6.5.2. Enantioselective C−H Acylation. In 2020, Huo and colleagues demonstrated the nickel/photoredox-catalyzed enantioselective C(sp^3)−H acylation of *N*-alkyl benzamides **344** with a chiral BOX ligand **L53**, providing various chiral *α*-amino ketones **346** in up to 99% yield and up to 96% *ee* (Scheme 73a).[292] Dimethyl dicarbonate (DMDC) was chosen to convert carboxylic acids **345** into the corresponding mixed anhydrides **Int103** as a means of *in situ* activation. The method could be performed on gram scale, illustrating its preparative utility, especially for the late-stage functionalization of functional molecules like pharmaceuticals. The bromide anion is essential to the success of this coupling reaction, presumably because bromine radical is formed upon photocatalytic oxidation. Subsequent HAT of the *α*-amino C(sp^3)−H bond forms a prochiral carbon radical that engages in Ni-catalyzed asymmetric acylation.[286,293] Notably, although a catalytic cycle involving a Ni(0)L* intermediate was proposed initially, which is similar to the photoredox/Ni-catalyzed enantioselective C−H arylation by Lu and co-workers, DFT calculations indicated that a Ni(I)/Ni(III)/Ni(II)/Ni(III)/Ni(I) mechanism is more energetically feasible (Scheme 73b).[294] With the oxidative addition of mixed anhydride **Int103** onto BOX-ligated Ni(I) complex **Int104**, a Ni(III) complex **Int105** is delivered, which is reduced by the Ir(II) through SET. The *α*-amino alkyl radical **Int107** from HAT was captured by the Ni(II) intermediate **Int106**, and the product **346** is constructed through C−C reductive elimination. Meanwhile, the origin of the enantioinduction was also revealed in this DFT analysis.

Subsequently, the Ni/photoredox-catalyzed enantioselective benzylic C(sp^3)−H acylation with carboxylic acids **349** was realized by Huo and collaborators under similar conditions (Scheme 73c).[295] In 2023, the same group then accomplished the asymmetric C(sp^3)−H acylation of saturated *N*-heterocycles **351** (Scheme 73d).[296] Interestingly, when both the *α*-amino and benzylic C−H bonds are present in the same molecule, the C−H cleavage via HAT takes place preferentially at the *α*-amino position with excellent site-selectivity. Recently, the direct

https://doi.org/10.1021/acs.chemrev.6c00255
Chem. Rev. XXXX, XXX, XXX−XXX

Scheme 68. Ni(0)/NHC-Catalyzed Three-Component Enantioselective C−H Alkylation

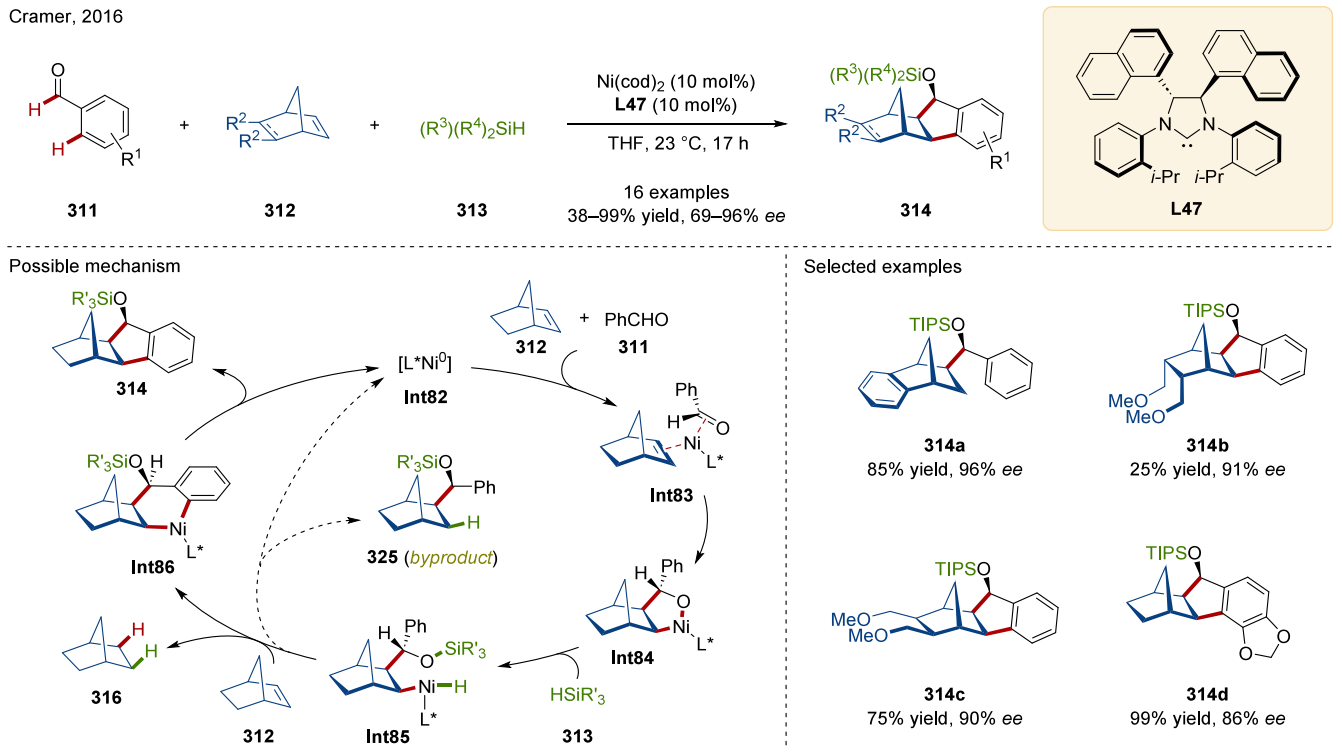

debrominative and decarboxylative enantioselective cross-coupling with aldehyde C−H bonds was also achieved by Huo and co-workers.[297,298]

6.5.3. Enantioselective C−H Olefination. In 2021, the Lu group disclosed a photoredox enantioselective benzylic C−H olefination via nickel-catalyzed radical relay, furnishing chiral allyl benzene compounds **356** in up to 82% yield and 93% *ee* (Scheme 74a).[299] One equivalent of 1,2-diphenylethene or 1-methoxy-4-styrylbenzene was added in this reaction to avoid the *E*/*Z* isomerization of both the alkenyl bromide **355** and the product **356** through inhibiting the photoinduced triplet energy transfer (EnT), ensuring high *E*/*Z*-selectivity of the final products **356** (up to >19:1 *E*/*Z*). At almost the same time, the Huo group achieved the Ni-catalyzed stereodivergent enantioselective C(sp^3)−H alkenylation, in which the *E*/*Z*-stereochemistry of products **359** could be controlled based on the identity of the counteranion of the iridium photocatalyst and the solvent (Scheme 74b).[300] Regarding the mechanism, control experiments indicated that the PF_6^- anion promotes the photoinduced *E* → *Z* isomerization to form *Z*-alkene product (*Z*)-**359**, while negligible isomerization was observed in the presence of chloride photocatalyst [Ir]Cl. Formal C(sp^3)−C(sp^3) cross-coupling could be realized through a one-pot tandem asymmetric C(sp^3)−H alkenylation/hydrogenation sequence. In 2023, Kong and co-workers then reported the nickel/photoredox-catalyzed enantioselective C(sp^3)−H olefination of oxacycles **332** with cyclic alkenyl bromides.[291]

6.5.4. Enantioselective C−H Alkylation. The catalytic stereoselective construction of C(sp^3)−C(sp^3) bonds via asymmetric cross-coupling remains a prominent challenge in organic synthesis. Although several nonstereoselective methodologies have been developed with a photocatalytic HAT strategy since 2017,[301] attempts to achieve enantiocontrol have been plagued by limited effectiveness of the available chiral ligands. In 2024 the Huo group reported a direct enantioselective *α*-amino C(sp^3)−H alkylation of saturated cyclic and acyclic benzamides **360**. The reaction leveraged synergistic photoredox and nickel catalysis to control radical generation and subsequent asymmetric cross-coupling, using redox-active *N*-hydrophthalimide (NHPI) esters as the alkylation reagents in combination with BOX ligand **L58** or **L59** (Scheme 75).[302] The reaction tolerated a broad range of functional groups, enabling late-stage diversification and expediting the total synthesis of drugs and natural products such as (−)-indolizidine 201 **363**, (−)-norbgugaine **364**, and a Ca-sensing receptor antagonist precursor.

Recently, inspired by the previous reports on asymmetric hydroalkylation of olefins through NiH-catalyzed radical relay[303] and the enantioselective alkylation of sulfonylimines via Ni-assisted paired electrolysis,[304] Kong, Ping, and colleagues described another approach for the Ni-catalyzed direct stereoselective C(sp^3)−H alkylation of saturated nitrogen and oxygen heterocycles **365**, **370**, and **373** with a different mechanism (Scheme 76).[305] In this reaction system, O−O homolysis of a peroxide (dicumyl peroxide, DCP; or di-*tert*-butyl peroxide, DTBP) generates an alkoxyl radical, which cleaves the target C(sp^3)−H bond via HAT. Meanwhile, an alkyl−Ni(II) intermediate is generated via rapid migratory insertion of unactivated olefins **366**, **367**, **371**, and **374** into an *in situ* formed nickel−hydride species. Subsequently, the *α*-amino/oxy alkyl radical is trapped by the L*Ni(II)(alkyl) intermediate, and C(sp^3)−H alkylated products **368**, **369**, **372**, and **375** are obtained through reductive elimination with concomitant regeneration of the catalytically active L*Ni(I) species. Strikingly, NiH catalysis could facilitate the chain-walking of internal alkenes **367** to remote terminal positions via *β*-H elimination and olefin reinsertion, allowing for linear-selective C−H alkylation of **365**. In some cases, chain walking can be suppressed; for example, *α*-boryl substitution stabilizes branched organonickel intermediates with internal alkenyl boron reagents **374**.[306] This protocol was employed in the

https://doi.org/10.1021/acs.chemrev.6c00255
Chem. Rev. XXXX, XXX, XXX−XXX

Scheme 69. Ni(II)/BINOL-Catalyzed Enantioselective C−H Alkynylation

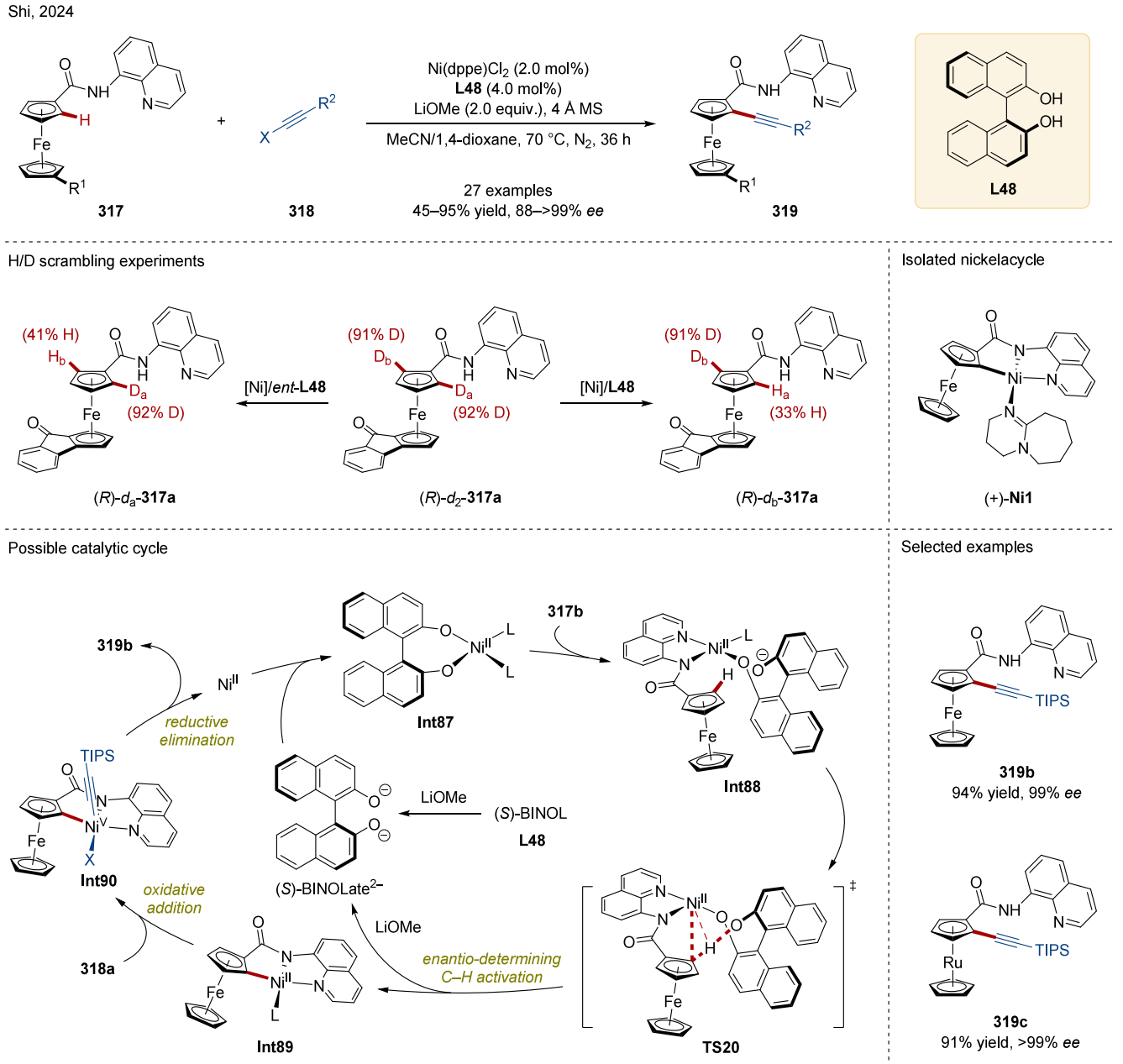

asymmetric total synthesis of biologically active compounds, including (−)-bgugaine **376**, (−)-irnidine **377**, (−)-coniceine **378**, (+)-α-lipoic acid **379**, (−)-tetrahydrolipstatin **380**, (−)-1-hydroxypyrrolizidine **381**, (−)-perhydro-8-indolizinol **382**, pumiliotoxin 251D **383**, (−)-trachelanthamidine **384**, (−)-tashiromine **385**, and 5-HT4 agonist SC-53606 **386**.

7. COPPER CATALYSIS

With its relatively high natural abundance in the earth's crust compared with other coinage metals, its low toxicity,[97] and accessible one- and two-electron redox processes across 0, +1, +2, and +3 oxidation states,[43,307] copper is a kind of versatile metal with numerous catalytic applications in organic chemistry.[308] In 1900s, Ullmann[309] and Goldberg[310] originally pioneered copper-catalyzed C−C and C−heteroatom bond forming reactions. Since those seminal studies, numerous copper-catalyzed transformations have been developed for cross-coupling, oxidation, addition, and radical pathway,[311] including enantioselective variants.[312] Encouraged by the progress in Cu-mediated radical[11k,246a,313] and carbenoid chemistry,[22,314] several outer-sphere enantioselective C−H functionalizations have been introduced during the past decades.[17b,315] However, as a group 11 metal with valence shell electron of $3d^{10}4s^1$,[43,307] copper has proven challenging to employ in inner-sphere asymmetric C−H activation due to lack of empty hybrid orbitals for C−H metalation after coordination with external ligands and/or directing groups present within substrates of interest. Only recently has this limitation been addressed with chiral ligands, such as NHC and BINOL.

7.1. Cu(I)/NHC Catalysis

The privileged nature of NHC ligands was discussed in the context of iron, cobalt, and nickel catalysis,[124,316] and along similar lines NHCs have found fertile ground in the realm of enantioselective C−H activation with copper. Building on their

https://doi.org/10.1021/acs.chemrev.6c00255
Chem. Rev. XXXX, XXX, XXX−XXX

Scheme 70. Ni(II)/Salox-Catalyzed Enantioselective C−H Annulation

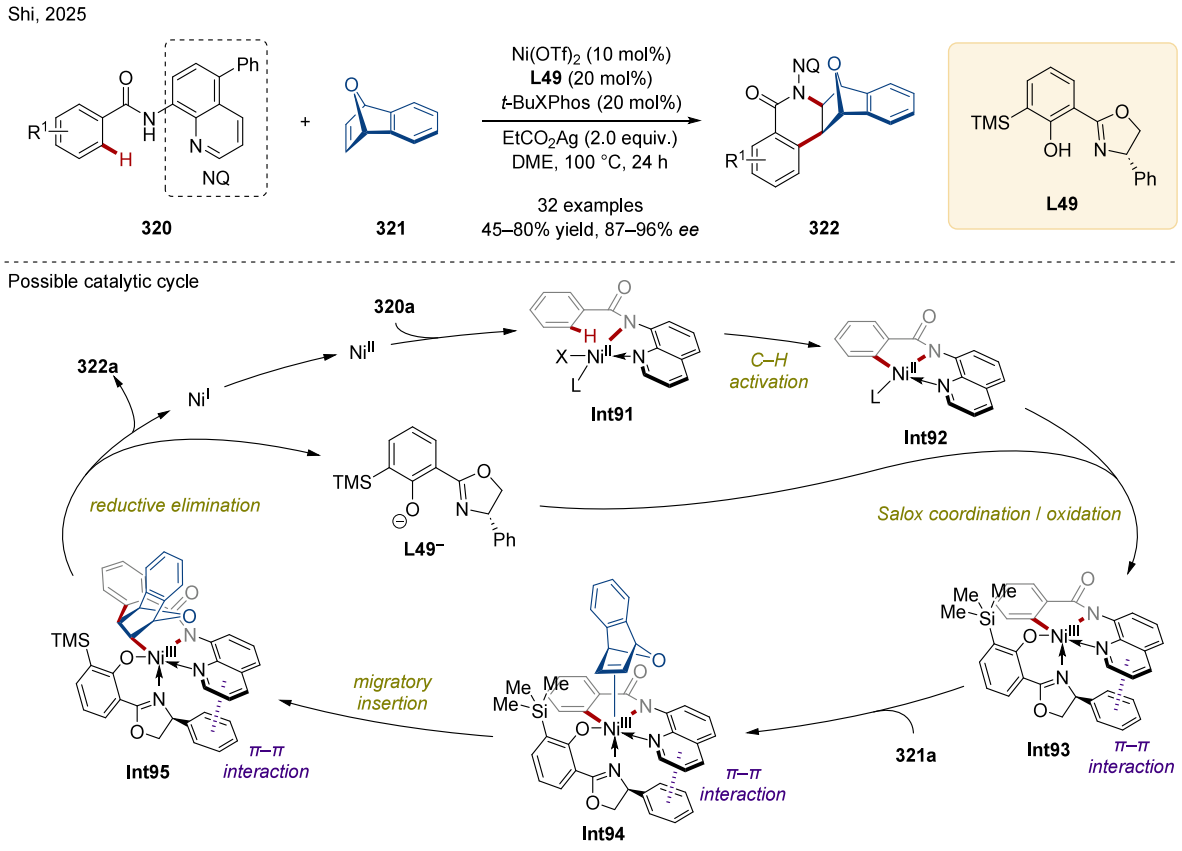

previous reports on Tsuji−Trost-type reactions,[317] in 2016 Sawamura, Ohmiya, and collaborators applied the sterically bulky NHC ligand **L62** featuring a naphtholic hydroxyl group in Cu(I)-catalyzed enantioselective C−H allylic alkylation of both benzothiazoles and oxazoles **387** (Scheme 77).[318] Employing γ,γ-disubstituted primary allyl phosphates **388** as the allyl electrophile, the corresponding products **389** bearing an all-carbon quaternary *C*-stereocenter at the α-position of the heteroaromatic ring were delivered with excellent branched regioselectivities under two subtly different conditions. Higher yields were obtained with CuCl in 1,4-dioxane, while enhanced enantioselectivities were achieved when the cationic precatalyst $[Cu(MeCN)_4]PF_6$ and a mixed solvent of THF and MeCN were used.

7.2. Cu(II)/BINOL Catalysis

The oxazoline-aniline moiety has been identified as a versatile bidentate directing group in Cu(II)-mediated C−H functionalization.[319] Rather than SET[320] or electrophilic attack mechanisms[321] that have been proposed previously, a CMD mechanism has been invoked for the C−H cleavage step in these transformations on the basis of detailed DFT calculations.[322] Moreover, the stereoselectivity can be controlled with a chiral oxazoline group, as exemplified in a report demonstrating C−H thiolation of ferrocene derivatives for the construction of planar chirality.[323] In 2023, Yu, Wang, and co-workers demonstrated the Cu(II)-mediated enantioselective C−H alkynylation of ferrocenes **390** with a 6,6′-dibromo-3,3′-dimethyl BINOL **L63** as the chiral ligand (Scheme 78a).[324] Through KIE studies, C−H cleavage was identified to be the rate-determining step. A CMD pathway was rationalized, rather than an SET mechanism,[325] with the process significantly accelerated by the BINOL ligand in a similar manner to Pd(II)/BINOL catalysis.

Simultaneously, our group independently achieved a catalytic C−H alkynylation that avoids the usage of stoichiometric copper.[326] The rection employed 8-aminoquinolyl fragment as a directing group and simple BINOL **L48** as the chiral ligand under mild conditions (0 °C), affording a wide range of chiral ferrocenes **395** in excellent yields and enantioselectivities (Scheme 78b). Notably, both chemical and electrochemical oxidation were compatible in this transformation.

Recently, the copper(II)-mediated enantioselective C−H thiolation between ferrocenyl carboxamides **397** and disulfides **398** has also been described by us with a catalyst loading of BINOL ligand as low as 2.5 mol% (Scheme 78c).[327] Intriguingly, although the reaction requires stoichiometric CuCl, it is catalytic in BINOL. Mechanistic studies revealed that the rate- and enantiodetermining C−H activation step is mediated by catalytic Cu(I) and BINOL and that the need for 1.2 equivalent of copper arises from deactivation of Cu(I) due to the accompanying formation of $CuSAr^1$ as a stoichiometric byproduct. The C−H cleavage was proposed to proceed via **TS21**, where stereoinduction arises through the involvement of the BINOLate ligand in the CMD process, analogous to the mechanism of the Ni(II)/BINOL system introduced above (Scheme 69).[281]

7.3. Cu(I) Catalysis with BOX Ligands and Their Analogues

7.3.1. Enantioselective C−H Cyanation. As a privileged ligand system in asymmetric copper catalysis,[308,312a,b,h] the BOX ligand has been initially applied in Cu(I)-catalyzed enantioselective allylic C−H acyloxylation, Kharasch−Sosnovsky oxidation,[328] throughout the late 20th century with substantial efforts

https://doi.org/10.1021/acs.chemrev.6c00255
Chem. Rev. XXXX, XXX, XXX−XXX

Scheme 71. Metallaphotoredox Enantioselective Benzylic C−H Arylation Catalyzed by Ni/BiIM and Ni/BOX

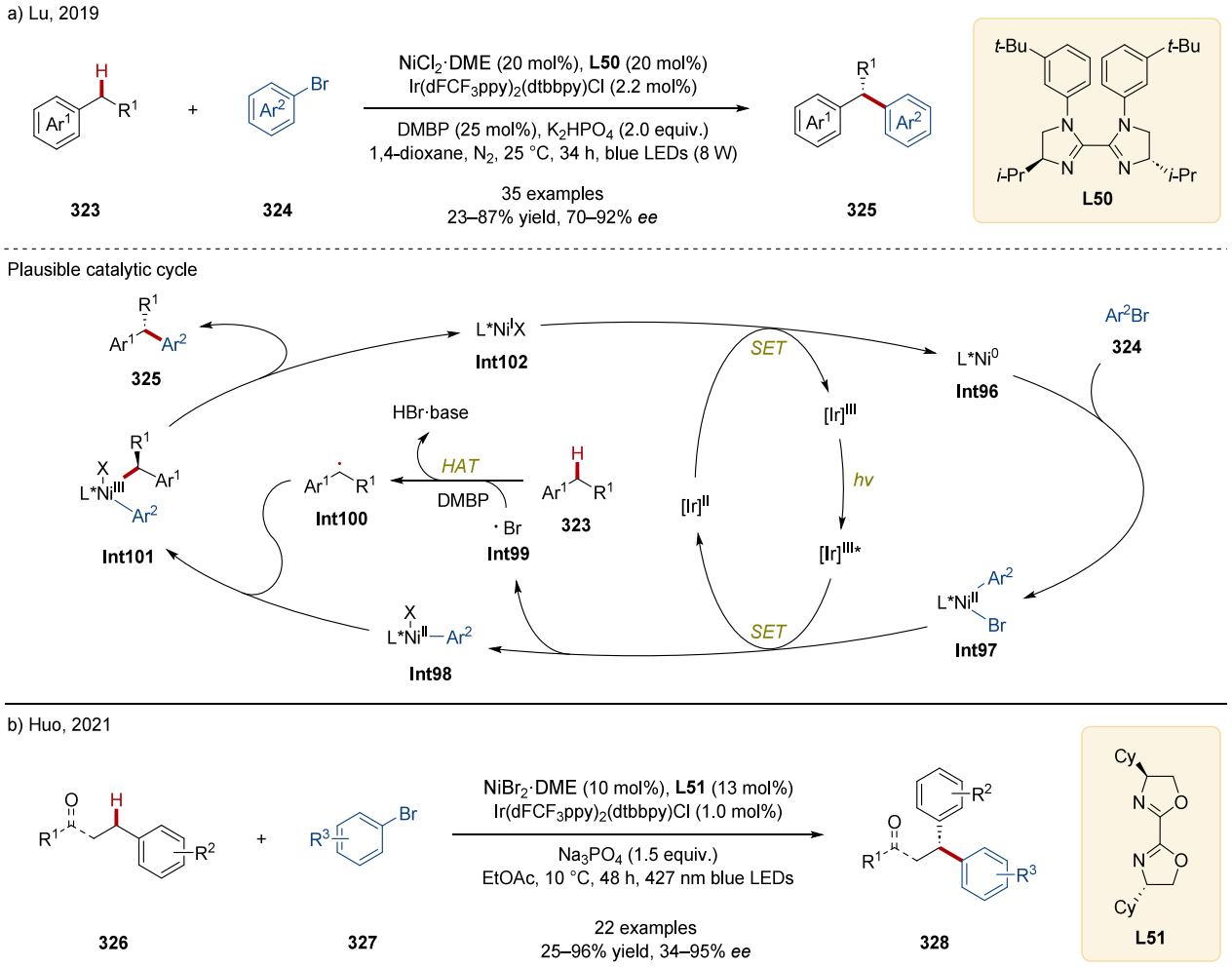

made to identify more universal conditions and explore superior stereocontrol.[329] Nevertheless, methods from this period were largely restricted to a limited scope of cyclic alkenes and required a large excess of the alkene substrates.[329,330] Only poor to moderate yields and enantioselectivities could be realized for more challenging acyclic alkenes.[331] The need for a large stoichiometric excess of alkene (relative to the other reactant) also restricts practical application of these C−H functionalization methodologies in organic synthesis.

In 2016, with the alkylarene substrates **399** employed as the limiting reagent, Liu, Stahl, and colleagues described an innovative desymmetrization strategy in which prochiral benzylic methylene C−H bonds undergo enantioselective cyanation via a radical relay mechanism (Scheme 79a).[332] Various nitriles **401** were produced in an enantioselective manner under mild conditions at room temperature. For those substrates containing two benzylic CH_2 moieties, C−H cyanation takes place at the α-position adjacent to a more electron-rich aromatic ring. Regarding the mechanism, the copper(I) catalyst **Int109** is oxidized to Cu(II) species **Int110** by *N*-fluorobenzenesulfonimide (NFSI), and the concurrently formed nitrogen radical **Int111** then serves as the H-atom acceptor to cleave the C−H bond in **399** via HAT. DFT calculations revealed that the capture between the BOX-chelated copper(II) cyanide species **Int112** and benzylic radical **Int113** to form alkyl−Cu(III) intermediate **Int114** is reversible and that subsequent C−C reductive elimination via transition state **TS22** is the enantiodetermining step.

Soon after, Liu, Lin, and co-workers described the Cu(I)-catalyzed site-, enantio-, and *E*/*Z*-stereoselective allylic C−H cyanation of olefins **302** using *N*-fluoroalkyl sulfonamide (NFAS) as the oxidant (Scheme 79b).[333] Intriguingly, since the regioselectivity is controlled by both the structure of NFAS and the chiral BOX ligand, it was surmised that the *N*-centered radical is coordinated to the copper(II) center during the HAT step (**TS23**). Indeed, the intermediacy of this tunable Cu(II)-bound nitrogen radical was supported by control experiments, EPR spectroscopy, and DFT calculations. Copper coordination in the HAT step amplifies the site-selectivity of allylic C−H bonds compared to the reactivity profile of free *N*-centered radical. Recently, several in-depth mechanistic investigations involving kinetic studies, computational analysis, and spectroscopy exploration were carried out to provide more insights into the details of this selective allylic C−H cyanation.[334] Some of the NFAS is consumed in side reactions with Cu(II)-bound *N*-centered radical [Cu(II)−NCR], which is quenched by excess TMSCN **400** to generate *N*-silylated sulfonamides and $(CN)_2$ as byproducts.[334b]

In 2021, Liu, Lin, and colleagues demonstrated a convenient approach to enantioenriched allenyl nitriles **405** through Cu(I)/BOX-catalyzed benzylic propargylic C−H cyanation, a method that exhibits exceptional site-, chemo-, and enantiocontrol

https://doi.org/10.1021/acs.chemrev.6c00255
Chem. Rev. XXXX, XXX, XXX−XXX

Scheme 72. Metallaphotoredox Enantioselective C−H Arylation at α-Position of Heteroatom Catalyzed by Ni/BiIM and Ni/PHOX

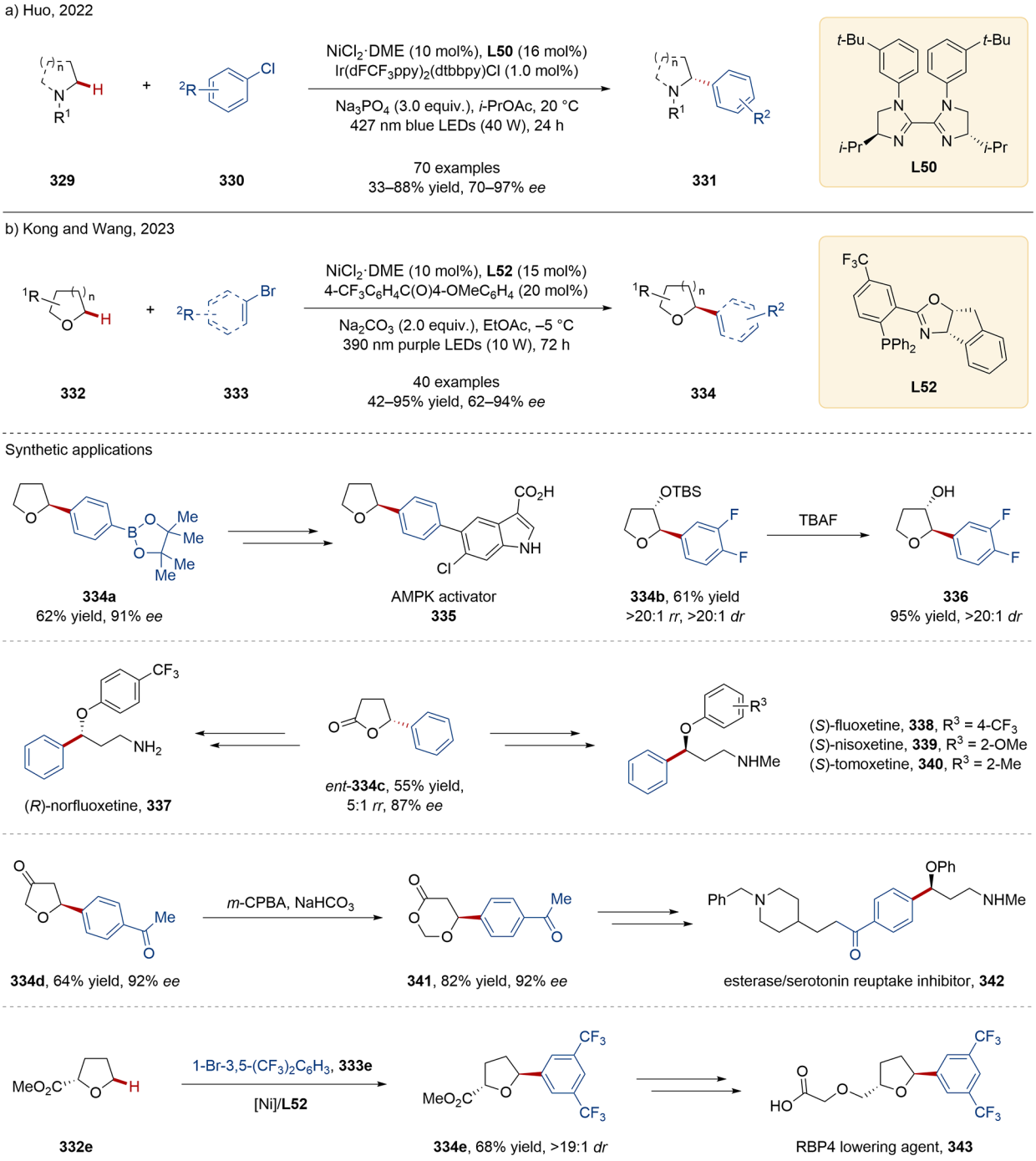

(Scheme 79c).[335] In terms of the mechanistic details, the coupling reaction between the resonance-stabilized carbon-centered radical and chiral dicyanide-coordinated copper(II) complex was proposed to be the regioselectivity-determining step, where the less sterically hindered allenyl radical reacts in preference to the propargylic radical upon tautomerization. This model was supported by DFT calculations, which indicated that the allenyl radical/copper coupling step is the enantiodetermining step as well, in contrast to the C(sp^3)−H cyanation system introduced above, in which reductive elimination is enantiodetermining.

In addition to intermolecular copper-bound *N*-centered-radical-promoted site-selective HAT, the regioselectivity of radical-mediated remote C−H functionalization could also be controlled via intramolecular 1,5-HAT, akin to the classical Hofmann−Löffler−Freytag (HLF) cyclization. In 2019, the Nagib group employed the uncommon divalent copper salt, $Cu(OTf)_2$, as the precatalyst in a series of interrupted HLF-type intramolecular annulations of NAFSs **406**. In this catalytic transformation, the carbon-centered radical generated upon 1,5-HAT is trapped with a chiral Cu(II) cyanide species (Scheme 80a).[336] Notably, this transformation provides access to 6-membered piperidines after downstream transformation of the

https://doi.org/10.1021/acs.chemrev.6c00255
Chem. Rev. XXXX, XXX, XXX−XXX

Scheme 73. Enantioselective C−H Acylation Catalyzed by Ni/BOX and its Analogues

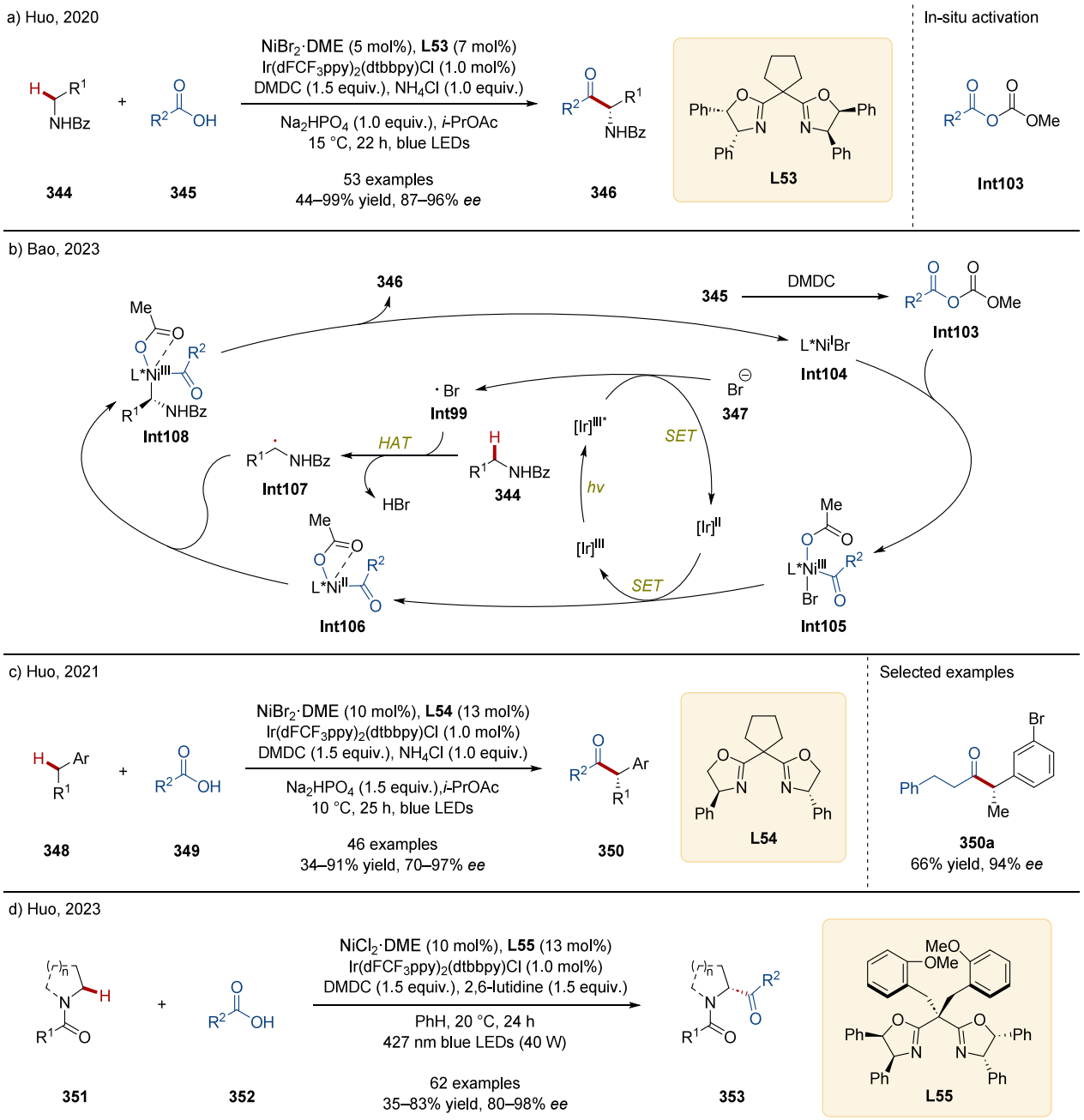

products—thereby complementing traditional HLF reactions that furnish pyrrolidines. Shortly thereafter, a similar report was described by the Wang, who employed copper in conjunction with chiral BOX ligand **L68** to facilitate the transformation (Scheme 80b).[337]

Building on their light-promoted enantioselective decarboxylative cyanation of NHPI esters,[338] at around the same time the Liu group developed an enantioselective C(sp^3)−H cyanation of NHPI ethers **410** facilitated by the synergistic photoredox and copper catalysis (Scheme 80c).[339] In the catalytic cycle a highly reactive oxygen-centered radical is generated upon SET reduction of the N−O bond by the excited state photocatalyst $Ir(ppy)_3$*. Intramolecular 1,5-HAT transposes the radical to the remote benzylic position, prior to enantioselective cyanative copper-mediated radical capture. The Zhu group then found *N*-alkoxypyridinium salts to be suitable precursors of the *O*-centered radical in a related report on Cu(I)-catalyzed enantioselective C(sp^3)−H cyanation.[340] A similar approach with *O*-benzoyl hydroxylamide **412** was then described by the Yu group (Scheme 80d).[341] In 2023, Liu, Chen, and colleagues also applied this strategy in the dual photo- and copper-catalyzed asymmetric cyanation of remote propargylic C(sp^3)−H bonds via 1,5-HAT (Scheme 80e).[342]

As introduced earlier in this review, electrochemistry provides an attractive platform for performing oxidative reactions without the need for stoichiometric chemical oxidants. Following successful development of enantioselective electrocatalytic cyanofunctionalization of alkenes with tailored copper/BOX catalysts,[343] in 2022 the Xu group merged electrocatalysis, photocatalysis, and copper/BOX catalysis to develop a site- and enantioselective benzylic C(sp^3)−H cyanation of alkylarenes **416** with a serine-derived BOX ligand **L70** without the need for

https://doi.org/10.1021/acs.chemrev.6c00255
Chem. Rev. XXXX, XXX, XXX−XXX

Scheme 74. Enantioselective C(sp^3)−H Olefination Catalyzed by Ni/BOX and its Analogues

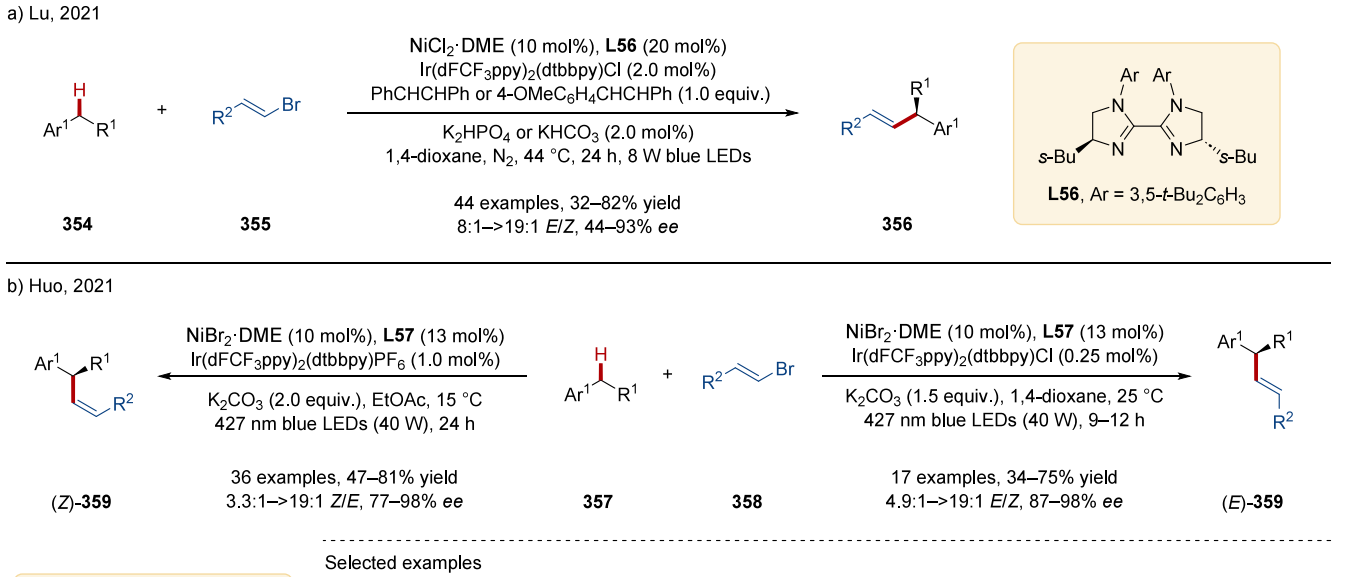

Scheme 75. Ni/BOX-Catalyzed Enantioselective C−H Alkylation with Redox-Active Esters

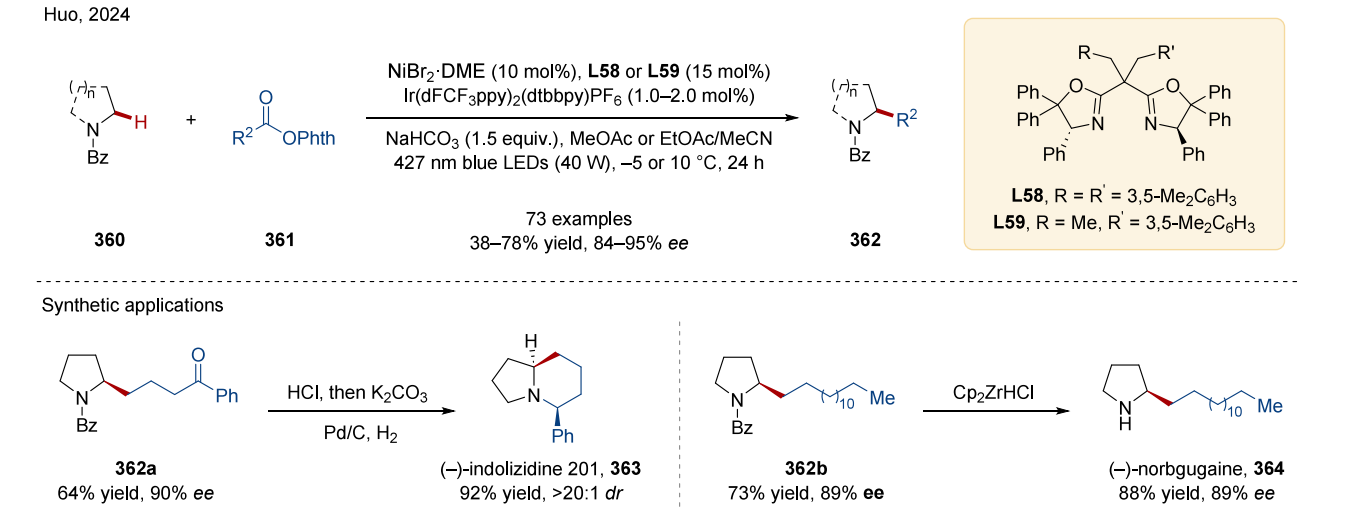

additional chemical oxidants (Scheme 81a).[344] Regarding the mechanism, two catalytic cycles take place in tandem. In the first cycle, the C−H bond of substrate **416** is cleaved by photoexcited disulfonate-substituted anthraquinone AQDS* via an electron-transfer, forming a key ion-radical pair [$AQDS^{\bullet-}$,$\mathbf{416}^{\bullet+}$] prior to site-selective proton transfer (PT), rather than conventional HAT.[345] In the second cycle, C−C bond formation generates chiral nitrile **417** through the final enantiodetermining C−C reductive elimination step, which is governed by the copper/BOX complex.[332] The semiquinone radical AQDS−H$^{\bullet}$ and Cu(I) species **Int115** are then oxidized on the anode to complete the catalytic cycle, with concomitant formation and release of H_2 gas on the cathode.

At nearly the same time, Liu, Wang, and co-workers independently reported the electrophotocatalytic Cu(I)/BOX-catalyzed asymmetric C(sp^3)−H cyanation (Scheme 81b).[346] By separating radical generation in photocatalytic cycle and radical capture in the copper cycle, these two processes could be modulated independently with minimal mutual interference. Specifically, tuning the electronic properties of the anthraquinone photocatalyst and adjust the applied current enabled site- and enantioselective C−H cyanation of substrates **418** that were unsuccessful in previous methodology,[332] particularly those containing electron-poor aryl rings.

7.3.2. Enantioselective C−H Arylation. Building on the mechanistic insights acquired from studies of nonstereoselective

https://doi.org/10.1021/acs.chemrev.6c00255
Chem. Rev. XXXX, XXX, XXX−XXX

Scheme 76. Ni/BOX-Catalyzed Enantioselective C−H Alkylation with Unactivated Alkenes

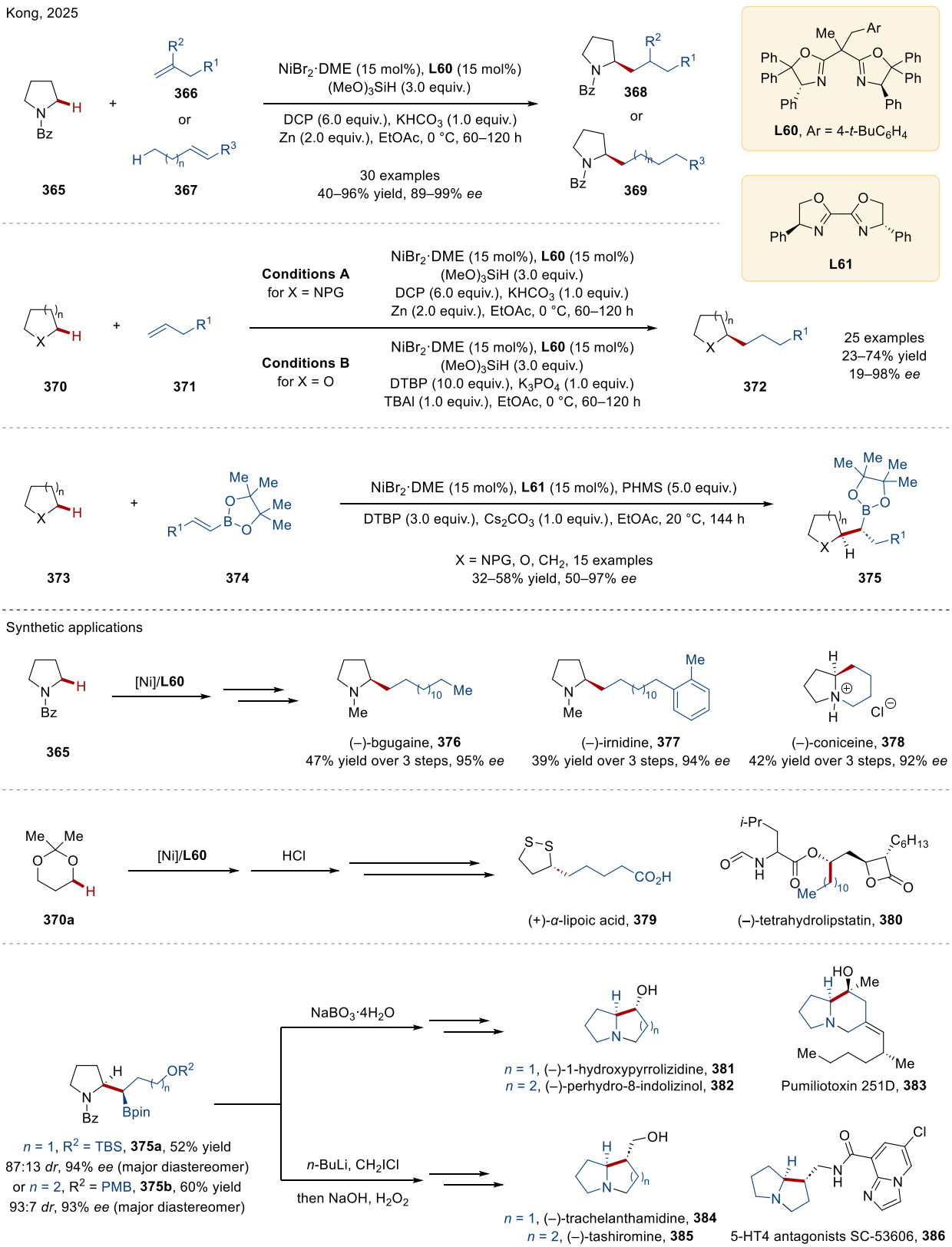

benzylic C−H arylation[347] and advances in asymmetric arylation of benzylic radical species generated via radical additions to olefins,[348] the Liu group reported an enantioselective benzylic C−H arylation of alkylarenes **420** in 2019 by employing the Cu(I)/BOX radical relay catalysis (Scheme 82).[349] In contrast to Ni-catalyzed asymmetric arylation of C−H bonds described in the preceding section which involved aryl halides (Scheme 71 and 72),[286,289−291] this copper(I)-catalyzed system uses arylboronic acids **421**. Introduction of an ester on the side arm[350] of the bulky BOX ligand **L71** accelerates the

https://doi.org/10.1021/acs.chemrev.6c00255
Chem. Rev. XXXX, XXX, XXX−XXX

Scheme 77. Cu(I)/NHC-Catalyzed Enantioselective C−H Allylic Alkylation

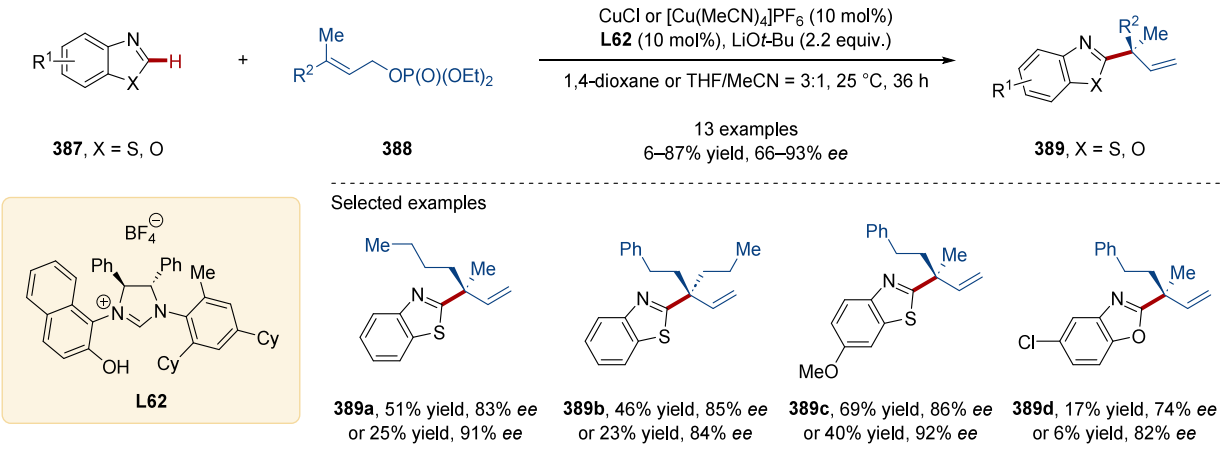

Scheme 78. Cu(II)/BINOL-Catalyzed (or -Mediated) Enantioselective C−H Alkynylation and Thiolation

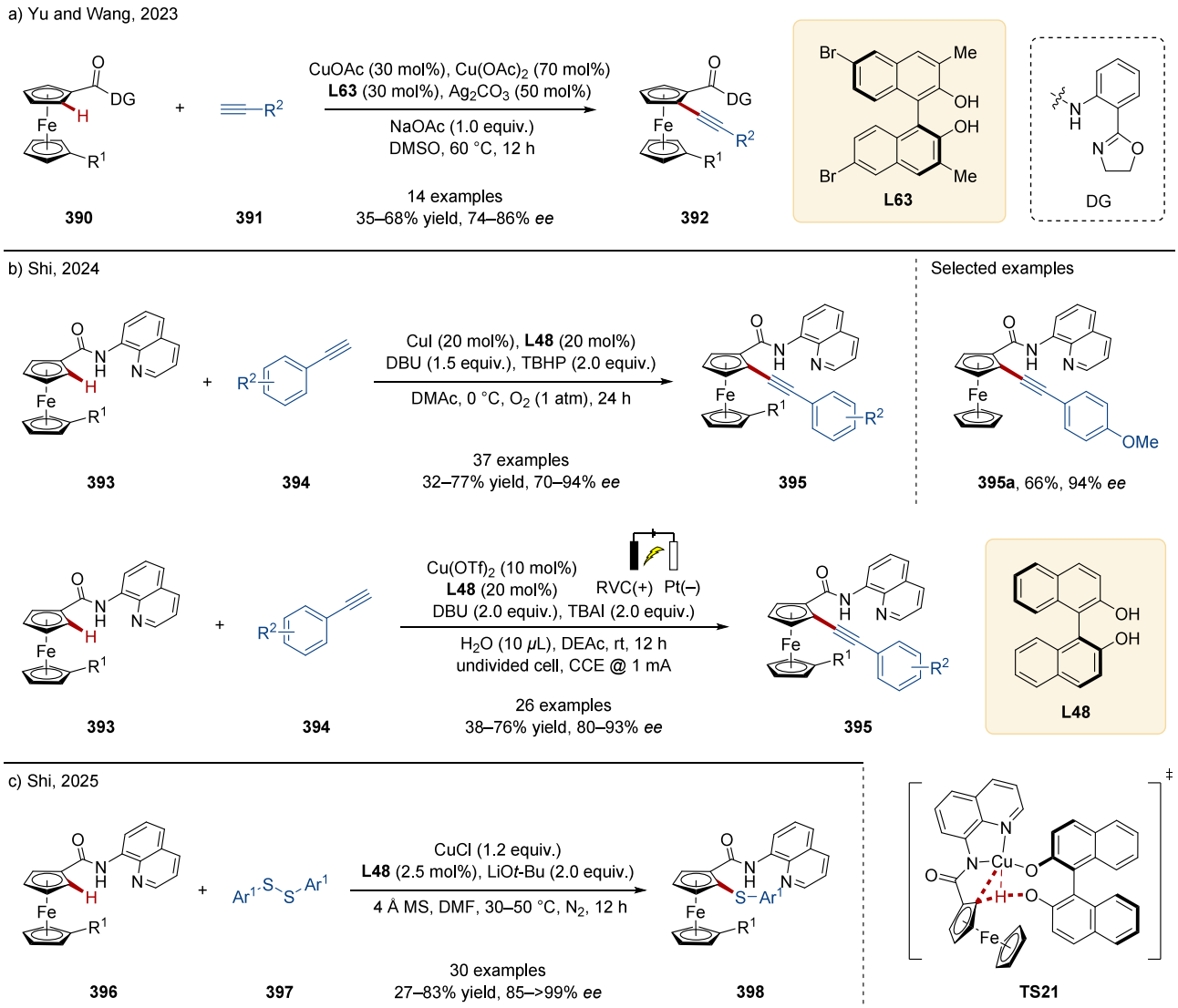

transmetalation between $Ar^1-B(OH)_2$ and the sterically hindered chiral divalent Cu species. This raises the concentration of the corresponding L*Cu(II)Ar^1 intermediate, promoting the benzylic radical trapping while inhibiting side reactions. Subsequently, the Nagib group disclosed an example of copper-catalyzed direct C−H arylation through intramolecular 1,5-HAT with excellent site-selectivity and moderate enantioselectivity.[351] The results could be improved to 87% yield and 90% *ee* with a new binaphthyl−BOX hybrid ligand designed by Maruoka and colleagues.[352]

https://doi.org/10.1021/acs.chemrev.6c00255
Chem. Rev. XXXX, XXX, XXX−XXX

Scheme 79. Cu(I)/BOX-Catalyzed Enantioselective C−H Cyanation Facilitated by Functional N−F Reagents

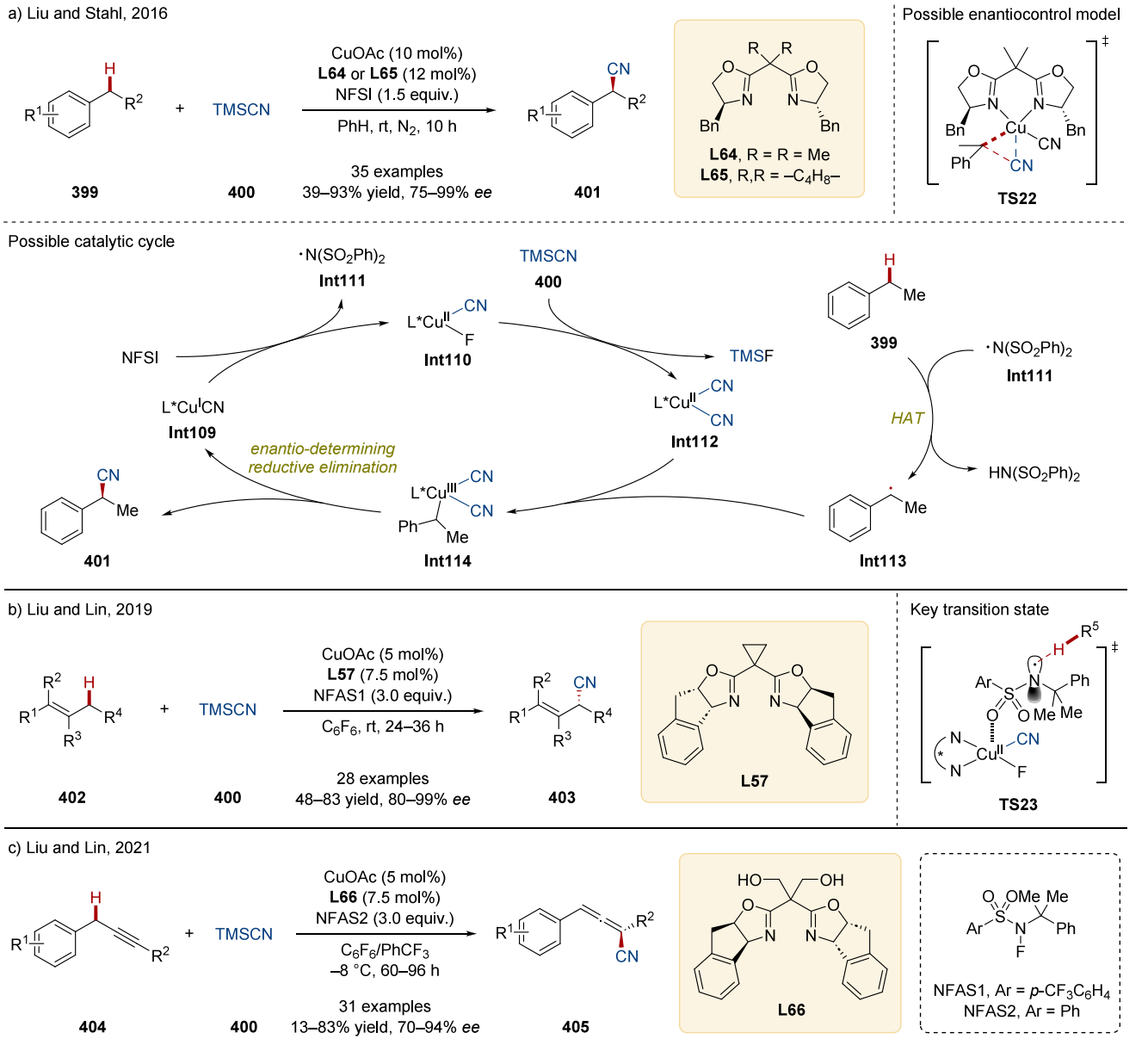

7.3.3. Enantioselective C−H Alkynylation. The dehydrogenative C(sp^3)−C(sp) cross-coupling of the α-amino C(sp^3)−H bonds and terminal alkynyl C(sp)−H bonds has been extensively studied in the context of nucleophilic addition of alkynylcopper species to iminium intermediates generated via oxidation.[353] Enantioselective variants have been developed through use of chiral metal catalysts, which simply function as Lewis acids.[354] Drawing on their prior experience in copper-catalyzed asymmetric radical coupling facilitated by cinchona alkaloid-based chiral ligands,[313b,c,355] in 2019 the Liu group unveiled an enantioselective Sonogashira-type C(sp^3)−H alkynylation with terminal alkynes **424** via copper radical relay catalysis (Scheme 83a).[356] In the proposed mechanism, a nitrogen-centered radical is formed via single-electron reduction of the N−F bond in *N*-fluoroamide **425** with Cu(I) complex bearing an *N,N,P*-ligand derived from a cinchona alkaloid. Intramolecular 1,5-HAT or 1,6-HAT occurs to provide a benzylic radical that is trapped by the chiral L*Cu(II)−alkynyl species to trigger asymmetric alkynylation. Shortly thereafter, Wang and colleagues achieved an analogous enantioselective C(sp^3)−H alkynylation with alkynylsilanes **427** under Cu(I)/BOX catalysis via a 1,5-HAT pathway, in which transmetalation generates the key chiral L*Cu(II)−alkynyl intermediate (Scheme 83b).[357]

In 2022, Zhang, Qi, Guo, and collaborators achieved another type of asymmetric C(sp^3)−H alkynylation through 1,5-HAT by merging photoredox and copper catalysis with a bisoxazoline diphenylamine (BOPA) **L73** and BINOL *ent*-**L48** cooperative ligand system (Scheme 83c).[358] Based on previous findings,[359] control experiments, and DFT calculations, the BOPA-ligated copper(I) acetylide species could act as a photosensitizer. Upon excitation by visible light, the excited state species reduces the 2-iodobenzamide derivative **429** via SET. The formation of a hydrogen-bonding complex with BINOL *ent*-**L48** lowers the reduction potential of the excited state species to facilitate this step. The resulting aryl radical then abstracts the H atom adjacent to nitrogen via 1,5-HAT, and the aliphatic carbon radical is captured by the Cu(II) acetylide intermediate to yield

https://doi.org/10.1021/acs.chemrev.6c00255
Chem. Rev. XXXX, XXX, XXX−XXX

Scheme 80. Cu(I)/BOX-Catalyzed Enantioselective C−H Cyanation via 1,5-HAT

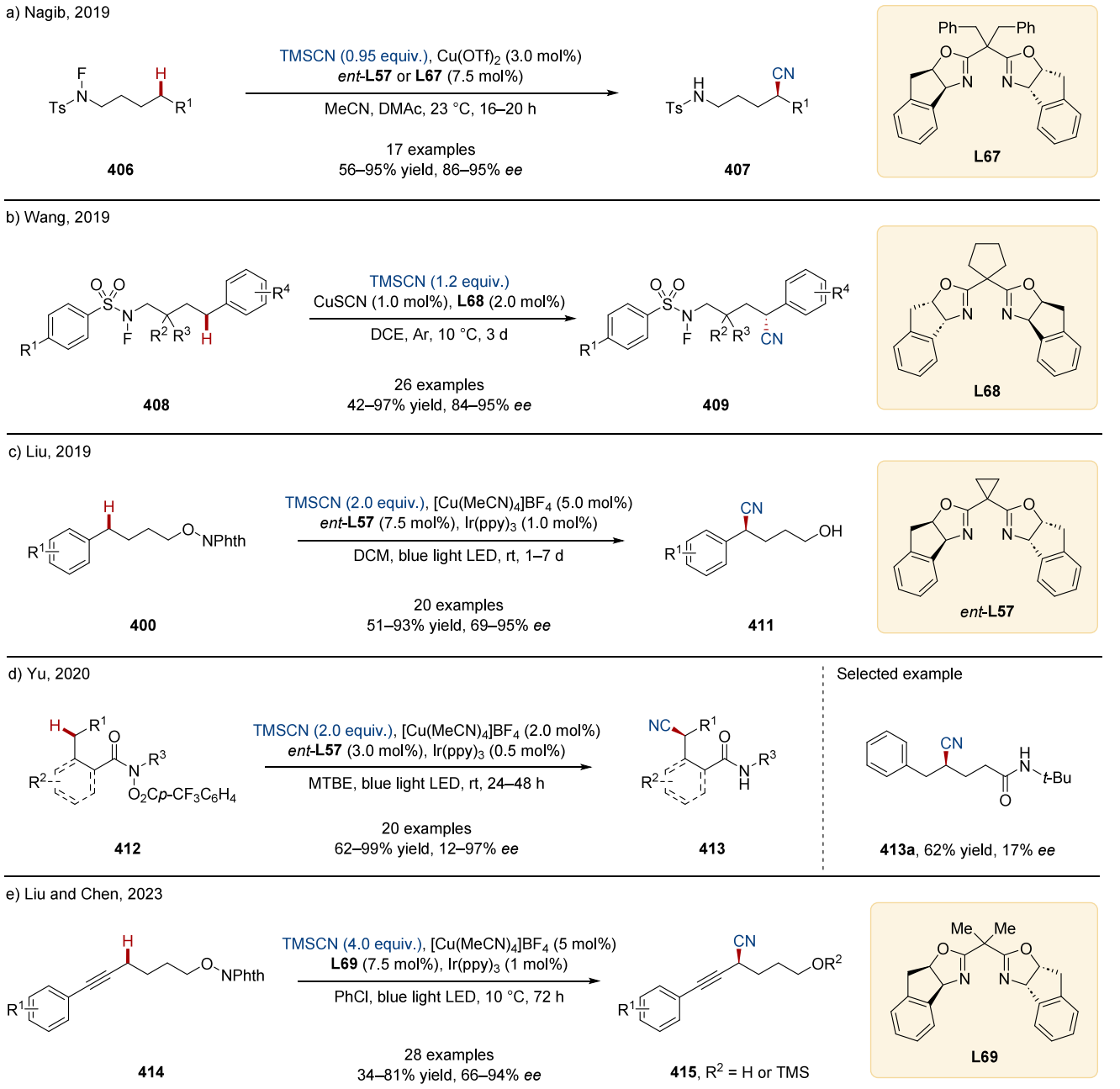

the enantioenriched cyclic amine **431** after the final stereoselective C(sp^3)−C(sp) reductive elimination step, of which the reduction potential might ulteriorly decreased by BINOL *ent*-**L48** with hydrogen-bond interactions.

Meanwhile, encouraged by their early accomplishments in asymmetric trifluoromethylalkynylation of olefins through radical relay,[360] in 2020 Liu, Lin, and co-workers then revealed a copper-catalyzed direct enantioselective C−H alkynylation of alkylarenes **432** with alkynylsilanes **433** in the presence of monocyclopentyl-substituted bisoxazoline ligand **L74** (Scheme 83d).[361] A subtly modified NFSI derivative was used as the nitrogen radical precursor. Intermolecular HAA furnishes the benzylic radical and a bisarenesulfonimide byproduct, which may also participate in the sequent functionalization step through coordination to copper center. DFT calculations excluded the possibility of the outer-sphere C−C coupling between benzylic carbon radical and the chiral L*Cu(II)−alkynyl intermediate and supported a conventional mechanism involving radical capture and asymmetric reductive elimination.

7.3.4. Enantioselective C−H (Fluoro)alkylation. In 2022, the Liu group reported the enantioselective trifluoromethylation of benzylic C−H bonds via Cu(I)/BOX catalysis in combination with photoinduced HAA (Scheme 84).[362] Guided by their prior work on asymmetric radical ring-opening trifluoromethylation[363] and MacMillan's aliphatic C−H trifluoromethylation,[364] the electrophilic Togni-II reagent **436** was used as the $CF_3^•$ source. Control experiments suggested that the reaction is initiated with the excited anthraquinone-type photosensitizer promoting HAT and generating a benzylic radical **Int121**. In contrast to the copper(I)/BOX radical relay catalysis described above for other C−H functionalization, the chiral L*Cu(I) catalyst **Int123** is first oxidized by Togni-II

https://doi.org/10.1021/acs.chemrev.6c00255
Chem. Rev. XXXX, XXX, XXX−XXX

Scheme 81. Cu(I)/BOX-Catalyzed Photoelectrochemical Enantioselective C−H Cyanation

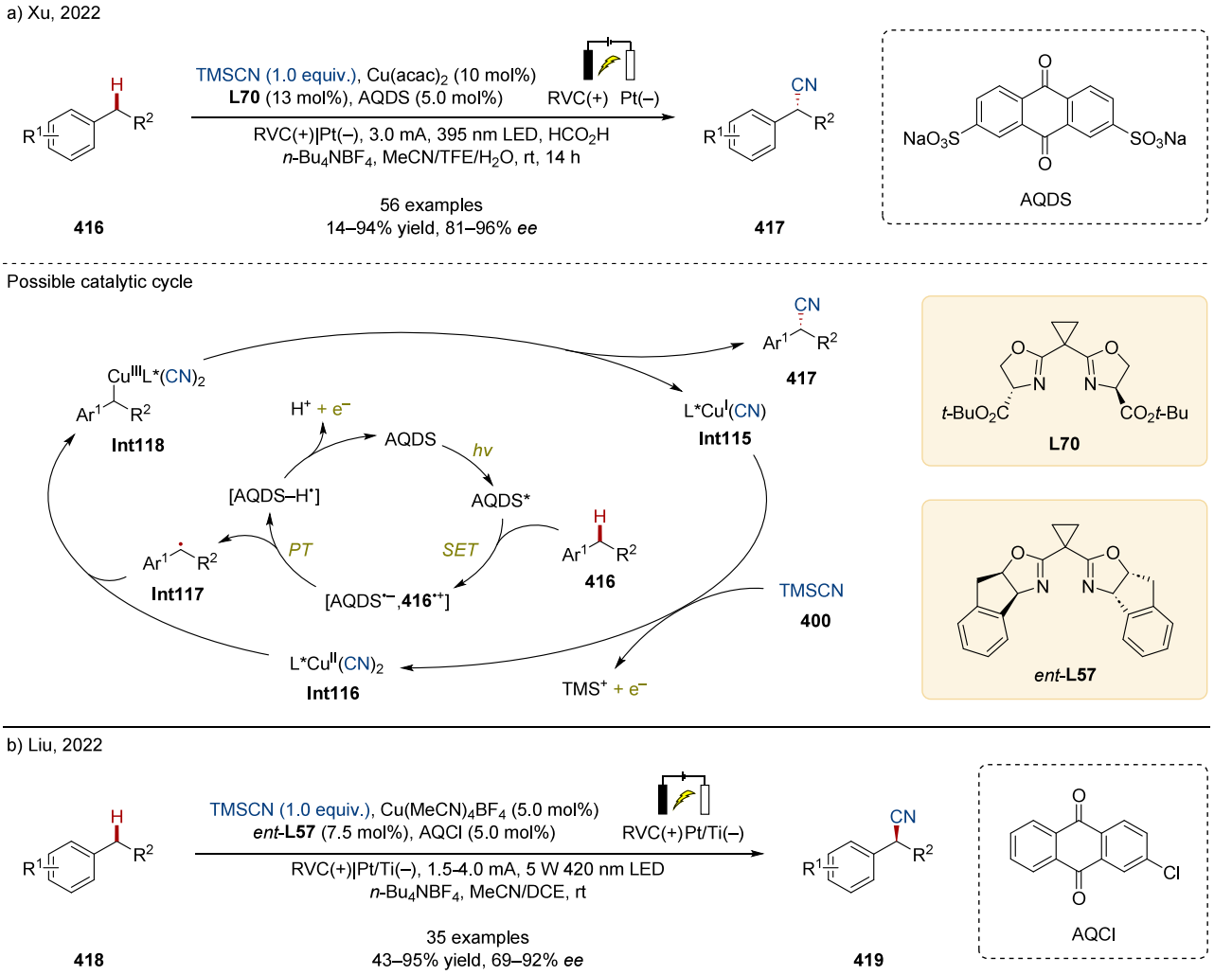

Scheme 82. Cu(I)/BOX-Catalyzed Enantioselective C−H Arylation

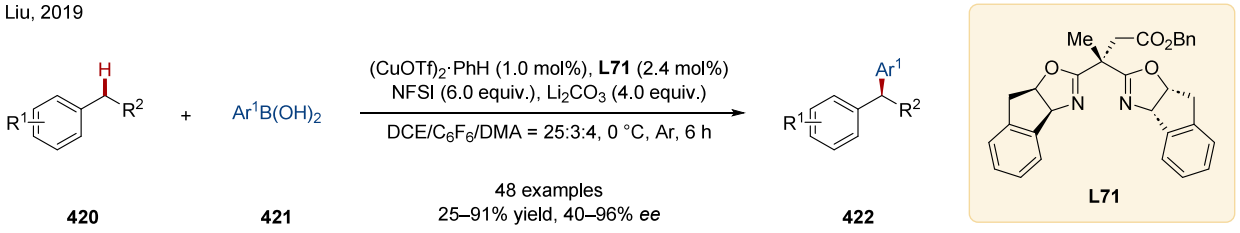

reagent **436** to a Cu(III) intermediate **Int124**. This Cu(III) species acts as a single-electron oxidant to regenerated the ground-state photocatalyst AQ from the AQ−H• radical, while concurrently releasing a L*Cu(II)−CF_3 complex **Int125** capable of reversible carbon-centered radical trapping.

Transition metal-catalyzed carbenoid insertion into C−H bonds is a well-established and versatile strategy for forming C−C bonds with broad functional group tolerance.[11d,314a,b] Numerous enantioselective carbenoid insertions have emerged through the development of a growing collection of chiral ligands.[11b,d,22,365] In 1997, the Schmalz group pioneered copper(I)/BOX-catalyzed carbenoid insertion into C(sp^2)−H bonds of ferrocenes **438** and **439** under mild conditions, using an intramolecularly tethered diazo group as the carbene precursor (Scheme 85a).[366] In 2007 Fraile, Mayoral, and co-workers then achieved stereoselective C(sp^3)−H alkylation at the α-position of oxacycles, albeit with poor to moderate enantiocontrol,[367] demonstrating the feasibility of copper-carbenoid insertion for constructing three-dimensional frameworks bearing continuous stereocenters, as further supported by subsequent reports from the authors and others.[368] Moreover, Maguire and colleagues disclosed a high regio- and enantioselective Cu(I)/BOX-catalyzed carbene insertion into C(sp^3)−H bonds, enabling 1,6- or 1,5-alkylation/annulation of α-diazo-β-keto sulfones **442** and **444** (Scheme 85b).[369] Follow up studies from the same group systematically elucidated the influence of carbene substituent, catalyst, ligand, additive, and counterion on this intramolecular C−H insertion.[370]

7.3.5. Enantioselective C−H Amination and Amidation. Although numerous early efforts toward asymmetric C−H

https://doi.org/10.1021/acs.chemrev.6c00255
Chem. Rev. XXXX, XXX, XXX−XXX

Scheme 83. Enantioselective C−H Alkynylation Catalyzed Cu(I)/*N,N,P*-Tridentate Ligand, BOPA, or BOX Complexes

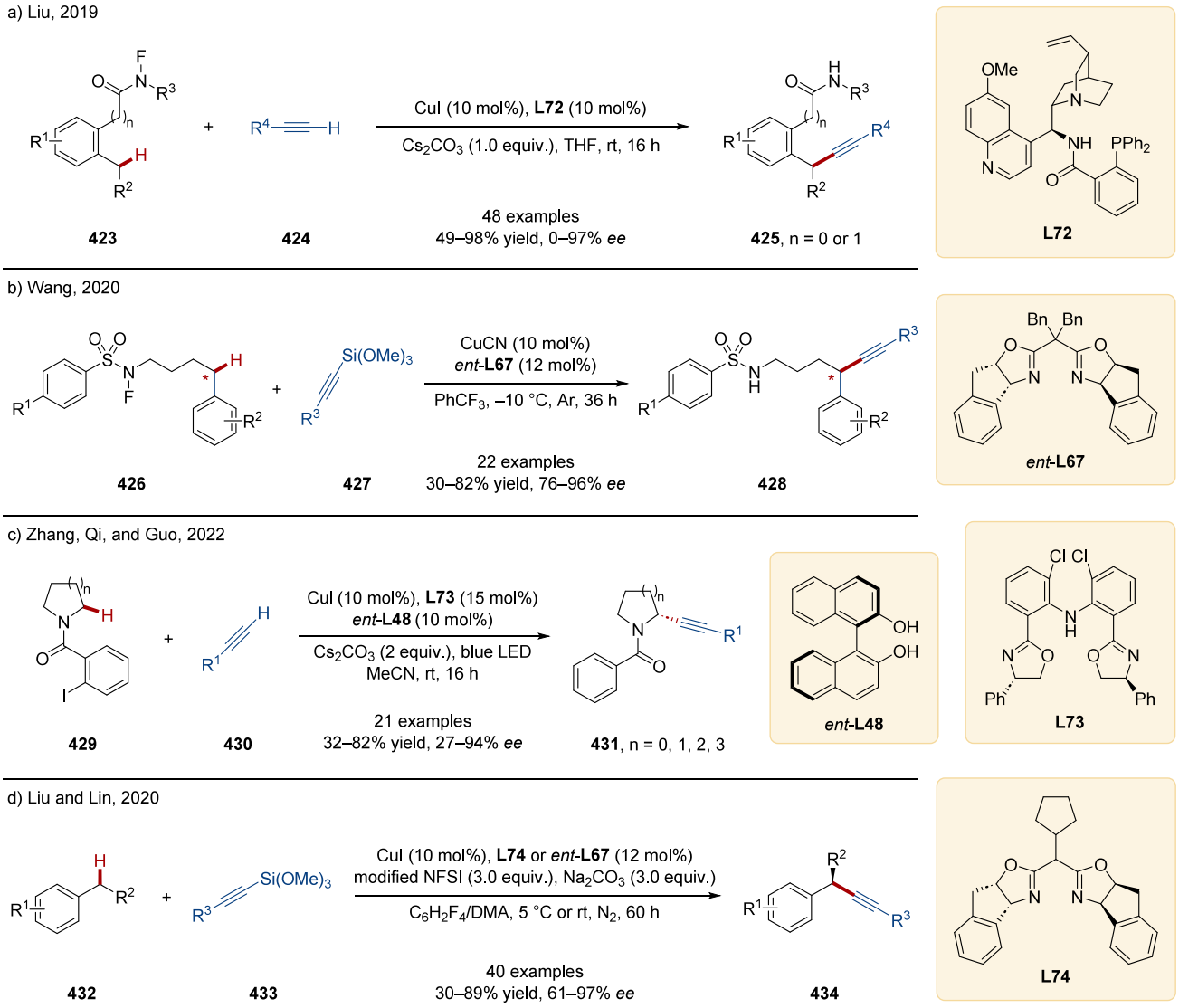

amidation via radical relay catalysis have been reported since 1997, these methods typically relied on super stoichiometric amounts of the cyclic alkene substrates and delivered only modest enantioselectivities.[371] Beyond direct C−C bond formation with high stereocontrol, photoassisted Cu(I)/BOX catalysis was extended to intramolecular asymmetric C−H amination/cyclization by the Nagib group in 2020 (Scheme 86a).[372] Oxime imidates **446**, generated *in situ* from diverse alcohols and imidoyl chlorides, initially coordinate to a Cu(I)/BOX catalyst. Upon energy transfer (EnT) from a photoexcited iridium catalyst, homolysis of the triplet-sensitized oxime N−O bond produces a Cu(II)-bound nitrogen-centered radical.[373] Subsequent experimental and computational mechanistic studies indicated that a regio- and enantioselective intramolecular 1,5-HAT occurs, furnishing chiral oxazoline products **447** either through a radical metalation/Cu(III) reductive elimination cascade[332,345,374] or via an outer-sphere direct radical coupling with the Cu(II) complex.[375]

In 2023, Karmer, Lian, and co-workers reported an efficient photopromoted enantioselective C−H amidation for the synthesis of chiral *N*-acyl or -carbamate benzylic amides **450** (Scheme 86b).[376] Inspired by earlier studies on asymmetric amidation of carbon-centered radicals,[377] a chiral *N,N*-bidentate BOX ligand **L64** was enlisted to enable radical relay catalysis,[332] wherein the benzylic radicals are generated via intermolecular HAT with *tert*-butoxy radicals formed from photoassisted DTBP homolysis.[301b] Nearly simultaneously, the Zhou group independently realized the same transformation for *ent*-**450** through copper radical relay catalysis without the use of photocatalysis (Scheme 86c).[378]

Notably, although the singlet acylnitrenoids typically favor concerted C−H insertion,[379] they may also tautomerize into open-shell L*Cu−nitrenoid species via spin crossover or orbital reorganization.[380] Such intermediates are closely analogous to the Cu(II)-bound nitrogen radicals featuring direct Cu−N coordination discussed above.[336,337,340,341,356,357,372] In 2023, the Chang group reported a Cu(I)/BOX-catalyzed intramolecular regio- and enantioselective δ-C(sp^3)−H amidation using dioxazolones **451** as nitrene precursors (Scheme 87).[381] In contrast to their earlier iridium-catalyzed asymmetric γ-C−H amidation of dioxazolones proceeding via Ir−nitrenoid insertion,[382] pronounced KIE as 3.5 ± 0.3,[379b,383] TEMPO trapping experiments, and DFT calculations collective support a stepwise mechanism. The mechanism involves initial 1,6-HAA

https://doi.org/10.1021/acs.chemrev.6c00255
Chem. Rev. XXXX, XXX, XXX−XXX

Scheme 84. Cu(I)/BOX-Catalyzed Enantioselective C−H Fluoroalkylation

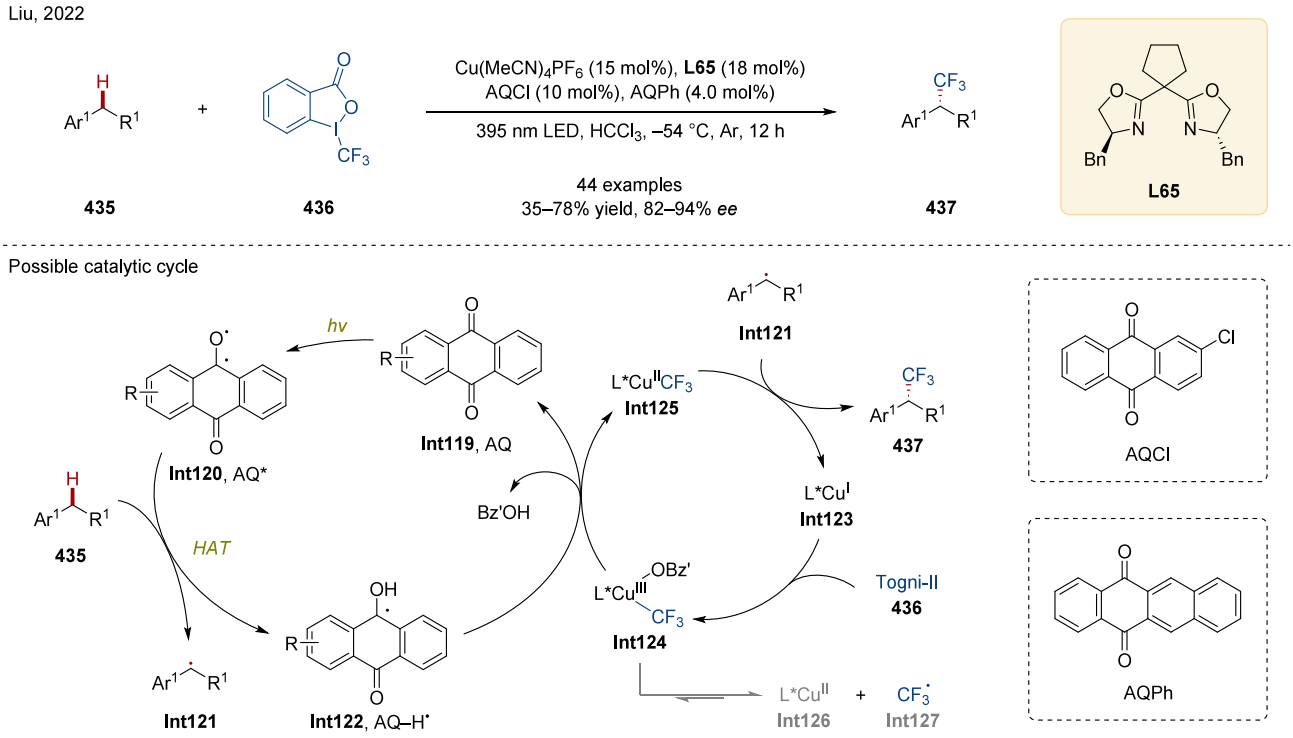

Scheme 85. Cu(I)/BOX-Catalyzed Enantioselective C−H Alkylation via Carbenoid Insertion

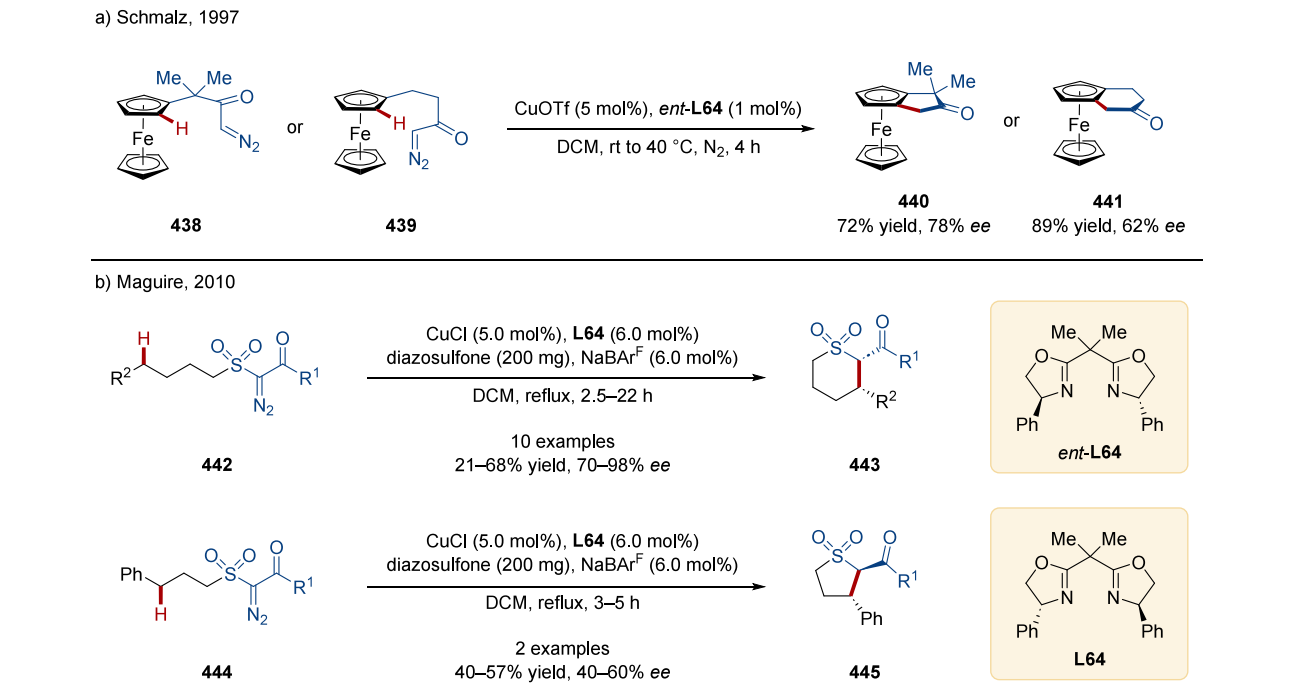

by an open-shell singlet Cu−acylnitrenoid species, followed by radical rebound C−N formation, with the former step governing regioselectivity and the latter dictating enantioselectivity.

7.3.6. Enantioselective C−H Acyloxylation. Although the copper-catalyzed asymmetric Kharasch−Sosnovsky oxidation has been investigated with a long history,[329] a large excess (usually 4−10 equivalent) of specific C−H substrates (typically a narrow scope of simple symmetrical cyclic alkenes) remains necessary to achieve satisfactory yields and selectivities.[329−331] Stimulated by Liu and Stahl's groundbreaking research on Cu(I)/BOX-catalyzed enantioselective C−H cyanation via radical relay,[332] in 2024, the Kramer group accomplished the photopromoted stereoselective allylic C(sp^3)−H acyloxylation of olefins **453** with the olefin as the limiting reagent (Scheme 88a).[384] Regarding the mechanism, a *tert*-butoxyl radical for the HAT step could be generated through either the traditional Kharasch−Sosnovsky oxidation mechanism[329,385] or the photoexcited homolysis of the perester **454**.[386] The authors favor the

https://doi.org/10.1021/acs.chemrev.6c00255
Chem. Rev. XXXX, XXX, XXX−XXX

Scheme 86. Cu(I)/BOX-Catalyzed Enantioselective C−H Amination and Amidation

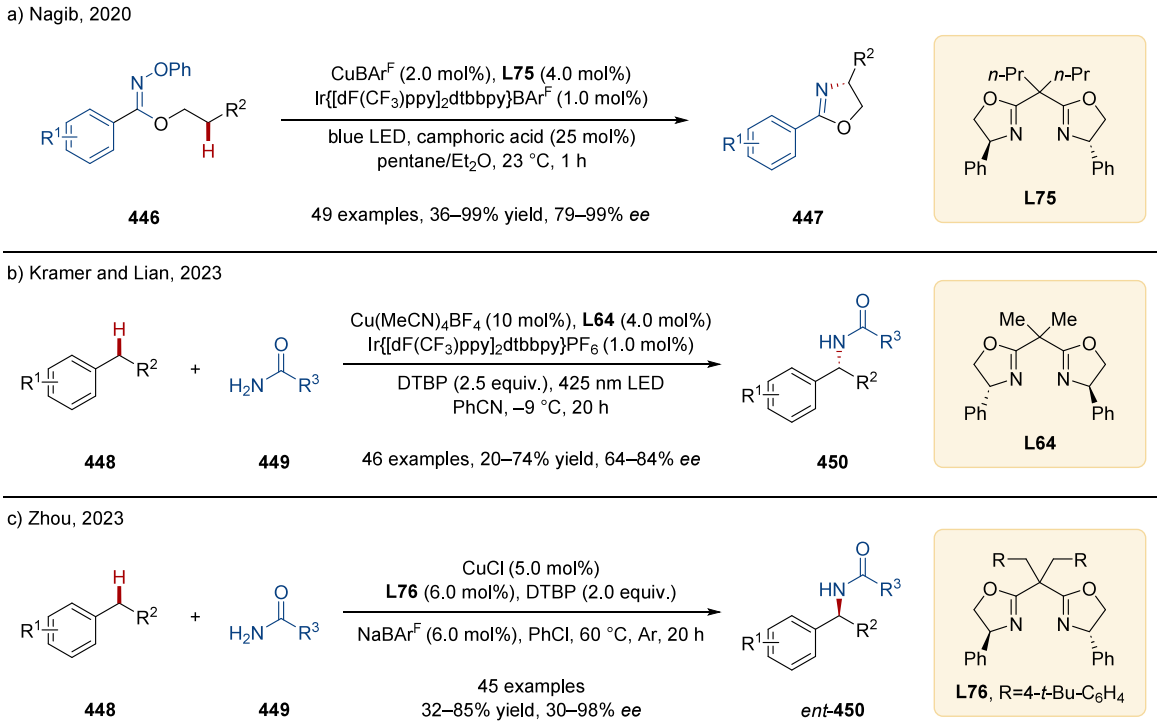

Scheme 87. Cu(I)/BOX-Catalyzed Enantioselective C−H Amidation via Nitrenoid Transfer

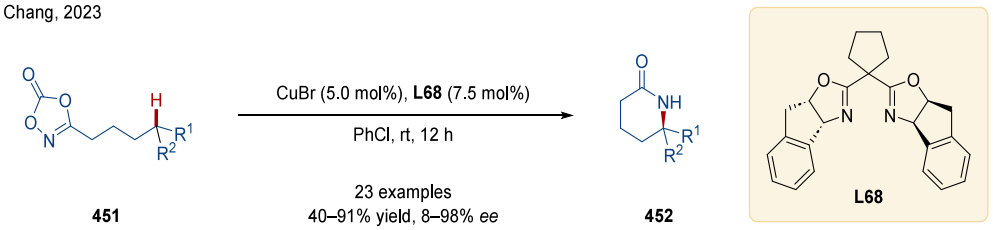

latter process as the major pathway since the former involves formation of copper(II) species **Int129** via SET oxidation by perester **454**. If the allylic radical is not formed or does not couple effectively, **Int129**, which is unable to initiate the catalytic cycle, can accumulate.[386c,387] A 1:1 *E*/*Z* mixture of 1-aryl-2-alkyl alkenes could be used directly in this transformation, providing the corresponding esters **455** in excellent regio- and enantioselectivities with a >20:1 *E*/*Z* ratio for all the examples, which is consistent with the results for pure *E*-isomer of substrate **453**. Reaction progress monitoring experiments revealed that both the (*E*)-**453** and (*Z*)-**453** could be converted into (*E*)-**455** in a convergent manner and that the consumption rates of both isomers were not significantly different. This result may be attributed to isomerization of the allylic radical intermediate **Int132**.[239] Shortly thereafter, the same group also illustrated the enantioselective benzylic C−H phosphorylation by dual photocatalysis and copper catalysis.[388]

In 2025, Liu, Lin, and co-workers demonstrated a biomimetic site- and enantioselective allylic oxidation of limiting C−H substrates **456** using a similar Cu(I)/BOX catalytic system. The reaction exhibited broad functional-group tolerance and accommodated structurally complex substrates, including those derived from natural products, pharmaceuticals, and their analogues (Scheme 88b).[389] Diethyl hydrazodicarboxylate was employed as a reductant for regenerating the catalytically reactive Cu(I) species. As the reactivity and enantioselectivity are reliant on the choice of solvent, in-depth mechanistic experiments and computational analysis were performed, revealing the involvement of a Cu(II)-bound *tert*-butoxy radical in the HAA process when TFE was used as the solvent, as represented by **TS24**. Strikingly, the involvement of Cu-associated radicals is consistent with mechanisms invoked in copper-based enzymatic C(sp^3)−H oxidations.[390] In contrast, in MeCN the conventional free *t*-BuO$^\bullet$ radical was detected by EPR with the spin trap DMPO, as reported previously.[385,391] By employing this allylic C−H acyloxylation methodology, the enantioenriched triol **460** was synthesized smoothly in 3 steps. In parallel, Yu, Dang, and collaborators (Scheme 89a)[392] as well as Zhou, Xiao, Xue, and colleagues (Scheme 89b)[393] independently developed visible light-mediated copper(I)-catalyzed enantioselective Kharasch−Sosnovsky oxidations of olefins with carboxylic acids **465** and **468**. In both cases, di-*tert*-butyl peroxide (DTBP) served as the oxidant, thereby eliminating the need to preform the corresponding peresters.

Beyond allylic C−H bonds, in 2024 Yu, Song, and co-workers described photoinduced Cu(I)/PyBOX-catalyzed enantioselective propargylic C(sp^3)−H acyloxylation with peroxides **457** (Scheme 90a).[394] The direct use of carboxylic acids together with DTBP was recognized as an advance toward practical C−H esterification. This transformation was then demonstrated by

https://doi.org/10.1021/acs.chemrev.6c00255
Chem. Rev. XXXX, XXX, XXX−XXX

Scheme 88. Cu(I)/BOX-Catalyzed Enantioselective Allylic C−H Acyloxylation with Alkene as the Limiting Reagent

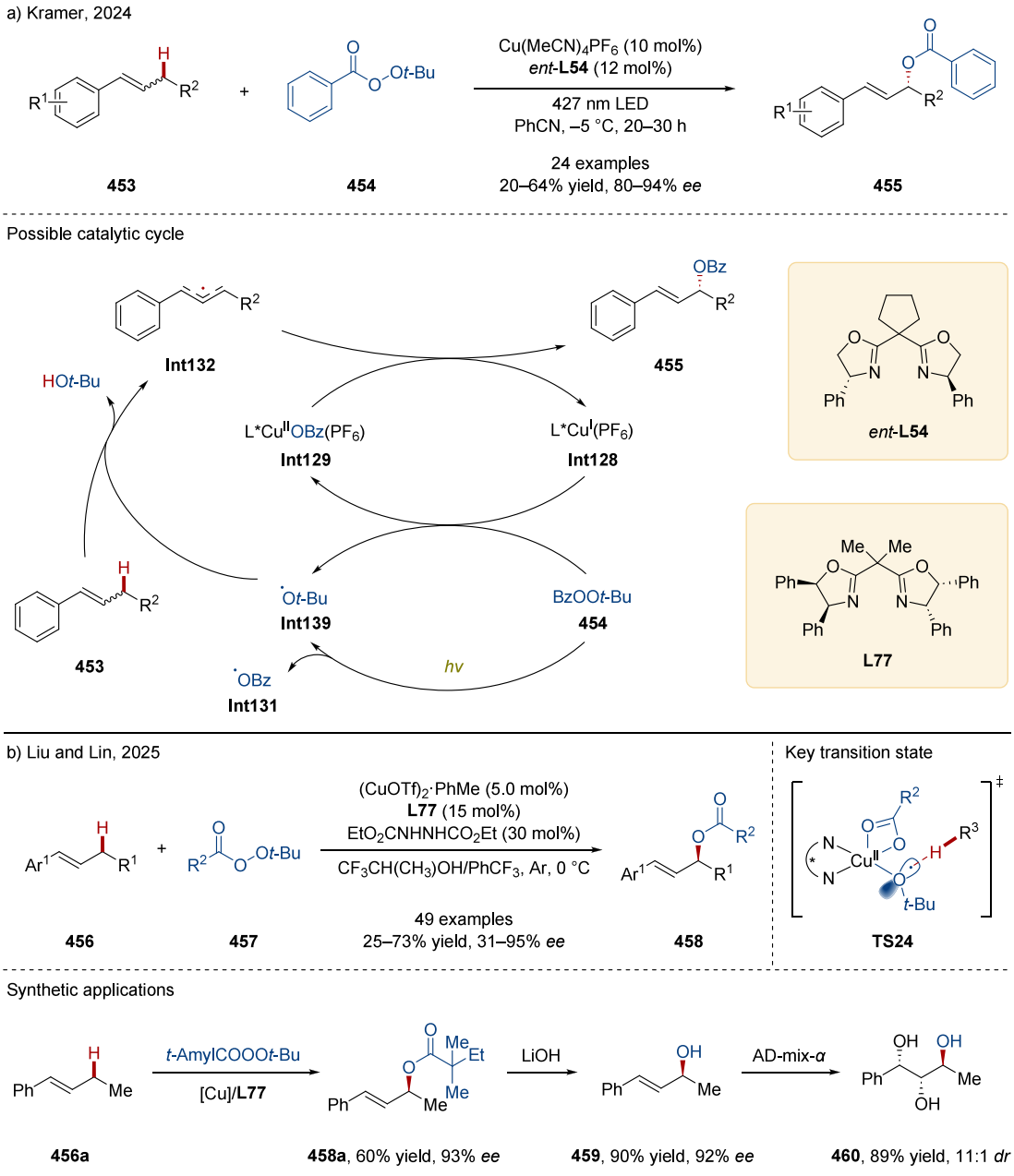

the Zhou group[393] and the Liu group[389] (Scheme 90b) employing either photocatalysis or chemical oxidation, and as reported by Liu and co-workers, this methodology also enabled formal syntheses of biologically active molecules, including alfaprostol **480**, virol A **481**, and virol C **482** (Scheme 90b).[389] Moreover, Bao, Zhu, and collaborators showcased the copper-catalyzed regio- and enantioselective benzylic propargylic C−H oxidation of arenes **461** with a tridentate PyBOX ligand **L81** (Scheme 90c).[395]

7.4. Cu(I)/CPA Catalysis

Building on their earlier success in chiral phosphate-mediated asymmetric functionalization of carbon radicals,[313b] the Liu group applied copper radical relay catalysis in the enantioselective allylic and benzylic C(sp^3)−H amidation/cyclization (Scheme 91a).[396] 2-Hydroxy-5-methoxyisoindoline-1,3-dione (4-OMe-NHPI) was employed as a stable HAT mediator[397] between the reactive alkoxy radical and the substrate **486**, enabling regio- and chemoselective C−H cleavage in the presence of both copper(II)−phosphate and zinc(II)−phosphate complexes. Notably, more than one CPA ligand **L83** participates in the stereodetermining C−N bond forming step, as evidenced by a pronounced nonlinear effect (NLE).

Concurrently, the same group reported the Cu(I)/CPA-catalyzed intramolecular enantioconvergent amidation of racemic tertiary C(sp^3)−H bonds via DKR (Scheme 91b).[398] Such a transformation is traditionally challenging for radical rebound[399] or C−H metalation pathways due to partial or complete retention of stereogenic configuration with insufficient racemization at the carbon stereocenter. In this protocol, racemic ketones were condensed with arenesulfonohydrazide (Ar^1NHNH_2) to generate *E*/*Z*-mixtures of racemic hydrazones **488**. H-atom abstraction from nitrogen by the *tert*-butoxy radical produces an *N*-centered radical, which undergoes rapid *E*/*Z*-isomerization facilitated by external acid.[400] Subsequent

https://doi.org/10.1021/acs.chemrev.6c00255
Chem. Rev. XXXX, XXX, XXX−XXX

Scheme 89. Photopromoted Cu(I)/BOX-Catalyzed Enantioselective Allylic C−H Acyloxylation

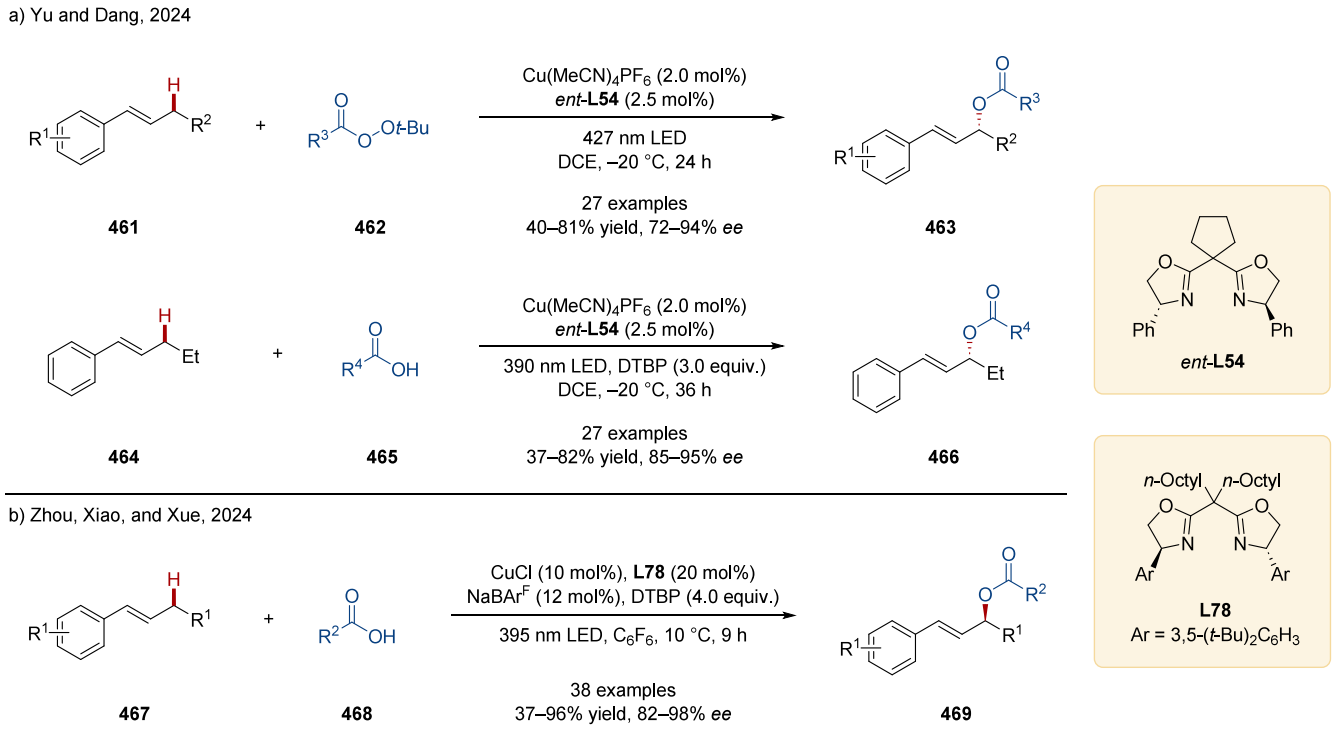

irreversible intramolecular 1,5-HAT, occurring in the absence of the copper−phosphate catalyst, furnishes a nearly planar prochiral tertiary carbon radical. Coordination of this radical to a chiral Cu(II) species then enables enantioselective C−N bond formation, delivering a variety of diazacycles **489** bearing a tetrasubstituted carbon stereocenter. In 2023, Liu, Yang, and co-workers further developed an efficient synthesis of chiral α-quaternary pyrrolidines **491** via asymmetric intramolecular C(sp^3)−H amidation using a related Cu(I)/CPA-catalyzed radical relay strategy (Scheme 91c).[401] In this case, the *N*-centered radical required for 1,5-HAT is generated through single-electron reduction of N−Cl bond.

7.5. Cu(I)/Phosphine Catalysis

In 2021, Xu, Wang, and co-workers reported a visible-light-assisted enantioselective C(sp^3)−H alkylation of quinolinyl-8-glycinate esters **492** using Cu(I)/bisphosphine catalysis (Scheme 92a).[402] This transformation proceeds through a mechanism distinct from previously discussed Cu(I)/oxazoline or Cu(I)/CPA radical relay pathways. Upon light excitation, the substrate−copper(I) complex **Int134** undergoes SET to reduce the NHPI ester **493**, generating an alkyl radical that recombines with copper to form a trivalent alkyl−Cu(III) adduct **Int135**. Subsequent ligand-to-metal charge transfer (LMCT) followed by 1,2-HAT furnishes a Cu(II) species **Int137** bearing a carbon-centered radical. Intramolecular capture of this radical by the copper center and enantiodetermining reductive elimination then deliver the alkylated product **494**. In 2023, the same group further disclosed an enantioselective cyanoalkylation of C-(sp^3)−H bonds at α-nitrogen position of glycine and peptide derivatives **495** containing an 8-amino-5-methoxy quinolyl directing group, enabled by planar chiral bisphosphine **L87** (Scheme 92b).[403] In this case, linear cyanoalkyl radicals are generated via β-C−C bond cleavage after single-electron reduction of cycloalkanone imine esters **496** by substrate-chelated copper(I) complex.

8. CONCLUSIONS AND PERSPECTIVES

Over the past two decades, enantioselective C−H functionalization catalyzed by 3d transition metals has developed rapidly. Through systematic exploration of practical chiral ligands, substantial progress has been achieved via both inner-sphere and outer-sphere pathways, including C−H metalation, HAA/radical rebound, HAA/radical relay, and metal−carbenoid insertion. These strategies have enabled a wide range of transformations of both C(sp^2)−H and C(sp^3)−H bonds. Particularly, unlike well-developed noble metal (e.g., Pd, Rh, Ir) catalysis which usually involves two-electron C−H functionalization processes, various radical relay (with Ni and Cu) and radical rebound (with Mn, Fe, Co, and Cu) pathways are incorporated in 3d metal catalysis, providing a complementary but broad avenue for C−H functionalization of more inert methylene groups. In this context, we have summarized key challenges, core design principles, and mechanistic insights underlying earth-abundant metal-catalyzed asymmetric C−H functionalization. Collectively, these advances open new opportunities for the imaginative design of direct and efficient synthetic routes to biologically active compounds and functional molecules with novel properties—offering promising alternatives to traditional noble metal catalysis.

Nevertheless, several critical challenges remain. First, most current reactions rely on either partially activated C−H bonds (e.g., benzylic, allylic, propargylic, or α-heteroatom) for radical relay and radical rebound catalysis, or the use of directing groups for C−H metalation processes (such as the bidentate 8-aminoquinolyl auxiliary, which may not be straightforward to cleave subsequently) to modulate the reactivity, site-selectivity, and enantioselectivity, restricting potential applications in organic synthesis. Developing catalysts capable of selectively functionalizing unactivated C−H bonds in simple substrates, especially more formidable aliphatic systems (such as hexane), would enable simple chemical feedstocks to be converted into a

https://doi.org/10.1021/acs.chemrev.6c00255
Chem. Rev. XXXX, XXX, XXX−XXX

Scheme 90. Cu(I)/BOX or PyBOX-Catalyzed Enantioselective Propargylic C−H Acyloxylation

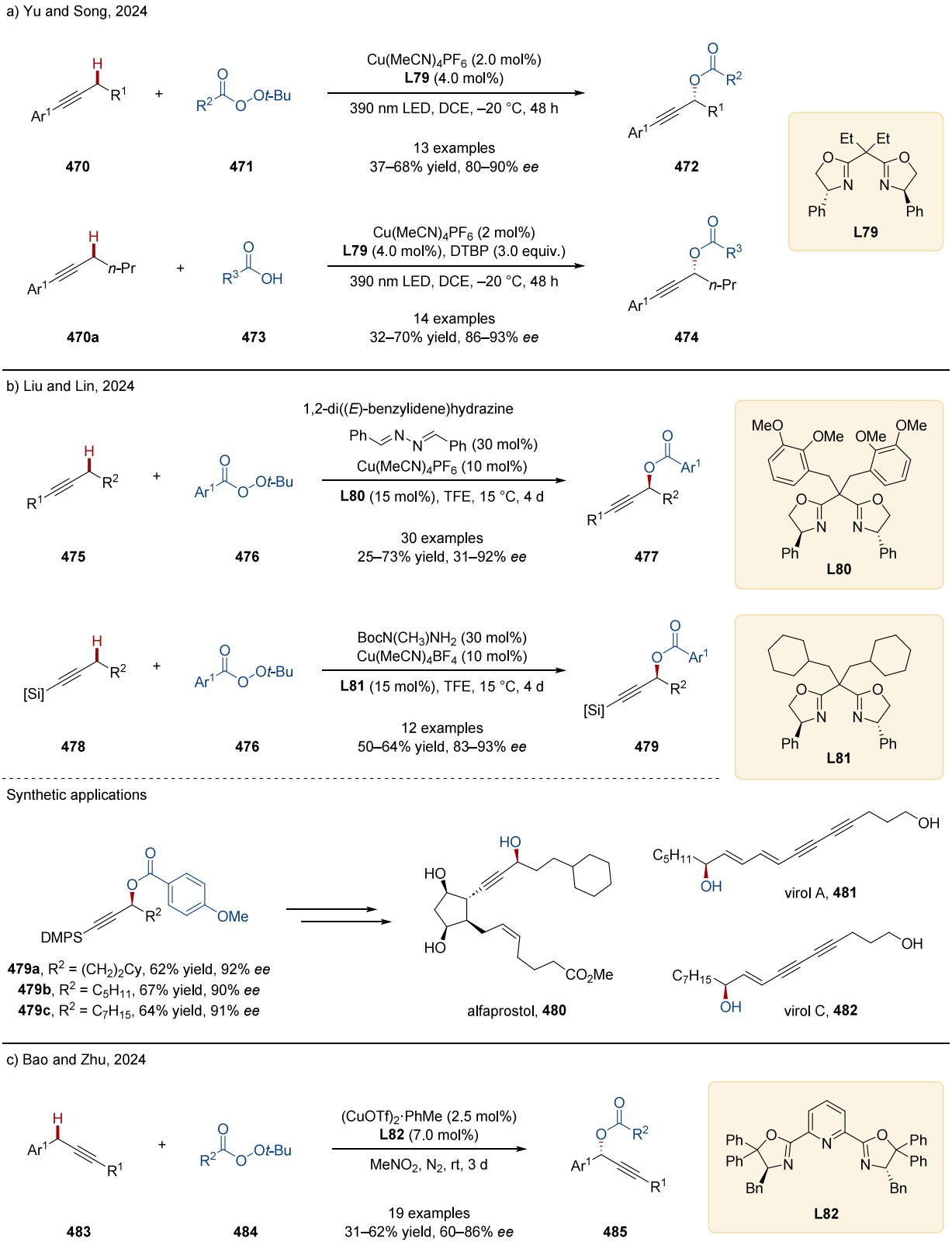

plethora of useful products. Second, the catalyst loading of the metal and ligand remains high in most cases (often 5−10 mol%), which can introduce downstream issues with metal sequestration. Improved catalyst designs are also expected to enhance catalytic turnover, thereby improving the practicality and industrial relevance of these methods. Third, owing to the limited availability of privileged ligands and robust catalytic systems, enantioselective C−H functionalization mediated by early 3d transition metals (e.g., Ti, V, and Cr) and post-transition metals (e.g., Zn) remains particularly challenging. Addressing this gap could unlock currently inaccessible transformations and further enrich the methodological toolbox

https://doi.org/10.1021/acs.chemrev.6c00255
Chem. Rev. XXXX, XXX, XXX−XXX

Scheme 91. Cu(I)/CPA-Catalyzed Enantioselective C−H Amidation

a) Liu, 2020

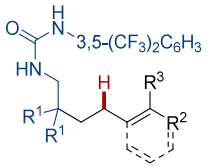

486

CuOAc or CuTc (10 mol%), **L83** or Zn(**L83**)$_2$ (15–20 mol%)
1-AdOCO$_3$*t*-Bu or 1-AdOCO$_3$*t*-Amyl (2.0–3.0 equiv.)
4-OMe-NHPI (0.2–1.0 equiv.)
ZnO (0–1.5 equiv.), DCM, 10 °C–rt, Ar, 1–7 d

34 examples, 14–88% yield, 36–94% *ee*

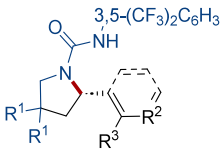

487

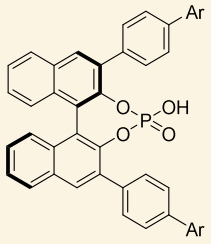

L83, Ar = 9-phenanthryl

b) Liu, 2020

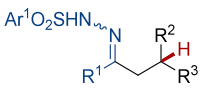

488

CuCN (10 mol%), **L84** (15 mol%)
$(NH_4)_2CO_3$ (5.0 mol%), Ph(CH_2)$_3$CO$_3$*t*-Bu (2.0 equiv.)
i-PrCO$_2$*i*-Pr, 35 °C, 96 h

47 examples
35–85% yield, 73–96% *ee*

489

Possible enantiocontrol model

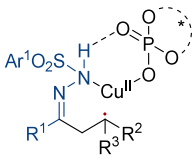

Int133

c) Liu and Yang, 2023

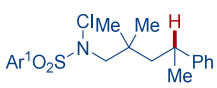

490

CuCN (10 mol%), **L85** (12 mol%)
Ag_2CO_3 (0.6 equiv.), 1,4-dioxane, rt, 24 h

6 examples, 17–35% yield, 61–81% *ee*

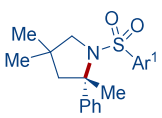

491

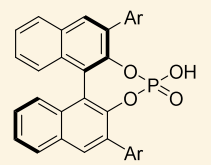

L84, Ar = 2,4,6-Me$_3$C$_6$H$_2$
L85, Ar = 9-phenanthryl

Scheme 92. Cu(I)/Phosphine-Catalyzed Enantioselective C−H Alkylation

a) Xu and Wang, 2021

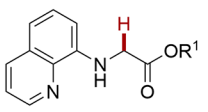

492

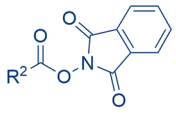

493

Cu(OTf)$_2$ (10 mol%)
L86 (11 mol%), DABCO (1.0 equiv.)
30 W blue LED
DMF, –10 °C, Ar, 60 h

35 examples
73–91% yield, 71–99% *ee*

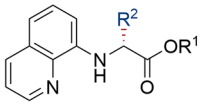

494

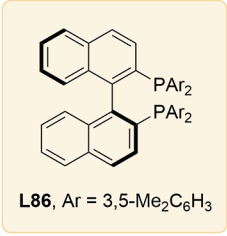

L86, Ar = 3,5-Me$_2$C$_6$H$_3$

Possible key intermediates

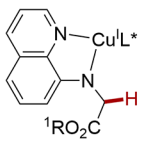

Int134

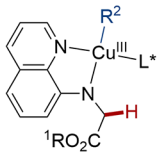

Int135

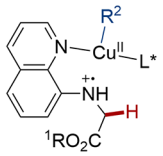

Int136

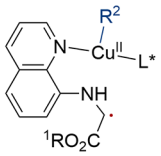

Int137

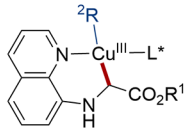

Int138

b) Xu and Wang, 2023

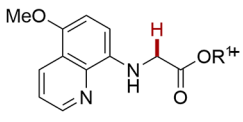

495

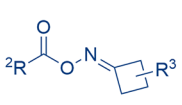

496

Cu(CH$_3$CN)$_4$PF$_6$ (10 mol%)
L87 (15 mol%)
DABCO (2.0 equiv.)
acetone, 0 °C, Ar, 18 h

26 examples
60–80% yield, 87–94% *ee*

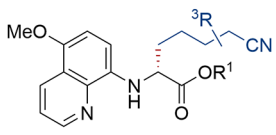

497

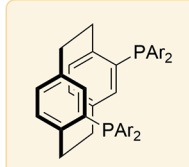

L87
Ar = 4-OMeC$_6$H$_4$

https://doi.org/10.1021/acs.chemrev.6c00255
Chem. Rev. XXXX, XXX, XXX−XXX

for asymmetric C−H activation, given the distinctive intrinsic properties of these metals. Finally, deeper integration of emerging technologies—including electrosynthesis, photochemistry, data science, and artificial intelligence (AI)—has the potential to dramatically accelerate progress in 3d metal catalysis. In particular, AI-empowered catalysis[404] and automation, informed by comprehensive mechanistic understanding, should enhance the entire workflow of reaction discovery, optimization, and scope assessment, and enable tailored catalysts and conditions to be discovered for individual substrates and transformations of interest. We anticipate that sustained and collaborative efforts in these directions will propel this field toward greater practicality, sustainability, and synthetic versatility, fostering impactful advances at the intersection of organic synthesis, organometallic chemistry, and asymmetric homogeneous catalysis in the years to come.

AUTHOR INFORMATION

Corresponding Authors

Bing-Feng Shi − *State Key Laboratory of Soil Pollution Control and Safety, Department of Chemistry, Zhejiang University, Hangzhou 310058, China;* orcid.org/0000-0003-0375-955X; Email: bfshi@zju.edu.cn

Keary M. Engle − *Department of Chemistry, The Scripps Research Institute, La Jolla, California 92037, United States;* orcid.org/0000-0003-2767-6556; Email: keary@scripps.edu

Authors

Pu-Fan Qian − *State Key Laboratory of Soil Pollution Control and Safety, Department of Chemistry, Zhejiang University, Hangzhou 310058, China;* orcid.org/0000-0003-2065-3669

Jia-Heng Hu − *State Key Laboratory of Soil Pollution Control and Safety, Department of Chemistry, Zhejiang University, Hangzhou 310058, China*

Yan-Xuan Wu − *State Key Laboratory of Soil Pollution Control and Safety, Department of Chemistry, Zhejiang University, Hangzhou 310058, China*

Yuan Xu − *State Key Laboratory of Soil Pollution Control and Safety, Department of Chemistry, Zhejiang University, Hangzhou 310058, China*

Complete contact information is available at: https://pubs.acs.org/10.1021/acs.chemrev.6c00255

Author Contributions

[§]J.-H.H., Y.-X.W., and Y.X. contributed equally to this work.

Notes

The authors declare no competing financial interest.

Biographies

Pu-Fan Qian was born in Zhejiang, China. He joined the research group of Prof. Bing-Feng Shi in 2019 and received a B.Sc. degree from Zhejiang University in 2022. Now he is a Ph.D. candidate in Zhejiang University under the guidance of Prof. Bing-Feng Shi. His research interests focus on the development of transition metal-catalyzed site- and enantioselective C−H functionalization and its application in the asymmetric synthesis of chiral functional molecules.

Jia-Heng Hu was born in Zhejiang, China. He commenced his undergraduate studies at Zhejiang University in 2022 and now conducts research under the supervision of Prof. Bing-Feng Shi. His research endeavors are centered on developing methodology of transition metal-catalyzed C−H functionalization.

Yan-Xuan Wu was born in Zhejiang, China. She received a B.Sc. degree from Zhengzhou University in 2024 (Advisors: Prof. Xuenian Chen and Dr. Yan-Na Ma) and now she is a Ph.D. student in Zhejiang University under the guidance of Prof. Bing-Feng Shi. Her research endeavors are centered on developing methodology of transition metal-catalyzed C−H functionalization.

Yuan Xu was born in Sichuan, China. He is currently pursuing a B.Sc. degree at Zhejiang University, under the supervision of Prof. Bing-Feng Shi, and also working as intern under Prof. Keary M. Engle. His research focuses on the methodology of metal-catalyzed enantioselective C−H functionalization.

Keary M. Engle was born in Lansing, Michigan, USA. He received his B.S. degree in Chemistry, Economics, Mathematics, and Statistics from the University of Michigan in 2007. He carried out graduate studies jointly at The Scripps Research Institute and the University of Oxford, earning a Ph.D. degree in Chemistry from The Scripps Research Institute under the guidance of Prof. Jin-Quan Yu and a D.Phil. degree in Biochemistry from the University of Oxford under the supervision of Prof. Véronique Gouverneur and Prof. John M. Brown in 2013. Following an NIH postdoctoral fellowship at the California Institute of Technology working with Prof. Robert H. Grubbs (2013−2015), he joined The Scripps Research Institute as an Assistant Professor in 2015 and was promoted to Professor in 2020. He currently serves as the John and Susan Diekman Dean of Graduate & Postdoctoral Studies at Scripps Research. His research interests focus on transition metal-catalyzed C−H functionalization and alkene difunctionalization.

Bing-Feng Shi was born in Shandong, China. He received his B.S. degree from Nankai University in 2001 and his Ph.D. degree from the Shanghai Institute of Organic Chemistry, Chinese Academy of Sciences, in 2006, under the supervision of Prof. Biao Yu. He then pursued postdoctoral studies with Prof. Michael S. VanNieuwenhze at the University of California, San Diego (2006−2007), before moving to The Scripps Research Institute, where he worked as a Research Associate with Prof. Jin-Quan Yu. In 2010, he joined the Department of Chemistry at Zhejiang University as a tenure-track professor, was promoted to Professor in 2014, and was appointed Qiushi Distinguished Professor in 2020. He currently serves as Vice Dean of the Faculty of Science at Zhejiang University and as an Associate Editor of *The Journal of Organic Chemistry*. His research focuses on transition metal-catalyzed C−H functionalization and its application in the synthesis of biologically important small molecules.

ACKNOWLEDGMENTS

Financial supports from National Natural Science Foundation of China (22525011, U25A20547, U22A20388, 92256302 for B.-F.S., 223B2118 for P.-F.Q.), National Key R&D Program of China (2022YFA1504302, 2021YFF0701603 for B.-F.S.), Fundamental and Interdisciplinary Disciplines Breakthrough Plan of the Ministry of Education of China (JYB2025XDXM407 for B.-F.S.) and Scripps Research Institute (for K.M.E.) are gratefully acknowledged.

ABBREVIATIONS

4CzIPN = 2,4,5,6-tetra(9*H*-carbazol-9-yl)isophthalonitrile
4-PPN = 4-phenylpyridine-*N*-oxide
σ-CAM = σ-complex assisted metathesis
Å = Ångstrom
AA = amino acids
Ac = acetyl

acac = acetylacetonate
Ad = adamantyl
AD = asymmetric dihydroxylation
AI = artificial intelligence
AMPK = adenosine monophosphate-activated protein kinase
AQ = anthraquinone
AQCl = 2-chloroanthraquinone
AQDS = disodium anthraquinone-2,7-disulfonate
AQPh = tetracene-5,12-dione
B_{Ar}^{F} = tetrakis[3,5-bis(trifluoromethyl)phenyl]borate
BDPP = 2,4-bis(diphenylphosphino)pentane
BiIM = biimidazoline
BINOL = 1,1′-bi-2-naphthol
Boc = *tert*-butyloxycarbonyl
BOPA = bisoxazoline diphenylamine
BOX = bisoxazoline
Bn = benzyl
Bu = butyl
Bz = benzoyl
CCA = chiral carboxylic acid
CMD = concerted metalation-deprotonation
cod = 1,5-cyclooctadiene
Cp = cyclopentadienyl
Cp^{X} = (chiral) substituted cyclopentadienyl
Cp* = pentamethylcyclopentadienyl
CPA = chiral phosphoric acid
CPME = cyclopentyl methyl ester
Cy = cyclohexyl
CYP450 = cytochrome P450
DABCO = triethylenediamine
DBU = 1,8-diazabicyclo[5.4.0]-7-undecene
DCP = dicumyl peroxide
DEAc = *N*,*N*-diethylacetamide
DFE = 2,2-difluoroethanol
DFT = density functional theory
DG = directing group
DHIQ = 1,2-dihydroisoquinoline
DHQ = 1,2-dihydroquinoline
DIAD = diisopropyl azodicarboxylate
Difluorphos = 5,5′-bis(diphenylphosphino)-2,2,2′,2′-tetrafluoro-4,4′-bi-1,3-benzodioxole
DIPAMP = (1*S*,1′*S*)-1,1′-(1,2-ethanediyl)bis[1-(2-methoxyphenyl)-1-phenylphosphine]
DIPEA = diisopropylethylamine
DKR = dynamic kinetic resolution
DMAc = *N*,*N*-dimethylacetamide
DMBA = 2,2-dimethylbutanoic acid
DMDC = dimethyl dicarbonate
DME = 1,2-dimethoxyethane
DMF = *N*,*N*-dimethylformamide
DMPB = bis(4-methoxyphenyl)methanone
DMPO = 5,5-dimethyl-1-pyrroline *N*-oxide
DMPS = dimethylphenylsilyl
dtbbpy = 4,4′-di-*tert*-butyl-2,2′-dipyridyl
DTBP = di-*tert*-butyl peroxide
ECD = electronic circular dichroism
EDCI = 1-(3-(dimethylamino)propyl)-3-ethylcarbodiimide hydrochloride
ee = enantiomeric excess
EnT = energy transfer
EPR = electron paramagnetic resonance
Et = ethyl
Et-BPE = 1,2-bis(2,5-diethylphospholano)ethane
HAA = hydrogen atom abstraction
HAT = hydrogen atom transfer
HBA = hydrogen-bond acceptor
HBD = hydrogen-bond donor
HFIP = 1,1,1,3,3,3-hexafluoro-2-propanol
HLF = Hofmann−Löffler−Freytag
HOBT = 1-hydroxybenzotriazole
HPA = phosphotungstic acid
KIE = kinetic isotope effect
KR = kinetic resolution
LED = light-emitting diode
LLHT = ligand-to-ligand hydrogen transfer
LMCT = ligand-to-metal charge transfer
MAD = methylaluminum bis(2,6-di-*tert*-butyl-4-methylphenoxide)
MBL = monoanionic bidentate ligand
Me = methyl
ML = machine learning
MPAA = monoprotected amino acid
MRC = metalloradical catalysis
MS = molecular sieve
MTBE = methyl *tert*-butyl ester
NCI = noncovalent interactions
NFAS = *N*-fluoroalkyl sulfonamide
NFSI = *N*-fluorobenzenesulfonimide
NHC = *N*-heterocyclic carbene
NHPI = *N*-hydroxyphthalimide
NLE = nonlinear effect
NMR = nuclear magnetic resonance
o-DCB = 1,2-dichlorobenzene
PA = picolinamide
PBS = phosphate buffered saline
PCF = planarly chiral ferrocene
PG = protecting group
Ph = phenyl
PHMS = polymethylhydrosiloxane
PHOX = phosphinooxazoline
Phth = phthaloyl
Ph-BPE = 1,2-bis(2,5-diphenylphospholano)ethane
PIFA = [bis(trifluoroacetoxy)iodo]benzene
PKR = parallel kinetic resolution
PMB = 4-methoxybenzyl
PMP = 4-methoxyphenyl
ppy = 2-phenylpyridine
Pr = propyl
Pro = proline
PT = proton transfer
PyBOX = pyridine-2,6-bisoxazoline
QuinoxP* = 2,3-bis(*t*-butylmethylphosphino)quinoxaline
RBP4 = retinol binding protein 4
ROS = reactive oxygen species
rt = room temperature
s = selectivity (factor)
Salan = *N*,*N*′-bis(2-hydroxybenzyl)ethylenediamine
Salen = *N*,*N*′-bis(salicylaldiminato)ethylenediamine
Salox = salicyloxazoline
SET = single-electron transfer
SOD = superoxide dismutase
SPO = secondary phosphine oxide
STRIP = 12-hydroxy-1,10-bis(2,4,6-triisopropylphenyl)-4,5,6,7-tetrahydrodiindeno[7,1-*de*:1′,7′-*fg*][1,3,2]-dioxaphosphocine 12-oxide

https://doi.org/10.1021/acs.chemrev.6c00255
Chem. Rev. XXXX, XXX, XXX−XXX

Taddol = 2,2-dimethyl-a,a,a′,a′-tetraphenyl-1,3-dioxopentane-4,5-diol
t-amyl = 2-methyl-2-butanyl
TBAF = tetrabutylammonium fluoride
TBAI = tetrabutylammonium iodide
TBDPS = *tert*-butyldiphenylsilyl
TBHP = *tert*-butyl hydroperoxide
TBS = *tert*-butyldimethylsilyl
Tc = thiophene-2-carboxylate
TCE = 1,1,2,2-tetrachloroethane
TEMPO = 2,2,6,6-tetramethylpiperidine-1-oxyl
Tf = trifluoromethanesulfonyl
TFE = 2,2,2-trifluoroethanol
THIQ = 1,2,3,4-tetrahydroisoquinoline
THQ = 1,2,3,4-tTetrahydroquinoline
TIBS = triisobutylsilyl
TIPS = triisopropylsilyl
Tle = *tert*-leucine
^{TM}Bn = 2,4,6-trimethylbenzyl
TMEDA = tetramethylethylenediamine
TMS = trimethylsilyl
TMP = 2,2,6,6-tetramethylpiperidine
TON = turnover number
TPFPP = 5,10,15,20-tetrakis(pentafluorophenyl)porphyrin
Troc = 2,2,2-Ttrichloroethoxycarbonyl

REFERENCES

(1) Simonyi, M.; Fitos, I.; Visy, J. Chirality of Bioactive Agents in Protein Binding Storage and Transport Processes. *Trends Pharmacol. Sci.* **1986**, *7*, 112−116.

(2) Crossley, R. *Chirality and the Biological Activity of Drugs*. CRC Press: Boca Raton, United States, 1995.

(3) (a) Noyori, R. Chemical Multiplication of Chirality: Science and Applications. *Chem. Soc. Rev.* **1989**, *18*, 187−208. (b) Yoon, T. P.; Jacobsen, E. N. Privileged Chiral Catalysts. *Science* **2003**, *299*, 1691−1693. (c) Desimoni, G.; Faita, G.; Jørgensen, K. A. C_2-Symmetric Chiral Bis(Oxazoline) Ligands in Asymmetric Catalysis. *Chem. Rev.* **2006**, *106*, 3561−3651. (d) Zhou, Q.-L. *Privileged Chiral Ligands and Catalysts*; VHCA & Wiley-VCH: Weinheim, Germany, 2011. (e) Moberg, C. The Role of Symmetry in Asymmetric Catalysis. *Isr. J. Chem.* **2012**, *52*, 653−662. (f) Parmar, D.; Sugiono, E.; Raja, S.; Rueping, M. Complete Field Guide to Asymmetric BINOL-Phosphate Derived Brønsted Acid and Metal Catalysis: History and Classification by Mode of Activation; Brønsted Acidity, Hydrogen Bonding, Ion Pairing, and Metal Phosphates. *Chem. Rev.* **2014**, *114*, 9047−9153. (g) Mas-Roselló, J.; Herraiz, A. G.; Audic, B.; Laverny, A.; Cramer, N. Chiral Cyclopentadienyl Ligands: Design, Syntheses, and Applications in Asymmetric Catalysis. *Angew. Chem., Int. Ed.* **2021**, *60*, 13198−13224. (h) Huang, Y.; Hayashi, T. Chiral Diene Ligands in Asymmetric Catalysis. *Chem. Rev.* **2022**, *122*, 14346−14404. (i) Dong, S.; Cao, W.; Pu, M.; Liu, X.; Feng, X. Ligand Acceleration in Chiral Lewis Acid Catalysis. *CCS Chem.* **2023**, *5*, 2717−2735. (j) Zhang, L.; Meggers, E. Chiral-at-Metal Catalysts: History, Terminology, Design, Synthesis, and Applications. *Chem. Soc. Rev.* **2025**, *54*, 1986−2005.

(4) Crassous, J. Chiral Transfer in Coordination Complexes: Towards Molecular Materials. *Chem. Soc. Rev.* **2009**, *38*, 830−845.

(5) Niu, X.; Zhao, R.; Yan, S.; Pang, Z.; Li, H.; Yang, X.; Wang, K. Chiral Materials: Progress, Applications, and Prospects. *Small* **2023**, *19*, 2303059.

(6) (a) Nicolaou, K. C.; Montagnon, T. *Molecules That Changed the World: A Brief History of the Art and Science of Synthesis and Its Impact on Society*; John Wiley & Sons: New York, 2008. (b) Barron, L. D. Chirality and Life. *Space Sci. Rev.* **2008**, *135*, 187−201.

(7) Eliel, E. L.; Wilen, S. H. *Stereochemistry of Organic Compounds*; John Wiley & Sons: New York, 1994.

(8) (a) Noyori, R. Asymmetric Catalysis: Science and Opportunities (Nobel Lecture). *Angew. Chem., Int. Ed.* **2002**, *41*, 2008−2022. (b) Sharpless, K. B. Searching for New Reactivity (Nobel Lecture). *Angew. Chem., Int. Ed.* **2002**, *41*, 2024−2032. (c) Trost, B. M.; Crawley, M. L. Asymmetric Transition-Metal-Catalyzed Allylic Alkylations: Applications in Total Synthesis. *Chem. Rev.* **2003**, *103*, 2921−2944. (d) Mukherjee, S.; Yang, J. W.; Hoffmann, S.; List, B. Asymmetric Enamine Catalysis. *Chem. Rev.* **2007**, *107*, 5471−5569. (e) Doyle, A. G.; Jacobsen, E. N. Small-Molecule H-Bond Donors in Asymmetric Catalysis. *Chem. Rev.* **2007**, *107*, 5713−5743. (f) Wang, Q.; Gu, Q.; You, S.-L. Enantioselective Carbonyl Catalysis Enabled by Chiral Aldehydes. *Angew. Chem., Int. Ed.* **2019**, *58*, 6818−6825. (g) He, Y.-M.; Cheng, Y.-Z.; Duan, Y.; Zhang, Y.-D.; Fan, Q.-H.; You, S.-L.; Luo, S.; Zhu, S.-F.; Fu, X.-F.; Zhou, Q.-L. Recent Progress of Asymmetric Catalysis from a Chinese Perspective. *CCS Chem.* **2023**, *5*, 2685−2716.

(9) (a) Newhouse, T.; Baran, P. S.; Hoffmann, R. W. The Economies of Synthesis. *Chem. Soc. Rev.* **2009**, *38*, 3010−3021. (b) Flerlage, H.; Slootweg, J. C. Modern Chemistry is Rubbish. *Nat. Rev. Chem.* **2023**, *7*, 593−594.

(10) (a) Trost, B. M. The Atom Economy—A Search for Synthetic Efficiency. *Science* **1991**, *254*, 1471−1477. (b) Trost, B. M. Atom Economy—A Challenge for Organic Synthesis: Homogeneous Catalysis Leads the Way. *Angew. Chem., Int. Ed. Engl.* **1995**, *34*, 259−281.

(11) (a) Labinger, J. A.; Bercaw, J. E. Understanding and Exploiting C−H Bond Activation. *Nature* **2002**, *417*, 507−514. (b) Davies, H. M. L.; Manning, J. R. Catalytic C−H Functionalization by Metal Carbenoid and Nitrenoid Insertion. *Nature* **2008**, *451*, 417−424. (c) Colby, D. A.; Bergman, R. G.; Ellman, J. A. Rhodium-Catalyzed C−C Bond Formation *via* Heteroatom-Directed C−H Bond Activation. *Chem. Rev.* **2010**, *110*, 624−655. (d) Doyle, M. P.; Duffy, R.; Ratnikov, M.; Zhou, L. Catalytic Carbene Insertion into C−H Bonds. *Chem. Rev.* **2010**, *110*, 704−724. (e) Lyons, T. W.; Sanford, M. S. Palladium-Catalyzed Ligand-Directed C−H Functionalization Reactions. *Chem. Rev.* **2010**, *110*, 1147−1169. (f) Hartwig, J. F. Evolution of C−H Bond Functionalization from Methane to Methodology. *J. Am. Chem. Soc.* **2016**, *138*, 2−24. (g) He, J.; Wasa, M.; Chan, K. S. L.; Shao, Q.; Yu, J.-Q. Palladium-Catalyzed Transformations of Alkyl C−H Bonds. *Chem. Rev.* **2017**, *117*, 8754−8786. (h) Yang, Y.; Lan, J.; You, J. Oxidative C−H/C−H Coupling Reactions between Two (Hetero)arenes. *Chem. Rev.* **2017**, *117*, 8787−8863. (j) Kim, D.-S.; Park, W.-J.; Jun, C.-H. Metal-Organic Cooperative Catalysis in C−H and C−C Bond Activation. *Chem. Rev.* **2017**, *117*, 8977−9015. (k) Yi, H.; Zhang, G.; Wang, H.; Huang, Z.; Wang, J.; Singh, A. K.; Lei, A. Recent Advances in Radical C−H Activation/Radical Cross-Coupling. *Chem. Rev.* **2017**, *117*, 9016−9085. (l) Park, Y.; Kim, Y.; Chang, S. Transition Metal-Catalyzed C−H Amination: Scope, Mechanism, and Applications. *Chem. Rev.* **2017**, *117*, 9247−9301. (m) Dong, Z.; Ren, Z.; Thompson, S. J.; Xu, Y.; Dong, G. Transition-Metal-Catalyzed C−H Alkylation Using Alkenes. *Chem. Rev.* **2017**, *117*, 9333−9403. (n) Sambiagio, C.; Schönbauer, D.; Blieck, R.; Dao-Huy, T.; Pototschnig, G.; Schaaf, P.; Wiesinger, T.; Zia, M. F.; Wencel-Delord, J.; Besset, T.; Maes, B. U. W.; Schnürch, M. Comprehensive Overview of Directing Groups Applied in Metal-Catalysed C−H Functionalisation Chemistry. *Chem. Soc. Rev.* **2018**, *47*, 6603−6743. (o) Liu, B.; Romine, A. M.; Rubel, C. Z.; Engle, K. M.; Shi, B.-F. Transition-Metal-Catalyzed, Coordination-Assisted Functionalization of Nonactivated C(sp^3)−H Bonds. *Chem. Rev.* **2021**, *121*, 14957−15074. (p) Grover, J.; Sebastian, A. T.; Maiti, S.; Bissember, A. C.; Maiti, D. Unified Approaches in Transition Metal Catalyzed C(sp^3)−H Functionalization: Recent Advances and Mechanistic Aspects. *Chem. Soc. Rev.* **2025**, *54*, 2006−2053.

(12) (a) Godula, K.; Sames, D. C−H Bond Functionalization in Complex Organic Synthesis. *Science* **2006**, *312*, 67−72. (b) Yamaguchi, J.; Yamaguchi, A. D.; Itami, K. C−H Bond Functionalization: Emerging Synthetic Tools for Natural Products and Pharmaceuticals. *Angew. Chem., Int. Ed.* **2012**, *51*, 8960−9009. (c) Wencel-Delord, J.; Glorius, F. C−H Bond Activation Enables the Rapid Construction and Late-Stage Diversification of Functional Molecules. *Nat. Chem.* **2013**, *5*, 369−375. (d) Cernak, T.; Dykstra, K. D.; Tyagarajan, S.; Vachal, P.; Krska, S. W.

The Medicinal Chemist's Toolbox for Late Stage Functionalization of Drug-Like Molecules. *Chem. Soc. Rev.* **2016**, *45*, 546−576. (e) Lam, N. Y. S.; Wu, K.; Yu, J.-Q. Advancing the Logic of Chemical Synthesis: C−H Activation as Strategic and Tactical Disconnections for C−C Bond Construction. *Angew. Chem., Int. Ed.* **2021**, *60*, 15767−15790. (f) de Jesus, R.; Hiesinger, K.; van Gemmeren, M. Preparative Scale Applications of C−H Activation in Medicinal Chemistry. *Angew. Chem., Int. Ed.* **2023**, *62*, No. e202306659. (g) Qian, P.-F.; Shi, B.-F. Enantioselective C−H Functionalization: Logic and Applications in the Total Synthesis of Natural Products. *Chem. Sci.* **2026**, *17*, 2969−2989.

(13) (a) Davies, H. M. L.; Beckwith, R. E. J. Catalytic Enantioselective C−H Activation by Means of Metal-Carbenoid-Induced C−H Insertion. *Chem. Rev.* **2003**, *103*, 2861−2904. (b) Giri, R.; Shi, B.-F.; Engle, K. M.; Maugel, N.; Yu, J.-Q. Transition Metal-Catalyzed C−H Activation Reactions: Diastereoselectivity and Enantioselectivity. *Chem. Soc. Rev.* **2009**, *38*, 3242−3272. (c) Zheng, C.; You, S.-L. Recent Development of Direct Asymmetric Functionalization of Inert C−H Bonds. *RSC Adv.* **2014**, *4*, 6173−6214. (d) Newton, C. G.; Wang, S.-G.; Oliveira, C. C.; Cramer, N. Catalytic Enantioselective Transformations Involving C−H Bond Cleavage by Transition-Metal Complexes. *Chem. Rev.* **2017**, *117*, 8908−8976. (e) Yoshino, T.; Satake, S.; Matsunaga, S. Diverse Approaches for Enantioselective C−H Functionalization Reactions Using Group 9 Cp^xM^{III} Catalysts. *Chem. - Eur. J.* **2020**, *26*, 7346−7357. (f) Shao, Q.; Wu, K.; Zhuang, Z.; Qian, S.; Yu, J.-Q. From $Pd(OAc)_2$ to Chiral Catalysts: The Discovery and Development of Bifunctional Mono-*N*-Protected Amino Acid Ligands for Diverse C−H Functionalization Reactions. *Acc. Chem. Res.* **2020**, *53*, 833−851. (g) Achar, T. K.; Maiti, S.; Jana, S.; Maiti, D. Transition Metal Catalyzed Enantioselective $C(sp^2)$−H Bond Functionalization. *ACS Catal.* **2020**, *10*, 13748−13793. (h) Zhan, B.-B.; Jin, L.; Shi, B.-F. Palladium-Catalyzed Enantioselective C−H Functionalization *via* C−H Palladation. *Trends Chem.* **2022**, *4*, 220−235. (i) Qian, P.-F.; Li, J.-Y.; Zhou, Y.-B.; Zhou, T.; Shi, B.-F. Half-Sandwich d^6-Metal (Co^{III}, Rh^{III}, Ir^{III}, Ru^{II})-Catalyzed Enantioselective C−H Activation. *SynOpen* **2023**, *7*, 466−485. (j) Liu, C.-X.; Yin, S.-Y.; Zhao, F.; Yang, H.; Feng, Z.; Gu, Q.; You, S.-L. Rhodium-Catalyzed Asymmetric C−H Functionalization Reactions. *Chem. Rev.* **2023**, *123*, 10079−10134. (k) Achar, T. K.; Al-Thabaiti, S. A.; Mokhtar, M.; Maiti, D. Enantioselective Annulation Reactions Through $C(sp^2)$−H activation with chiral Cp^xM^{III} catalysts. *Chem. Catal.* **2023**, *3*, 100575.

(14) (a) Emsley, J. *Nature's Building Blocks: An A−Z. Guide to the Elements*. Oxford University Press: Oxford, UK, 2001. (b) Wolczanski, P. T. Elemental Aspects of Transition Metals Pertinent to Organometallic Chemistry: Properties, Periodicity, Curiosities, and Related Main Group Issues. *Organometallics* **2024**, *43*, 787−801.

(15) (a) Shang, R.; Ilies, L.; Nakamura, E. Iron-Catalyzed C−H Bond Activation. *Chem. Rev.* **2017**, *117*, 9086−9139. (b) Pototschnig, G.; Maulide, N.; Schnürch, M. Direct Functionalization of C−H Bonds by Iron, Nickel, and Cobalt Catalysis. *Chem. - Eur. J.* **2017**, *23*, 9206−9232. (c) Gandeepan, P.; Müller, T.; Zell, D.; Cera, G.; Warratz, S.; Ackermann, L. 3d Transition Metals for C−H Activation. *Chem. Rev.* **2019**, *119*, 2192−2452. (d) Liu, Y.; You, T.; Wang, H.-X.; Tang, Z.; Zhou, C.-Y.; Che, C.-M. Iron- and Cobalt-Catalyzed $C(sp^3)$−H Bond Functionalization Reactions and Their Application in Organic Synthesis. *Chem. Soc. Rev.* **2020**, *49*, 5310−5358. (e) Wang, X.; He, J.; Wang, Y.-N.; Zhao, Z.; Jiang, K.; Yang, W.; Zhang, T.; Jia, S.; Zhong, K.; Niu, L.; Lan, Y. Strategies and Mechanisms of First-Row Transition Metal-Regulated Radical C−H Functionalization. *Chem. Rev.* **2024**, *124*, 10192−10280.

(16) (a) Tasker, S. Z.; Standley, E. A.; Jamison, T. F. Recent Advances in Homogeneous Nickel Catalysis. *Nature* **2014**, *509*, 299−309. (b) Bauer, I.; Knölker, H.-J. Iron Catalysis in Organic Synthesis. *Chem. Rev.* **2015**, *115*, 3170−3387. (c) Chen, J.; Lu, Z. Asymmetric Hydrofunctionalization of Minimally Functionalized Alkenes *via* Earth Abundant Transition Metal Catalysis. *Org. Chem. Front.* **2018**, *5*, 260−272. (d) Li, L.-J.; He, Y.; Yang, Y.; Guo, J.; Lu, Z.; Wang, C.; Zhu, S.; Zhu, S.-F. Recent Advances in Mn, Fe, Co, and Ni-Catalyzed Organic Reactions. *CCS Chem.* **2024**, *6*, 537−584. (e) Yang, C.-J.; Liu, L.; Gu, Q.-S.; Liu, X.-Y. Research Progress in Enantioselective Radical Desymmetrization Reactions. *CCS Chem.* **2024**, *6*, 1612−1627. (f) Huang, T.; Du, P.; Lin, Y.-M. Recent Advances in Photoactive First-Row Transition Metal Complexes for Organic Synthesis. *Chin. J. Chem.* **2025**, *43*, 2566−2587.

(17) (a) Woźniak, Ł.; Cramer, N. Enantioselective C−H Bond Functionalizations by 3d Transition-Metal Catalysts. *Trends Chem.* **2019**, *1*, 471−484. (b) Zhang, C.; Li, Z.-L.; Gu, Q.-S.; Liu, X.-Y. Catalytic Enantioselective $C(sp^3)$−H Functionalization Involving Radical Intermediates. *Nat. Commun.* **2021**, *12*, 475. (c) Zhang, Z.; Chen, P.; Liu, G. Copper-Catalyzed Radical Relay in $C(sp^3)$−H Functionalization. *Chem. Soc. Rev.* **2022**, *51*, 1640−1658. (d) Lee, W.-C. C.; Zhang, X. P. Metalloradical Catalysis: General Approach for Controlling Reactivity and Selectivity of Homolytic Radical Reactions. *Angew. Chem., Int. Ed.* **2024**, *63*, No. e202320243. (e) Palone, A.; Bietti, M.; Costas, M. Enzymatic and Bio-Inspired Enantioselective Oxidation of Non-Activated $C(sp^3)$−H Bonds. *Synthesis* **2025**, *57*, 1280−1294.

(18) (a) Xue, X.-S.; Ji, P.; Zhou, B.; Cheng, J.-P. The Essential Role of Bond Energetics in C−H Activation/Functionalization. *Chem. Rev.* **2017**, *117*, 8622−8648. (b) Chu, J. C. K.; Rovis, T. Complementary Strategies for Directed $C(sp^3)$−H Functionalization: A Comparison of Transition-Metal-Catalyzed Activation, Hydrogen Atom Transfer, and Carbene/Nitrene Transfer. *Angew. Chem., Int. Ed.* **2018**, *57*, 62−101. (c) Saint-Denis, T. G.; Zhu, R.-Y.; Chen, G.; Wu, Q.-F.; Yu, J.-Q. Enantioselective $C(sp^3)$−H Bond Activation by Chiral Transition Metal Catalysts. *Science* **2018**, *359*, No. eaao4798.

(19) Hartwig, J. F. *Organotransition Metal Chemistry: From Bonding to Catalysis*. University Science Books: Sausalito, United States, 2010.

(20) (a) Gunay, A.; Theopold, K. H. C−H Bond Activations by Metal Oxo Compounds. *Chem. Rev.* **2010**, *110*, 1060−1081. (b) Borovik, A. S. Role of Metal−Oxo Complexes in the Cleavage of C−H Bonds. *Chem. Soc. Rev.* **2011**, *40*, 1870−1874. (c) Bryliakov, K. P. Mechanisms of $C(sp^3)$−H and C═C Selective Oxidative Heterofunctionalizations by Non-Heme Fe and Mn Mimics of Oxygenase Enzymes. *Coord. Chem. Rev.* **2024**, *508*, 215793.

(21) Huang, H.-M.; Garduño-Castro, M. H.; Morrill, C.; Procter, D. J. Catalytic Cascade Reactions by Radical Relay. *Chem. Soc. Rev.* **2019**, *48*, 4626−4638.

(22) Teng, M.-Y.; Han, T.; Huang, E.-H.; Ye, L.-W. Research Progress on Enantioselective Desymmetrization Reactions Involving Metal Carbenes. *Chin. J. Org. Chem.* **2022**, *42*, 3295−3301.

(23) During the preparation of this review, several reports on this topic appeared and highlighted the importance of 3d metal catalysts: (a) Yang, F.; Chi, L.; Ye, Z.; Gong, L. Photoinduced Regiodivergent and Enantioselective Cross-Coupling of Glycine Derivatives with Hydrocarbon Feedstocks. *J. Am. Chem. Soc.* **2025**, *147*, 1767−1780. (b) Mishra, A.; Hu, J.; Cong, X.; Zhuo, Q.; Nishiura, M.; Luo, G.; Hou, Z. Enantioselective [3 + 2] Annulation of Aldimines with Alkynes by Scandium-Catalyzed C−H Activation. *Angew. Chem., Int. Ed.* **2025**, *64*, No. e202419567. (c) Hu, J.; Tan, X.; Li, Y.; Luo, L.; Wang, X.; Cao, D.; Luo, G. Theoretical Insights into Rare-Earth-Catalyst-Controlled Diastereo- and Enantioselective [3 + 2] Annulation of Aromatic Aldimines with Styrenes. *Inorg. Chem.* **2025**, *64*, 3120−3128. (d) Dana, S.; Pandit, N. K.; Boos, P.; von Münchow, T.; Peters, S. E.; Trienes, S.; Haberstock, L.; Herbst-Irmer, R.; Stalke, D.; Ackermann, L. Parametrization of κ^2-*N*,*O*-Oxazoline Preligands for Enantioselective Cobaltaelectro-Catalyzed C−H Activations. *ACS Catal.* **2025**, *15*, 4450−4459. (e) Murata, A.; Endo, T.; Hirata, Y.; Higashida, K.; Yoshino, T.; Matsunaga, S. Enantioselective C−H Amidation of Sulfondiimines for the Synthesis of 1,2,4-Benzothiadiazine-1-Imines under Cobalt Catalysis. *Org. Chem. Front.* **2025**, *12*, 4236−4241. (f) Kim, J. H.; Warrington, E. M.; Lee, K. S.; Hu, D. B.; Berry, J. F.; Schomaker, J. M. Solvent-Driven Mechanistic Insights into Cu-Catalyzed Asymmetric C−H Amidation *via* Nitrene Transfer. *ChemCatChem.* **2025**, *17*, No. e202402077. (g) Dai, L.; Chen, Y.-Y.; Wang, J.-J.; Chen, J.-J.; Zhou, Q.-L. Photoinduced Copper-Catalysed Enantioselective Amination of Allylic and Propargylic C−H Bonds. *Chem. Sci.* **2025**, *16*, 9213−9219. (h) Huang, F.-R.; Teng, M.-Y.; Qiu, H.; Yao, Q.-J.; Shi, B.-F. Modification of [2.2]Paracyclophanes *via* Cobalt/Salox-Catalyzed Enantioselective Electrooxidative or Photo-

redox C−H Acyloxylation and Alkoxylation. *Angew. Chem., Int. Ed.* **2025**, *64*, No. e202506465. (i) Lv, D.; Zhu, X.; Bao, H. Copper-Catalyzed Enantioselective Radical Cyanation of Allenic C(sp^2)-H Bonds to Access Tri- and Tetrasubstituted Chiral Allenes. *ACS Catal.* **2025**, *15*, 7741−7748. (j) Cheng, Z.; Zhang, G.; Deng, Y.; Zhang, Y.; Li, X.; Chen, P.; Liu, G. Copper-Catalyzed Asymmetric Cyanation of Propargylic Radicals Derived From Silyl-Substituted Allenes and Alkynes. *Angew. Chem., Int. Ed.* **2025**, *64*, No. e202505939. (k) Palone, A.; Call, A.; Garcia-Roca, A.; Luis, J. M.; Sigman, M. S.; Bietti, M.; Nevado, C.; Costas, M. Shaping of a Reactive Manganese Catalyst Enables Access to Polyfunctionalized Cyclohexanes *via* Enantioselective C(sp^3)−H Bond Oxidation of 1,3-meso Diethers. *Angew. Chem., Int. Ed.* **2025**, *64*, No. e202507755. (l) Lin, J.; Song, D.; Zhang, W.; Zheng, C.; Zheng, C.; Lv, J.; Xue, J.; Zhong, W.; Ling, F. Design of a Polymer Supported Chiral Cobalt Catalyst for Heterogeneous Enantioselective C−H Activations. *Green Chem.* **2025**, *27*, 8251−8259. (m) Wu, Z.; Li, K.; Liao, M.; Pan, C.; Yang, B.; Ma, X.; Huo, H.; Tu, B.; Zhang, G.; Guo, R. Photoinduced Copper-Catalyzed Enantioselective Alkylalkynylation of Alkenes *via* Polarity-Matched Hydrogen Atom Transfer. *J. Am. Chem. Soc.* **2025**, *147*, 22072−22083. (n) Zhou, Y.; Chen, P.; Liu, G. Copper-Catalyzed Highly Efficient and Asymmetric Allylic C−H Oxidation of 3-Aryl-Substituted Terminal Alkenes. *J. Am. Chem. Soc.* **2025**, *147*, 22873−22882. (o) Cindy; Lee, W.-C.; Wang, D.-S.; Deb, A.; Zhu, Y.; Zhang, X. P. Asymmetric C−H Amination *via* Fe(III)-Metalloradical Catalysis Featuring α-Fe(IV)-Aminyl Radicals as Key Intermediates. *J. Am. Chem. Soc.* **2025**, *147*, 24001−24013. (p) Xu, Y.; Pandit, N. K.; Meraviglia, S.; Boos, P.; Stark, P. A. M.; Surke, M.; Herbst-Irmer, R.; Stalke, D.; Ackermann, L. Stereocontrolled Construction of Multi-Chiral [2.2]Paracyclophanes *via* Cobaltaphotoredox Dual Catalysis. *ACS Catal.* **2025**, *15*, 11716−11725. (q) Wu, X.; Tian, Q.; Ge, J.; Liu, Y.; Li, Z.; Zhang, J.; Cheng, G. Cobalt-Catalyzed Regio, Diastereo, and Enantioselective C−H Annulation of Aminoquinoline Amides with Internal Alkynes for the Construction of Diaxes. *Chin. J. Chem.* **2025**, *43*, 2669−2676. (r) Mishra, A.; Lin, X.; Maji, K.; Nishiura, M.; Cong, X.; Hou, Z. Diastereo- and Enantioselective Synthesis of Polycyclic Amines by Cascade Cyclization of Aromatic Aldimines with Tethered Alkenes *via* Scandium-Catalyzed C−H Activation. *J. Am. Chem. Soc.* **2025**, *147*, 26116−26123. (s) Das, A.; Kumaran, S.; Maity, P.; Premkumar, J. R.; Sundararaju, B. Cobalt-Catalyzed Enantioselective and Diastereodivergent Construction of C−N Atropisomers. *J. Am. Chem. Soc.* **2025**, *147*, 26226−26237. (t) Yang, F.; Gong, L. Visible Light-Triggered Regiodivergent and Enantioselective Alkylation of Glycine Derivatives. *Synlett* **2025**, *36*, 3121−3127. (u) Kurganskiy, V. I.; Bryliakova, A. A.; Medvedev, A. G.; Shashkov, M. V.; Bryliakov, K. P. Mn-Catalyzed Regio- and Stereoselective C(sp^3)−H Lactonization of Carboxylic Acids with H_2O_2. *ACS Catal.* **2025**, *15*, 14938−14954. (v) Ghosh, S.; Saha, P. S.; Saha, S. N.; Chandrasekharan, S. P.; Koner, M.; Baidya, M. Cobalt-Catalyzed Regio- and Stereoselective Synthesis of Atropisomers with *Vicinal* C−C and C−N Diaxes. *Chem. Commun.* **2025**, *61*, 15231−15234. (w) Stroek, W.; Rowlinson, N. A. V.; Hudson, L. A.; Albrecht, M. Enantioselective C−H Amination Catalyzed by Homoleptic Iron Salox Complexes. *Chem. Commun.* **2025**, *61*, 15274−15277. (x) Koner, M.; Ballav, N.; Varma, A. J.; Ghosh, S.; Mondal, T.; Kuniyil, R.; Baidya, M. Multifaceted Photocatalysis Enables Cobalt Catalyzed Enantioselective C−H Activation and APEX Reaction for C−N Axially Chiral Molecules. *Chem. Sci.* **2025**, *16*, 19296−19303. (y) Lv, G.; Wang, X.; Zhang, P.; Zhang, J.; Ye, F.; Tian, X.; Wu, Y. Photoredox Copper-Catalyzed Asymmetric C(sp^3)−H Glycosylation for Access to Chiral Heterobenzylic Amines. *Organometallics* **2025**, *44*, 2250−2259. (z) Almaraz-Ortiz, W. E.; Cramer, N. Cobalt(III)-Catalyzed Synthesis of Chiral 1,2-Amino Alcohols by C−H Carboamidation. *ACS Catal.* **2025**, *15*, 17436−17442. (aa) Zhou, Q.; Zhang, Y.; Shang, J.; Qi, R.; Ren, X.; Xu, Z.; Wang, C. Photoinduced and Copper-Catalyzed Asymmetric Alkylation of Glycine Derivatives *via* a Synergistic Electron/Atom Transfer Process. *ACS Catal.* **2025**, *15*, 17504−17512. (ab) Chen, J.-H.; Jiang, T.-Y.; Yao, Q.-J.; Feng, Y.-L.; Zhong, M.-Y.; Huang, F.-R.; Shi, B.-F. Synthesis of Acyclic All-Carbon Quaternary Stereocenters through Nickel-Catalyzed Enantioselective C(sp^3)−H Amination. *J. Am. Chem. Soc.* **2025**, *147*, 39060−39066. (ac) Zhang, H.; Gu, W.; Zheng, J.; Lu, J.; Li, Q.; Liu, Y.; Qi, X.; Zhang, G.; Guo, R. Ligand Evolution-Enabled Enantioselective C(sp^3)−H Azidation. *J. Am. Chem. Soc.* **2025**, *147*, 40010−40023. (ad) Liu, Q.-F.; Peng, Q.-Q.; Hao, S.-S.; Liu, L.; Zhang, F.-H.; Shi, Z.-J.; Xie, J.-H.; Ai, C.-R.; Wang, X.-C. Borane/Transition Metal-Catalyzed Allenylic and Allylic Alkylation of Unactivated 2-Alkylbenzoxazoles. *J. Am. Chem. Soc.* **2025**, *147*, 40799−40806. (ae) Jiang, B.; Shi, S.-L. A Chiral Bifunctional NHC Ligand Promoted Ni/Al-Catalyzed Regio- and Enantioselective C_6−H Alkylation of Pyrimidines. *ACS Catal.* **2025**, *15*, 18824−18833. (af) Peng, Y.; Zhong, D.; Song, Y.; Wang, Q.; Huang, K.; Huo, H.; Wang, C. Iridium Photosensitizers Immobilized on Metal-Organic Layers Lead to Enhanced Enantioselectivity in Ni/Ir Dual Photocatalysis. *Angew. Chem., Int. Ed.* **2025**, *64*, No. e202518424. (ag) He, Z.; de Wit, S. W. J.; van der Loo, S. M.; Tromp, D. S.; Bauer, A. K.; Neidig, M. L.; Mathew, S.; Ehlers, A. W.; de Bruin, B.; van der Vlugt, J. I. Selective Chiral Diamine-Bisoxazoline Iron(II) Catalysts for Pyrrolidine Formation *via* Intramolecular C(sp^3)−H Amination of Aliphatic Azides. *J. Am. Chem. Soc.* **2025**, *147*, 44273−44284. (ah) Wang, B.-J.; Jiang, T.-Y.; Jiang, Y.-L; Wu, X.; Yao, Q.-J.; Shi, B.-F. Catalytic Enantioselective Synthesis of Planar-Chiral Cyclophanes *via* a Chiral Octahedral Cobalt(III)-Templated C−H Macrocyclization. *J. Am. Chem. Soc.* **2025**, *147*, 45785−45792. (ai) Zhao, P.; Deng, Y.; Chen, P.; Liu, G. Copper-Catalyzed Asymmetric Alkynylation of sp^2 Allenic C−H Bonds for the Synthesis of Skipped Diynes. *J. Am. Chem. Soc.* **2025**, *147*, 46847−46853. (aj) Hinterlang, L.; Demirel, N.; Ivlev, S. I.; Meggers, E. An Achiral Tetradentate Cis-α-Coordinating NCCN Ligand Gives Rise to a Configurationally Stable Chiral-at-Iron Complex for Enantioselective Catalysis. *Chem. - Eur. J.* **2026**, *32*, No. e03221. (ak) Xiao, T.-F.; Jian, K.-R.; Gu, Y.-C.; Xu, G.-Q.; Xu, P.-F. Asymmetric Vicinal C(sp^3)−H Difunctionalization of Saturated Cyclic Amines *via* Synergistic Photoredox, Copper and Chiral Phosphoric Acid Catalysis. *Chem. Sci.* **2026**, *17*, 3240−3247. (al) Yang, Q.-L.; Gao, C.; Wang, D.-C.; Wang, H.-X.; Guo, H.-M. Enantioselective Cobalt-Catalyzed C−H Activation and Annulation of Indole-3-carboxamides with Alkynes: Access to Axially Chiral γ-Carbolinones. *Org. Lett.* **2026**, *28*, 123−129. (am) Brunard, E.; Huang, F.; Díaz-Jiménez, À.; Kostiukovska, S.; Wencel-Delord, J. Intermolecular Enantioselective Nickel-Catalyzed Arylation of Un-Activated C(sp^3)−H Bond. *Angew. Chem., Int. Ed.* **2026**, *65*, No. e23241. (an) Biswas, D. D.; Das, S.; Pal, D.; Gupta, S. S. Enantioselective C−H Bond Oxidation Using a Bio-Inspired Chiral Fe-TAML Catalyst. *Chem. Commun.* **2026**, *62*, 1289−1292. (ao) Li, W.; Fu, L.; Xu, Y.; Zhou, Y.; Qu, J.; Wang, B. Atroposelective Synthesis of Isoquinolinone Bearing Two Distinct C−N Axes *via* Cobalt-Catalyzed Enantioselective C−H Activation/annulation. *Chem. Commun.* **2026**, *62*, 4276−4279. (ap) Li, H.; Bai, J.; Wang, F.; Li, X.-X.; Wang, M.; Li, X. Harnessing Cooperative Hydrogen-Atom Transfer and Nitrene-Primed Radical-Polar Crossover for Asymmetric C−H Amidation of α-Amino Carbonyls. *J. Am. Chem. Soc.* **2026**, *148*, 7905−7918.

(24) (a) Kobayashi, S.; Sugiura, M.; Kitagawa, H.; Lam, W. W.-L. Rare-Earth Metal Triflates in Organic Synthesis. *Chem. Rev.* **2002**, *102*, 2227−2302. (b) Zeimentz, P. M.; Arndt, S.; Elvidge, B. R.; Okuda, J. Cationic Organometallic Complexes of Scandium, Yttrium, and the Lanthanoids. *Chem. Rev.* **2006**, *106*, 2404−2433. (c) Li, X.; Hou, Z. Organometallic Catalysts for Copolymerization of Cyclic Olefins. *Coord. Chem. Rev.* **2008**, *252*, 1842−1869. (d) Nishiura, M.; Hou, Z. Novel Polymerization Catalysts and Hydride Clusters from Rare-Earth Metal Dialkyls. *Nat. Chem.* **2010**, *2*, 257−268.

(25) (a) Johnson, K. R. D.; Hayes, P. G. Cyclometalative C−H Bond Activation in Rare Earth and Actinide Metal Complexes. *Chem. Soc. Rev.* **2013**, *42*, 1947−1960. (b) Waterman, R. σ-Bond Metathesis: A 30-Year Retrospective. *Organometallics* **2013**, *32*, 7249−7263. (c) Arnold, P. L.; McMullon, M. W.; Rieb, J.; Kühn, F. E. C−H Bond Activation by f-Block Complexes. *Angew. Chem., Int. Ed.* **2015**, *54*, 82−100.

(26) (a) Sun, Q.; Xu, X.; Xu, X. Recent Advances in Rare-Earth Metal-Catalyzed C−H Functionalization Reactions. *ChemCatChem.* **2022**, *14*, No. e202201083. (b) Cong, X.; Huang, L.; Hou, Z. C−H Functionalization with Alkenes, Allenes, and Alkynes by Half-Sandwich Rare-Earth Catalysts. *Tetrahedron* **2023**, *135*, 133323.

(27) Nishiura, M.; Guo, F.; Hou, Z. Half-Sandwich Rare-Earth-Catalyzed Olefin Polymerization, Carbometalation, and Hydroarylation. *Acc. Chem. Res.* **2015**, *48*, 2209−2220.
(28) Song, G.; O, W. W. N.; Hou, Z. Enantioselective C−H Bond Addition of Pyridines to Alkenes Catalyzed by Chiral Half-Sandwich Rare-Earth Complexes. *J. Am. Chem. Soc.* **2014**, *136*, 12209−12212.
(29) Guan, B.-T.; Hou, Z. Rare-Earth-Catalyzed C−H Bond Addition of Pyridines to Olefins. *J. Am. Chem. Soc.* **2011**, *133*, 18086−18089.
(30) Luo, G.; Luo, Y.; Qu, J.; Hou, Z. Mechanistic Investigation on Scandium-Catalyzed C−H Addition of Pyridines to Olefins. *Organometallics* **2012**, *31*, 3930−3937.
(31) Gladysz, J. A.; Boone, B. J. Chiral Recognition in π Complexes of Alkenes, Aldehydes, and Ketones with Transition Metal Lewis Acids; Development of a General Model for Enantioface Binding Selectivities. *Angew. Chem., Int. Ed. Engl.* **1997**, *36*, 550−583.
(32) Zhan, G.; Teng, H.-L.; Luo, Y.; Lou, S.-J.; Nishiura, M.; Hou, Z. Enantioselective Construction of Silicon-Stereogenic Silanes by Scandium-Catalyzed Intermolecular Alkene Hydrosilylation. *Angew. Chem., Int. Ed.* **2018**, *57*, 12342−12346.
(33) Luo, Y.; Teng, H.-L.; Nishiura, M.; Hou, Z. Asymmetric Yttrium-Catalyzed C(sp^3)−H Addition of 2-Methyl Azaarenes to Cyclopropenes. *Angew. Chem., Int. Ed.* **2017**, *56*, 9207−9210.
(34) Lou, S.-J.; Mo, Z.; Nishiura, M.; Hou, Z. Construction of All-Carbon Quaternary Stereocenters by Scandium-Catalyzed Intramolecular C−H Alkylation of Imidazoles with 1,1-Disubstituted Alkenes. *J. Am. Chem. Soc.* **2020**, *142*, 1200−1205.
(35) Mishra, A.; Cong, X.; Nishiura, M.; Hou, Z. Enantioselective Synthesis of 1-Aminoindanes *via* [3 + 2] Annulation of Aldimines with Alkenes by Scandium-Catalyzed C−H Activation. *J. Am. Chem. Soc.* **2023**, *145*, 17468−17477.
(36) (a) Liu, F.; Luo, G.; Hou, Z.; Luo, Y. Mechanistic Insights into Scandium-Catalyzed Hydroaminoalkylation of Olefins with Amines: Origin of Regioselectivity and Charge-Based Prediction Model. *Organometallics* **2017**, *36*, 1557−1565. (b) Luo, G.; Liu, F.; Luo, Y.; Zhou, G.; Kang, X.; Hou, Z.; Luo, L. Computational Investigation of Scandium-Based Catalysts for Olefin Hydroaminoalkylation and C−H Addition. *Organometallics* **2019**, *38*, 1887−1896.
(37) (a) Cong, X.; Zhuo, Q.; Hao, N.; Mo, Z.; Zhan, G.; Nishiura, M.; Hou, Z. Regio- and Diastereoselective [3 + 2] Annulation of Aliphatic Aldimines with Alkenes by Scandium-Catalyzed β-C(sp^3)−H Activation. *Angew. Chem., Int. Ed.* **2022**, *61*, No. e202115996. (b) Cong, X.; Zhuo, Q.; Hao, N.; Mishra, A.; Nishiura, M.; Hou, Z. Divergent Synthesis of Multi-Substituted Aminotetralins *via* [4 + 2] Annulation of Aldimines with Alkenes by Rare-Earth-Catalyzed Benzylic C(sp^3)−H Activation. *Angew. Chem., Int. Ed.* **2024**, *63*, No. e202318203. (c) Cong, X.; Hao, N.; Mishra, A.; Zhuo, Q.; An, K.; Nishiura, M.; Hou, Z. Regio- and Diastereoselective Annulation of α,β-Unsaturated Aldimines with Alkenes *via* Allylic C(sp^3)−H Activation by Rare-Earth Catalysts. *J. Am. Chem. Soc.* **2024**, *146*, 10187−10198.
(38) Lou, S.-J.; Luo, G.; Yamaguchi, S.; An, K.; Nishiura, M.; Hou, Z. Modular Access to Spiro-dihydroquinolines *via* Scandium-Catalyzed Dearomative Annulation of Quinolines with Alkynes. *J. Am. Chem. Soc.* **2021**, *143*, 20462−20471.
(39) Shao, J.; Huang, L.; Lou, S.-J.; Ohno, A.; Yamada, Y. M. A.; Nishiura, M.; Murahashi, T.; Hou, Z. Synthesis of Rigid Stepladder Polymers *via* Scandium-Catalyzed Polyspiroannulation of Quinoline with Alkyne. *J. Am. Chem. Soc.* **2025**, *147*, 1416−1420.
(40) Lou, S.-J.; Zhuo, Q.; Nishiura, M.; Luo, G.; Hou, Z. Enantioselective C−H Alkenylation of Ferrocenes with Alkynes by Half-Sandwich Scandium Catalyst. *J. Am. Chem. Soc.* **2021**, *143*, 2470−2476.
(41) Lou, S.-J.; Zhang, L.; Luo, Y.; Nishiura, M.; Luo, G.; Luo, Y.; Hou, Z. Regiodivergent C−H Alkylation of Quinolines with Alkenes by Half-Sandwich Rare-Earth Catalysts. *J. Am. Chem. Soc.* **2020**, *142*, 18128−18137.
(42) Sun, Q.; Feng, X.; Wang, X.; Shi, H.; Su, J.; Wang, M.; Luo, G.; Xu, X. Enantioselective ortho-C−H Addition of Aromatic Amines to Alkenes by Bulky Chiral Anilido-Oxazoline Scandium Complexes. *J. Am. Chem. Soc.* **2025**, *147*, 13658−13666.
(43) Cotton, A. F.; Wilkinson, G.; Bochmann, M.; Murillo, C. A. *Advanced Inorganic Chemistry*; Wiley: Weinheim, Germany, 1999.
(44) (a) Carney, J. R.; Dillon, B. R.; Thomas, S. P. Recent Advances of Manganese Catalysis for Organic Synthesis. *Eur. J. Org. Chem.* **2016**, *2016*, 3912−3929. (b) Baglia, R. A.; Zaragoza, J. P. T.; Goldberg, D. P. Biomimetic Reactivity of Oxygen-Derived Manganese and Iron Porphyrinoid Complexes. *Chem. Rev.* **2017**, *117*, 13320−13352.
(45) (a) Zhang, W.; Loebach, J. L.; Wilson, S. R.; Jacobsen, E. N. Enantioselective Epoxidation of Unfunctionalized Olefins Catalyzed by Salen Manganese Complexes. *J. Am. Chem. Soc.* **1990**, *112*, 2801−2803. (b) Katsuki, T. Some Recent Advances in Metallosalen Chemistry. *Synlett* **2003**, 281−297. (c) McGarrigle, E. M.; Gilheany, D. G. Chromium- and Manganese-Salen Promoted Epoxidation of Alkenes. *Chem. Rev.* **2005**, *105*, 1563−1602.
(46) Costa, L. G.; Aschner, M. *Manganese in Health and Disease*; Royal Society of Chemistry: Cambridge, UK, 2015.
(47) (a) Lewis, J. C.; Coelho, P. S.; Arnold, F. H. Enzymatic Functionalization of Carbon−Hydrogen Bonds. *Chem. Soc. Rev.* **2011**, *40*, 2003−2021. (b) Liu, W.; Groves, J. T. Manganese Catalyzed C−H Halogenation. *Acc. Chem. Res.* **2015**, *48*, 1727−1735. (c) Milan, M.; Bietti, M.; Costas, M. Enantioselective Aliphatic C−H Bond Oxidation Catalyzed by Bioinspired Complexes. *Chem. Commun.* **2018**, *54*, 9559−9570. (d) Chen, J.; Jiang, Z.; Fukuzumi, S.; Nam, W.; Wang, B. Artificial Nonheme Iron and Manganese Oxygenases for Enantioselective Olefin Epoxidation and Alkane Hydroxylation Reactions. *Coord. Chem. Rev.* **2020**, *421*, 213443. (e) Vicens, L.; Olivo, G.; Costas, M. Rational Design of Bioinspired Catalysts for Selective Oxidations. *ACS Catal.* **2020**, *10*, 8611−8631. (f) Costas, M. Site and Enantioselective Aliphatic C−H Oxidation with Bioinspired Chiral Complexes. *Chem. Rec.* **2021**, *21*, 4000−4014.
(48) (a) Hu, Y.; Zhou, B.; Wang, C. Inert C−H Bond Transformations Enabled by Organometallic Manganese Catalysis. *Acc. Chem. Res.* **2018**, *51*, 816−827. (b) Anusree, G.; Devi, P. S.; Anilkumar, G. Recent Advances and Prospects in Manganese-Catalyzed C−H Activation. *Adv. Synth. Catal.* **2024**, *366*, 3963−3999.
(49) Larrow, J. F.; Jacobsen, E. N. Kinetic Resolution of 1,2-Dihydronaphthalene Oxide and Related Epoxides *via* Asymmetric C−H Hydroxylation. *J. Am. Chem. Soc.* **1994**, *116*, 12129−12130.
(50) Hamachi, K.; Irie, R.; Katsuki, T. Asymmetric Benzylic Oxidation Using a Mn-Salen Complex as Catalyst. *Tetrahedron Lett.* **1996**, *37*, 4979−4982.
(51) Hamada, T.; Irie, R.; Mihara, J.; Hamachi, K.; Katsuki, T. Highly Enantioselective Benzylic Hydroxylation with Concave Type of (Salen)manganese(III) Complex. *Tetrahedron* **1998**, *54*, 10017−10028.
(52) Murahashi, S.-I.; Noji, S.; Komiya, N. Catalytic Enantioselective Oxidation of Alkanes and Alkenes Using (Salen)Manganese Complexes Bearing a Chiral Binaphthyl Strapping Unit. *Adv. Synth. Catal.* **2004**, *346*, 195−198.
(53) Herrmann, P.; Bach, T. Diastereotopos-Differentiating C−H Activation Reactions at Methylene Groups. *Chem. Soc. Rev.* **2011**, *40*, 2022−2038.
(54) Miyafuji, A.; Katsuki, T. Asymmetric Desymmetrization of *Meso*-Tetrahydrofuran Derivatives by Highly Enantiotopic Selective C−H Oxidation. *Tetrahedron* **1998**, *54*, 10339−10348.
(55) (a) Punniyamurthy, T.; Miyafuji, A.; Katsuki, T. Chiral Mn-Salen Catalyzed Enantiotopic Selective C−H Oxidation of *Meso*-Pyrrolidine Derivatives. *Tetrahedron Lett.* **1998**, *39*, 8295−8298. (b) Punniyamurthy, T.; Katsuki, T. Asymmetric Desymmetrization of *Meso*-Pyrrolidine Derivatives by Enantiotopic Selective C−H Hydroxylation Using (Salen)manganese(III) Complexes. *Tetrahedron* **1999**, *55*, 9439−9454.
(56) (a) Mao, Y.; Wang, Z.; Wang, G.; Zhao, R.; Kan, L.; Pan, X.; Liu, L. Redox Deracemization of Tertiary Stereocenters Adjacent to an Electron-Withdrawing Group. *ACS Catal.* **2020**, *10*, 7785−7791. (b) Ma, Y.; Liu, X.; Mao, Y.; Huang, J.; Ma, S.; Liu, L. Redox Deracemization of Diarylmethyl Alkynes. *Org. Chem. Front.* **2020**, *7*, 2526−2530.
(57) Cao, M.; Wang, H.; Hou, F.; Zhu, Y.; Liu, Q.; Tung, C.-H.; Liu, L. Catalytic Enantioselective Hydroxylation of Tertiary Propargylic

C(sp^3)−H Bonds in Acyclic Systems: A Kinetic Resolution Study. *J. Am. Chem. Soc.* **2024**, *146*, 18396−18406.
(58) Komiya, N.; Noji, S.; Murahashi, S.-I. Manganese Catalyzed Asymmetric Oxidation of Alkanes to Optically Active Ketones Bearing Asymmetric Center at the α-Position. *Tetrahedron Lett.* **1998**, *39*, 7921−7924.
(59) Murahashi, S.-I.; Noji, S.; Hirabayashi, T.; Komiya, N. Manganese-Catalyzed Enantioselective Oxidation of C−H Bonds of Alkanes and Silyl Ethers to Optically Active Ketones. *Tetrahedron: Asymmetry* **2005**, *16*, 3527−3535.
(60) (a) Pellissier, H. Recent Developments in Non-Enzymatic Oxidative Kinetic Resolution of Secondary Alcohols. *Tetrahedron* **2018**, *74*, 3459−3468. (b) Ahmad, I.; Shagufta; AlMallah, A. R. Advances in Asymmetric Oxidative Kinetic Resolution of Racemic Secondary Alcohols Catalyzed by Chiral Mn(III) Salen Complexes. *Chirality* **2017**, *29*, 798−810. (c) Chandra, P.; Ghosh, T.; Choudhary, N.; Mohammad, A.; Mobin, S. M. Recent Advancement in Oxidation or Acceptorless Dehydrogenation of Alcohols to Valorised Products Using Manganese Based Catalysts. *Coord. Chem. Rev.* **2020**, *411*, 213241.
(61) Sun, S.; Yang, Y.; Zhao, R.; Zhang, D.; Liu, L. Site- and Enantiodifferentiating C(sp^3)−H Oxidation Enables Asymmetric Access to Structurally and Stereochemically Diverse Saturated Cyclic Ethers. *J. Am. Chem. Soc.* **2020**, *142*, 19346−19353.
(62) Sun, S.; Ma, Y.; Liu, Z.; Liu, L. Oxidative Kinetic Resolution of Cyclic Benzylic Ethers. *Angew. Chem., Int. Ed.* **2021**, *60*, 176−180.
(63) (a) Wang, G.; Lu, R.; He, C.; Liu, L. Kinetic Resolution of Indolines by Asymmetric Hydroxylamine Formation. *Nat. Commun.* **2021**, *12*, 2512. (b) Wang, G.; Chen, T.; Jia, K.; Ma, W.; Tung, C.-H.; Liu, L. Catalytic Asymmetric Oxidation of Amines to Hydroxylamines. *J. Am. Chem. Soc.* **2023**, *145*, 22276−22283.
(64) Ye, P.; Feng, A.; Wang, L.; Cao, M.; Zhu, R.; Liu, L. Kinetic Resolution of Cyclic Benzylic Azides Enabled by Site- and Enantioselective C(sp^3)−H Oxidation. *Nat. Commun.* **2022**, *13*, 1621.
(65) (a) Kurahashi, T.; Fujii, H. Chiral Distortion in a Mn^{IV}(salen)-$(N_3)_2$ Derived from Jacobsen's Catalyst as a Possible Conformation Model for Its Enantioselective Reactions. *Inorg. Chem.* **2008**, *47*, 7556−7567. (b) Kurahashi, T.; Hada, M.; Fujii, H. Critical Role of External Axial Ligands in Chirality Amplification of trans-Cyclohexane-1,2-diamine in Salen Complexes. *J. Am. Chem. Soc.* **2009**, *131*, 12394−12405.
(66) Huang, X.; Bergsten, T. M.; Groves, J. T. Manganese-Catalyzed Late-Stage Aliphatic C−H Azidation. *J. Am. Chem. Soc.* **2015**, *137*, 5300−5303.
(67) Cao, M.; Wang, H.; Ma, Y.; Tung, C.-H.; Liu, L. Site- and Enantioselective Manganese-Catalyzed Benzylic C−H Azidation of Indolines. *J. Am. Chem. Soc.* **2022**, *144*, 15383−15390.
(68) Meunier, B. Metalloporphyrins as Versatile Catalysts for Oxidation Reactions and Oxidative DNA Cleavage. *Chem. Rev.* **1992**, *92*, 1411−1456.
(69) (a) Groves, J. T.; Kruper, W. J.; Haushalter, R. C. Hydrocarbon Oxidations with Oxometalloporphinates. Isolation and Reactions of a (Porphinato)manganese(V) Complex. *J. Am. Chem. Soc.* **1980**, *102*, 6375−6377. (b) Groves, J. T.; Lee, J.; Marla, S. S. Detection and Characterization of an Oxomanganese(V) Porphyrin Complex by Rapid-Mixing Stopped-Flow Spectrophotometry. *J. Am. Chem. Soc.* **1997**, *119*, 6269−6273. (c) Jin, N.; Ibrahim, M.; Spiro, T. G.; Groves, J. T. Trans-dioxo Manganese(V) Porphyrins. *J. Am. Chem. Soc.* **2007**, *129*, 12416−12417.
(70) Srour, H.; Le Maux, P.; Simonneaux, G. Enantioselective Manganese-Porphyrin-Catalyzed Epoxidation and C−H Hydroxylation with Hydrogen Peroxide in Water/Methanol Solutions. *Inorg. Chem.* **2012**, *51*, 5850−5856.
(71) Halterman, R. L.; Jan, S. T. Catalytic Asymmetric Epoxidation of Unfunctionalized Alkenes Using the First D4-Symmetric Metallotetraphenylporphyrin. *J. Org. Chem.* **1991**, *56*, 5253−5254.
(72) Nicolas, I.; Le Maux, P.; Simonneaux, G. Synthesis of Chiral Water-Soluble Metalloporphyrins (Fe, Ru): New Catalysts for Asymmetric Carbene Transfer in Water. *Tetrahedron Lett.* **2008**, *49*, 5793−5795.
(73) (a) De Angelis, F.; Jin, N.; Car, R.; Groves, J. T. Electronic Structure and Reactivity of Isomeric Oxo-Mn(V) Porphyrins: Effects of Spin-State Crossing and pK_a Modulation. *Inorg. Chem.* **2006**, *45*, 4268−4276. (b) Jin, N.; Lahaye, D. E.; Groves, J. T. A "Push-Pull" Mechanism for Heterolytic O−O Bond Cleavage in Hydroperoxo Manganese Porphyrins. *Inorg. Chem.* **2010**, *49*, 11516−11524.
(74) (a) Fackler, P.; Berthold, C.; Voss, F.; Bach, T. Hydrogen-Bond-Mediated Enantio- and Regioselectivity in a Ru-Catalyzed. *J. Am. Chem. Soc.* **2010**, *132*, 15911−15913. (b) Fackler, P.; Huber, S. M.; Bach, T. Enantio- and Regioselective Epoxidation of Olefinic Double Bonds in Quinolones, Pyridones, and Amides Catalyzed by a Ruthenium Porphyrin Catalyst with a Hydrogen Bonding Site. *J. Am. Chem. Soc.* **2012**, *134*, 12869−12878. (c) Frost, J. R.; Huber, S. M.; Breitenlechner, S.; Bannwarth, C.; Bach, T. Enantiotopos-Selective C−H Oxygenation Catalyzed by a Supramolecular Ruthenium Complex. *Angew. Chem., Int. Ed.* **2015**, *54*, 691−695.
(75) Burg, F.; Gicquel, M.; Breitenlechner, S.; Pöthig, A.; Bach, T. Site- and Enantioselective C−H Oxygenation Catalyzed by a Chiral Manganese Porphyrin Complex with a Remote Binding Site. *Angew. Chem., Int. Ed.* **2018**, *57*, 2953−2957.
(76) (a) Das, S.; Incarvito, C. D.; Crabtree, R. H.; Brudvig, G. W. Molecular Recognition in the Selective Oxygenation of Saturated C−H Bonds by a Dimanganese Catalyst. *Science* **2006**, *312*, 1941−1943. (b) Das, S.; Brudvig, G. W.; Crabtree, R. H. High Turnover Remote Catalytic Oxygenation of Alkyl Groups: How Steric Exclusion of Unbound Substrate Contributes to High Molecular Recognition Selectivity. *J. Am. Chem. Soc.* **2008**, *130*, 1628−1637.
(77) Burg, F.; Breitenlechner, S.; Jandl, C.; Bach, T. Enantioselective Oxygenation of Exocyclic Methylene Groups by a Manganese Porphyrin Catalyst with a Chiral Recognition Site. *Chem. Sci.* **2020**, *11*, 2121−2129.
(78) Ahmed, H.; Pöthig, A.; Truong, K.-N.; Bach, T. Remote Enantioselective Epoxidation Reactions Catalyzed by Chiral Iron Porphyrin Complexes with a Hydrogen-Bonding Site. *Synlett* **2024**, *35*, 983−988.
(79) (a) Chen, M. S.; White, M. C. A Predictably Selective Aliphatic C−H Oxidation Reaction for Complex Molecule Synthesis. *Science* **2007**, *318*, 783−787. (b) Chen, M. S.; White, M. C. Combined Effects on Selectivity in Fe-Catalyzed Methylene Oxidation. *Science* **2010**, *327*, 566−571. (c) Bigi, M. A.; Reed, S. A.; White, M. C. Diverting Non-Haem Iron Catalysed Aliphatic C−H Hydroxylations towards Desaturations. *Nat. Chem.* **2011**, *3*, 216−222. (d) Bigi, M. A.; Reed, S. A.; White, M. C. Directed Metal (Oxo) Aliphatic C−H Hydroxylations: Overriding Substrate Bias. *J. Am. Chem. Soc.* **2012**, *134*, 9721−9726.
(80) Talsi, E. P.; Samsonenko, D. G.; Ottenbacher, R. V.; Bryliakov, K. P. Highly Enantioselective C−H Oxidation of Arylalkanes with H_2O_2 in the Presence of Chiral Mn-Aminopyridine Complexes. *ChemCatChem.* **2017**, *9*, 4580−4586.
(81) Dantignana, V.; Milan, M.; Cussó, O.; Company, A.; Bietti, M.; Costas, M. Chemoselective Aliphatic C−H Bond Oxidation Enabled by Polarity Reversal. *ACS Cent. Sci.* **2017**, *3*, 1350−1358.
(82) Ottenbacher, R. V.; Talsi, E. P.; Rybalova, T. V.; Bryliakov, K. P. Enantioselective Benzylic Hydroxylation of Arylalkanes with H_2O_2 in Fluorinated Alcohols in the Presence of Chiral Mn Aminopyridine Complexes. *ChemCatChem.* **2018**, *10*, 5323−5330.
(83) Ottenbacher, R. V.; Talsi, E. P.; Bryliakov, K. P. Highly Enantioselective Undirected Catalytic Hydroxylation of Benzylic CH_2 groups with H_2O_2. *J. Catal.* **2020**, *390*, 170−177.
(84) Masferrer-Rius, E.; Li, F.; Lutz, M.; Klein Gebbink, R. J. M. Exploration of Highly Electron-Rich Manganese Complexes in Enantioselective Oxidation Catalysis; a Focus on Enantioselective Benzylic Oxidation. *Catal. Sci. Technol.* **2021**, *11*, 7751−7763.
(85) Sun, Q.; Sun, W. Catalytic Enantioselective Methylene C(sp^3)−H Hydroxylation Usinga Chiral Manganese Complex/Carboxylic Acid System. *Org. Lett.* **2020**, *22*, 9529−9533.
(86) Palone, A.; Casadevall, G.; Ruiz-Barragan, S.; Call, A.; Osuna, S.; Bietti, M.; Costas, M. C−H Bonds as Functional Groups: Simultaneous Generation of Multiple Stereocenters by Enantioselective Hydrox-

ylation at Unactivated Tertiary C−H Bonds. *J. Am. Chem. Soc.* **2023**, *145*, 15742−15753.
(87) (a) Milan, M.; Bietti, M.; Costas, M. Highly Enantioselective Oxidation of Nonactivated Aliphatic C−H Bonds with Hydrogen Peroxide Catalyzed by Manganese Complexes. *ACS Cent. Sci.* **2017**, *3*, 196−204. (b) Wang, F.; Liu, G. Setting Cyclohexane Stereochemistry with Oxidation. *ACS Cent. Sci.* **2017**, *3*, 161−162.
(88) Milan, M.; Bietti, M.; Costas, M. Aliphatic C−H Bond Oxidation with Hydrogen Peroxide Catalyzed by Manganese Complexes: Directing Selectivity through Torsional Effects. *Org. Lett.* **2018**, *20*, 2720−2723.
(89) Call, A.; Palone, A.; Liles, J. P.; Romer, N. P.; Read, J. A.; Luis, J. M.; Sigman, M. S.; Bietti, M.; Costas, M. Understanding Catalytic Enantioselective C−H Bond Oxidation at Nonactivated Methylenes Through Predictive Statistical Modeling Analysis. *ACS Catal.* **2025**, *15*, 2110−2123.
(90) Qiu, B.; Xu, D.; Sun, Q.; Miao, C.; Lee, Y.-M.; Li, X.-X.; Nam, W.; Sun, W. Highly Enantioselective Oxidation of Spirocyclic Hydrocarbons by Bioinspired Manganese Catalysts and Hydrogen Peroxide. *ACS Catal.* **2018**, *8*, 2479−2487.
(91) Qiu, B.; Xu, D.; Sun, Q.; Lin, J.; Sun, W. Manganese-Catalyzed Asymmetric Oxidation of Methylene C−H of Spirocyclic Oxindoles and Dihydroquinolinones with Hydrogen Peroxide. *Org. Lett.* **2019**, *21*, 618−622.
(92) (a) White, M. C.; Zhao, J. Aliphatic C−H Oxidations for Late-Stage Functionalization. *J. Am. Chem. Soc.* **2018**, *140*, 13988−14009. (b) Olivo, G.; Cussó, O.; Borrell, M.; Costas, M. Oxidation of Alkane and Alkene Moieties with Biologically Inspired Nonheme Iron Catalysts and Hydrogen Peroxide: From Free Radicals to Stereoselective Transformations. *J. Biol. Inorg. Chem.* **2017**, *22*, 425−452. (c) Bryliakov, K. P. Catalytic Asymmetric Oxygenations with the Environmentally Benign Oxidants H_2O_2 and O_2. *Chem. Rev.* **2017**, *117*, 11406−11459.
(93) Cianfanelli, M.; Olivo, G.; Milan, M.; Klein Gebbink, R. J. M.; Ribas, X.; Bietti, M.; Costas, M. Enantioselective C−H Lactonization of Unactivated Methylenes Directed by Carboxylic Acids. *J. Am. Chem. Soc.* **2020**, *142*, 1584−1593.
(94) Call, A.; Capocasa, G.; Palone, A.; Vicens, L.; Aparicio, E.; Choukairi Afailal, N.; Siakavaras, N.; López Saló, M. E.; Bietti, M.; Costas, M. Highly Enantioselective Catalytic Lactonization at Non-activated Primary and Secondary γ-C−H Bonds. *J. Am. Chem. Soc.* **2023**, *145*, 18094−18103.
(95) (a) Vicens, L.; Bietti, M.; Costas, M. General Access to Modified α-Amino Acids by Bioinspired Stereoselective γ-C−H Bond Lactonization. *Angew. Chem., Int. Ed.* **2021**, *60*, 4740−4746. (b) Call, A.; Cianfanelli, M.; Besalú-Sala, P.; Olivo, G.; Palone, A.; Vicens, L.; Ribas, X.; Luis, J. M.; Bietti, M.; Costas, M. Carboxylic Acid Directed γ-Lactonization of Unactivated Primary C−H Bonds Catalyzed by Mn Complexes: Application to Stereoselective Natural Product Diversification. *J. Am. Chem. Soc.* **2022**, *144*, 19542−19558.
(96) (a) Ortiz de Montellano, P. R. Hydrocarbon Hydroxylation by Cytochrome P450 Enzymes. *Chem. Rev.* **2010**, *110*, 932−948. (b) King-Smith, E.; Zwick, C. R., III; Renata, H. Applications of Oxygenases in the Chemoenzymatic Total Synthesis of Complex Natural Products. *Biochemistry* **2018**, *57*, 403−412. (c) Zhang, R. K.; Huang, X.; Arnold, F. H. Selective C−H Bond Functionalization with Engineered Heme Proteins: New Tools to Generate Complexity. *Curr. Opin. Chem. Biol.* **2019**, *49*, 67−75. (d) Li, Y.; Yuan, B.; Sun, Z.; Zhang, W. C−H Bond Functionalization Reactions Enabled by Photobiocatalytic Cascades. *Green Synth. Catal.* **2021**, *2*, 267−274. (e) Ren, X.; Fasan, R. Engineered and Artificial Metalloenzymes for Selective C−H Functionalization. *Curr. Opin. Green Sustain. Chem.* **2021**, *31*, 100494. (f) Das, A.; Gao, S.; Athavale, S. V.; Alfonzo, E.; Long, Y.; Arnold, F. H. Directed evolution of P411 Enzymes for Amination of Inert C−H Bonds. *Methods Enzymol.* **2023**, *693*, 1−30.
(97) Egorova, K. S.; Ananikov, V. P. Which Metals are Green for Catalysis? Comparison of the Toxicities of Ni, Cu, Fe, Pd, Pt, Rh, and Au Salts. *Angew. Chem., Int. Ed.* **2016**, *55*, 12150−12162.
(98) (a) Enthaler, S.; Junge, K.; Beller, M. Sustainable Metal Catalysis with Iron: From Rust to a Rising Star? *Angew. Chem., Int. Ed.* **2008**, *47*, 3317−3321. (b) Correa, A.; Garcia Mancheno, O.; Bolm, C. Iron-Catalysed Carbon−Heteroatom and Heteroatom−Heteroatom Bond Forming Processes. *Chem. Soc. Rev.* **2008**, *37*, 1108−1117. (c) Fürstner, A. Iron Catalysis in Organic Synthesis: A Critical Assessment of What It Takes to Make This Base Metal a Multitasking Champion. *ACS Cent. Sci.* **2016**, *2*, 778−789. (d) Olivo, G.; Cussó, O.; Borrell, M.; Costas, M. Oxidation of Alkane and Alkene Moieties with Biologically Inspired Nonheme Iron Catalysts and Hydrogen Peroxide: from Free Radicals to Stereoselective Transformations. *J. Biol. Inorg. Chem.* **2017**, *22*, 425−452. (e) Casnati, A.; Lanzi, M.; Cera, G. Recent Advances in Asymmetric Iron Catalysis. *Molecules* **2020**, *25*, 3889. (f) Zhang, J.; Wu, J. Recent Progress in Asymmetric Radical Reactions Enabled by Chiral Iron Catalysts. *Chem. Commun.* **2024**, *60*, 12633−12649.
(99) (a) Nakamura, E.; Yoshikai, N. Low-Valent Iron-Catalyzed C−C Bond Formation-Addition, Substitution, and C−H Bond Activation. *J. Org. Chem.* **2010**, *75*, 6061−6067. (b) Kal, S.; Xu, S.; Que, L., Jr. Bioinspired Nonheme Iron Oxidation Catalysis: Involvement of Oxoiron(V) Oxidants in Cleaving Strong C−H Bonds. *Angew. Chem., Int. Ed.* **2020**, *59*, 7332−7349. (c) Pradhan, C.; Punji, B. Advancement in the C−H Bond Alkylation of (Hetero)arenes Catalyzed by the Most Abundant Transition Metal-Iron. *Org. Chem. Front.* **2024**, *11*, 2397−2417. (d) Yu, K.; Ward, T. R. C−H Functionalization Reactions Catalyzed by Artificial Metalloenzymes. *J. Inorg. Biochem.* **2024**, *258*, 112621. (e) Talsi, E. P.; Bryliakov, K. P. Nonheme Fe Based Enzyme Mimics for Fine Organic Synthesis: Catalytic C−H and C═C Oxygenations. *Eur. J. Org. Chem.* **2024**, *27*, No. e202400664.
(100) (a) Meunier, B.; de Visser, S. P.; Shaik, S. Mechanism of Oxidation Reactions Catalyzed by Cytochrome P450 Enzymes. *Chem. Rev.* **2004**, *104*, 3947−3980. (b) Oloo, W. N.; Que, L., Jr. Bioinspired Nonheme Iron Catalysts for C−H and C═C Bond Oxidation: Insights into the Nature of the Metal-Based Oxidants. *Acc. Chem. Res.* **2015**, *48*, 2612−2621. (c) Huang, X.; Groves, J. T. Beyond Ferryl-Mediated Hydroxylation: 40 Years of the Rebound Mechanism and C−H Activation. *J. Biol. Inorg. Chem.* **2017**, *22*, 185−207. (d) Collins, T. J.; Ryabov, A. D. Targeting of High-Valent Iron-TAML Activators at Hydrocarbons and Beyond. *Chem. Rev.* **2017**, *117*, 9140−9162. (e) Huang, X.; Groves, J. T. Oxygen Activation and Radical Transformations in Heme Proteins and Metalloporphyrins. *Chem. Rev.* **2018**, *118*, 2491−2553.
(101) Li, H.-H.; Chen, X.; Kramer, S. Recent Developments for Intermolecular Enantioselective Amination of Non-Acidic C(sp^3)−H Bonds. *Chem. Sci.* **2023**, *14*, 13278−13289.
(102) Groves, J. T.; Nemo, T. E. Aliphatic Hydroxylation Catalyzed by Iron Porphyrin Complexes. *J. Am. Chem. Soc.* **1983**, *105*, 6243−6248.
(103) (a) Groves, J. T.; Viski, P. Asymmetric Hydroxylation by a Chiral Iron Porphyrin. *J. Am. Chem. Soc.* **1989**, *111*, 8537−8538. (b) Groves, J. T.; Viski, P. Asymmetric Hydroxylation, Epoxidation, and Sulfoxidation Catalyzed by Vaulted Binaphthyl Metalloporphyrins. *J. Org. Chem.* **1990**, *55*, 3628−3634.
(104) (a) Ini, S.; Kapon, M.; Cohen, S.; Gross, Z. Self Assembly Assisted Preparation of a Homochiral Porphyrin. *Tetrahedron: Asymmetry* **1996**, *7*, 659−662. (b) Gross, Z.; Ini, S. Asymmetric Catalysis by a Chiral Ruthenium Porphyrin: Epoxidation, Hydroxylation, and Partial Kinetic Resolution of Hydrocarbons. *Org. Lett.* **1999**, *1*, 2077−2080.
(105) Le Maux, P.; Srour, H. F.; Simonneaux, G. Enantioselective Water-Soluble Iron-Porphyrin-Catalyzed Epoxidation with Aqueous Hydrogen Peroxide and Hydroxylation with Iodobenzene Diacetate. *Tetrahedron* **2012**, *68*, 5824−5828.
(106) Das, S. K.; Roy, S.; Khatua, H.; Chattopadhyay, B. Iron-Catalyzed Amination of Strong Aliphatic C(sp^3)−H Bonds. *J. Am. Chem. Soc.* **2020**, *142*, 16211−16217.
(107) Wang, H.-H.; Shao, H.; Huang, G.; Fan, J.; To, W.-P.; Dang, L.; Liu, Y.; Che, C.-M. Chiral Iron Porphyrins Catalyze Enantioselective Intramolecular C(sp^3)−H Bond Amination Upon Visible-Light Irradiation. *Angew. Chem., Int. Ed.* **2023**, *62*, No. e202218577.

(108) Lu, R.; Cao, L.; Guan, H.; Liu, L. Iron-Catalyzed Aerobic Dehydrogenative Kinetic Resolution of Cyclic Secondary Amines. *J. Am. Chem. Soc.* **2019**, *141*, 6318−6324.
(109) (a) Glaser, T.; Pawelke, R. H.; Heidemeier, M. Z. Synthesis, Structure, and Spectroscopic Properties of a Dinuclear $Fe^{III}(\mu_2\text{-}O)Fe^{III}$ Complex Using a Strongly Electron-Donating Ligand: Implications for the Generation of New High-Valent Species. *Z. Anorg. Allg. Chem.* **2003**, *629*, 2274−2281. (b) Strautmann, J. B. H.; George, S. D.; Bothe, E.; Bill, E.; Weyhermuller, T.; Stammler, A.; Bogge, H.; Glaser, T. Molecular and Electronic Structures of Mononuclear Iron Complexes Using Strongly Electron-Donating Ligands and their Oxidized Forms. *Inorg. Chem.* **2008**, *47*, 6804−6824.
(110) (a) Egami, H.; Katsuki, T. Iron-catalyzed Asymmetric Aerobic Oxidation: Oxidative Coupling of 2-Naphthols. *J. Am. Chem. Soc.* **2009**, *131*, 6082−6083. (b) Egami, H.; Matsumoto, K.; Oguma, T.; Kunisu, T.; Katsuki, T. Enantioenriched Synthesis of C_1-Symmetric BINOLs: Iron-Catalyzed Cross-Coupling of 2-Naphthols and Some Mechanistic Insight. *J. Am. Chem. Soc.* **2010**, *132*, 13633−13635. (c) Matsumoto, K.; Egami, H.; Oguma, T.; Katsuki, T. What Factors Influence the Catalytic Activity of Iron-Salan Complexes for Aerobic Oxidative Coupling of 2-Naphthols? *Chem. Commun.* **2012**, *48*, 5823−5825.
(111) (a) Armstrong, W. H.; Spool, A.; Papaefthymiou, G. C.; Frankel, R. B.; Lippard, S. J. Assembly and Characterization of an Accurate Model for the Diiron Center in Hemerythrin. *J. Am. Chem. Soc.* **1984**, *106*, 3653−3667. (b) Rabion, A.; Chen, S.; Wang, J.; Buchanan, R. M.; Seris, J.-L.; Fish, R. H. Biomimetic Oxidation Studies. 9. Mechanistic Aspects of the Oxidation of Alcohols with Functional, Active Site Methane Monooxygenase Enzyme Models in Aqueous Solution. *J. Am. Chem. Soc.* **1995**, *117*, 12356−12357. (c) Que, L., Jr.; Ho, R. Y. N. Dioxygen Activation by Enzymes with Mononuclear Non-Heme Iron Active Sites. *Chem. Rev.* **1996**, *96*, 2607−2624. (d) Jonas, R. T.; Stack, T. D. P. C−H Bond Activation by a Ferric Methoxide Complex: A Model for the Rate-Determining Step in the Mechanism of Lipoxygenase. *J. Am. Chem. Soc.* **1997**, *119*, 8566−8567. (e) Roth, J. P.; Mayer, J. M. Hydrogen Transfer Reactivity of a Ferric Bi-imidazoline Complex that Models the Activity of Lipoxygenase Enzymes. *Inorg. Chem.* **1999**, *38*, 2760−2761.
(112) Mekmouche, Y.; Duboc-Toia, C.; Ménage, S.; Lambeaux, C.; Fontecave, M. Hydroxylation of Alkanes Catalysed by a Chiral μ-Oxo Diferric Complex: A Metal-Based Mechanism. *J. Mol. Catal. A: Chem.* **2000**, *156*, 85−89.
(113) (a) Huo, H.; Shen, X.; Wang, C.; Zhang, L.; Röse, P.; Chen, L.-A.; Harms, K.; Marsch, K.; Hilt, G.; Meggers, E. Asymmetric Photoredox Transition-Metal Catalysis Activated by Visible Light. *Nature* **2014**, *515*, 100−103. (b) Zhang, L.; Meggers, E. Steering Asymmetric Lewis Acid Catalysis Exclusively with Octahedral Metal-Centered Chirality. *Acc. Chem. Res.* **2017**, *50*, 320−330.
(114) (a) Zheng, Y.; Tan, Y.; Harms, K.; Marsch, M.; Riedel, R.; Zhang, L.; Meggers, E. Octahedral Ruthenium Complex with Exclusive Metal-Centered Chirality for Highly Effective Asymmetric Catalysis. *J. Am. Chem. Soc.* **2017**, *139*, 4322−4325. (b) Zhou, Z.; Chen, S.; Qin, J.; Nie, X.; Zheng, X.; Harms, K.; Riedel, R.; Houk, K. N.; Meggers, E. Catalytic Enantioselective Intramolecular $C(sp^3)$−H Amination of 2-Azidoacetamides. *Angew. Chem., Int. Ed.* **2019**, *58*, 1088−1093. (c) Qin, J.; Zhou, Z.; Cui, T.; Hemming, M.; Meggers, E. Enantioselective Intramolecular C−H Amination of Aliphatic Azides by Dual Ruthenium and Phosphine Catalysis. *Chem. Sci.* **2019**, *10*, 3202−3207.
(115) Ye, C.-X.; Shen, X.; Chen, S.; Meggers, E. Stereocontrolled 1,3-Nitrogen Migration to Access Chiral α-Amino Acids. *Nat. Chem.* **2022**, *14*, 566−573.
(116) Zhou, B.; Ye, C.-X.; Meggers, E. *N*-Boc-Protected α-Amino Acids by 1,3-Migratory Nitrene $C(sp^3)$−H Insertion. *Eur. J. Org. Chem.* **2023**, *26*, No. e202300296.
(117) Cui, T.; Ye, C.-X.; Thelemann, J.; Jenisch, D.; Meggers, E. Enantioselective and Enantioconvergent Iron-Catalyzed $C(sp^3)$−H Aminations to Chiral 2-Imidazolidinones. *Chin. J. Chem.* **2023**, *41*, 2065−2070.
(118) Li, J.; Bao, R.; Yang, X.; Cen, S.; Zhang, Z. Chiral Phenanthroline Ligand-Promoted Iron-Catalyzed Enantioselective Intramolecular $C(sp^3)$−H Amination. *J. East China Univ. Sci. Technol.* **2024**, *50*, 524−533.
(119) Seo, K.; Zhang, Y.; Trinh, T. A.; Kim, J.; Qi, L.; Guzei, I. A.; Clark, J. R.; Liu, P.; Schomaker, J. M. Mechanistic and Computational Insights into Asymmetric Intramolecular Iron-Catalyzed Nitrene Transfer into Benzylic C−H Bonds. *ACS Catal.* **2025**, *15*, 3789−3798.
(120) Ye, C.-X.; Dansby, D. R.; Chen, S.; Meggers, E. Expedited Synthesis of α-Amino Acids by Single-Step Enantioselective α-Amination of Carboxylic Acids. *Nat. Synth.* **2023**, *2*, 645−652.
(121) Cera, G.; Haven, T.; Ackermann, L. Expedient Iron-Catalyzed C−H Allylation/Alkylation by Triazole Assistance with Ample Scope. *Angew. Chem., Int. Ed.* **2016**, *55*, 1484−1488.
(122) Schmiel, D.; Butenschön, H. Directed Iron-Catalyzed *ortho*-Alkylation and Arylation: Toward the Stereoselective Catalytic Synthesis of 1,2-Disubstituted Planar-Chiral Ferrocene Derivatives. *Organometallics* **2017**, *36*, 4979−4989.
(123) Loup, J.; Zell, D.; Oliveira, J. C. A.; Keil, H.; Stalke, D.; Ackermann, L. Asymmetric Iron-Catalyzed C−H Alkylation Enabled by Remote Ligand meta-Substitution. *Angew. Chem., Int. Ed.* **2017**, *56*, 14197−14201.
(124) (a) Fliedel, C.; Labande, A.; Manoury, E.; Poli, R. Chiral *N*-Heterocyclic Carbene Ligands with Additional Chelating Group(s) Applied to Homogeneous Metal-Mediated Asymmetric Catalysis. *Coord. Chem. Rev.* **2019**, *394*, 65−103. (b) Liang, Q.; Song, D. Iron *N*-Heterocyclic Carbene Complexes in Homogeneous Catalysis. *Chem. Soc. Rev.* **2020**, *49*, 1209−1232. (c) Zhao, Q.; Meng, G.; Nolan, S. P.; Szostak, M. *N*-Heterocyclic Carbene Complexes in C−H Activation Reactions. *Chem. Rev.* **2020**, *120*, 1981−2048. (d) Thongpaen, J.; Manguin, R.; Baslé, O. Chiral *N*-Heterocyclic Carbene Ligands Enable Asymmetric C−H Bond Functionalization. *Angew. Chem., Int. Ed.* **2020**, *59*, 10242−10251. (e) Bera, A.; Kabadwal, L. M.; Bera, S.; Banerjee, D. Recent Advances on Non-Precious Metal-Catalyzed C−H Functionalization of *N*-Heteroarenes. *Chem. Commun.* **2021**, *58*, 10−28.
(125) Wong, M. Y.; Yamakawa, T.; Yoshikai, N. Iron-Catalyzed Directed C2-Alkylation and Alkenylation of Indole with Vinylarenes and Alkynes. *Org. Lett.* **2015**, *17*, 442−445.
(126) Loup, J.; Parchomyk, T.; Lülf, S.; Demeshko, S.; Meyer, F.; Koszinowski, K.; Ackermann, L. Mössbauer and Mass Spectrometry Support for Iron(II) Catalysts in Enantioselective C−H Activation. *Dalton Trans.* **2019**, *48*, 5135−5139.
(127) (a) Guihaumé, J.; Halbert, S.; Eisenstein, O.; Perutz, R. N. Hydrofluoroarylation of Alkynes with Ni Catalysts. C−H Activation *via* Ligand-to-Ligand Hydrogen Transfer, an Alternative to Oxidative Addition. *Organometallics* **2012**, *31*, 1300−1314. (b) Bair, J. S.; Schramm, Y.; Sergeev, A. G.; Clot, E.; Eisenstein, O.; Hartwig, J. F. Linear-Selective Hydroarylation of Unactivated Terminal and Internal Olefins with Trifuoromethyl-Substituted Arenes. *J. Am. Chem. Soc.* **2014**, *136*, 13098−13101. (c) Xiao, L.-J.; Fu, X.-N.; Zhou, M.-J.; Xie, J.-H.; Wang, L.-X.; Xu, X.-F.; Zhou, Q.-L. Nickel-Catalyzed Hydroacylation of Styrenes with Simple Aldehydes: Reaction Development and Mechanistic Insights. *J. Am. Chem. Soc.* **2016**, *138*, 2957−2960. (d) Tang, S.; Eisenstein, O.; Nakao, Y.; Sakaki, S. Aromatic C−H σ-Bond Activation by Ni^0, Pd^0, and Pt^0 Alkene Complexes: Concerted Oxidative Addition to Metal *vs* Ligand-to-Ligand H Transfer Mechanism. *Organometallics* **2017**, *36*, 2761−2771. (e) Eisenstein, O.; Milani, J.; Perutz, R. N. Selectivity of C−H Activation and Competition between C−H and C-F Bond Activation at Fluorocarbons. *Chem. Rev.* **2017**, *117*, 8710−8753.
(128) Zhang, Z.-J.; Jacob, N.; Bhatia, S.; Boos, P.; Chen, X.; DeMuth, J. C.; Messinis, A. M.; Jei, B. B.; Oliveira, J. C. A.; Radović, A.; Neidig, M. L.; Wencel-Delord, J.; Ackermann, L. Iron-Catalyzed Stereoselective C−H Alkylation for Simultaneous Construction of C−N Axial and *C*-central Chirality. *Nat. Commun.* **2024**, *15*, 3503.
(129) (a) Silva, J. J. R. F.; Williams, R. J. P. *The Biological Chemistry of the Elements: The Inorganic Chemistry of Life*, 2nd ed.; Oxford University Press: Oxford, UK, 2001. (b) Sigel, A.; Sigel, H.; Sigel, R. K. O. *Interrelations between Essential Metal Ions and Human Diseases*; Springer: Dordrecht, 2013.

(130) (a) Khand, I. U.; Knox, G. R.; Pauson, P. L.; Watts, W. E. A Cobalt Induced Cleavage Reaction and a New Series of Arenecobalt Carbonyl Complexes. *J. Chem. Soc. D* **1971**, 36a. (b) Khand, I. U.; Knox, G. R.; Pauson, P. L.; Watts, W. E. Organocobalt Complexes. Part I. Arene Complexes Derived from Dodecacarbonyltetracobalt. *J. Chem. Soc., Perkin Trans. 1* **1973**, 975−977. (c) Lautens, M.; Klute, W.; Tam, W. Transition Metal-Mediated Cycloaddition Reactions. *Chem. Rev.* **1996**, *96*, 49−92. (d) Hebrard, F.; Kalck, P. Cobalt-Catalyzed Hydroformylation of Alkenes: Generation and Recycling of the Carbonyl Species, and Catalytic Cycle. *Chem. Rev.* **2009**, *109*, 4272−4282. (e) Cahiez, G.; Moyeux, A. Cobalt-Catalyzed Cross-Coupling Reactions. *Chem. Rev.* **2010**, *110*, 1435−1462. (f) Pellissier, H.; Clavier, H. Enantioselective Cobalt-Catalyzed Transformations. *Chem. Rev.* **2014**, *114*, 2775−2823. (g) Gandeepan, P.; Cheng, C.-H. Cobalt Catalysis Involving π Components in Organic Synthesis. *Acc. Chem. Res.* **2015**, *48*, 1194−1206.

(131) (a) Murahashi, S. Synthesis of Phthalimidines from Schiff Bases and Carbon Monoxide. *J. Am. Chem. Soc.* **1955**, *77*, 6403−6404. (b) Murahashi, S.; Horiie, S. The Reaction of Azobenzene and Carbon Monoxide. *J. Am. Chem. Soc.* **1956**, *78*, 4816−4817.

(132) (a) Gao, K.; Yoshikai, N. Low-Valent Cobalt Catalysis: New Opportunities for C−H Functionalization. *Acc. Chem. Res.* **2014**, *47*, 1208−1219. (b) Tilly, D.; Dayaker, G.; Bachu, P. Cobalt Mediated C−H Bond Functionalization: Emerging Tools for Organic Synthesis. *Catal. Sci. Technol.* **2014**, *4*, 2756−2777. (c) Hyster, T. K. High-Valent Co(III)- and Ni(II)-Catalyzed C−H Activation. *Catal. Lett.* **2015**, *145*, 458−467. (d) Moselage, M.; Li, J.; Ackermann, L. Cobalt-Catalyzed C−H Activation. *ACS Catal.* **2016**, *6*, 498−525. (e) Wei, D.; Zhu, X.; Niu, J.-L.; Song, M.-P. High-Valent-Cobalt-Catalyzed C−H Functionalization Based on Concerted Metalation-Deprotonation and Single-Electron-Transfer Mechanisms. *ChemCatChem.* **2016**, *8*, 1242−1263. (f) Kommagalla, Y.; Chatani, N. Cobalt(II)-Catalyzed C−H Functionalization using an *N,N'*-Bidentate Directing Group. *Coord. Chem. Rev.* **2017**, *350*, 117−135. (g) Yoshino, T.; Matsunaga, S. Cobalt-Catalyzed C(sp^3)−H Functionalization Reactions. *Asian J. Org. Chem.* **2018**, *7*, 1193−1205. (h) Baccalini, A.; Vergura, S.; Dolui, P.; Zanoni, G.; Maiti, D. Recent Advances in Cobalt-Catalysed C−H Functionalizations. *Org. Biomol. Chem.* **2019**, *17*, 10119−10141. (i) Lukasevics, L.; Cizikovs, A.; Grigorjeva, L. C−H Bond Functionalization by High-Valent Cobalt Catalysis: Current Progress, Challenges and Future Perspectives. *Chem. Commun.* **2021**, *57*, 10827−10841.

(133) (a) Xu, W.; Ye, M. Enantioselective Cobalt-Catalyzed C−H Functionalization. *Synthesis* **2022**, *54*, 4773−4783. (b) Zheng, Y.; Zheng, C.; Gu, Q.; You, S.-L. Enantioselective C−H Functionalization Reactions Enabled by Cobalt Catalysis. *Chem. Catal.* **2022**, *2*, 2965−2985. (c) Garai, B.; Das, A.; Kumar, D. V.; Sundararaju, B. Enantioselective C−H Bond Functionalization under Co(III)-Catalysis. *Chem. Commun.* **2024**, *60*, 3354−3369. (d) Yao, Q.-J.; Shi, B.-F. Cobalt(III)-Catalyzed Enantioselective C−H Functionalization: Ligand Innovation and Reaction Development. *Acc. Chem. Res.* **2025**, *58*, 971−990. (e) Yang, T.; Zhang, Y.; Dou, Y.; Yang, D.; Niu, J.-L. Earth-Abundant Cobalt-Catalyzed Enantioselective C−H Functionalizations. *Sci. China Chem.* **2026**, *69*, 659−679.

(134) (a) Willis, M. C. Transition Metal Catalyzed Alkene and Alkyne Hydroacylation. *Chem. Rev.* **2010**, *110*, 725−748. (b) Wang, H.; Ye, M. Research Advance on Enantioselective Transition Metal-Catalyzed Hydroacylation Reactions. *Chin. J. Org. Chem.* **2022**, *42*, 3152−3166.

(135) Gao, K.; Lee, P.-S.; Fujita, T.; Yoshikai, N. Cobalt-Catalyzed Hydroarylation of Alkynes through Chelation-Assisted C−H Bond Activation. *J. Am. Chem. Soc.* **2010**, *132*, 12249−12251.

(136) Yang, J.; Yoshikai, N. Cobalt-Catalyzed Enantioselective Intramolecular Hydroacylation of Ketones and Olefins. *J. Am. Chem. Soc.* **2014**, *136*, 16748−16751.

(137) (a) Omura, S.; Fukuyama, T.; Murakami, Y.; Okamoto, H.; Ryu, I. Hydroruthenation Triggered Catalytic Conversion of Dialdehydes and Keto Aldehydes to Lactones. *Chem. Commun.* **2009**, 6741−6743. (b) Murphy, S. K.; Dong, V. M. Enantioselective Ketone Hydroacylation Using Noyori's Transfer Hydrogenation Catalyst. *J. Am. Chem. Soc.* **2013**, *135*, 5553−5556.

(138) Yang, J.; Rérat, A.; Lim, Y. J.; Gosmini, C.; Yoshikai, N. Cobalt-Catalyzed Enantio- and Diastereoselective Intramolecular Hydroacylation of Trisubstituted Alkenes. *Angew. Chem., Int. Ed.* **2017**, *56*, 2449−2453.

(139) Bosnich, B. Asymmetric Catalysis. A Comparative Study of the Mechanisms of Intramolecular Hydroacylation and Hydrosilation. *Acc. Chem. Res.* **1998**, *31*, 667−674.

(140) Kim, D. K.; Riedel, J.; Kim, R. S.; Dong, V. M. Cobalt Catalysis for Enantioselective Cyclobutanone Construction. *J. Am. Chem. Soc.* **2017**, *139*, 10208−10211.

(141) Whyte, A.; Bajohr, J.; Torelli, A.; Lautens, M. Enantioselective Cobalt-Catalyzed Intermolecular Hydroacylation of 1,6-Enynes. *Angew. Chem., Int. Ed.* **2020**, *59*, 16409−16413.

(142) Zell, D.; Bursch, M.; Müller, V.; Grimme, S.; Ackermann, L. Full Selectivity Control in Cobalt(III)-Catalyzed C−H Alkylations by Switching of the C−H Activation Mechanism. *Angew. Chem., Int. Ed.* **2017**, *56*, 10378−10382.

(143) Santhoshkumar, R.; Mannathan, S.; Cheng, C.-H. Ligand-Controlled Divergent C−H Functionalization of Aldehydes with Enynes by Cobalt Catalysts. *J. Am. Chem. Soc.* **2015**, *137*, 16116−16120.

(144) (a) Ishida, M.; Shibata, Y.; Noguchi, K.; Tanaka, K. Rhodium-Catalyzed Asymmetric [2 + 2 + 2] Cyclization of 1,6-Enynes and Aldehydes. *Chem. - Eur. J.* **2011**, *17*, 12578−12581. (b) Wu, C.; Yoshikai, N. Cobalt-Catalyzed Intramolecular Reactions between a Vinylcyclopropane and an Alkyne: Switchable [5 + 2] Cycloaddition and Homo-Ene Pathways. *Angew. Chem., Int. Ed.* **2018**, *57*, 6558−6562.

(145) Lee, P.-S.; Yoshikai, N. Cobalt-Catalyzed Enantioselective Directed C−H Alkylation of Indole with Styrenes. *Org. Lett.* **2015**, *17*, 22−25.

(146) Whyte, A.; Torelli, A.; Mirabi, B.; Prieto, L.; Rodríguez, J. F.; Lautens, M. Cobalt-Catalyzed Enantioselective Hydroarylation of 1,6-Enynes. *J. Am. Chem. Soc.* **2020**, *142*, 9510−9517.

(147) (a) Kazerouni, A. M.; McKoy, Q. A.; Blakey, S. B. Recent Advances in Oxidative Allylic C−H Functionalization *via* Group IX-Metal Catalysis. *Chem. Commun.* **2020**, *56*, 13287−13300. (b) Wang, P.-S.; Gong, L.-Z. Pd-Catalyzed Asymmetric Allylic C−H Functionalization. *Chin. J. Chem.* **2023**, *41*, 1841−1848.

(148) Mita, T.; Hanagata, S.; Michigami, K.; Sato, Y. Co-Catalyzed Direct Addition of Allylic C(sp^3)−H Bonds to Ketones. *Org. Lett.* **2017**, *19*, 5876−5879.

(149) Zhang, H.; Huang, J.; Meng, F. Cobalt-Catalyzed Diastereo- and Enantioselective Allyl Addition to Aldehydes and α-Ketoesters through Allylic C−H Functionalization. *Cell Rep. Phys. Sci.* **2021**, *2*, 100406.

(150) Yamada, K.; Hashiyama, R.; Yasui, T.; Yamamoto, Y. Cobalt-Catalyzed Enantioselective Desymmetrization and Chemodivergent Parallel Kinetic Resolution of Unsaturated Substrates *via* C(sp^3)−H Bond Activation. *ACS Catal.* **2025**, *15*, 3860−3872.

(151) Yamada, K.; Koga, N.; Yasui, T.; Yamamoto, Y. Cobalt/Organophotoredox Dual-Catalysis-Enabled Cyclization of 1,5,10-Enediynes Involving Metallole-Mediated Remote C(sp^3)−H Bond Activation Leading to Axially Chiral Aryl Alkenes. *ACS Catal.* **2024**, *14*, 2049−2057.

(152) Jacob, N.; Zaid, Y.; Oliveira, J. C. A.; Ackermann, L.; Wencel-Delord, J. Cobalt-Catalyzed Enantioselective C−H Arylation of Indoles. *J. Am. Chem. Soc.* **2022**, *144*, 798−806.

(153) Oliveira, J. C. A.; Dhawa, U.; Ackermann, L. Insights into the Mechanism of Low-Valent Cobalt-Catalyzed C−H Activation. *ACS Catal.* **2021**, *11*, 1505−1515.

(154) Luc, A.; Oliveira, J. C. A.; Boos, P.; Jacob, N.; Ackermann, L.; Wencel-Delord, J. Double Cobalt-Catalyzed Atroposelective C−H Activation: One-Step Synthesis of Atropisomeric Indoles Bearing *Vicinal* C−C and C−N Diaxes. *Chem. Catal.* **2023**, *3*, 100765.

(155) Yoshino, T.; Ikemoto, H.; Matsunaga, S.; Kanai, M. A Cationic High-Valent Cp*Co^{III} Complex for the Catalytic Generation of Nucleophilic Organometallic Species: Directed C−H Bond Activation. *Angew. Chem., Int. Ed.* **2013**, *52*, 2207−2211.

(156) Yoshino, T.; Matsunaga, S. (Pentamethylcyclopentadienyl)-Cobalt(III)-Catalyzed C−H Bond Functionalization: From Discovery to Unique Reactivity and Selectivity. *Adv. Synth. Catal.* **2017**, *359*, 1245−1262.
(157) Ozols, K.; Jang, Y.-S.; Cramer, N. Chiral Cyclopentadienyl Cobalt(III) Complexes Enable Highly Enantioselective 3d-Metal-Catalyzed C−H Functionalizations. *J. Am. Chem. Soc.* **2019**, *141*, 5675−5680.
(158) Avilés, T.; Dinis, A.; Gonçalves, J. O.; Félix, V.; Calhorda, M. J.; Prazeres, Â.; Drew, M. G. B.; Alves, H.; Henriques, R. T.; da Gama, V.; Zanello, P.; Fontani, M. Synthesis, X-Ray Structures, Electro-Chemistry, Magnetic Properties, and Theoretical Studies of the Novel Monomeric $[CoI_2(dppfO_2)]$ and Polymeric Chain $[CoI_2(\mu\text{-}dppfO_2)_n]$. *J. Chem. Soc., Dalton Trans.* **2002**, *31*, 4595−4602.
(159) Sun, B.; Yoshino, T.; Matsunaga, S.; Kanai, M. Air-Stable Carbonyl(pentamethylcyclopentadienyl)cobalt Diiodide Complex as a Precursor for Cationic (Pentamethylcyclopentadienyl)cobalt(III) Catalysis: Application for Directed C-2 Selective C−H Amidation of Indoles. *Adv. Synth. Catal.* **2014**, *356*, 1491−1495.
(160) Ozols, K.; Onodera, S.; Woźniak, Ł.; Cramer, N. Cobalt(III)-Catalyzed Enantioselective Intermolecular Carboamination by C−H Functionalization. *Angew. Chem., Int. Ed.* **2021**, *60*, 655−659.
(161) Lerchen, A.; Knecht, T.; Daniliuc, C. G.; Glorius, F. Unnatural Amino Acid Synthesis Enabled by the Regioselective Cobalt(III)-Catalyzed Intermolecular Carboamination of Alkenes. *Angew. Chem., Int. Ed.* **2016**, *55*, 15166−15170.
(162) (a) Piou, T.; Rovis, T. Rhodium-Catalysed *syn*-Carboamination of Alkenes *via* a Transient Directing Group. *Nature* **2015**, *527*, 86−90. (b) Hu, Z.; Tong, X.; Liu, G. Rhodium(III) Catalyzed Carboamination of Alkenes Triggered by C−H Activation of *N*-Phenoxyacetamides under Redox-Neutral Conditions. *Org. Lett.* **2016**, *18*, 1702−1705.
(163) Zheng, Y.; Zhang, W.-Y.; Gu, Q.; Zheng, C.; You, S.-L. Cobalt(III)-Catalyzed Asymmetric Ring-Opening of 7-Oxabenzonorbornadienes *via* Indole C−H Functionalization. *Nat. Commun.* **2023**, *14*, 1094.
(164) Verdhi, L. K.; Wodrich, M. D.; Cramer, N. Enantioselective Cobalt(III)-Catalyzed [4 + 1] Annulation of Benzamides: Cyclopropenes as One-Carbon Synthons. *J. Am. Chem. Soc.* **2025**, *147*, 15041−15049.
(165) Boerth, J. A.; Hummel, J. R.; Ellman, J. A. Highly Stereoselective Cobalt(III)-Catalyzed Three-Component C−H Bond Addition Cascade. *Angew. Chem., Int. Ed.* **2016**, *55*, 12650−12654.
(166) Herraiz, A. G.; Cramer, N. Cobalt(III)-Catalyzed Diastereo- and Enantioselective Three-Component C−H Functionalization. *ACS Catal.* **2021**, *11*, 11938−11944.
(167) Zheng, Y.; Xie, P.-P.; Zheng, C.; You, S.-L. Cobalt-Catalyzed Asymmetric Synthesis of Planar Chiral Ferrocene Derivatives *via* $C(sp^2)-C(sp^3)$ Bond Formation. *CCS Chem.* **2025**, *7*, 1202−1215.
(168) (a) Ackermann, L. Carboxylate-Assisted Transition-Metal-Catalyzed C−H Bond Functionalizations: Mechanism and Scope. *Chem. Rev.* **2011**, *111*, 1315−1345. (b) Davies, D. L.; Macgregor, S. A.; McMullin, C. L. Computational Studies of Carboxylate-Assisted C−H Activation and Functionalization at Group 8−10 Transition Metal Centers. *Chem. Rev.* **2017**, *117*, 8649−8709.
(169) Yoshino, T.; Matsunaga, S. Chiral Carboxylic Acid Assisted Enantioselective C−H Activation with Achiral Cp^xM^{III} (M = Co, Rh, Ir) Catalysts. *ACS Catal.* **2021**, *11*, 6455−6466.
(170) Pesciaioli, F.; Dhawa, U.; Oliveira, J. C. A.; Yin, R.; John, M.; Ackermann, L. Enantioselective Cobalt(III)-Catalyzed C−H Activation Enabled by Chiral Carboxylic Acid Cooperation. *Angew. Chem., Int. Ed.* **2018**, *57*, 15425−15429.
(171) Zhang, Z.-J.; Li, S.-W.; Oliveira, J. C. A.; Li, Y.; Chen, X.; Zhang, S.-Q.; Xu, L.-C.; Rogge, T.; Hong, X.; Ackermann, L. Data-Driven Design of New Chiral Carboxylic Acid for Construction of Indoles with *C*-Central and C−N Axial Chirality *via* Cobalt Catalysis. *Nat. Commun.* **2023**, *14*, 3149.
(172) Kurihara, T.; Kojima, M.; Yoshino, T.; Matsunaga, S. Cp^*Co^{III}/Chiral Carboxylic Acid-Catalyzed Enantioselective 1,4-Addition Reactions of Indoles to Maleimides. *Asian J. Org. Chem.* **2020**, *9*, 368−371.
(173) Qian, P.-F.; Zhou, T.; Shi, B.-F. Transition-Metal-Catalyzed Atroposelective Synthesis of Axially Chiral Styrenes. *Chem. Commun.* **2023**, *59*, 12669−12684.
(174) Shen, C.; Zhu, Y.; Shen, W.; Jin, S.; Zhong, G.; Luo, S.; Xu, L.; Zhong, L.; Zhang, J. Access to Axially Chiral Aryl 1,3-Dienes by Transient Group Directed Asymmetric C−H Alkenylations. *Org. Chem. Front.* **2022**, *9*, 2109−2115.
(175) (a) Fanourakis, A.; Docherty, P. J.; Chuentragool, P.; Phipps, R. J. Recent Developments in Enantioselective Transition Metal Catalysis Featuring Attractive Noncovalent Interactions between Ligand and Substrate. *ACS Catal.* **2020**, *10*, 10672−10714. (b) Liao, G.; Wu, Y.-J.; Shi, B.-F. Noncovalent Interaction in Transition Metal-Catalyzed Selective C−H Activation. *Acta Chim. Sinica* **2020**, *78*, 289−298.
(176) Liu, Y.-H.; Xie, P.-P.; Liu, L.; Fan, J.; Zhang, Z.-Z.; Hong, X.; Shi, B.-F. Cp*Co(III)-Catalyzed Enantioselective Hydroarylation of Unactivated Terminal Alkenes *via* C−H Activation. *J. Am. Chem. Soc.* **2021**, *143*, 19112−19120.
(177) Liu, L.; Liu, Y.-H.; Shi, B.-F. Synthesis of Amino Acids and Peptides with Bulky Side Chains *via* Ligand-Enabled Carboxylate-Directed γ-$C(sp^3)$−H Arylation. *Chem. Sci.* **2020**, *11*, 290−294.
(178) (a) Fukagawa, S.; Kato, Y.; Tanaka, R.; Kojima, M.; Yoshino, T.; Matsunaga, S. Enantioselective $C(sp^3)$−H Amidation of Thioamides Catalyzed by a $Cobalt^{III}$/Chiral Carboxylic Acid Hybrid System. *Angew. Chem., Int. Ed.* **2019**, *58*, 1153−1157. (b) Sekine, D.; Ikeda, K.; Fukagawa, S.; Kojima, M.; Yoshino, T.; Matsunaga, S. Chiral 2-Aryl Ferrocene Carboxylic Acids for the Catalytic Asymmetric $C(sp^3)$−H Activation of Thioamides. *Organometallics* **2019**, *38*, 3921−3926.
(179) Tan, P. W.; Mak, A. M.; Sullivan, M. B.; Dixon, D. J.; Seayad, J. Thioamide-Directed Cobalt(III)-Catalyzed Selective Amidation of $C(sp^3)$−H Bonds. *Angew. Chem., Int. Ed.* **2017**, *56*, 16550−16554.
(180) Liu, Y.-H.; Li, P.-X.; Yao, Q.-J.; Zhang, Z.-Z.; Huang, D.-Y.; Le, M. D.; Song, H.; Liu, L.; Shi, B.-F. Cp*Co(III)/MPAA-Catalyzed Enantioselective Amidation of Ferrocenes Directed by Thioamides under Mild Conditions. *Org. Lett.* **2019**, *21*, 1895−1899.
(181) Zhou, Y.-B.; Zhou, T.; Qian, P.-F.; Li, J.-Y.; Shi, B.-F. Synthesis of Sulfur-Stereogenic Sulfoximines *via* Co(III)/Chiral Carboxylic Acid-Catalyzed Enantioselective C−H Amidation. *ACS Catal.* **2022**, *12*, 9806−9811.
(182) Hirata, Y.; Sekine, D.; Kato, Y.; Lin, L.; Kojima, M.; Yoshino, T.; Matsunaga, S. Cobalt(III)/Chiral Carboxylic Acid-Catalyzed Enantioselective Synthesis of Benzothiadiazine-1-oxides *via* C−H Activation. *Angew. Chem., Int. Ed.* **2022**, *61*, No. e202205341.
(183) (a) Cui, Y.-M.; Lin, Y.; Xu, L.-W. Catalytic Synthesis of Chiral Organoheteroatom Compounds of Silicon, Phosphorus, and Sulfur *via* Asymmetric Transition Metal-Catalyzed C−H Functionalization. *Coord. Chem. Rev.* **2017**, *330*, 37−52. (b) Diesel, J.; Cramer, N. Generation of Heteroatom Stereocenters by Enantioselective C−H Functionalization. *ACS Catal.* **2019**, *9*, 9164−9177. (c) Qian, P.-F.; Li, J.-Y.; Zhou, T.; Shi, B.-F. Synthesis of *P*- and *S*-Stereogenic Compounds *via* Enantioselective C−H Functionalization. *Synthesis* **2022**, *54*, 4784−4794. (d) Suleman, M.; Huang, T.; Zhou, T.; Chen, Z.; Shi, B.-F. Recent Advances in Asymmetric Synthesis of Chiral-at-Sulfur Sulfoximines. *ACS Catal.* **2025**, *15*, 5511−5530.
(184) (a) Zhou, T.; Qian, P.-F.; Li, J.-Y.; Zhou, Y.-B.; Li, H.-C.; Chen, H.-Y.; Shi, B.-F. Efficient Synthesis of Sulfur-Stereogenic Sulfoximines *via* Ru(II)-Catalyzed Enantioselective C−H Functionalization Enabled by Chiral Carboxylic Acid. *J. Am. Chem. Soc.* **2021**, *143*, 6810−6816. (b) Li, J.-Y.; Xie, P.-P.; Zhou, T.; Qian, P.-F.; Zhou, Y.-B.; Li, H.-C.; Hong, X.; Shi, B.-F. Ir(III)-Catalyzed Asymmetric C−H Activation/Annulation of Sulfoximines Assisted by the Hydrogen-Bonding Interaction. *ACS Catal.* **2022**, *12*, 9083−9091. (c) Qian, P.-F.; Zhou, T.; Li, J.-Y.; Zhou, Y.-B.; Shi, B.-F. Ru(II)/Chiral Carboxylic Acid-Catalyzed Asymmetric [4 + 3] Annulation of Sulfoximines with α,β-Unsaturated Ketones. *ACS Catal.* **2022**, *12*, 13876−13883. (d) Zhou, G.; Zhou, T.; Jiang, A.-L.; Qian, P.-F.; Li, J.-Y.; Jiang, B.-Y.; Chen, Z.-J.; Shi, B.-F. Electrooxidative Rhodium(III)/Chiral Carboxylic Acid-

Catalyzed Enantioselective C−H Annulation of Sulfoximines with Alkynes. *Angew. Chem., Int. Ed.* **2024**, *63*, No. e202319871.
(185) Staronova, L.; Yamazaki, K.; Xu, X.; Shi, H.; Bickelhaupt, F. M.; Hamlin, T. A.; Dixon, D. J. Cobalt-Catalyzed Enantio- and Regioselective C(sp^3)-H Alkenylation of Thioamides. *Angew. Chem., Int. Ed.* **2024**, *63*, No. e202316021.
(186) Yuan, W.-K.; Shi, B.-F. Synthesis of Chiral Spirolactams *via* Sequential C−H Olefination/Asymmetric [4 + 1] Spirocyclization under a Simple Co^{II}/Chiral Spiro Phosphoric Acid Binary System. *Angew. Chem., Int. Ed.* **2021**, *60*, 23187−23192.
(187) (a) Chen, D.-F.; Gong, L.-Z. Organo/Transition-Metal Combined Catalysis Rejuvenates Both in Asymmetric Synthesis. *J. Am. Chem. Soc.* **2022**, *144*, 2415−2437. (b) Tran, V. T.; Nimmagadda, S. K.; Liu, M.; Engle, K. M. Recent Applications of Chiral Phosphoric Acids in Palladium Catalysis. *Org. Biomol. Chem.* **2020**, *18*, 618−637.
(188) von Münchow, T.; Dana, S.; Xu, Y.; Yuan, B.; Ackermann, L. Enantioselective Electrochemical Cobalt-Catalyzed Aryl C−H Activation Reactions. *Science* **2023**, *379*, 1036−1042.
(189) (a) Grigorjeva, L.; Daugulis, O. Cobalt-Catalyzed, Aminoquinoline-Directed C(sp^2)-H Bond Alkenylation by Alkynes. *Angew. Chem., Int. Ed.* **2014**, *53*, 10209−10212. (b) Grigorjeva, L.; Daugulis, O. Cobalt-Catalyzed, Aminoquinoline-Directed Coupling of sp^2 C−H Bonds with Alkenes. *Org. Lett.* **2014**, *16*, 4684−4687.
(190) Yao, Q.-J.; Chen, J.-H.; Song, H.; Huang, F.-R.; Shi, B.-F. Cobalt/Salox-Catalyzed Enantioselective C−H Functionalization of Arylphosphinamides. *Angew. Chem., Int. Ed.* **2022**, *61*, No. e202202892.
(191) (a) Bolm, C.; Weickhardt, K.; Zehnder, M.; Ranff, T. Synthesis of Optically Active Bis(2-Oxazolines): Crystal Structure of a 1,2-Bis(2-Oxazolinyl) Benzene $ZnCl_2$ Complex. *Chem. Ber.* **1991**, *124*, 1173−1180. (b) Bolm, C.; Weickhardt, K.; Zehnder, M.; Glasmacher, D. Syntheses and Crystal Structures of 4,5-Dihydro-2-(2′-hydroxyphenyl)-oxazole-Containing Metal Complexes. *Helv. Chim. Acta* **1991**, *74*, 717−726. (c) Shi, B.-F.; Chen, J.-H. 2-(4,5-Dihydro-4-phenyl-2-oxazolyl)-phenol. In *Encyclopedia of Reagents for Organic Synthesis [Online]*; John Wiley & Sons: Bognor Regis, UK, 2005; pp 1−5.
(192) (a) Liu, T.; Zhang, W.; Xu, C.; Xu, Z.; Song, D.; Qian, W.; Lu, G.; Zhang, C.-J.; Zhong, W.; Ling, F. Synthesis of *P*-Stereogenic Cyclicphosphinic Amides *via* Electrochemically Enabled Cobalt-Catalyzed Enantioselective C−H Annulation. *Green Chem.* **2023**, *25*, 3606−3614. (b) Lin, Y.; von Münchow, T.; Ackermann, L. Cobaltaelectro-Catalyzed C−H Annulation with Allenes for Atropochiral and *P*-Stereogenic Compounds: Late-Stage Diversification and Continuous Flow Scale-Up. *ACS Catal.* **2023**, *13*, 9713−9723.
(193) Das, A.; Mandal, R.; Ravi Sankar, H. S.; Kumaran, S.; Premkumar, J. R.; Borah, D.; Sundararaju, B. Reversal of Regioselectivity in Asymmetric C−H Bond Annulation with Bromoalkynes under Cobalt Catalysis. *Angew. Chem., Int. Ed.* **2024**, *63*, No. e202315005.
(194) Wu, Y.-J.; Chen, J.-H.; Teng, M.-Y.; Li, X.; Jiang, T.-Y.; Huang, F.-R.; Yao, Q.-J.; Shi, B.-F. Cobalt-Catalyzed Enantioselective C−H Annulation of Benzylamines with Alkynes: Application to the Modular and Asymmetric Syntheses of Bioactive Molecules. *J. Am. Chem. Soc.* **2023**, *145*, 24499−24505.
(195) Si, X.-J.; Yang, D.; Sun, M.-C.; Wei, D.; Song, M.-P.; Niu, J.-L. Atroposelective Isoquinolinone Synthesis through Cobalt-Catalysed C−H Activation and Annulation. *Nat. Synth.* **2022**, *1*, 709−718.
(196) Wang, X.; Si, X.-J.; Sun, Y.; Wei, Z.; Xu, M.; Yang, D.; Shi, L.; Song, M.-P.; Niu, J.-L. C−N Axially Chiral Heterobiaryl Isoquinolinone Skeletons Construction *via* Cobalt-Catalyzed Atroposelective C−H Activation/Annulation. *Org. Lett.* **2023**, *25*, 6240−6245.
(197) Lin, Y.; von Münchow, T.; Ackermann, L. Cobaltaelectro-Catalyzed C−H Annulation with Allenes for Atropochiral and *P*-Stereogenic Compounds: Late-Stage Diversification and Continuous Flow Scale-Up. *ACS Catal.* **2023**, *13*, 9713−9723.
(198) Xu, Y.; Lin, Y.; Homölle, S. L.; Oliveira, J. C. A.; Ackermann, L. Enantioselective Cobaltaphotoredox-Catalyzed C−H Activation. *J. Am. Chem. Soc.* **2024**, *146*, 24105−24113.
(199) Si, X.-J.; Zhao, X.; Wang, J.; Wang, X.; Zhang, Y.; Yang, D.; Song, M.-P.; Niu, J.-L. Cobalt-Catalyzed Enantioselective C−H/N-H Annulation of Aryl Sulfonamides with Allenes or Alkynes: Facile Access to C−N Axially Chiral Sultams. *Chem. Sci.* **2023**, *14*, 7291−7303.
(200) Zhang, Y.; Liu, S.-L.; Li, T.; Xu, M.; Wang, Q.; Yang, D.; Song, M.-P.; Niu, J.-L. *N*,*O*-Auxiliary Enabled Cobaltaelectro-Catalyzed Atroposelective C−H Annulation. *ACS Catal.* **2024**, *14*, 1−9.
(201) (a) Wencel-Delord, J.; Panossian, A.; Leroux, F. R.; Colobert, F. Recent Advances and New Concepts for the Synthesis of Axially Stereoenriched Biaryls. *Chem. Soc. Rev.* **2015**, *44*, 3418−3430. (b) Wu, Y.-J.; Liao, G.; Shi, B.-F. Stereoselective Construction of Atropisomers Featuring a C−N Chiral Axis. *Green Synth. Catal.* **2022**, *3*, 117−136. (c) Cheng, J. K.; Xiang, S.-H.; Li, S.; Ye, L.; Tan, B. Recent Advances in Catalytic Asymmetric Construction of Atropisomers. *Chem. Rev.* **2021**, *121*, 4805−4902. (d) Liao, G.; Shi, B.-F. Synthesis of Axially Chiral Compounds *via* Transition Metal-Catalyzed Atroposelective C−H Functionalization. *Acc. Chem. Res.* **2025**, *58*, 1562−1579.
(202) Li, T.; Shi, L.; Wang, X.; Yang, C.; Yang, D.; Song, M.-P.; Niu, J.-L. Cobalt-Catalyzed Atroposelective C−H Activation/Annulation to Access N−N Axially Chiral Frameworks. *Nat. Commun.* **2023**, *14*, 5271.
(203) Cai, J.; Li, L.; Wang, C.; Qin, S.; Li, Y.; Liao, S.-Y.; Wang, S.; Gao, H.; Zhou, Z.; Huang, Y.; Yi, W.; Zeng, Z. N−N Atropisomer Synthesis *via* Electrolyte- and Base-Free Electrochemical Cobalt-Catalysed C−H Annulation. *Green Chem.* **2024**, *26*, 11524−11530.
(204) Sun, Y.; Yang, T.; Wang, Q.; Shi, L.; Song, M.-P.; Niu, J.-L. Atroposelective N−N Axes Synthesis *via* Electrochemical Cobalt Catalysis. *Org. Lett.* **2024**, *26*, 5063−5068.
(205) (a) Liao, G.; Zhou, T.; Yao, Q.-J.; Shi, B.-F. Recent Advances in the Synthesis of Axially Chiral Biaryls *via* Transition Metal-Catalysed Asymmetric C−H Functionalization. *Chem. Commun.* **2019**, *55*, 8514−8523. (b) Feng, K.; Yao, C.; Xu, H. Biaxially Chiral Compounds: Research and Development of Synthesis. *Chem. Commun.* **2025**, *61*, 2217−2234.
(206) Wang, B.-J.; Xu, G.-X.; Huang, Z.-W.; Wu, X.; Hong, X.; Yao, Q.-J.; Shi, B.-F. Single-Step Synthesis of Atropisomers with *Vicinal* C−C and C−N Diaxes by Cobalt-Catalyzed Atroposelective C−H Annulation. *Angew. Chem., Int. Ed.* **2022**, *61*, No. e202208912.
(207) Qian, P.-F.; Wu, Y.-X.; Hu, J.-H.; Chen, J.-H.; Zhou, T.; Yao, Q.-J.; Zhang, Z.-H.; Wang, B.-J.; Shi, B.-F. Atroposelective Synthesis of Pyridoindolones Bearing Two Remote Distinct C−N Axes through Cobalt-Catalyzed Enantioselective C−H Activation. *J. Am. Chem. Soc.* **2025**, *147*, 10791−10802.
(208) (a) Dalla Cort, A; Mandolini, L.; Pasquini, C.; Schiaffino, L. "Inherent Chirality" and Curvature. *New J. Chem.* **2004**, *28*, 1198−1199. (b) Szumna, A. Inherently Chiral Concave Molecules—from Synthesis to Applications. *Chem. Soc. Rev.* **2010**, *39*, 4274−4285. (c) Zhu, K.; Spring, D. R.; Shi, B.-F.; Zhang, F. Recent Progress Towards Catalytic Asymmetric Construction of Inherently Chiral Scaffolds. *Chem. Soc. Rev.* **2025**, *54*, 10856−10879.
(209) Qian, P.-F.; Zhou, G.; Hu, J.-H.; Wang, B.-J.; Jiang, A.-L.; Zhou, T.; Yuan, W.-K.; Yao, Q.-J.; Chen, J.-H.; Kong, K.-X.; Shi, B.-F. Asymmetric Synthesis of Chiral Calix[4]arenes with Both Inherent and Axial Chirality *via* Cobalt-Catalyzed Enantioselective Intermolecular C−H Annulation. *Angew. Chem., Int. Ed.* **2024**, *63*, No. e202412459.
(210) Li, T.; Zhang, Y.; Du, C.; Yang, D.; Song, M.-P.; Niu, J.-L. Simultaneous Construction of Inherent and Axial Chirality by Cobalt-Catalyzed Enantioselective C−H Activation of Calix[4]arenes. *Nat. Commun.* **2024**, *15*, 7673.
(211) Yao, Q.-J.; Huang, F.-R.; Chen, J.-H.; Zhong, M.-Y.; Shi, B.-F. Enantio- and Regioselective Electrooxidative Cobalt-Catalyzed C−H/N-H Annulation with Alkenes. *Angew. Chem., Int. Ed.* **2023**, *62*, No. e202218533.
(212) Yang, D.; Zhang, X.; Wang, X.; Si, X.-J.; Wang, J.; Wei, D.; Song, M.-P.; Niu, J.-L. Cobalt-Catalyzed Enantioselective C−H Annulation with Alkenes. *ACS Catal.* **2023**, *13*, 4250−4260.
(213) von Münchow, T.; Liu, Y.-R.; Parmar, R.; Peters, S. E.; Trienes, S.; Ackermann, L. Cobaltaelectro-Catalyzed C−H Activation for Central and Axial Double Enantio-Induction. *Angew. Chem., Int. Ed.* **2024**, *63*, No. e202405423.
(214) Huang, F.-R.; Yao, Q.-J.; Zhang, P.; Teng, M.-Y.; Chen, J.-H.; Jiang, L.-C.; Shi, B.-F. Cobalt-Catalyzed Domino Transformations *via*

https://doi.org/10.1021/acs.chemrev.6c00255
Chem. Rev. XXXX, XXX, XXX−XXX

Enantioselective C−H Activation/Nucleophilic [3 + 2] Annulation toward Chiral Bridged Bicycles. *J. Am. Chem. Soc.* **2024**, *146*, 15576−15586.
(215) von Münchow, T.; Pandit, N. K.; Dana, S.; Boos, P.; Peters, S. E.; Boucat, J.; Liu, Y.-R.; Scheremetjew, A.; Ackermann, L. Enantioselective C−H Annulations Enabled by Either Nickel- or Cobalt-Electrocatalysed C−H Activation for Catalyst-Controlled Chemodivergence. *Nat. Catal.* **2025**, *8*, 257−269.
(216) Teng, M.-Y.; Liu, D.-Y.; Mao, S.-Y.; Wu, X.; Chen, J.-H.; Zhong, M.-Y.; Huang, F.-R.; Yao, Q.-J.; Shi, B.-F. Asymmetric Dearomatization of Indoles through Cobalt-Catalyzed Enantioselective C−H Functionalization Enabled by Photocatalysis. *Angew. Chem., Int. Ed.* **2024**, *63*, No. e202407640.
(217) Das, A.; Kumaran, S.; Ravi Sankar, H. S.; Premkumar, J. R.; Sundararaju, B. A Dual Cobalt-Photoredox Catalytic Approach for Asymmetric Dearomatization of Indoles with Aryl Amides *via* C−H Activation. *Angew. Chem., Int. Ed.* **2024**, *63*, No. e202406195.
(218) Chen, J.-H.; Teng, M.-Y.; Huang, F.-R.; Song, H.; Wang, Z.-K.; Zhuang, H.-L.; Wu, Y.-J.; Wu, X.; Yao, Q.-J.; Shi, B.-F. Cobalt/Salox-Catalyzed Enantioselective Dehydrogenative C−H Alkoxylation and Amination. *Angew. Chem., Int. Ed.* **2022**, *61*, No. e202210106.
(219) Zhou, G.; Chen, J.-H.; Yao, Q.-J.; Huang, F.-R.; Wang, Z.-K.; Shi, B.-F. Base-Promoted Electrochemical Co^{II}-catalyzed Enantioselective C−H Oxygenation. *Angew. Chem., Int. Ed.* **2023**, *62*, No. e202302964.
(220) Wang, Z.-K.; Wu, Y.-J.; Yao, Q.-J.; Shi, B.-F. Synthesis of Chiral Diarylmethylamines by Cobalt-Catalyzed Enantioselective C−H Alkoxylation. *Angew. Chem., Int. Ed.* **2023**, *62*, No. e202304706.
(221) Huang, F.-R.; Zhang, P.; Yao, Q.-J.; Shi, B.-F. Construction of Planar Chiral Ferrocenes by Cobalt-Catalyzed Enantioselective C−H Acyloxylation Enabled by Dual Ligands. *CCS Chem.* **2024**, *6*, 2783−2793.
(222) Zhang, L.; Yang, C.; Wang, X.; Yang, T.; Yang, D.; Dou, Y.; Niu, J.-L. Enantioselective Electrosynthesis of Inherently Chiral Calix[4]-arenes *via* a Cobalt-Catalyzed Aryl C−H Acyloxylation. *Green Chem.* **2024**, *26*, 10232−10239.
(223) Xia, X.; Zheng, C.; Hang, Y.; Guo, J.; Liu, T.; Song, D.; Chen, Z.; Zhong, W.; Ling, F. Electrochemically Enabled Cobalt Catalyzed Enantioselective C−H Acyloxylation of Aryl Phosphamide with Carboxylic Acid. *Green Chem.* **2024**, *26*, 8323−8329.
(224) Li, T.; Shi, L.; Zhao, X.; Wang, J.; Si, X.-J.; Yang, D.; Song, M.-P.; Niu, J.-L. C−N Axially Chiral Heterobiaryl Skeletons Construction *via* Cobalt-Catalyzed Atroposelective Annulation. *Org. Lett.* **2023**, *25*, 5191−5196.
(225) Teng, M.-Y.; Wu, Y.-J.; Chen, J.-H.; Huang, F.-R.; Liu, D.-Y.; Yao, Q.-J.; Shi, B.-F. Cobalt-Catalyzed Enantioselective C−H Carbonylation towards Chiral Isoindolinones. *Angew. Chem., Int. Ed.* **2024**, *63*, No. e202318803.
(226) Wu, Y.-J.; Wang, Z.-K.; Jia, Z.-S.; Chen, J.-H.; Huang, F.-R.; Zhan, B.-B.; Yao, Q.-J.; Shi, B.-F. Synthesis of Axially Chiral Biaryls through Cobalt(II)-Catalyzed Atroposelective C−H Arylation. *Angew. Chem., Int. Ed.* **2023**, *62*, No. e202310004.
(227) (a) Simonneaux, G.; Le Maux, P. Optically Active Ruthenium Porphyrins: Chiral Recognition and Asymmetric Catalysis. *Coord. Chem. Rev.* **2002**, *228*, 43−60. (b) Thompson, S. J.; Brennan, M. R.; Lee, S. Y.; Dong, G. Synthesis and Applications of Rhodium Porphyrin Complexes. *Chem. Soc. Rev.* **2018**, *47*, 929−981. (c) Dar, U. A.; Shahnawaz, M.; Taneja, P.; Dar, M. A. Recent Advances in Main Group Coordination Driven Porphyrins: A Comprehensive Review. *ChemistrySelect* **2024**, *9*, No. e202304817.
(228) (a) Lu, H.; Zhang, X. P. Catalytic C−H Functionalization by Metalloporphyrins: Recent Developments and Future Directions. *Chem. Soc. Rev.* **2011**, *40*, 1899−1909. (b) Che, C.-M.; Lo, V. K.-Y.; Zhou, C.-Y.; Huang, J.-S. Selective Functionalisation of Saturated C−H Bonds with Metalloporphyrin Catalysts. *Chem. Soc. Rev.* **2011**, *40*, 1950−1975. (c) Singh, R.; Mukherjee, A. Metalloporphyrin Catalyzed C−H Amination. *ACS Catal.* **2019**, *9*, 3604−3617.
(229) Kuijpers, P. F.; Tiekink, M. J.; Breukelaar, W. B.; Broere, D. L. J.; van Leest, N. P.; van der Vlugt, J. I.; Reek, J. N. H.; de Bruin, B. Cobalt-Porphyrin-Catalysed Intramolecular Ring-Closing C−H Amination of Aliphatic Azides: A Nitrene-Radical Approach to Saturated Heterocycles. *Chem.—Eur. J.* **2017**, *23*, 7945−7952.
(230) Lu, H.; Jiang, H.; Wojtas, L.; Zhang, X. P. Selective Intramolecular C−H Amination through the Metalloradical Activation of Azides: Synthesis of 1,3-Diamines under Neutral and Nonoxidative Conditions. *Angew. Chem., Int. Ed.* **2010**, *49*, 10192−10196.
(231) Li, C.; Lang, K.; Lu, H.; Hu, Y.; Cui, X.; Wojtas, L.; Zhang, X. P. Catalytic Radical Process for Enantioselective Amination of C(sp^3)−H Bonds. *Angew. Chem., Int. Ed.* **2018**, *57*, 16837−16841.
(232) Lang, K.; Torker, S.; Wojtas, L.; Zhang, X. P. Asymmetric Induction and Enantiodivergence in Catalytic Radical C−H Amination *via* Enantiodifferentiative H-Atom Abstraction and Stereoretentive Radical Substitution. *J. Am. Chem. Soc.* **2019**, *141*, 12388−12396.
(233) Hu, Y.; Lang, K.; Tao, J.; Marshall, M.; Cheng, Q.; Cui, X.; Wojtas, L.; Zhang, X. P. Next-Generation D2-Symmetric Chiral Porphyrins for Co(II)-Based Metalloradical Catalysis: Catalyst Engineering by Distal Bridging. *Angew. Chem., Int. Ed.* **2019**, *58*, 2670−2674.
(234) Lang, K.; Li, C.; Kim, I.; Zhang, X. P. Enantioconvergent Amination of Racemic Tertiary C−H Bonds. *J. Am. Chem. Soc.* **2020**, *142*, 20902−20911.
(235) Lang, K.; Hu, Y.; Lee, W.-C. C.; Zhang, X. P. Combined Radical and Ionic Approach for the Enantioselective Synthesis of *β*-Functionalized Amines from Alcohols. *Nat. Synth.* **2022**, *1*, 548−557.
(236) Zhu, Y.; Lee, W.-C. C.; Zhang, X. P. Catalytic Metalloradical System for Radical 1,6-C(sp^3)−H Amination with Concurrent Control of Site-, Chemo-, and Enantio-selectivity. *J. Am. Chem. Soc.* **2025**, *147*, 15755−15766.
(237) Hu, Y.; Lang, K.; Li, C.; Gill, J. B.; Kim, I.; Lu, H.; Fields, K. B.; Marshall, M.; Cheng, Q.; Cui, X.; Wojtas, L.; Zhang, X. P. Enantioselective Radical Construction of 5-Membered Cyclic Sulfonamides by Metalloradical C−H Amination. *J. Am. Chem. Soc.* **2019**, *141*, 18160−18169.
(238) Jin, L.-M.; Xu, P.; Xie, J.; Zhang, X. P. Enantioselective Intermolecular Radical C−H Amination. *J. Am. Chem. Soc.* **2020**, *142*, 20828−20836.
(239) Xu, P.; Xie, J.; Wang, D.-S.; Zhang, X. P. Metalloradical Approach for Concurrent Control in Intermolecular Radical Allylic C−H Amination. *Nat. Chem.* **2023**, *15*, 498−507.
(240) Cui, X.; Xu, X.; Jin, L.-M.; Wojtas, L.; Zhang, X. P. Stereoselective Radical C−H Alkylation with Acceptor/Acceptor-Substituted Diazo Reagents *via* Co(II)-Based Metalloradical Catalysis. *Chem. Sci.* **2015**, *6*, 1219−1224.
(241) Karns, A. S.; Goswami, M.; de Bruin, B. Catalytic Synthesis of Indolines by Hydrogen Atom Transfer to Cobalt(III)−Carbene Radicals. *Chem. - Eur. J.* **2018**, *24*, 5253−5258.
(242) Wen, X.; Wang, Y.; Zhang, X. P. Enantioselective Radical Process for Synthesis of Chiral Indolines by Metalloradical Alkylation of Diverse C(sp^3)−H Bonds. *Chem. Sci.* **2018**, *9*, 5082−5086.
(243) Wang, Y.; Wen, X.; Cui, X.; Zhang, X. P. Enantioselective Radical Cyclization for Construction of 5-Membered Ring Structures by Metalloradical C−H Alkylation. *J. Am. Chem. Soc.* **2018**, *140*, 4792−4796.
(244) Xie, J.; Xu, P.; Zhu, Y.; Wang, J.; Lee, W.-C. C.; Zhang, X. P. New Catalytic Radical Process Involving 1,4-Hydrogen Atom Abstraction: Asymmetric Construction of Cyclobutanones. *J. Am. Chem. Soc.* **2021**, *143*, 11670−11678.
(245) (a) Nakao, Y. Hydroarylation of Alkynes Catalyzed by Nickel. *Chem. Rec.* **2011**, *11*, 242−251. (b) Diccianni, J.; Lin, Q.; Diao, T. Mechanisms of Nickel-Catalyzed Coupling Reactions and Applications in Alkene Functionalization. *Acc. Chem. Res.* **2020**, *53*, 906−919. (c) Zhang, Z.; Bera, S.; Fan, C.; Hu, X. Streamlined Alkylation *via* Nickel−Hydride-Catalyzed Hydrocarbonation of Alkenes. *J. Am. Chem. Soc.* **2022**, *144*, 7015−7029. (d) Liu, Y.; Li, F.-Y.; Bhat, M.-u.-S.; Tian, L.; Zhang, H.-R.; Meng, H.; Zhao, H.-T.; Li, Y.-L.; Shu, W. Recent Progress on Nickel-Catalyzed Reductive Dicarbofunctionalization of Alkenes. *Chin. J. Chem.* **2025**, *43*, 3637−3658.

(246) (a) Choi, J.; Fu, G. C. Transition Metal-Catalyzed Alkyl−Alkyl Bond Formation: Another Dimension in Cross-Coupling Chemistry. *Science* **2017**, *356*, No. eaaf7230. (b) Poremba, K. E.; Dibrell, S. E.; Reisman, S. E. Nickel-Catalyzed Enantioselective Reductive Cross-Coupling Reactions. *ACS Catal.* **2020**, *10*, 8237−8246. (c) Zhu, C.; Yue, H.; Jia, J.; Rueping, M. Nickel-Catalyzed C−Heteroatom Cross-Coupling Reactions under Mild Conditions *via* Facilitated Reductive Elimination. *Angew. Chem., Int. Ed.* **2021**, *60*, 17810−17831. (d) Li, Z.; Li, C.; Ding, Y.; Huo, H. Photoinduced Nickel-Catalyzed Enantioselective Coupling Reactions. *Coord. Chem. Rev.* **2022**, *460*, 214479. (e) Dawson, G. A.; Spielvogel, E. H.; Diao, T. Nickel-Catalyzed Radical Mechanisms: Informing Cross-Coupling for Synthesizing Non-Canonical Biomolecules. *Acc. Chem. Res.* **2023**, *56*, 3640−3653. (f) Chen, L. M.; Reisman, S. E. Enantioselective $C(sp^2)-C(sp^3)$ Bond Construction by Ni Catalysis. *Acc. Chem. Res.* **2024**, *57*, 751−762.

(247) (a) Gui, Y.-Y.; Sun, L.; Lu, Z.-P.; Yu, D.-G. Photoredox Sheds New Light on Nickel Catalysis: From Carbon−Carbon to Carbon−Heteroatom Bond Formation. *Org. Chem. Front.* **2016**, *3*, 522−526. (b) Diccianni, J. B.; Diao, T. Mechanisms of Nickel-Catalyzed Cross-Coupling Reactions. *Trends Chem.* **2019**, *1*, 830−844.

(248) Ananikov, V. P. Nickel: The "Spirited Horse" of Transition Metal Catalysis. *ACS Catal.* **2015**, *5*, 1964−1971.

(249) Kleiman, J. P.; Dubeck, M. The Preparation of Cyclopentadienyl [*o*-(Phenylazo)phenyl]nickel. *J. Am. Chem. Soc.* **1963**, *85*, 1544−1545.

(250) (a) Castro, L. C M.; Chatani, N. Nickel Catalysts/*N*,*N*′-Bidentate Directing Groups: An Excellent Partnership in Directed C−H Activation Reactions. *Chem. Lett.* **2015**, *44*, 410−421. (b) Yamaguchi, J.; Muto, K.; Itami, K. Nickel-Catalyzed Aromatic C−H Functionalization. *Top. Curr. Chem.* **2016**, *374*, 55. (c) Khake, S. M.; Chatani, N. Chelation-Assisted Nickel-Catalyzed C−H Functionalizations. *Trends Chem.* **2019**, *1*, 524−539. (d) Liu, Y.-H.; Xia, Y.-N.; Shi, B.-F. Ni-Catalyzed Chelation-Assisted Direct Functionalization of Inert C−H Bonds. *Chin. J. Chem.* **2020**, *38*, 635−662.

(251) (a) Ping, Y.; Xu, S.; Kong, W. Stereoselective Nondirected α-$C(sp^3)$−H Functionalization of Oxygen Heterocycles. *Acc. Chem. Res.* **2025**, *58*, 2477−2495. (b) Yao, F.; Shi, B.-F. Nickel-Catalyzed Enantioselective C−H Functionalization. *Chem. Commun.* **2026**, *62*, 1745−1757.

(252) (a) Nakao, Y.; Idei, H.; Kanyiva, K. S.; Hiyama, T. Hydrocarbamoylation of Unsaturated Bonds by Nickel/Lewis-Acid Catalysis. *J. Am. Chem. Soc.* **2009**, *131*, 5070−5071. (b) Miyazaki, Y.; Yamada, Y.; Nakao, Y.; Hiyama, T. Regioselective Hydrocarbamoylation of 1-Alkenes. *Chem. Lett.* **2012**, *41*, 298−300.

(253) Xu, M.; Xu, W.; Ye, M. Chiral Secondary Phosphine Oxide Ligands in Asymmetric Ni−Al Bimetallic Catalysis. *Eur. J. Org. Chem.* **2025**, *28*, No. e202401000.

(254) Donets, P. A.; Cramer, N. Diaminophosphine Oxide Ligand Enabled Asymmetric Nickel-Catalyzed Hydrocarbamoylations of Alkenes. *J. Am. Chem. Soc.* **2013**, *135*, 11772−11775.

(255) Luan, Y.-X.; Ye, M. Ligand-Ligated Ni−Al Bimetallic Catalysis for C−H and C−C Bond Activation. *Chem. Commun.* **2022**, *58*, 12260−12273.

(256) Xu, W.; Sun, Y.; Jiang, Y.; Yan, X.; Gao, Z.; Wang, H.; Huang, G.; Zhou, Q.-L.; Ye, M. Enantioselective Carbonylative Cyclization of Alkenes with C−H Bonds for Synthesis of γ-Lactams Bearing an α-Quaternary Carbon. *J. Am. Chem. Soc.* **2025**, *147*, 96−103.

(257) Wang, Y.-X.; Qi, S.-L.; Luan, Y.-X.; Han, X.-W.; Wang, S.; Chen, H.; Ye, M. Enantioselective Ni−Al Bimetallic Catalyzed *exo*-Selective C−H Cyclization of Imidazoles with Alkenes. *J. Am. Chem. Soc.* **2018**, *140*, 5360−5364.

(258) Tsai, A. S.; Wilson, R. M.; Harada, H.; Bergman, R. G.; Ellman, J. A. Rhodium Catalyzed Enantioselective Cyclization of Substituted Imidazoles *via* C−H Bond Activation. *Chem. Commun.* **2009**, *26*, 3910−3912.

(259) Zhang, Y.; Ni, Q.; Pan, B.; Jiang, L.; Qiu, L. Development of Sterically Hindered SPOs and Enantioselective Ni−Al Bimetallic Catalyzed C−H Cyclization of 4-Oxoquinazolines with Tethered Alkenes. *Chin. Chem. Lett.* **2023**, *34*, 108017.

(260) (a) Landert, H.; Spindler, F.; Wyss, A.; Blaser, H.-U.; Pugin, B.; Ribourduoille, Y.; Gschwend, B.; Ramalingam, B.; Pfaltz, A. *Angew. Chem., Int. Ed.* **2010**, *49*, 6873−6876. (b) Xu, K.; Thieme, N.; Breit, B. Unlocking the N^2 Selectivity of Benzotriazoles: Regiodivergent and Highly Selective Coupling of Benzotriazoles with Allenes. *Angew. Chem., Int. Ed.* **2014**, *53*, 7268−7271.

(261) Loup, J.; Müller, V.; Ghorai, D.; Ackermann, L. Enantioselective Aluminum-Free Alkene Hydroarylations through C−H Activation by a Chiral Nickel/JoSPOphos Manifold. *Angew. Chem., Int. Ed.* **2019**, *58*, 1749−1753.

(262) Li, J.-F.; Pan, D.; Wang, H.-R.; Zhang, T.; Li, Y.; Huang, G.; Ye, M. Enantioselective C2−-H Alkylation of Pyridines with 1,3-Dienes *via* Ni−Al Bimetallic Catalysis. *J. Am. Chem. Soc.* **2022**, *144*, 18810−18816.

(263) Zhang, Z.-J.; Simon, M. M.; Yu, S.; Li, S.-W.; Chen, X.; Cattani, S.; Hong, X.; Ackermann, L. Nickel-Catalyzed Atroposelective C−H Alkylation Enabled by Bimetallic Catalysis with Air-Stable Heteroatom-Substituted Secondary Phosphine Oxide Preligands. *J. Am. Chem. Soc.* **2024**, *146*, 9172−9180.

(264) Chen, H.; Wang, Y.-X.; Luan, Y.-X.; Ye, M. Enantioselective Twofold C−H Annulation of Formamides and Alkynes without Built-in Chelating Groups. *Angew. Chem., Int. Ed.* **2020**, *59*, 9428−9432.

(265) Alberico, D.; Scott, M. E.; Lautens, M. Aryl−Aryl Bond Formation by Transition-Metal-Catalyzed Direct Arylation. *Chem. Rev.* **2007**, *107*, 174−238.

(266) Wang, R.-H.; Li, J.-F.; Li, Y.; Qi, S.-L.; Zhang, T.; Luan, Y.-X.; Ye, M. Selective $C(sp^3)$−H Cleavage of Enamides for Synthesis of 2-Pyridones *via* Ligand-Enabled Ni−Al Bimetallic Catalysis. *ACS Catal.* **2021**, *11*, 858−864.

(267) Wang, Y.-X.; Zhang, F.-P.; Chen, H.; Li, Y.; Li, J.-F.; Ye, M. Enantioselective Nickel-Catalyzed $C(sp^3)$−H Activation of Formamides. *Angew. Chem., Int. Ed.* **2022**, *61*, No. e202209625.

(268) Diesel, J.; Cramer, N. Modular Chiral N-Heterocyclic Carbene Ligands for the Nickel-Catalyzed Enantioselective C−H Functionalization of Heterocycles. *Chimia* **2020**, *74*, 278−284.

(269) Hirsch-Weil, D.; Abboud, K. A.; Hong, S. Isoquinoline-Based Chiral Monodentate *N*-Heterocyclic Carbenes. *Chem. Commun.* **2010**, *46*, 7525−7527.

(270) Donets, P. A.; Cramer, N. Ligand-Controlled Regiodivergent Nickel-Catalyzed Annulation of Pyridones. *Angew. Chem., Int. Ed.* **2015**, *54*, 633−637.

(271) (a) Albright, A.; Eddings, D.; Black, R.; Welch, C. J.; Gerasimchuk, N. N.; Gawley, R. E. Design and Synthesis of C_2-Symmetric *N*-Heterocyclic Carbene Precursors and Metal Carbenoids. *J. Org. Chem.* **2011**, *76*, 7341−7351. (b) Albright, A.; Gawley, R. E. Application of a C_2-Symmetric Copper Carbenoid in the Enantioselective Hydrosilylation of Dialkyl and Aryl−Alkyl Ketones. *J. Am. Chem. Soc.* **2011**, *133*, 19680−19683.

(272) Maruoka, K.; Itoh, T.; Yamamoto, H. Methylaluminum Bis(2,6-di-tert-butyl-4-alkylphenoxide). A New Reagent for Obtaining Unusual Equatorial and Anti-Cram Selectivity in Carbonyl Alkylation. *J. Am. Chem. Soc.* **1985**, *107*, 4573−4576.

(273) Diesel, J.; Finogenova, A. M.; Cramer, N. Nickel-Catalyzed Enantioselective Pyridone C−H Functionalizations Enabled by a Bulky *N*-Heterocyclic Carbene Ligand. *J. Am. Chem. Soc.* **2018**, *140*, 4489−4493.

(274) Shen, D.; Zhang, W.-B.; Li, Z.; Shi, S.-L.; Xu, Y. Nickel/NHC−Catalyzed Enantioselective Cyclization of Pyridones and Pyrimidones with Tethered Alkenes. *Adv. Synth. Catal.* **2020**, *362*, 1125−1130.

(275) Zhang, W.-B.; Yang, X.-T.; Ma, J.-B.; Su, Z.-M.; Shi, S.-L. Regio- and Enantioselective C−H Cyclization of Pyridines with Alkenes Enabled by a Nickel/*N*-Heterocyclic Carbene Catalysis. *J. Am. Chem. Soc.* **2019**, *141*, 5628−5634.

(276) Diesel, J.; Grosheva, D.; Kodama, S.; Cramer, N. A Bulky Chiral N-Heterocyclic Carbene Nickel Catalyst Enables Enantioselective C−H Functionalizations of Indoles and Pyrroles. *Angew. Chem., Int. Ed.* **2019**, *58*, 11044−11048.

(277) Cai, Y.; Ye, X.; Liu, S.; Shi, S.-L. Nickel/NHC−Catalyzed Asymmetric C−H Alkylation of Fluoroarenes with Alkenes: Synthesis

of Enantioenriched Fluorotetralins. *Angew. Chem., Int. Ed.* **2019**, *58*, 13433−13437.
(278) Ahlin, J. S. E.; Cramer, N. Chiral *N*-Heterocyclic Carbene Ligand Enabled Nickel(0)-Catalyzed Enantioselective Three-Component Couplings as Direct Access to Silylated Indanols. *Org. Lett.* **2016**, *18*, 3242−3245.
(279) Ogata, K.; Atsuumi, Y.; Shimada, D.; Fukuzawa, S.-i. Nickel-Catalyzed Three-Component Coupling between Aryl Aldehydes, Norbornenes, and Silanes Leading to Indanols through Aromatic C−H Bond Activation of Aryl Aldehydes. *Angew. Chem., Int. Ed.* **2011**, *50*, 5896−5899.
(280) Seiders, T. J.; Ward, D. W.; Grubbs, R. H. Enantioselective Ruthenium-Catalyzed Ring-Closing Metathesis. *Org. Lett.* **2001**, *3*, 3225−3228.
(281) Yao, Q.-J.; Huang, F.-R.; Chen, J.-H.; Shi, B.-F. Nickel(II)/BINOL-Catalyzed Enantioselective C−H Activation *via* Desymmetrization and Kinetic Resolution. *Nat. Commun.* **2024**, *15*, 7135.
(282) (a) Omer, H. M.; Liu, P. Computational Study of Ni-Catalyzed C−H Functionalization: Factors that Control the Competition of Oxidative Addition and Radical Pathways. *J. Am. Chem. Soc.* **2017**, *139*, 9909−9920. (b) Haines, B. E.; Yu, J.-Q.; Musaev, D. G. The Mechanism of Directed Ni(II)-Catalyzed C−H Iodination with Molecular Iodine. *Chem. Sci.* **2018**, *9*, 1144−1154. (c) Beattie, D. D.; Grunwald, A. C.; Perse, T.; Schafer, L. L.; Love, J. A. Understanding Ni(II)-Mediated C(sp^3)−H Activation: Tertiary Ureas as Model Substrates. *J. Am. Chem. Soc.* **2018**, *140*, 12602−12610. (d) Roy, P.; Bour, J. R.; Kampf, J. W.; Sanford, M. S. Catalytically Relevant Intermediates in the Ni-Catalyzed C(sp^2)-H and C(sp^3)−H Functionalization of Aminoquinoline Substrates. *J. Am. Chem. Soc.* **2019**, *141*, 17382−17387.
(283) Chen, J.-H.; Yao, Q.-J.; Zhong, M.-Y.; Jiang, T.-Y.; Huang, F.-R.; Li, X.; Shi, B.-F. Nickel(II)/Salox-Catalyzed Enantioselective C−H Functionalization. *ACS Cent. Sci.* **2025**, *11*, 127−135.
(284) Zuo, Z.; Ahneman, D. T.; Chu, L.; Terrett, J. A.; Doyle, A. G.; MacMillan, D. W. C. Merging Photoredox with Nickel Catalysis: Coupling of α-Carboxyl sp^3-Carbons with Aryl Halides. *Science* **2014**, *345*, 437−440.
(285) (a) Capaldo, L.; Ravelli, D.; Fagnoni, M. Direct Photocatalyzed Hydrogen Atom Transfer (HAT) for Aliphatic C−H Bonds Elaboration. *Chem. Rev.* **2022**, *122*, 1875−1924. (b) Holmberg-Douglas, N.; Nicewicz, D. A. Photoredox-Catalyzed C−H Functionalization Reactions. *Chem. Rev.* **2022**, *122*, 1925−2016. (c) Golden, D. L.; Suh, S. E.; Stahl, S. S. Radical C(sp^3)−H Functionalization and Cross-Coupling Reactions. *Nat. Rev. Chem.* **2022**, *6*, 405−427. (d) Bellotti, P.; Huang, H.-M.; Faber, T.; Glorius, F. Photocatalytic Late-Stage C−H Functionalization. *Chem. Rev.* **2023**, *123*, 4237−4352.
(286) Cheng, X.; Lu, H.; Lu, Z. Enantioselective Benzylic C−H Arylation *via* Photoredox and Nickel Dual Catalysis. *Nat. Commun.* **2019**, *10*, 3549.
(287) Heitz, D. R.; Tellis, J. C.; Molander, G. A. Photochemical Nickel-Catalyzed C−H Arylation: Synthetic Scope and Mechanistic Investigations. *J. Am. Chem. Soc.* **2016**, *138*, 12715−12718.
(288) (a) Shaw, M. H.; Shurtleff, V. W.; Terrett, J. A.; Cuthbertson, J. D.; MacMillan, D. W. C. Native Functionality in Triple Catalytic Cross-Coupling: sp^3 C−H Bonds as Latent Nucleophiles. *Science* **2016**, *352*, 1304−1308. (b) Shields, B. J.; Doyle, A. G. Direct C(sp^3)−H Cross Coupling Enabled by Catalytic Generation of Chlorine Radicals. *J. Am. Chem. Soc.* **2016**, *138*, 12719−12722. (c) Zhang, H.-H.; Zhao, J.-J.; Yu, S. Enantioselective Allylic Alkylation with 4-Alkyl-1,4-dihydropyridines Enabled by Photoredox/Palladium Cocatalysis. *J. Am. Chem. Soc.* **2018**, *140*, 16914−16919. (d) Shen, Y.; Gu, Y.; Martin, R. sp^3 C−H Arylation and Alkylation Enabled by the Synergy of Triplet Excited Ketones and Nickel Catalysts. *J. Am. Chem. Soc.* **2018**, *140*, 12200−12209.
(289) Zhang, W.; Shu, X.; Huan, L.; Cheng, B.; Huo, H. Enantioselective β-C(sp^3)−H Arylation of Amides *via* Synergistic Nickel and Photoredox Catalysis. *Org. Biomol. Chem.* **2021**, *19*, 9407−9409.
(290) Shu, X.; Zhong, D.; Lin, Y.; Qin, X.; Huo, H. Modular Access to Chiral α-(Hetero)aryl Amines *via* Ni/Photoredox-Catalyzed Enantioselective Cross-Coupling. *J. Am. Chem. Soc.* **2022**, *144*, 8797−8806.
(291) Xu, S.; Ping, Y.; Li, W.; Guo, H.; Su, Y.; Li, Z.; Wang, M.; Kong, W. Enantioselective C(sp^3)−H Functionalization of Oxacycles *via* Photo-HAT/Nickel Dual Catalysis. *J. Am. Chem. Soc.* **2023**, *145*, 5231−5241.
(292) Shu, X.; Huan, L.; Huang, Q.; Huo, H. Direct Enantioselective C(sp^3)−H Acylation for the Synthesis of α-Amino Ketones. *J. Am. Chem. Soc.* **2020**, *142*, 19058−19064.
(293) (a) Zhang, P.; Le, C. C.; MacMillan, D. W. C. Silyl Radical Activation of Alkyl Halides in Metallaphotoredox Catalysis: A Unique Pathway for Cross-Electrophile Coupling. *J. Am. Chem. Soc.* **2016**, *138*, 8084−8087. (b) Kawasaki, T.; Ishida, N.; Murakami, M. Dehydrogenative Coupling of Benzylic and Aldehydic C−H Bonds. *J. Am. Chem. Soc.* **2020**, *142*, 3366−3370. (c) Kawasaki, T.; Ishida, N.; Murakami, M. Photoinduced Specific Acylation of Phenolic Hydroxy Groups with Aldehydes. *Angew. Chem., Int. Ed.* **2020**, *59*, 18267−18271.
(294) Liu, R.; Lv, K.; Bao, X. Mechanistic Insights into Enantioselective C(sp^3)−H Acylation to Construct α-Amino Ketones *via* Photoredox and Ni(II) Dual Catalysis: A DFT Study. *Chem. - Asian J.* **2023**, *18*, No. e202201266.
(295) Huan, L.; Shu, X.; Zu, W.; Zhong, D.; Huo, H. Asymmetric Benzylic C(sp^3)−H Acylation *via* Dual Nickel and Photoredox Catalysis. *Nat. Commun.* **2021**, *12*, 3536.
(296) Shu, X.; Zhong, D.; Huang, Q.; Huan, L.; Huo, H. Site- and Enantioselective Cross-Coupling of Saturated *N*-Heterocycles with Carboxylic Acids by Cooperative Ni/Photoredox Catalysis. *Nat. Commun.* **2023**, *14*, 125.
(297) Li, C.; Cheng, J.; Wan, X.; Li, J.; Zu, W.; Xu, Y.; Huang, Y.; Huo, H. Ni/Photoredox-Catalyzed Enantioselective Acylation of α-Bromobenzoates with Aldehydes: A Formal Approach to Aldehyde-Aldehyde Cross-Coupling. *J. Am. Chem. Soc.* **2024**, *146*, 19909−19918.
(298) Li, T.; Xu, Z.; Huang, Y.; Zu, W.; Huo, H. Enantioselective Alkyl−Acyl Radical Cross-Coupling Enabled by Metallaphotoredox Catalysis. *J. Am. Chem. Soc.* **2025**, *147*, 10999−11009.
(299) Cheng, X.; Li, T.; Liu, Y.; Lu, Z. Stereo- and Enantioselective Benzylic C−H Alkenylation *via* Photoredox/Nickel Dual Catalysis. *ACS Catal.* **2021**, *11*, 11059−11065.
(300) Xu, J.; Li, Z.; Xu, Y.; Shu, X.; Huo, H. Stereodivergent Synthesis of Both *Z*- and *E*-Alkenes by Photoinduced, Ni-Catalyzed Enantioselective C(sp^3)−H Alkenylation. *ACS Catal.* **2021**, *11*, 13567−13574.
(301) (a) Le, C.; Liang, Y.; Evans, R. W.; Li, X.; MacMillan, D. W. C. Selective sp^3 C−H Alkylation *via* Polarity-Match-Based Cross-Coupling. *Nature* **2017**, *547*, 79−83. (b) Vasilopoulos, A.; Krska, S. W.; Stahl, S. S. C(sp^3)−H Methylation Enabled by Peroxide Photosensitization and Ni-Mediated Radical Coupling. *Science* **2021**, *372*, 398−403. (c) Mao, E.; MacMillan, D. W. C. Late-Stage C(sp^3)−H Methylation of Drug Molecules. *J. Am. Chem. Soc.* **2023**, *145*, 2787−2793.
(302) Li, J.; Cheng, B.; Shu, X.; Xu, Z.; Li, C.; Huo, H. Enantioselective Alkylation of α-Amino C(sp^3)−H Bonds *via* Photoredox and Nickel Catalysis. *Nat. Catal.* **2024**, *7*, 889−899.
(303) Shi, J.-L.; Wang, Y.; Han, Y.; Chen, J.; Pu, X.; Xia, Y. Hydroalkylation of Unactivated Olefins with C(sp^3)−H Compounds Enabled by NiH-Catalyzed Radical Relay. *Sci. Adv.* **2024**, *10*, No. eads6885.
(304) Tao, Y.; Ma, W.; Sun, R.; Huang, C.; Lu, Q. Asymmetric Paired Electrolysis: Enantioselective Alkylation of Sulfonylimines *via* C(sp^3)−H Functionalization. *Angew. Chem., Int. Ed.* **2024**, *63*, No. e202409222.
(305) Zhou, Z.; Ke, Y.; Miao, R.; Hu, F.; Wang, X.; Ping, Y.; Xu, S.; Kong, W. Direct Stereoselective C(sp^3)−H Alkylation of Saturated Heterocycles Using Olefins. *Nat. Chem.* **2025**, *17*, 344−355.
(306) (a) Bera, S.; Hu, X. Nickel-Catalyzed Regioselective Hydroalkylation and Hydroarylation of Alkenyl Boronic Esters. *Angew. Chem., Int. Ed.* **2019**, *58*, 13854−13859. (b) Zhang, Y.; Han, B.; Zhu, S. Rapid Access to Highly Functionalized Alkyl Boronates by NiH-Catalyzed Remote Hydroarylation of Boron-Containing Alkenes. *Angew. Chem., Int. Ed.* **2019**, *58*, 13860−13864. (c) Bera, S.; Mao, R.; Hu, X.

https://doi.org/10.1021/acs.chemrev.6c00255
Chem. Rev. XXXX, XXX, XXX−XXX

Enantioselective C(sp^3)−C(sp^3) Cross-Coupling of Non-Activated Alkyl Electrophiles *via* Nickel Hydride Catalysis. *Nat. Chem.* **2021**, *13*, 270−277.
(307) (a) DiMucci, I. M.; Lukens, J. T.; Chatterjee, S.; Carsch, K. M.; Titus, C. J.; Lee, S. J.; Nordlund, D.; Betley, T. A.; MacMillan, S. N.; Lancaster, K. M. The myth of d^8 Copper(III). *J. Am. Chem. Soc.* **2019**, *141*, 18508−18520. (b) Weingarten, A. Copper Comeuppance. *Nat. Rev. Chem.* **2020**, *4*, 3.
(308) Krause, N. *Modern Organocopper Chemistry*; Wiley-VCH: Weinheim, Germany, 2002.
(309) Ullmann, F.; Bielecki, J. Ueber Synthesen in der Biphenylreihe. *Ber. Dtsch. Chem. Ges.* **1901**, *34*, 2174−2185.
(310) Goldberg, I. Ueber Phenylirungen bei Gegenwart von Kupfer als Katalysator. *Ber. Dtsch. Chem. Ges.* **1906**, *39*, 1691−1692.
(311) (a) Fanta, P. E. The Ullmann Synthesis of Biaryls, 1945−1963. *Chem. Rev.* **1964**, *64*, 613−632. (b) Hassan, J.; Sévignon, M.; Gozzi, C.; Schulz, E.; Lemaire, M. Aryl−Aryl Bond Formation One Century after the Discovery of the Ullmann Reaction. *Chem. Rev.* **2002**, *102*, 1359−1470. (c) Reymond, S.; Cossy, J. Copper-Catalyzed Diels−Alder Reactions. *Chem. Rev.* **2008**, *108*, 5359−5406. (d) Punniyamurthy, T.; Rout, L. Recent Advances in Copper-Catalyzed Oxidation of Organic Compounds. *Coord. Chem. Rev.* **2008**, *252*, 134−154. (e) Yoshikai, N.; Nakamura, E. Mechanisms of Nucleophilic Organocopper(I) Reactions. *Chem. Rev.* **2012**, *112*, 2339−2372. (f) Zhang, C.; Tang, C.; Jiao, N. Recent Advances in Copper-Catalyzed Dehydrogenative Functionalization *via* a Single Electron Transfer (SET) Process. *Chem. Soc. Rev.* **2012**, *41*, 3464−3484. (g) Allen, S. E.; Walvoord, R. R.; Padilla-Salinas, R.; Kozlowski, M. C. Aerobic Copper-Catalyzed Organic Reactions. *Chem. Rev.* **2013**, *113*, 6234−6458. (h) Sambiagio, C.; Marsden, S. P.; Blacker, A. J.; McGowan, P. C. Copper Catalysed Ullmann Type Chemistry: from Mechanistic Aspects to Modern Development. *Chem. Soc. Rev.* **2014**, *43*, 3525−3550. (i) Ryland, B. L.; Stahl, S. S. Practical Aerobic Oxidations of Alcohols and Amines with Homogeneous Copper/TEMPO and Related Catalyst Systems. *Angew. Chem., Int. Ed.* **2014**, *53*, 8824−8838. (j) McCann, S. D.; Stahl, S. S. Copper-Catalyzed Aerobic Oxidations of Organic Molecules: Pathways for Two-Electron Oxidation with a Four-Electron Oxidant and a One-Electron Redox-Active Catalyst. *Acc. Chem. Res.* **2015**, *48*, 1756−1766. (k) Evano, G.; Blanchard, N. *Copper-Mediated Cross-Coupling Reactions*. Wiley: Hoboken, United States, 2014. (l) Zhu, X.; Chiba, S. Copper-Catalyzed Oxidative Carbon−Heteroatom Bond Formation: A Recent Update. *Chem. Soc. Rev.* **2016**, *45*, 4504−4523. (m) Pirnot, M. T.; Wang, Y.-M.; Buchwald, S. L. Copper Hydride Catalyzed Hydroamination of Alkenes and Alkynes. *Angew. Chem., Int. Ed.* **2016**, *55*, 48−57.
(312) (a) Johnson, J. S.; Evans, D. A. Chiral Bis(oxazoline) Copper(II) Complexes: Versatile Catalysts for Enantioselective Cycloaddition, Aldol, Michael, and Carbonyl Ene Reactions. *Acc. Chem. Res.* **2000**, *33*, 325−335. (b) Desimoni, G.; Faita, G.; Jørgensen, K. A. C_2-Symmetric Chiral Bis(Oxazoline) Ligands in Asymmetric Catalysis. *Chem. Rev.* **2006**, *106*, 3561−3651. (c) Alexakis, A.; Bäckvall, J. E.; Krause, N.; Pàmies, O.; Diéguez, M. Enantioselective Copper-Catalyzed Conjugate Addition and Allylic Substitution Reactions. *Chem. Rev.* **2008**, *108*, 2796−2823. (d) Yamada, K.-i.; Tomioka, K. Copper-Catalyzed Asymmetric Alkylation of Imines with Dialkylzinc and Related Reactions. *Chem. Rev.* **2008**, *108*, 2874−2886. (e) Stanley, L. M.; Sibi, M. P. Enantioselective Copper-Catalyzed 1,3-Dipolar Cycloadditions. *Chem. Rev.* **2008**, *108*, 2887−2902. (f) Poulsen, T. B.; Jørgensen, K. A. Catalytic Asymmetric Friedel−Crafts Alkylation Reactions—Copper Showed the Way. *Chem. Rev.* **2008**, *108*, 2903−2915. (g) Jerphagnon, T.; Pizzuti, M. G.; Minnaard, A. J.; Feringa, B. L. Recent Advances in Enantioselective Copper-Catalyzed 1,4-Addition. *Chem. Soc. Rev.* **2009**, *38*, 1039−1075. (h) Alexakis, A.; Krause, N.; Woodward, S. *Copper-Catalyzed Asymmetric Synthesis*; Wiley-VCH: Weinheim, Germany, 2014. (i) Liu, R. Y.; Buchwald, S. L. CuH-Catalyzed Olefin Functionalization: From Hydroamination to Carbonyl Addition. *Acc. Chem. Res.* **2020**, *53*, 1229−1243.
(313) (a) Hossain, A.; Bhattacharyya, A.; Reiser, O. Copper's Rapid Ascent in Visible-Light Photoredox Catalysis. *Science* **2019**, *364*, No. eaav9713. (b) Gu, Q.-S.; Li, Z.-L.; Liu, X.-Y. Copper(I)-Catalyzed Asymmetric Reactions Involving Radicals. *Acc. Chem. Res.* **2020**, *53*, 170−181. (c) Li, Z.-L.; Fang, G.-C.; Gu, Q.-S.; Liu, X.-Y. Recent Advances in Copper-Catalysed Radical-Involved Asymmetric 1,2-Difunctionalization of Alkenes. *Chem. Soc. Rev.* **2020**, *49*, 32−48. (d) Song, L.; Cai, L.; Gong, L.; Van der Eycken, E. V. Photoinduced Copper-Catalyzed Enantioselective Coupling Reactions. *Chem. Soc. Rev.* **2023**, *52*, 2358−2376.
(314) (a) Kirmse, W. Copper Carbene Complexes: Advanced Catalysts, New Insights. *Angew. Chem., Int. Ed.* **2003**, *42*, 1088−1093. (b) Davies, H. M. L.; Hedley, S. J. Intermolecular Reactions of Electron-Rich Heterocycles with Copper and Rhodium Carbenoids. *Chem. Soc. Rev.* **2007**, *36*, 1109−1119. (c) Zhu, S.-F.; Zhou, Q.-L. Transition-Metal-Catalyzed Enantioselective Heteroatom−Hydrogen Bond Insertion Reactions. *Acc. Chem. Res.* **2012**, *45*, 1365−1377. (d) Gillingham, D.; Fei, N. Catalytic X−H Insertion Reactions Based on Carbenoids. *Chem. Soc. Rev.* **2013**, *42*, 4918−4931.
(315) (a) Wang, F.; Chen, P.; Liu, G. Copper-Catalyzed Radical Relay for Asymmetric Radical Transformations. *Acc. Chem. Res.* **2018**, *51*, 2036−2046. (b) Zhang, Z.; Chen, P.; Liu, G. Copper-Catalyzed Radical Relay in C(sp^3)−H Functionalization. *Chem. Soc. Rev.* **2022**, *51*, 1640−1658. (c) Wang, F.; Chen, P.; Liu, G. Copper-Catalysed Asymmetric Radical Cyanation. *Nat. Synth.* **2022**, *1*, 107−116.
(316) Beig, N.; Goyal, V.; Bansal, R. K. Application of *N*-Heterocyclic Carbene-Cu(I) Complexes as Catalysts in Organic Synthesis: A Review. *Beilstein J. Org. Chem.* **2023**, *19*, 1408−1442.
(317) (a) Makida, Y.; Ohmiya, H.; Sawamura, M. Regio- and Stereocontrolled Introduction of Secondary Alkyl Groups to Electron-Deficient Arenes through Copper-Catalyzed Allylic Alkylation. *Angew. Chem., Int. Ed.* **2012**, *51*, 4122−4127. (b) Makida, Y.; Takayama, Y.; Ohmiya, H.; Sawamura, M. Copper-Catalyzed γ-Selective and Stereospecific Direct Allylic Alkylation of Terminal Alkynes: Synthesis of Skipped Enynes. *Angew. Chem., Int. Ed.* **2013**, *52*, 5350−5354. (c) Harada, A.; Makida, Y.; Sato, T.; Ohmiya, H.; Sawamura, M. Copper-Catalyzed Enantioselective Allylic Alkylation of Terminal Alkyne Pronucleophiles. *J. Am. Chem. Soc.* **2014**, *136*, 13932−13939.
(318) Ohmiya, H.; Zhang, H.; Shibata, S.; Harada, A.; Sawamura, M. Construction of Quaternary Stereogenic Carbon Centers through Copper-Catalyzed Enantioselective Allylic Alkylation of Azoles. *Angew. Chem., Int. Ed.* **2016**, *55*, 4777−4780.
(319) (a) Shang, M.; Sun, S.-Z.; Dai, H.-X.; Yu, J.-Q. Cu(II)-Mediated C−H Amidation and Amination of Arenes: Exceptional Compatibility with Heterocycles. *J. Am. Chem. Soc.* **2014**, *136*, 3354−3357. (b) Shang, M.; Wang, H.-L.; Sun, S.-Z.; Dai, H.-X.; Yu, J.-Q. Cu(II)-Mediated *ortho* C−H Alkynylation of (Hetero)Arenes with Terminal Alkynes. *J. Am. Chem. Soc.* **2014**, *136*, 11590−11593. (c) Shang, M.; Sun, S.-Z.; Wang, H.-L.; Laforteza, B. N.; Dai, H.-X.; Yu, J.-Q. Exceedingly Fast Copper(II)-Promoted *ortho* C−H Trifluoromethylation of Arenes using $TMSCF_3$. *Angew. Chem., Int. Ed.* **2014**, *53*, 10439−10442.
(320) Chen, X.; Hao, X.-S.; Goodhue, C. E.; Yu, J.-Q. Cu(II)-Catalyzed Functionalizations of Aryl C−H Bonds Using O_2 as an Oxidant. *J. Am. Chem. Soc.* **2006**, *128*, 6790−6791.
(321) (a) Phipps, R. J.; Grimster, N. P.; Gaunt, M. J. Cu(II)-Catalyzed Direct and Site-Selective Arylation of Indoles Under Mild Conditions. *J. Am. Chem. Soc.* **2008**, *130*, 8172−8174. (b) Phipps, R. J.; Gaunt, M. J. A *Meta*-Selective Copper-Catalyzed C−H Bond Arylation. *Science* **2009**, *323*, 1593−1597.
(322) Xu, L.-P.; Haines, B. E.; Ajitha, M. J.; Yu, J.-Q.; Musaev, D. G. Unified Mechanistic Concept of the Copper-Catalyzed and Amide-Oxazoline-Directed C(sp^2)-H Bond Functionalization. *ACS Catal.* **2021**, *11*, 12620−12631.
(323) Kong, W.-J.; Shao, Q.; Li, M.-H.; Zhou, Z.-L.; Xu, H.; Dai, H.-X.; Yu, J.-Q. Copper-Mediated Diastereoselective C−H Thiolation of Ferrocenes. *Organometallics* **2018**, *37*, 2832−2836.
(324) Kuang, X.; Li, J.-J.; Liu, T.; Ding, C.-H.; Wu, K.; Wang, P.; Yu, J.-Q. Cu-Mediated Enantioselective C−H Alkynylation of Ferrocenes with Chiral BINOL Ligands. *Nat. Commun.* **2023**, *14*, 7698.
(325) Suess, A. M.; Ertem, M. Z.; Cramer, C. J.; Stahl, S. S. Divergence Between Organometallic and Single-Electron-Transfer Mechanisms in

Copper(II)-Mediated Aerobic C−H Oxidation. *J. Am. Chem. Soc.* **2013**, *135*, 9797−9804.
(326) Zhang, Z.-Z.; Zhou, G.; Yue, Q.; Yao, Q.-J.; Shi, B.-F. Copper/BINOL-Catalyzed Enantioselective C−H Functionalization toward Planar Chiral Ferrocenes Under Mild Conditions. *ACS Catal.* **2024**, *14*, 4030−4039.
(327) Ma, J.-Y.; Yao, Q.-J.; Jiang, L.-C.; Huang, F.-R.; Yue, Q.; Shi, B.-F. Copper-Mediated Enantioselective C−H Thiolation of Ferrocenes Enabled by the BINOL Ligand. *J. Am. Chem. Soc.* **2025**, *147*, 7061−7069.
(328) (a) Kharasch, M. S.; Sosnovsky, G. The Reactions of *t*-Butyl Perbenzoate and Olefins-a Stereospecific Reaction. *J. Am. Chem. Soc.* **1958**, *80*, 756. (b) Kharasch, M. S.; Fono, A. Radical Substitution Reactions. *J. Org. Chem.* **1958**, *23*, 325−326.
(329) (a) Rawlinson, D. J.; Sosnovsky, G. One-Step Substitutive Acyloxylation at Carbon. Part I. Reactions Involving Peroxides. *Synthesis* **1972**, *1972*, 1−28. (b) Eames, J.; Watkinson, M. Catalytic Allylic Oxidation of Alkenes Using an Asymmetric Kharasch−Sosnovsky Reaction. *Angew. Chem., Int. Ed.* **2001**, *40*, 3567−3571. (c) Andrus, M. B.; Lashley, J. C. Copper Catalyzed Allylic Oxidation with Peresters. *Tetrahedron* **2002**, *58*, 845−866. (d) Bayeh, L.; Tambar, U. K. Catalytic Asymmetric Intermolecular Allylic Functionalization of Unactivated Internal Alkenes. *ACS Catal.* **2017**, *7*, 8533−8543. (e) Samadi, S.; Arvinnezhad, H.; Nazari, S.; Majidian, S. Enantioselective Allylic C−H Bond Oxidation of Olefins Using Copper Complexes of Chiral Oxazoline Based Ligands. *Top. Curr. Chem.* **2022**, *380*, 20.
(330) (a) Andrus, M. B.; Zhou, Z. Highly Enantioselective Copper-Bisoxazoline-Catalyzed Allylic Oxidation of Cyclic Olefins with *tert*-Butyl *p*-Nitroperbenzoate. *J. Am. Chem. Soc.* **2002**, *124*, 8806−8807. (b) Ginotra, S. K.; Singh, V. K. Enantioselective Oxidation of Olefins Catalyzed by Chiral Copper Bis(oxazolinyl)pyridine Complexes: A Reassessment. *Tetrahedron* **2006**, *62*, 3573−3581. (c) Hoang, V. D. M.; Reddy, P. A. N.; Kim, T.-J. Asymmetric Allylic Oxidation Catalyzed by Copper(I) Complexes of Chiral (Iminophosphoranyl)ferrocenes. *Organometallics* **2008**, *27*, 1026−1027. (d) Tan, Q.; Hayashi, M. Asymmetric Desymmetrization of 4,5-Epoxycyclohex-1-ene by Enantioselective Allylic Oxidation. *Org. Lett.* **2009**, *11*, 3314−3317. (e) Samadi, S.; Arvinnezhad, H.; Mansoori, S.; Parsa, H. Preparation and DFT Studies of Chiral Cu(I)-Complexes of Biphenyl Bisoxazolines and Their Application in Enantioselective Kharasch−Sosnovsky Reaction. *Sci. Rep.* **2022**, *12*, 15038.
(331) (a) Andrus, M. B.; Argade, A. B.; Chen, X.; Pamment, M. G. The Asymmetric Kharasch Reaction. Catalytic Enantioselective Allylic Acyloxylation of Olefins with Chiral Copper(I) Complexes and *tert*-Butyl Perbenzoate. *Tetrahedron Lett.* **1995**, *36*, 2945−2948. (b) Zhang, B.; Zhu, S.-F.; Zhou, Q.-L. Copper-Catalyzed Enantioselective Allylic Oxidation of Acyclic Olefins. *Tetrahedron Lett.* **2013**, *54*, 2665−2668.
(332) Zhang, W.; Wang, F.; McCann, S. D.; Wang, D.; Chen, P.; Stahl, S. S.; Liu, G. Enantioselective Cyanation of Benzylic C−H Bonds *via* Copper-Catalyzed Radical Relay. *Science* **2016**, *353*, 1014−1018.
(333) Li, J.; Zhang, Z.; Wu, L.; Zhang, W.; Chen, P.; Lin, Z.; Liu, G. Site-Specific Allylic C−H Bond Functionalization with a Copper-Bound *N*-Centred Radical. *Nature* **2019**, *574*, 516−521.
(334) (a) Mandal, M.; Buss, J. A.; Chen, S.-J.; Cramer, C. J.; Stahl, S. S. Mechanistic Insights into Radical Formation and Functionalization in Copper/*N*-Fluorobenzenesulfonimide Radical-Relay Reactions. *Chem. Sci.* **2024**, *15*, 1364−1373. (b) Li, J.; Yang, T.; Chen, P.; Shiri, F.; Guan, H.; Lin, Z.; Liu, G. Mechanistic Insights into Copper-Catalyzed Asymmetric Cyanation of Allylic C−H Bonds. *J. Am. Chem. Soc.* **2025**, *147*, 14756−14768.
(335) Lu, R.; Yang, T.; Chen, X.; Fan, W.; Chen, P.; Lin, Z.; Liu, G. Enantioselective Copper-Catalyzed Radical Cyanation of Propargylic C−H Bonds: Easy Access to Chiral Allenyl Nitriles. *J. Am. Chem. Soc.* **2021**, *143*, 14451−14457.
(336) Zhang, Z.; Zhang, X.; Nagib, D. A. Chiral Piperidines from Acyclic Amines *via* Enantioselective, Radical-Mediated δ C−H Cyanation. *Chem.* **2019**, *5*, 3127−3134.
(337) Wang, C.-Y.; Qin, Z.-Y.; Huang, Y.-L.; Jin, R.-X.; Lan, Q.; Wang, X.-S. Enantioselective Copper-Catalyzed Cyanation of Remote C-(sp^3)−H Bonds Enabled by 1,5-Hydrogen Atom Transfer. *iScience* **2019**, *21*, 490−498.
(338) Wang, D.; Zhu, N.; Chen, P.; Lin, Z.; Liu, G. Enantioselective Decarboxylative Cyanation Employing Cooperative Photoredox Catalysis and Copper Catalysis. *J. Am. Chem. Soc.* **2017**, *139*, 15632−15635.
(339) Cheng, Z.; Chen, P.; Liu, G. Enantioselective Cyanation of Remote C−H Bonds *via* Cooperative Photoredox and Copper Catalysis. *Acta Chim. Sinica* **2019**, *77*, 856−860.
(340) Bao, X.; Wang, Q.; Zhu, J. Dual Photoredox/Copper Catalysis for the Remote C(sp^3)−H Functionalization of Alcohols and Alkyl Halides by *N*-Alkoxypyridinium Salts. *Angew. Chem., Int. Ed.* **2019**, *58*, 2139−2143.
(341) Chen, H.; Jin, W.; Yu, S. Enantioselective Remote C(sp^3)−H Cyanation *via* Dual Photoredox and Copper Catalysis. *Org. Lett.* **2020**, *22*, 5910−5914.
(342) Deng, Y.; Lu, R.; Chen, P.; Liu, G. Enantioselective Cyanation of Propargylic C−H Bonds *via* Cooperative Photoredox and Copper Catalysis. *Chem. Commun.* **2023**, *59*, 4656−4659.
(343) (a) Fu, N.; Song, L.; Liu, J.; Shen, Y.; Siu, J. C.; Lin, S. New Bisoxazoline Ligands Enable Enantioselective Electrocatalytic Cyanofunctionalization of Vinylarenes. *J. Am. Chem. Soc.* **2019**, *141*, 14480−14485. (b) Song, L.; Fu, N.; Ernst, B. G.; Lee, W. H.; Frederick, M. O.; DiStasio, R. A., Jr.; Lin, S. Dual Electrocatalysis Enables Enantioselective Hydrocyanation of Conjugated Alkenes. *Nat. Chem.* **2020**, *12*, 747−754.
(344) Cai, C.-Y.; Lai, X.-L.; Wang, Y.; Hu, H.-H.; Song, J.; Yang, Y.; Wang, C.; Xu, H.-C. Photoelectrochemical Asymmetric Catalysis Enables Site- and Enantioselective Cyanation of Benzylic C−H Bonds. *Nat. Catal.* **2022**, *5*, 943−951.
(345) (a) Wagner, P. J.; Truman, R. J.; Puchalski, A. E.; Wake, R. Extent of Charge Transfer in the Photoreduction of Phenyl Ketones by Alkylbenzenes. *J. Am. Chem. Soc.* **1986**, *108*, 7727−7738. (b) Grampp, G.; Galán, M.; Sacher, M. Kinetics of Photoinduced Electron Transfer Reactions of Some Anthraquinone Radical Anions with Various Inorganic Ions: Comparison with Marcus Cross-Relation. *Ber. Bunsenges. Phys. Chem.* **1995**, *99*, 111−117. (c) Rathore, R.; Hubig, S. M.; Kochi, J. K. Direct Observation and Structural Characterization of the Encounter Complex in Bimolecular Electron Transfers with Photoactivated Acceptors. *J. Am. Chem. Soc.* **1997**, *119*, 11468−11480.
(346) Fan, W.; Zhao, X.; Deng, Y.; Chen, P.; Wang, F.; Liu, G. Electrophotocatalytic Decoupled Radical Relay Enables Highly Efficient and Enantioselective Benzylic C−H Functionalization. *J. Am. Chem. Soc.* **2022**, *144*, 21674−21682.
(347) (a) Vasilopoulos, A.; Zultanski, S. L.; Stahl, S. S. Feedstocks to Pharmacophores: Cu-Catalyzed Oxidative Arylation of Inexpensive Alkylarenes Enabling Direct Access to Diarylalkanes. *J. Am. Chem. Soc.* **2017**, *139*, 7705−7708. (b) Zhang, W.; Chen, P.; Liu, G. Copper-Catalyzed Arylation of Benzylic C−H Bonds with Alkylarenes as the Limiting Reagents. *J. Am. Chem. Soc.* **2017**, *139*, 7709−7712.
(348) Wu, L.; Wang, F.; Wan, X.; Wang, D.; Chen, P.; Liu, G. Asymmetric Cu-Catalyzed Intermolecular Trifluoromethylarylation of Styrenes: Enantioselective Arylation of Benzylic Radicals. *J. Am. Chem. Soc.* **2017**, *139*, 2904−2907.
(349) Zhang, W.; Wu, L.; Chen, P.; Liu, G. Enantioselective Arylation of Benzylic C−H Bonds by Copper-Catalyzed Radical Relay. *Angew. Chem., Int. Ed.* **2019**, *58*, 6425−6429.
(350) Liao, S.; Sun, X.-L.; Tang, Y. Sidearm Strategy for Catalyst Design Based on Bisoxazolines in the Remote Control of Enantioselection and Related. *Acc. Chem. Res.* **2014**, *47*, 2260−2272.
(351) Zhang, Z.; Stateman, L. M.; Nagib, D. A. δ C−H (Hetero)-arylation *via* Cu-Catalyzed Radical Relay. *Chem. Sci.* **2019**, *10*, 1207−1211.
(352) Sakurai, S.; Matsumoto, A.; Kano, T.; Maruoka, K. Cu-Catalyzed Enantioselective Alkylarylation of Vinylarenes Enabled by Chiral Binaphthyl-BOX Hybrid Ligands. *J. Am. Chem. Soc.* **2020**, *142*, 19017−19022.

(353) Li, C.-J. Cross-Dehydrogenative Coupling (CDC): Exploring C−C Bond Formations Beyond Functional Group Transformations. *Acc. Chem. Res.* **2009**, *42*, 335−344.
(354) (a) Li, Z.; Li, C.-J. Catalytic Enantioselective Alkynylation of Prochiral sp^3 C−H Bonds Adjacent to a Nitrogen Atom. *Org. Lett.* **2004**, *6*, 4997−4999. (b) Li, Z.; Macleod, P. D.; Li, C.-J. Studies on Cu-Catalyzed Asymmetric Alkynylation of Tetrahydroisoquinoline Derivatives. *Tetrahedron: Asymmetry* **2006**, *17*, 590−597. (c) Lin, W.; Cao, T.; Fan, W.; Han, Y.; Kuang, J.; Luo, H.; Miao, B.; Tang, X.; Yu, Q.; Yuan, W.; Zhang, J.; Zhu, C.; Ma, S. Enantioselective Double Manipulation of Tetrahydroisoquinolines with Terminal Alkynes and Aldehydes under Copper(I) Catalysis. *Angew. Chem., Int. Ed.* **2014**, *53*, 277−281. (d) Huang, T.; Liu, X.; Lang, J.; Xu, J.; Lin, L.; Feng, X. Asymmetric Aerobic Oxidative Cross-Coupling of Tetrahydroisoquinolines with Alkynes. *ACS Catal.* **2017**, *7*, 5654−5660. (e) Gao, P.-S.; Weng, X.-J.; Wang, Z.-H.; Zheng, C.; Sun, B.; Chen, Z.-H.; You, S.-L.; Mei, T.-S. Cu^{II}/TEMPO-Catalyzed Enantioselective C(sp^3)−H Alkynylation of Tertiary Cyclic Amines through Shono-Type Oxidation. *Angew. Chem., Int. Ed.* **2020**, *59*, 15254−15259. (f) Chan, J. Z.; Yesilcimen, A.; Cao, M.; Zhang, Y.; Zhang, B.; Wasa, M. Direct Conversion of *N*-Alkylamines to *N*-Propargylamines through C−H Activation Promoted by Lewis Acid/Organocopper Catalysis: Application to Late-Stage Functionalization of Bioactive Molecules. *J. Am. Chem. Soc.* **2020**, *142*, 16493−16505.
(355) (a) Li, X.-T.; Gu, Q.-S.; Dong, X.-Y.; Meng, X.; Liu, X.-Y. A Copper Catalyst with a Cinchona-Alkaloid-Based Sulfonamide Ligand for Asymmetric Radical Oxytrifluoromethylation of Alkenyl Oximes. *Angew. Chem., Int. Ed.* **2018**, *57*, 7668−7672. (b) Dong, X.-Y.; Zhang, Y.-F.; Ma, C.-L.; Gu, Q.-S.; Wang, F.-L.; Li, Z.-L.; Jiang, S.-P.; Liu, X.-Y. A General Asymmetric Copper-Catalysed Sonogashira C(sp^3)-C(sp) Coupling. *Nat. Chem.* **2019**, *11*, 1158−1166.
(356) Zhang, Z.-H.; Dong, X.-Y.; Du, X.-Y.; Gu, Q.-S.; Li, Z.-L.; Liu, X.-Y. Copper-Catalyzed Enantioselective Sonogashira-Type Oxidative Cross-Coupling of Unactivated C(sp^3)−H Bonds with Alkynes. *Nat. Commun.* **2019**, *10*, 5689.
(357) Wang, C.-Y.; Qin, Z.-Y.; Huang, Y.-L.; Hou, Y.-M.; Jin, R.-X.; Li, C.; Wang, X.-S. Enantioselective Copper-Catalyzed Remote C(sp^3)−H Alkynylation of Linear Primary Sulfonamides. *Org. Lett.* **2020**, *22*, 4006−4009.
(358) Guo, R.; Xiao, H.; Li, S.; Luo, Y.; Bai, J.; Zhang, M.; Guo, Y.; Qi, X.; Zhang, G. Photoinduced Copper-Catalyzed Asymmetric C(sp^3)−H Alkynylation of Cyclic Amines by Intramolecular 1,5-Hydrogen Atom Transfer. *Angew. Chem., Int. Ed.* **2022**, *61*, No. e202208232.
(359) (a) Zhang, Y.; Sun, Y.; Chen, B.; Xu, M.; Li, C.; Zhang, D.; Zhang, G. Copper-Catalyzed Photoinduced Enantioselective Dual Carbofunctionalization of Alkenes. *Org. Lett.* **2020**, *22*, 1490−1494. (b) Cao, Z.; Li, J.; Sun, Y.; Zhang, H.; Mo, X.; Cao, X.; Zhang, G. Photo-Induced Copper-Catalyzed Alkynylation and Amination of Remote Unactivated C(sp^3)−H Bonds. *Chem. Sci.* **2021**, *12*, 4836−4840. (c) Yam, V. W.-W.; Lo, K. K.-W.; Wong, K. M.-C. Luminescent Polynuclear Metal Acetylides. *J. Organomet. Chem.* **1999**, *578*, 3−30.
(360) Fu, L.; Zhou, S.; Wan, X.; Chen, P.; Liu, G. Enantioselective Trifluoromethylalkynylation of Alkenes *via* Copper-Catalyzed Radical Relay. *J. Am. Chem. Soc.* **2018**, *140*, 10965−10969.
(361) Fu, L.; Zhang, Z.; Chen, P.; Lin, Z.; Liu, G. Enantioselective Copper-Catalyzed Alkynylation of Benzylic C−H Bonds *via* Radical Relay. *J. Am. Chem. Soc.* **2020**, *142*, 12493−12500.
(362) Xu, P.; Fan, W.; Chen, P.; Liu, G. Enantioselective Radical Trifluoromethylation of Benzylic C−H Bonds *via* Cooperative Photoredox and Copper Catalysis. *J. Am. Chem. Soc.* **2022**, *144*, 13468−13474.
(363) Jiang, C.; Wang, L.; Zhang, H.; Chen, P.; Guo, Y.-L.; Liu, G. Enantioselective Copper-Catalyzed Trifluoromethylation of Benzylic Radicals *via* Ring Opening of Cyclopropanols. *Chem.* **2020**, *6*, 2407−2419.
(364) Sarver, P. J.; Bacauanu, V.; Schultz, D. M.; DiRocco, D. A.; Lam, Y.-H.; Sherer, E. C.; MacMillan, D. W. C. The Merger of Decatungstate and Copper Catalysis to Enable Aliphatic C(sp^3)−H Trifluoromethylation. *Nat. Chem.* **2020**, *12*, 459−467.
(365) Hansen, J.; Davies, H. M. L. High Symmetry Dirhodium(II) Paddlewheel Complexes as Chiral Catalysts. *Coord. Chem. Rev.* **2008**, *252*, 545−555.
(366) Siegel, S.; Schmalz, H.-G. Insertion of Carbenoids into Cp-H Bonds of Ferrocenes: An Enantioselective-Catalytic Entry to Planar-Chiral Fertocenes. *Angew. Chem., Int. Ed. Engl.* **1997**, *36*, 2456−2458.
(367) Fraile, J. M.; García, J. I.; Mayoral, J. A.; Roldán, M. Simple and Efficient Heterogeneous Copper Catalysts for Enantioselective C−H Carbene Insertion. *Org. Lett.* **2007**, *9*, 731−733.
(368) (a) Fraile, J. M.; López-Ram-de-Viu, P.; Mayoral, J. A.; Roldán, M.; Santafé-Valero, J. Enantioselective C−H Carbene Insertions with Homogeneous and Immobilized Copper Complexes. *Org. Biomol. Chem.* **2011**, *9*, 6075−6081. (b) Zhang, X.; Li, Z.; Chu, J. C. K.; Chiu, P. Desymmetrization of *meso* [3.2.1]Oxabicyclic Systems Using Metal-Catalysed Asymmetric Intramolecular C−H Insertion. *Tetrahedron Lett.* **2011**, *52*, 6763−6766.
(369) Flynn, C. J.; Elcoate, C. J.; Lawrence, S. E.; Maguire, A. R. Highly Enantioselective Intramolecular Copper Catalyzed C−H Insertion Reactions of α-Diazosulfones. *J. Am. Chem. Soc.* **2010**, *132*, 1184−1185.
(370) (a) Slattery, C. N.; Maguire, A. R. Asymmetric Copper-Catalysed Intramolecular C−H Insertion Reactions of α-Diazo-β-keto Sulfones. *Org. Biomol. Chem.* **2011**, *9*, 667−669. (b) Slattery, C. N.; Clarke, L.-A.; O'Neill, S.; Ring, A.; Ford, A.; Maguire, A. R. Investigation of Additive Effects in Enantioselective Copper-Catalysed C−H Insertion and Aromatic Addition Reactions of α-Diazocarbonyl Compounds. *Synlett* **2012**, *23*, 765−767. (c) Slattery, C. N.; Clarke, L.-A.; Ford, A.; Maguire, A. R. Catalyst, Additive and Counterion Effects on the Efficiency and Enantioselectivity of Copper-Catalysed C−H Insertion Reactions of α-Diazosulfones. *Tetrahedron* **2013**, *69*, 1297−1301. (d) Clarke, L. A.; Ring, A.; Ford, A.; Sinha, A. S.; Lawrence, S. E.; Maguire, A. R. Enantioselective Copper Catalysed C−H Insertion Reaction of 2-Sulfonyl-2-diazoacetamides to Form γ-Lactams. *Org. Biomol. Chem.* **2014**, *12*, 7612−7628. (e) Shiely, A. E.; Slattery, C. N.; Ford, A.; Eccles, K. S.; Lawrence, S. E.; Maguire, A. R. Enantioselective Copper Catalysed Intramolecular C−H Insertion Reactions of α-Diazo-β-keto Sulfones, α-Diazo-β-keto Phosphine Oxides and 2-Diazo-1,3-diketones; the Influence of the Carbene Substituent. *Org. Biomol. Chem.* **2017**, *15*, 2609−2628.
(371) (a) Kohmura, Y.; Kawasaki, K.; Katsuki, T. Benzylic and Allylic Amination. *Synlett* **1997**, *12*, 1456−1458. (b) Clark, J. S.; Roche, C. Tuneable Asymmetric Copper-Catalysed Allylic Amination and Oxidation Reactions. *Chem. Commun.* **2005**, 5175−5177.
(372) Nakafuku, K. M.; Zhang, Z.; Wappes, E. A.; Stateman, L. M.; Chen, A. D.; Nagib, D. A. Enantioselective Radical C−H Amination for the Synthesis of β-Amino Alcohols. *Nat. Chem.* **2020**, *12*, 697−704.
(373) (a) Kochi, J. K. Electron-Transfer Mechanisms for Organometallic Intermediates in Catalytic Reactions. *Acc. Chem. Res.* **1974**, *7*, 351−360. (b) Welin, E. R.; Le, C.; Arias-Rotondo, D. M.; McCusker, J. K.; MacMillan, D. W. C. Photosensitized, Energy Transfer-Mediated Organometallic Catalysis through Electronically Excited Nickel(II). *Science* **2017**, *355*, 380−385. (c) Strieth-Kalthoff, F.; James, M. J.; Teders, M.; Pitzer, L.; Glorius, F. Energy Transfer Catalysis Mediated by Visible Light: Principles, Applications, Directions. *Chem. Soc. Rev.* **2018**, *47*, 7190−7202.
(374) Gutierrez, O.; Tellis, J. C.; Primer, D. N.; Molander, G. A.; Kozlowski, M. C. Nickel-Catalyzed Cross-Coupling of Photoredox-Generated Radicals: Uncovering a General Manifold for Stereoconvergence in Nickel-Catalyzed Cross-Couplings. *J. Am. Chem. Soc.* **2015**, *137*, 4896−4899.
(375) Kainz, Q. M.; Matier, C. D.; Bartoszewicz, A.; Zultanski, S. L.; Peters, J. C.; Fu, G. C. Asymmetric Copper-Catalyzed C−N Cross-Couplings Induced by Visible Light. *Science* **2016**, *351*, 681−684.
(376) Chen, X.; Lian, Z.; Kramer, S. Enantioselective Intermolecular Radical Amidation and Amination of Benzylic C−H Bonds *via* Dual Copper and Photocatalysis. *Angew. Chem., Int. Ed.* **2023**, *62*, No. e202217638.

(377) Chen, C.; Peters, J. C.; Fu, G. C. Photoinduced Copper-Catalysed Asymmetric Amidation *via* Ligand Cooperativity. *Nature* **2021**, *596*, 250−256.
(378) Dai, L.; Chen, Y.-Y.; Xiao, L.-J.; Zhou, Q.-L. Intermolecular Enantioselective Benzylic C(sp^3)−H Amination by Cationic Copper Catalysis. *Angew. Chem., Int. Ed.* **2023**, *62*, No. e202304427.
(379) (a) van Vliet, K. M.; de Bruin, B. Dioxazolones: Stable Substrates for the Catalytic Transfer of Acyl Nitrenes. *ACS Catal.* **2020**, *10*, 4751−4769. (b) Hong, S. Y.; Hwang, Y.; Lee, M.; Chang, S. Mechanism-Guided Development of Transition-Metal-Catalyzed C−N Bond-Forming Reactions Using Dioxazolones as the Versatile Amidating Source. *Acc. Chem. Res.* **2021**, *54*, 2683−2700.
(380) (a) Schröder, D.; Shaik, S.; Schwarz, H. Two-State Reactivity as a New Concept in Organometallic Chemistry. *Acc. Chem. Res.* **2000**, *33*, 139−145. (b) Ju, M.; Schomaker, J. M. Nitrene Transfer Catalysts for Enantioselective C−N Bond Formation. *Nat. Rev. Chem.* **2021**, *5*, 580−594. (c) He, P.; Zhu, S.-F. Spin Crossover and Its Application in Organometallic Catalysis: Concepts and Recent Progress. *Chem. - Eur. J.* **2024**, *30*, No. e202403437.
(381) Kim, S.; Song, S. L.; Zhang, J.; Kim, D.; Hong, S.; Chang, S. Regio- and Enantioselective Catalytic δ-C−H Amidation of Dioxazolones Enabled by Open-Shell Copper-Nitrenoid Transfer. *J. Am. Chem. Soc.* **2023**, *145*, 16238−16248.
(382) (a) Hong, S. Y.; Park, Y.; Hwang, Y.; Kim, Y. B.; Baik, M.-H.; Chang, S. Selective Formation of γ-Lactams *via* C−H Amidation Enabled by Tailored Iridium Catalysts. *Science* **2018**, *359*, 1016−1021. (b) Park, Y.; Chang, S. Asymmetric Formation of γ-Lactams *via* C−H Amidation Enabled by Chiral Hydrogen-Bond-Donor Catalysts. *Nat. Catal.* **2019**, *2*, 219−227. (c) Wang, H.; Park, Y.; Bai, Z.; Chang, S.; He, G.; Chen, G. Iridium-Catalyzed Enantioselective C(sp^3)−H Amidation Controlled by Attractive Noncovalent Interactions. *J. Am. Chem. Soc.* **2019**, *141*, 7194−7201.
(383) Bakhoda, A.; Jiang, Q.; Badiei, Y. M.; Bertke, J. A.; Cundari, T. R.; Warren, T. H. Copper-Catalyzed C(sp^3)−H Amidation: Sterically Driven Primary and Secondary C−H Site-Selectivity. *Angew. Chem., Int. Ed.* **2019**, *58*, 3421−3425.
(384) Chen, X.; Li, H.-H.; Kramer, S. Photoinduced Copper-Catalyzed Enantioselective Allylic C(sp^3)−H Oxidation of Acyclic 1-Aryl-2-alkyl Alkenes as Limiting Substrates. *Angew. Chem., Int. Ed.* **2024**, *63*, No. e202413190.
(385) (a) Mayoral, J. A.; Rodríguez-Rodríguez, S.; Salvatella, L. Theoretical Insights into Enantioselective Catalysis: The Mechanism of the Kharasch−Sosnovsky Reaction. *Chem. - Eur. J.* **2008**, *14*, 9274−9285. (b) Gephart, R. T., III; McMullin, C. L.; Sapiezynski, N. G.; Jang, E. S.; Aguila, M. J. B.; Cundari, T. R.; Warren, T. H. Reaction of Cu^{I} with Dialkyl Peroxides: Cu^{II}-Alkoxides, Alkoxy Radicals, and Catalytic C−H Etherification. *J. Am. Chem. Soc.* **2012**, *134*, 17350−17353.
(386) (a) Zheng, Y.-W.; Narobe, R.; Donabauer, K.; Yakubov, S.; König, B. Copper(II)-Photocatalyzed N−H Alkylation with Alkanes. *ACS Catal.* **2020**, *10*, 8582−8589. (b) Balakrishna, B.; Mossin, S.; Kramer, S. Photo-Induced Metal-Free Dehydrogenative N−N Homo-Coupling. *Chem. Commun.* **2022**, *58*, 10977−10980. (c) Golden, D. L.; Zhang, C.; Chen, S.-J.; Vasilopoulos, A.; Guzei, I. A.; Stahl, S. S. Benzylic C−H Esterification with Limiting C−H Substrate Enabled by Photochemical Redox Buffering of the Cu Catalyst. *J. Am. Chem. Soc.* **2023**, *145*, 9434−9440.
(387) Hu, H.; Chen, S.-J.; Mandal, M.; Pratik, S. M.; Buss, J. A.; Krska, S. W.; Cramer, C. J.; Stahl, S. S. Copper-Catalysed Benzylic C−H Coupling with Alcohols *via* Radical Relay Enabled by Redox Buffering. *Nat. Catal.* **2020**, *3*, 358−367.
(388) Li, H.-H.; Liu, Y.; Kramer, S. Benzylic C(sp^3)−H Phosphonylation *via* Dual Photo and Copper Catalysis. *Angew. Chem., Int. Ed.* **2025**, *64*, No. e202420613.
(389) Zhang, H.; Zhou, Y.; Yang, T.; Wu, J.; Chen, P.; Lin, Z.; Liu, G. Site- and Enantioselective Allylic and Propargylic C−H Oxidation Enabled by Copper-Based Biomimetic Catalysis. *Nat. Catal.* **2025**, *8*, 58−66.
(390) (a) Lieberman, R. L.; Rosenzweig, A. C. Crystal Structure of a Membrane-Bound Metalloenzyme that Catalyses the Biological Oxidation of Methane. *Nature* **2005**, *434*, 177−182. (b) Balasubramanian, R.; Smith, S. M.; Rawat, S.; Yatsunyk, L. A.; Stemmler, T. L.; Rosenzweig, A. C. Oxidation of Methane by a Biological Dicopper Centre. *Nature* **2010**, *465*, 115−119.
(391) (a) Walling, C.; Zavitsas, A. A. The Copper-Catalyzed Reaction of Peresters with Hydrocarbons. *J. Am. Chem. Soc.* **1963**, *85*, 2084−2090. (b) Kochi, J. K.; Mains, H. E. Studies on the Mechanism of the Reaction of Peroxides and Alkenes with Copper Salts. *J. Org. Chem.* **1965**, *30*, 1862−1872. (c) Beckwith, A. L. J.; Zavitsas, A. A. Allylic Oxidations by Peroxy Esters Catalyzed by Copper Salts. The Potential for Stereoselective Syntheses. *J. Am. Chem. Soc.* **1986**, *108*, 8230−8234. (d) Smith, K.; Hupp, C. D.; Allen, K. L.; Slough, G. A. Catalytic Allylic Amination *versus* Allylic Oxidation: A Mechanistic Dichotomy. *Organometallics* **2005**, *24*, 1747−1755.
(392) Tang, S.; Xu, H.; Dang, Y.; Yu, S. Photoexcited Copper-Catalyzed Enantioselective Allylic C(sp^3)−H Acyloxylation of Acyclic Internal Alkenes. *J. Am. Chem. Soc.* **2024**, *146*, 27196−27203.
(393) Liu, X.-M.; Li, F.; Wang, T.; Dai, L.; Yang, Y.; Jiang, N.-Q.; Xue, L.-Y.; Liu, J.-Y.; Xue, X.-S.; Xiao, L.-J.; Zhou, Q.-L. Catalytic Asymmetric Oxidative Coupling between C(sp^3)−H Bonds and Carboxylic Acids. *J. Am. Chem. Soc.* **2025**, *147*, 627−635.
(394) Tang, S.; Song, H.; Yu, S. Enantioselective Propargylic C(sp^3)−H Acyloxylation Enabled by Photoexcited Copper Catalysis. *Org. Lett.* **2024**, *26*, 10036−10040.
(395) Xi, J.; Zhu, X.; Bao, H. Copper-Catalyzed Enantioselective Radical Esterification of Propargylic C−H Bonds. *Synthesis* **2024**, *56*, 1393−1400.
(396) Ye, L.; Tian, Y.; Meng, X.; Gu, Q.-S.; Liu, X.-Y. Enantioselective Copper(I)/Chiral Phosphoric Acid Catalyzed Intramolecular Amination of Allylic and Benzylic C−H Bonds. *Angew. Chem., Int. Ed.* **2020**, *59*, 1129−1133.
(397) Minisci, F.; Recupero, F.; Cecchetto, A.; Gambarotti, C.; Punta, C.; Paganelli, R.; Pedulli, G. F.; Fontana, F. Solvent and Temperature Effects in the Free Radical Aerobic Oxidation of Alkyl and Acyl Aromatics Catalysed by Transition Metal Salts and *N*-Hydroxyphthalimide: New Processes for the Synthesis of *p*-Hydroxybenzoic Acid, Diphenols, and Dienes for Liquid Crystals and Cross-Linked Polymers. *Org. Process Res. Dev.* **2004**, *8*, 163−168.
(398) Yang, C.-J.; Zhang, C.; Gu, Q.-S.; Fang, J.-H.; Su, X.-L.; Ye, L.; Sun, Y.; Tian, Y.; Li, Z.-L.; Liu, X.-Y. Cu-Catalysed Intramolecular Radical Enantioconvergent Tertiary β-C(sp^3)−H Amination of Racemic Ketones. *Nat. Catal.* **2020**, *3*, 539−546.
(399) Yang, Y.; Cho, I.; Qi, X.; Liu, P.; Arnold, F. H. An Enzymatic Platform for the Asymmetric Amination of Primary, Secondary and Tertiary C(sp^3)−H Bonds. *Nat. Chem.* **2019**, *11*, 987−993.
(400) Duan, X.-Y.; Yang, X.-L.; Jia, P.-P.; Zhang, M.; Han, B. Hydrazonyl Radical-Participated Tandem Reaction: A Strategy for the Synthesis of Pyrazoline-Functionalized Oxindoles. *Org. Lett.* **2015**, *17*, 6022−6025.
(401) Gao, A.; Ren, Y.-Q.; Luan, C.; Tian, Y.; Liu, L.; Gu, Q.-S.; Li, Z.-L.; Yang, C.-J.; Liu, X.-Y. Copper-Catalyzed Intramolecular Radical Amination of Tertiary C(sp^3)−H Bonds to Access α-Quaternary Pyrrolidines. *Asian J. Org. Chem.* **2023**, *12*, No. e202300220.
(402) Qi, R.; Wang, C.; Huo, Y.; Chai, H.; Wang, H.; Ma, Z.; Liu, L.; Wang, R.; Xu, Z. Visible Light Induced Cu-Catalyzed Asymmetric C(sp^3)−H Alkylation. *J. Am. Chem. Soc.* **2021**, *143*, 12777−12783.
(403) Qi, R.; Chen, Q.; Liu, L.; Ma, Z.; Pan, D.; Wang, H.; Li, Z.; Wang, C.; Xu, Z. Copper-Catalyzed Asymmetric C(sp^3)−H Cyanoalkylation of Glycine Derivatives and Peptides. *Nat. Commun.* **2023**, *14*, 3295.
(404) Zahrt, A. F.; Henle, J. J.; Rose, B. T.; Wang, Y.; Darrow, W. T.; Denmark, S. E. Prediction of Higher-Selectivity Catalysts by Computer-Driven Workflow and Machine Learning. *Science* **2019**, *363*, No. eaau5631.